PHOTOCHEMICAL ISOMERIZATION OF ERGOSTEROL--A KINETIC STUDY

By

Horatio S. Stillo

A THESIS

Submitted to the School of Advanced Graduate Studies
of Michigan State University of Agriculture and
Applied Science in partial fulfillment of
the requirements for the degree of

DOCTOR OF PHILOSOPHY

Department of Chemistry

1959

ACKNOWLEDGMENT

It is with sincere appreciation that I acknowledge the assistance and valuable counsel of Professor James C. Sternberg under whose direction this investigation was conducted.

I also wish to express my gratitude to the staff of the Chemistry Department for assistance and advice on many matters. In particular, I gratefully acknowledge the suggestions offered by Professor Richard H. Schwendeman that pertained to the computational analytical procedure.

I am indebted to Mr. W. H. C. Shaw of Glaxo Laboratories, Ltd., Greenford, England, for his kind furnishing of samples and spectral data. Acknowledgment is also due the National Institutes of Health for their grants supporting this work.

Last, but by no means least, I wish to thank Irene, my wife, for her patience and understanding, and for her willingness to leave a secure and comfortable station in order that I might complete this phase of my education.

****

PHOTOCHEMICAL ISOMERIZATION OF ERGOSTEROL--A KINETIC STUDY

By

Horatio S. Stillo

AN ABSTRACT

Submitted to the School of Advanced Graduate Studies
of Michigan State University of Agriculture and
Applied Science in partial fulfillment of
the requirements for the degree of

DOCTOR OF PHILOSOPHY

Department of Chemistry

Year 1959

Approved James C. Sternberg

ABSTRACT

A kinetic investigation of the photochemical isomerization of ergosterol has been carried out. The kinetic data have been obtained in solvents with a range of viscosity, but fixed chemical nature, at different wavelengths in a stirred reaction cell.

A spectrophotometric analytical procedure based on a least-squares curve-fitting technique has been developed, verified, and employed to determine the requisite concentration vs. time data. A novel photometric technique has also been developed and actinometrically calibrated to make possible the absolute determination of the absorbed light intensity as a function of time of irradiation. Combination of these data with the spectrophotometric analytical results has furnished the absorbed light intensity for each component as a function of time, making possible the elimination of the "inner filter" effect and the use of a new type of photochemical kinetic expression.

Stereochemical information and considerations of the excited states of the components of the irradiation mixture have been utilized to formulate a kinetic mechanism expressed in general and in specific terms. The general formulation is a special photochemical application of generalized first order series and parallel reaction kinetics, and has been shown to lead to expressions for concentrations of the components as linear combinations of definite integrals representing the amounts of radiation absorbed by the individual components during a given irradiation

interval. In the specific cases of interest, the expressions reduce to simple linear relationships between individual concentrations and single integrals.

A comparison of the results of the kinetic runs with the derived rate expressions furnishes values for the quantum yield, ϕ_E, for the conversion of ergosterol to total products, the quantum yield, ϕ_{PT}, for the conversion of precalciferol$_2$ to tachysterol$_2$, and the quantum yield, ϕ_{EL}, for the conversion of ergosterol to lumisterol$_2$. The values of the quantum yields have been found as functions of wavelength and viscosity.

The value of ϕ_E is in accord with bioassay results and the value of ϕ_{PT} supports recent data of Havinga obtained by direct irradiation of precalciferol$_2$. This agreement with the results of investigations based on other analytical techniques substantiates both the novel photometric technique and the validity of the analytical scheme. The results also indicate that the solvent effect is truly a viscosity effect and show the direction of the viscosity dependence for ϕ_{PT} to be opposite to that obtained for ϕ_E and ϕ_{EL}. In addition, an appreciable wavelength dependence for ϕ_E and ϕ_{PT}, entirely apart from inner filter effect, is demonstrated.

An interpretation or description of the proposed mechanism has been made with the following features: (a) the optical excited state is a singlet state, (b) the optical excited state for ergosterol differs from that for precalciferol$_2$, (c) conversions occur through cross-overs of potential energy surfaces along coordinates corresponding to internal

rotations, (d) the solvent exerts an effect through its viscous resistance to internal rotation, and (e) the excess energy per quantum of radiation at shorter wavelengths helps overcome the barrier to internal rotation.

An alternative non-mechanistic interpretation has been presented but is ruled out on the basis of the available data.

The results of this investigation have been utilized to suggest other studies which would help further to establish the complete mechanism.

TABLE OF CONTENTS

TABLE OF CONTENTS - Continued

TABLE OF CONTENTS - Continued

TABLE OF CONTENTS - Continued

LIST OF TABLES

LIST OF TABLES - Continued

LIST OF FIGURES

LIST OF FIGURES - Continued

FIGURE Page

I. INTRODUCTION

A kinetic study of the photochemical isomerization of ergosterol to calciferol$_2$ is of interest, since this reaction affords the only practical synthesis of the biologically important compound, calciferol$_2$. From a fundamental point of view, this reaction is representative of a very important class of photochemical reactions of excited molecules. Despite the expenditure of a vast amount of effort in the study of the photochemical isomerization of ergosterol over the past thirty years, an extensive kinetic investigation capable of quantitative treatment had not been made until the present study. Sebrell and Harris (35) have summarized the results of these investigations up to the year 1952. More recent work has been summarized by Sharpe (37). In view of the publication of these works, the historical discussion of the topic will be limited.

The early workers in this field, i.e., A. Windaus, O. Rosenheim, J. Waddell, and others, established ergosterol as an important provitamin that could be activated to calciferol$_2$ by ultraviolet irradiation. Windaus was one of the principal investigators and did much of the work that resulted in the characterization of a number of the irradiation products of ergosterol. As a result of this early work a mechanism was proposed in which the irradiation reaction proceeded irreversibly through the identified intermediates as follows:

$$\text{ergosterol} \xrightarrow{h\nu} \text{lumisterol}_2 \xrightarrow{h\nu} \text{tachysterol}_2$$

$$\xrightarrow{h\nu} \text{calciferol}_2 \xrightarrow{h\nu} \text{overirradiation products.}$$

In 1948-49 Velluz (42) and his associates announced the characterization of a hitherto overlooked intermediate which they called precalciferol$_2$. They observed that the newly discovered compound was transformed to calciferol$_2$ by a thermal reaction. An equilibrium exists between the two compounds in which increasing temperature favors calciferol$_2$. Precalciferol$_2$ had escaped detection because the "working up" of the irradiated provitamin or resin was quite involved and required time during which precalciferol$_2$ was largely converted to calciferol$_2$.

The components of the ergosterol irradiation sequence are isomers, and their structural formulae showing generally accepted stereochemical details are presented in Figure 1. The stereochemical details are quite important with respect to the development of this thesis and will be discussed in the body of the text.

The discovery of precalciferol* by Velluz and his associates has stimulated a great deal of interest in this field; in the decade following this important discovery, three groups working in Europe have made extensive contributions directly in the study of the photochemical isomerization of ergosterol. These groups have been under the direction

---

*For convenience, the subscript 2 will not be employed from this point in the text. All of the work of this investigation was performed with ergosterol as the starting material, and consequently discussion pertaining to this investigation will refer to the irradiation products with subscript 2--i.e., the products derived from ergosterol. The pertinent chemistry of the products derived from ergosterol is identical with that of the products derived from 7-dehydrocholesterol (subscript 3), and general discussion will be equally applicable to both the ergosterol and 7-dehydrocholesterol irradiation sequences.

Figure 1. Structural Formulae of the Components of the Irradiation Mixture.

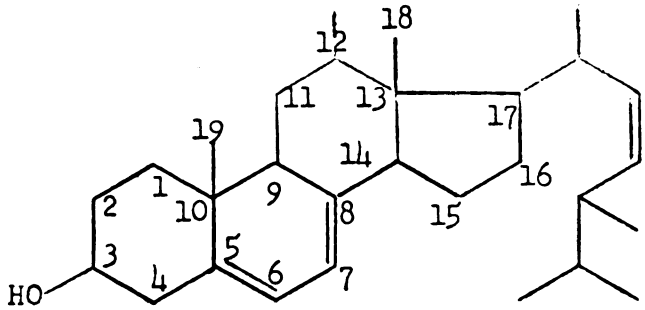

ERGOSTEROL

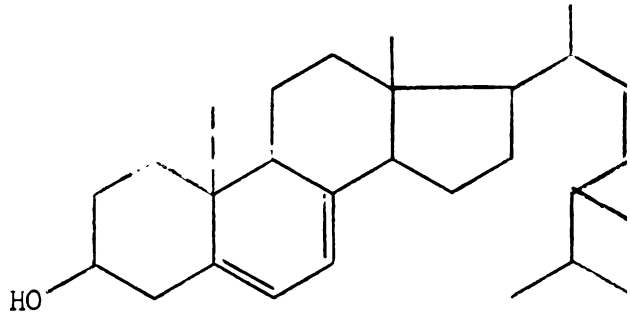

LUMISTEROL

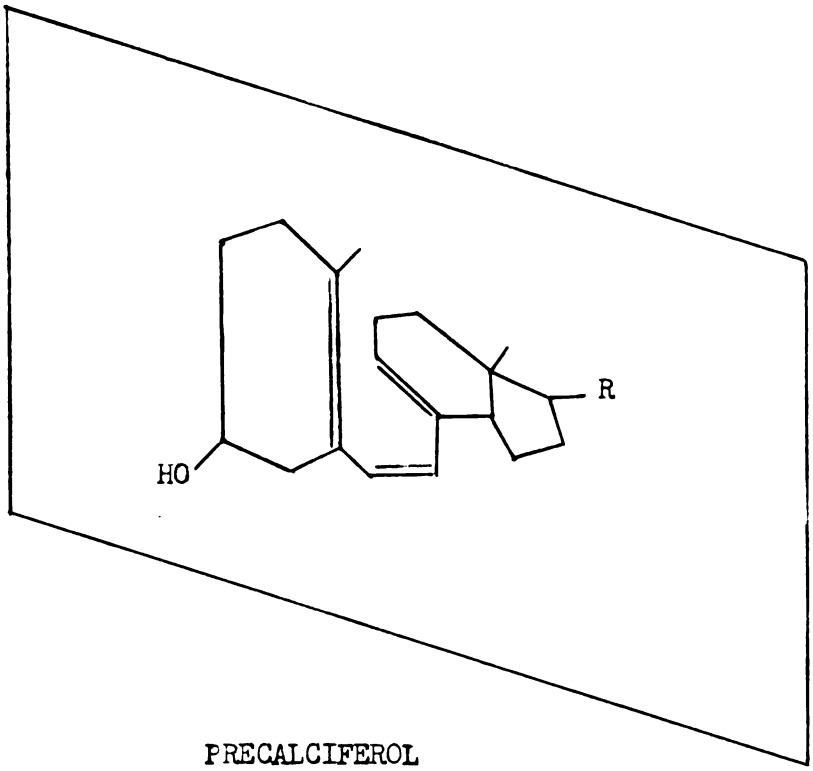

PRECALCIFEROL
Proposed Nonplanar Structure

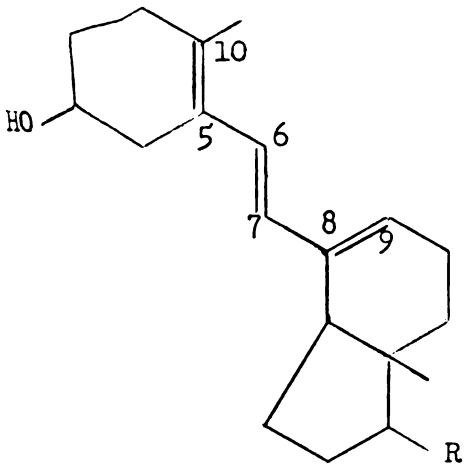

TACHYSTEROL

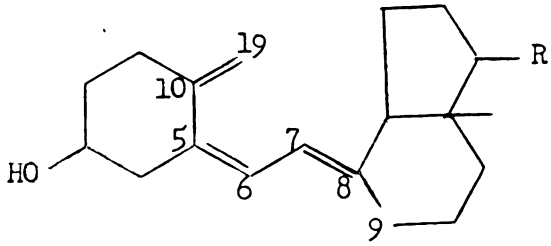

CALCIFEROL

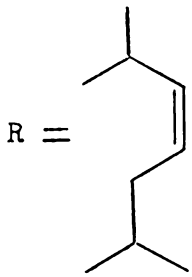

of Vellnz (42,43,44, and 45), Havinga (18,19,20,27,33,34,46,47,48,49,50), and Inhoffen (22,23,24,25,26). These groups have reported the results of investigations on the mechanism, stereochemistry, and general chemical details of the photochemical isomerization of ergosterol. In addition the studies of this reaction have stimulated other investigations on related reactions of other compounds containing similar structural details. For example, Buchi and Yang (6) have reported their results of photochemical isomerization of certain dienones. Also typical of related work is the investigation of the irradiation of dehydroergosterol by Barton and Kende (2). Investigations are also being made of the reactions of the components of the ergosterol irradiation sequence. A recent contribution (11) has been the elucidation of the structure of suprasterol II, one of the over-irradiation products of the photochemical isomerization of ergosterol. Brande and Wheeler (4) have explored new synthetic routes to simple analogues that contain the chromophores of the components of the ergosterol irradiation mixture. Important contributions with respect to analytical procedures applicable to this field have been made by Shaw and his associates (39).

Havinga and his associates have re-examined the early mechanism postulated for the photochemical isomerization of ergosterol and have cited evidence that refutes the original formulation of the reaction sequence. Essentially their contribution has been to demonstrate that lumisterol and tachysterol are not essential intermediates in the formation of calciferol. They have also reported--concurrently with the results of this investigation--that precalciferol is the primary product of the reaction.

Kinetic studies of the reaction have been quite limited. Dasler (10) had reported a kinetic study in which only the concentration of ergosterol was followed as a function of time. More recently, results of limited kinetic studies have been reported and interpreted in the light of recent knowledge of the reaction (33,34). However, an extensive kinetic investigation which is capable of explaining such observations as the wavelength and specific solvent effects had not been made. For example, in a given solvent, the short wavelengths (about 2500 A^{o}) favor a rapid conversion of ergosterol and fast formation of tachysterol. Irradiation with wavelengths at the longer wavelength limit of the absorption band (about 3000 A^{o}) results in a slower rate of conversion of ergosterol and favors the formation of lumisterol. In addition, a specific solvent effect has been observed in which the maximum obtainable yield of calciferol is apparently greater in ether than in alcohol.

The major obstacle to a successful completion of a kinetic study has been the lack of a suitable analytical procedure. Recent advances have been made in analysis of the complex irradiation mixtures through combination of chromatographic and colorimetric procedures (34,39), but it seemed desirable to find a more rapid analysis which could be carried out at time intervals during the irradiation without disturbing the irradiation mixture. The possibility of carrying out the analysis entirely on the basis of ultraviolet spectrophotometry was therefore re-examined.

The irradiation mixture may contain the following principal components: ergosterol, lumisterol, tachysterol, precalciferol, and

calciferol, and possible over-irradiation products. Ergosterol and the four other major components are isomers and have very similar ultraviolet absorption spectra (cf. Figure 2), complicating the utilization of spectrophotometric techniques. Past attempts for obtaining the composition of the irradiation mixture, based upon the direct application of the Beer-Lambert-Bouger Law to the ultraviolet absorption spectra of the mixtures, failed because the system of five simultaneous linear equations obtained lacked sufficient independence. This failure has generally been attributed to the lack of accuracy with which the spectra of the components were known.

It appeared that it might be possible to obtain with reasonable accuracy the compositions of the irradiation mixtures by application of curve-fitting techniques to the spectra, utilizing the available spectral data for the components. Sharpe (37) employed a curve fitting technique, which involved a comparison of experimental absorption spectra with curves calculated on the basis of the Beer-Lambert-Bouger Law, and utilizing IBM punched card machines for performing the calculations and comparisons; this method proved partially successful. However, the procedure yielded several compositions that would equally well satisfy the conditions for the comparison. In addition, one of the major components of the irradiation mixture, precalciferol, was neglected in making the calculations, since the existence of precalciferol in appreciable quantities in the irradiation mixture was not generally recognized at the time the calculations were initiated. This omission has invalidated the results of the calculations, although the method appears sound.

Figure 2. Ultraviolet Absorption Spectra of the Components of the Ergosterol Irradiation Mixture in Absolute Ethanol (40).

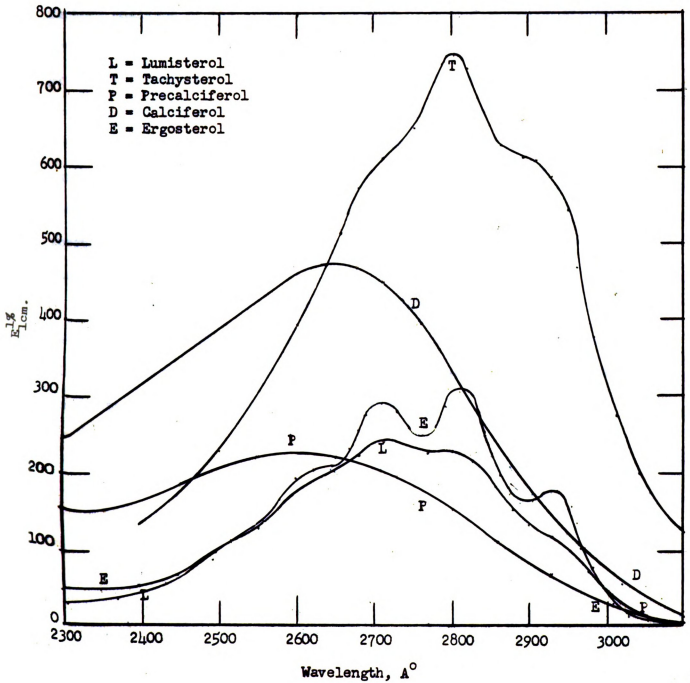

The recent availability of more reliable spectra of the pure components (39,40), and the use of a more convenient statistical averaging technique to obtain the best least squares fit of the calculated results to spectrophotometric data, have now made it possible to obtain satisfactory analyses of the irradiation mixture by purely spectrophotometric procedures. When this investigation was initiated, plans were made to prepare the components that were not available in order to obtain more accurate spectral data and to verify the analytical procedure by application of the computational procedure to the spectra of synthetic mixtures. While this work was in progress, Mr. W. H. C. Shaw of Glaxo Laboratories, Ltd., Greenford, England, kindly furnished the necessary spectral data and samples of the components, and the preparative work was discontinued.

With the development of the computational analytical procedure, it was possible to achieve the objective of this study, i.e., an extensive kinetic study which would serve as the basis for an interpretation of the photochemical isomerization of ergosterol.

TABLE OF CONTENTS

II. EXPERIMENTAL

A. Preparative

1. Irradiation Procedure and Apparatus

Solutions of ergosterol in isopropyl alcohol were subjected to ultraviolet radiation in a flow system illustrated in Figure 3. A cylindrical low pressure mercury lamp was employed as the source of radiation. The mercury lamp was placed in the center of three concentric cylindrical quartz chambers. Tap water was circulated through the inner chamber--next to the lamp--to cool the system; a copper sulfate solution was circulated through the middle chamber to filter out ultraviolet radiation and provide further cooling of the system. Adjustment of the concentration of the copper sulfate solution permitted a variation of the wavelength of cut-off of the radiation; this factor will be discussed further in a succeeding paragraph. The ergosterol solution that was to be irradiated was circulated through the outermost chamber. The irradiated ergosterol solution and the copper sulfate solution were cooled by passing them through heat exchangers through which ice water was circulated. Centrifugal pumps were employed to circulate the cell solution and the filter solution. A packing consisting of Teflon shavings and Silicone grease was employed in the pump in the irradiation circuit. With the exception of the steel pump, the irradiation circuit consisted entirely of quartz, glass, and Teflon tubing, which was employed to join the components of the system.

Figure 3

Preparative Irradiation Apparatus

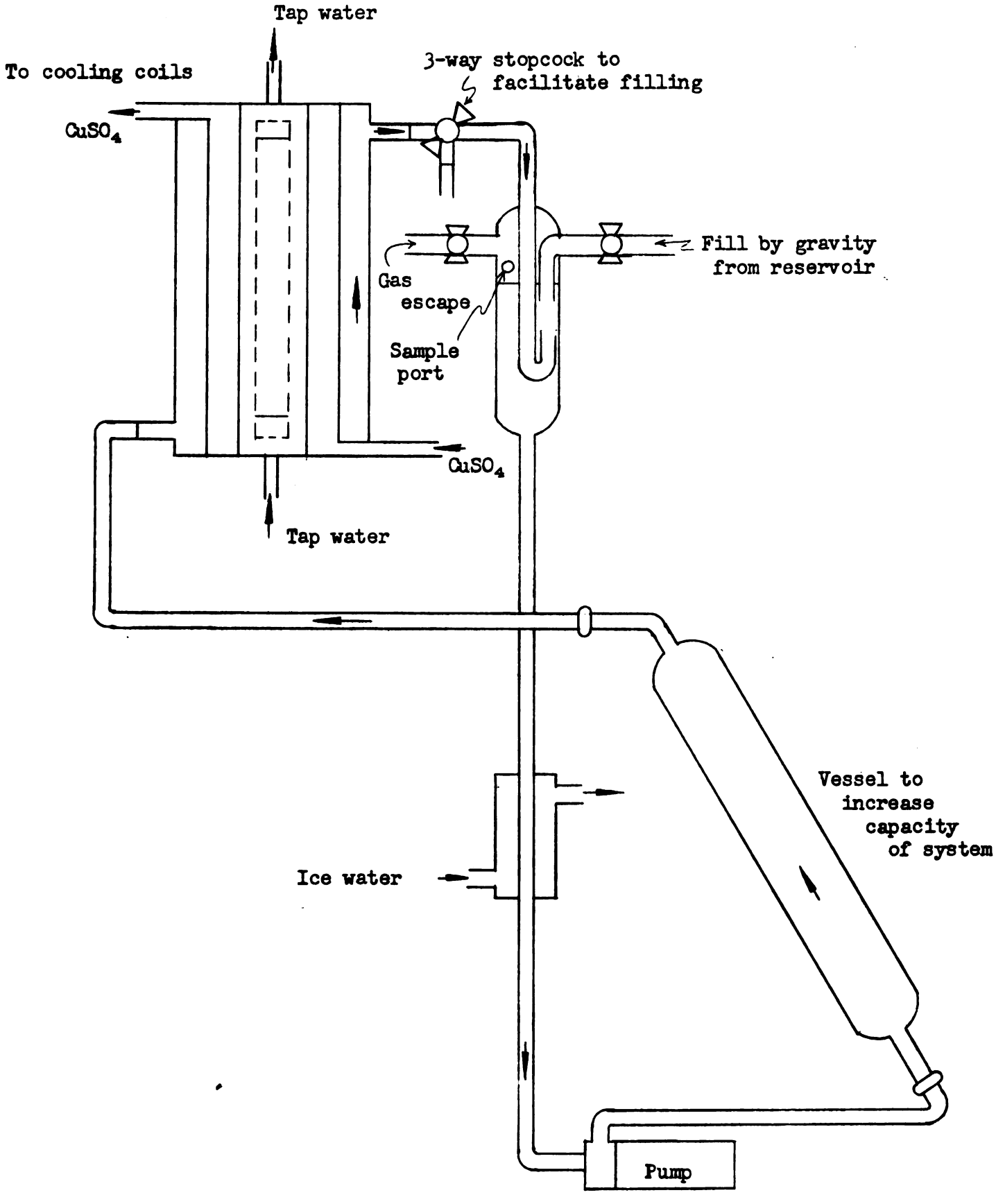

The capacity of the irradiation system was increased from about 500 ml. to approximately 900 ml. by the inclusion of the vessel indicated in Figure 3. The thickness of the chamber containing the solution being irradiated was 0.50 cm. Prior to filling the system with ergosterol solution, nitrogen was passed through the irradiation circuit. The solvent was also purged with nitrogen prior to the preparation of the ergosterol solution.

The course of the irradiation was followed by determination of the ultraviolet absorption spectrum of the irradiated solution. Samples of the cell solution were withdrawn periodically through the sampling port, cf. Figure 3. A suitable dilution was made and the spectrum determined on a Beckman DK-2 spectrophotometer.

At the time the experimental work was started, it was believed that radiation of wave length greater than 296 mμ would favor the formation of precalciferol, which was the product to be prepared initially. The reasons for this belief will be discussed in a later section. In order to achieve this condition, the bulk of ultraviolet radiation of short wave length was filtered out by an aqueous copper sulfate solution of appropriate concentration which was chosen from the data summarized in Table I; the absorption spectra of aqueous copper sulfate solutions were determined at varying concentrations. The wave length at which the percent transmission was reduced to 10% was considered as the lower wave length cut-off.

TABLE I

ULTRAVIOLET ABSORPTION OF AQUEOUS COPPER SULFATE SOLUTIONS

Path Length = 1.00 cm.

Concentration g./100 ml. water	Wave Length at Which Percent Transmission = 10, mμ
20.0	318
10.0	312
6.7	309
5.0	307
2.5	298
1.25	290
0.625	279
0.312	265

2. Preparation of Irradiated Solution for Chromatographic Separation

The irradiated solution was evaporated to dryness in a vacuum evaporation apparatus that utilized a dry ice bath as a heat sink. Liquid in the evaporator was stirred by means of a magnetic stirring bar to increase the rate of evaporation and to prevent "bumping" of the liquid. The temperature of the liquid in the evaporator was maintained below 0° C. by the vaporization process.

The resin (the residue in the evaporator) was dissolved in methanol--about 25 ml. of solvent per gram of crude irradiation product--and allowed to stand overnight at about 5° C. The mixture was placed in an ice-salt bath for several hours; the unreacted ergosterol was separated

from the soluble irradiation product by filtration. The filtrate was evaporated to dryness in the vacuum evaporation apparatus described above.

3. Chromatographic Separation and Preparation of Derivatives

The subsequent treatment of the resin was that of Shaw et al. (39). The resin was taken up in petroleum ether and chromatographed on an alumina column with a height of 50 cm. and diameter of 3 cm. and employing a mixture consisting of 6% acetone in petroleum ether (v/v) as eluent. The column was filled with petroleum ether to a height of 40 cm. and alumina was poured through the solvent to form a 50 cm. column.

Alumina with an activity of III on the Brockmann scale (5,52) was employed in the chromatographic procedure. The activity of alumina is determined by its behavior toward binary mixtures of certain azo dyes. A test solution consisting of Sudan red and Sudan yellow 0.04% w/v of each dye--in a solvent with a composition of 20% benzene and 80% petroleum ether v/v, is employed in the test for Grade III activity. Ten ml. of the test solution are introduced into an alumina column 5 cm. in length and with a diameter of 1.5 cm. The column is developed with 20 ml. of solvent. An activity of Grade III is indicated if the Sudan yellow band, which is the lower band, is still held on the column about 3-4 cm. from the top. The alumina employed--Merck Reagent Grade, marked suitable for chromatographic absorption--possessed an activity of III without further treatment.

The column was eluted at the rate of 3-4 ml. per minute and 15 ml. fractions were collected. Each fraction was checked with antimony

trichloride reagent in order to detect the appearance of bands in the eluent. A 0.05 ml. portion of each fraction was evaporated to dryness and 0.5 ml. of the antimony trichloride reagent was added to the residue. A yellowish-pink or bronze color is developed which reaches maximum intensity within 30 seconds and is stable for 4-5 minutes. The relative intensity of the antimony trichloride color that is developed by the components of the irradiation mixture (on the basis of the color of calciferol as 100%) is as follows (39):

	Antimony Trichloride Color
Ergosterol	< 1% yellow
Lumisterol	< 1% yellow
Precalciferol	100% orange
Tachysterol	96-100% orange
Calciferol	100% orange

Lyness and Quackenbush have reported similar observations with regard to the antimony trichloride color (28).

Shaw et al. (39) have reported that the components of the irradiation mixture are resolved into three bands as follows:

First Band

Precalciferol
Lumisterol
Suprasterol II
Pyrocalciferol

Second Band

Calciferol
Tachysterol
Suprasterol

Third Band

Ergosterol
Isopyrocalciferol

The procedure of Kield et al. (31) was employed for the preparation of the antimony trichloride reagent. Merck's reagent chloroform was washed seven times with equal portions of distilled water and then shaken with an excess of phosphorus pentoxide, followed by a rapid filtration through filter paper. The chloroform was distilled through a fractionating column and the appropriate fractions were used to prepare the reagent. Then 15-22 grams of antimony trichloride (Mallinckrodt Analytical Reagent grade) were dissolved per 100 ml. of the purified chloroform, and the mixture was warmed to 35-45° to facilitate rapid solution of the salt. The mixture was filtered and 2.0 ml. of freshly distilled acetyl chloride were added to every 100 ml. of the filtrate. The reagent was stored in 100 ml. glass-stoppered dark bottles.

The liquid of the band that contained precalciferol was evaporated to dryness in vacuo, and the 3,5 dinitrobenzoate was prepared by reacting the residue with freshly prepared 3,5 dinitrobenzoyl chloride in a solvent consisting of 3 parts benzene and 1 part pyridine. The reaction was allowed to proceed at tap water temperature for about one hour, and then the reaction flask was allowed to stand in an ice bath for four hours.

The reaction mixture was poured into water, sodium carbonate was added, and the layers were separated. The aqueous layer was extracted with benzene, and the combined benzene extracts were added to the original benzene layer. The benzene solution was dried over sodium sulfate and evaporated to dryness in vacuo. A recrystallization solvent mixture employed by Vellaz et al.(42) was utilized. The crude product was dissolved in a solvent consisting of 3 parts absolute ethanol and 1 part 2-butanone. Part of the solvent was evaporated in vacuo at 0° C. until crystallization began. The precipitate was filtered by suction and washed with the cold solvent. All operations were carried out with the apparatus immersed in an ice bath.

B. Kinetic Studies

1. Apparatus

The two basic types of data required for the kinetic study were the concentrations of the components of the irradiation mixture as a function of time and the amount of radiation absorbed by the sample solution during the period of irradiation. The concentration-time data were obtained by the spectrophotometric analytical procedure described in another section, utilizing data taken with a Beckman DK-2 Recording Spectrophotometer. Since this is a standard commercial instrument, it will not be described here. The irradiation of the solutions with monochromatized light required a source and monochromator, and the measurements of absorbed light intensity during the irradiation required construction of a photometer designed for that purpose. These portions of the

apparatus will now be considered in detail. The optical components of the apparatus are shown in Figure 4.

a. Source and Monochromator

The source of ultraviolet light for the irradiations of the kinetic study was an Hanovia Sun Burner Type SH--a medium pressure mercury arc. The mercury arc was used in conjunction with a Bausch and Lomb Grating Monochromator which had a focal length of 250 millimeters, a linear dispersion of 66 A° per millimeter and an effective aperture of f/4.4. The grating, which was blazed for first-order in the range 2000-14000 A°, contained 600 lines per millimeter on a surface 50 x 50 millimeters. The slit widths were adjustable and were maintained at 1.5 and 2.0 millimeters as indicated in the presentation of the data.

A quartz lens at the exit slit of the monochromator imaged the grating at a point about 60 mm. in front of the monochromator housing. A quartz collecting lens was placed about 50 mm. beyond the point at which the grating was imaged; the collecting lens possessed a focal length of about 50 mm. The result of this geometry was a slowly converging beam of radiation emanating from the collecting lens.

b. The Photometer Section

(1) Optics for Splitting the Radiation into Sample and Reference Beams. A quartz plate was placed in the path of the radiation at a distance of 50 mm. beyond the collecting lens, and inclined at an angle of about 45° to the beam. The incident beam was divided into a beam which was slightly reduced in intensity and slightly deflected from the

Figure 4.

Irradiation Apparatus for Kinetic Studies--
Optical Components

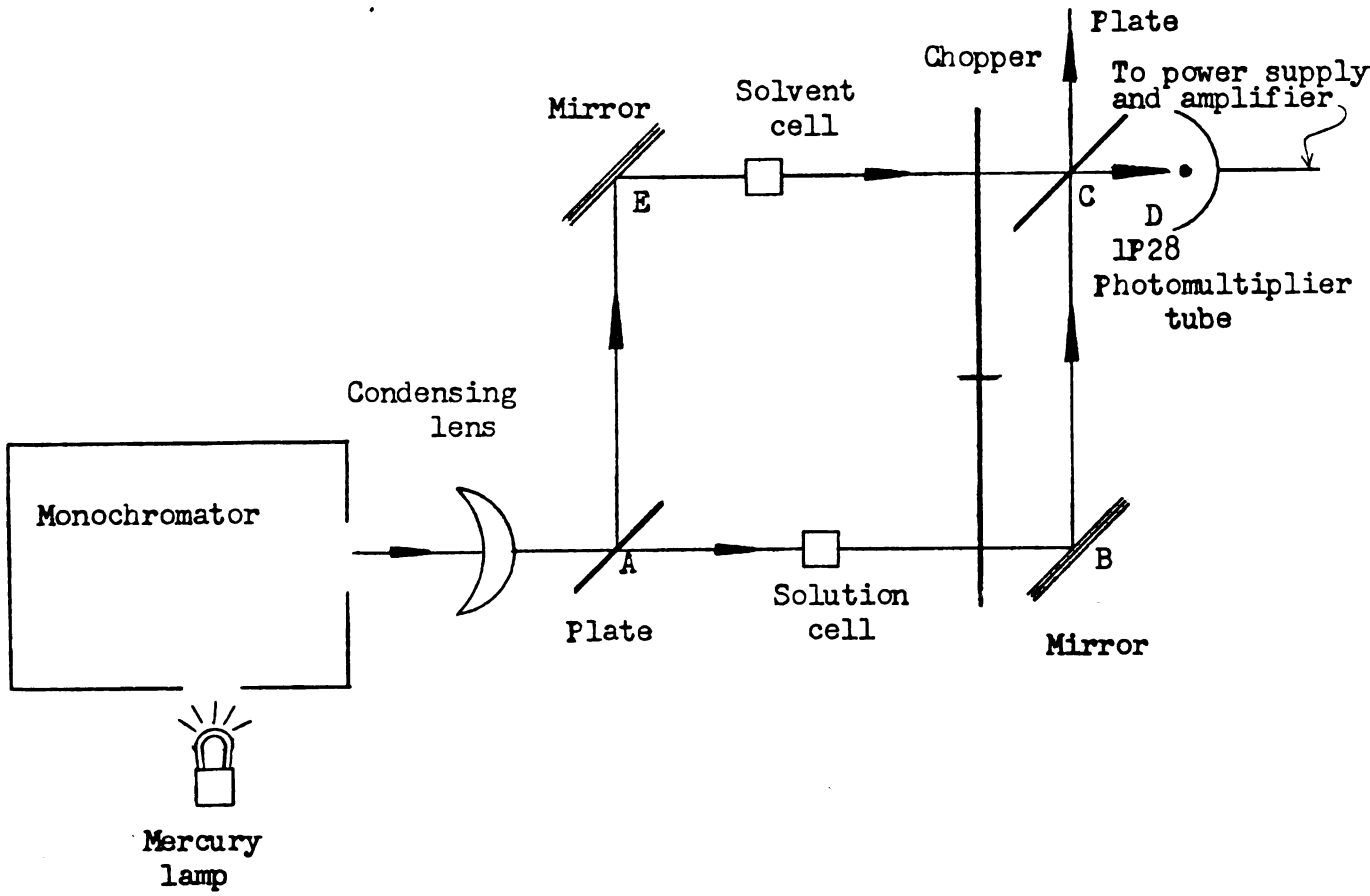

original direction, and a second beam, with a fraction of the intensity of the incident beam, which was reflected to a direction approximately perpendicular to the original direction of propagation.

(2) The Sample Beam. The solution to be irradiated was contained in a Beckman spectrophotometer quartz cell with a path length of 1.00 cm. The irradiation cell was placed in the path of the major portion of the incident beam about 16 cm. beyond the quartz plate; this placed the irradiation cell slightly in front of the focal point of the beam. The image incident on the front side of the cell was rectangular in shape with the dimensions of 2x:0.3 mm. at a slit width of 1.50 mm. These dimensions were increased to about 2x:0.4 mm. when an exit slit width of 2.00 mm. was employed. Stirring in the irradiation cell was achieved by a magnetic stirrer which consisted of a coil constructed from the fine alloy steel wire employed for cleaning hypodermic needles. The magnetic stirrer motor was mounted beneath an aluminum track which served as a mounting for a cell holder of the type employed with the Beckman Model DU Spectrophotometer. The solution spectrophotometer cell was placed in the cell holder.

The radiation that passed through the solution being irradiated was reflected from an aluminum front-surfaced mirror placed in the path of the beam, about 15 cm. beyond the irradiation cell and inclined at an angle of 45° to the direction of propagation. This reflected beam was again divided by a quartz plate placed about 10 cm. from the mirror and inclined at an angle of 45° to the new direction of the beam. The major portion of this beam passed through the quartz plate and was absorbed by

the walls of cover of the apparatus; the remaining portion was reflected to a photomultiplier tube (1P28). The tube was mounted in a housing which was equipped with an aperture and shutter.

(3) The Reference Beam. The radiation absorbed by the solution is measured by comparison of the intensities of the radiation striking the phototube from the beam just described and from a beam which travels an identical path except for the contents of the cell (solvent rather than solution). The second beam originates as the reflected portion of the radiation which strikes the first quartz plate beyond the collecting lens, cf. Figure 3. The reflected fraction is again reflected by an aluminum front surfaced mirror placed at 45° to the direction of the beam and 10 cm. from the quartz plate. A Beckman spectrophotometer cell with a path length of 1.00 cm. and containing solvent is placed in the path of the beam slightly in front of the focal point of the beam. The solvent cell is mounted in the optical path in a manner similar to that described above for the solution cell. The solvent beam is divided by the quartz plate in front of the phototube into a reflected portion and a transmitted fraction which strikes the phototube.

(4) The Chopper. A semicircular chopper with a period of about five minutes was placed in a plane perpendicular to the direction of the solvent and solution beams and between solvent and solution cells and the plate and mirror at C and B to alternately mask the solvent and solution beams from the detector.

All components were rigidly mounted on optical benches, which in turn were bolted to one another forming a rigid matrix. The apparatus

was covered with a box which had been painted with a flat black paint on both the exterior and interior sides.

(5) Principle of Operation of the Photometer. It is apparent that the path of the solution beam, ABCD, is equivalent to that of the solvent beam, AECD, with the exception that the latter beam traverses a cell containing solvent only, while the solution beam traverses a cell containing solution. Therefore the difference between the amounts of radiation striking the detector from the two beams is a measure of the amount of radiation absorbed by the solution.

The signal from the phototube is amplified and fed continuously to a recorder (the electrical components are described more fully in a succeeding paragraph). The recorder pattern produced by the alternate signals from the solvent and solution beams is shown in Figure 5. The difference between the scale deflection produced by the reference beam and that of the solvent beam at any given instant is a measure of the rate that radiation is being absorbed; the area between the curves connecting the individual deflections provides an integration in time and is a measure of the amount of radiation absorbed during a given interval of time. In order to obtain an absolute measure of the radiation absorbed, it is necessary to relate the area between the curves to an absolute amount of radiation; this was achieved by calibration with a chemical actinometer as described in the next section. Two thicknesses of Monel metal wire screen, 40 mesh, were placed directly in front of the detector to reduce the intensity of the beam striking the detector; this will also be discussed further in the next section.

Figure 5

Actinometer Recorder Pattern

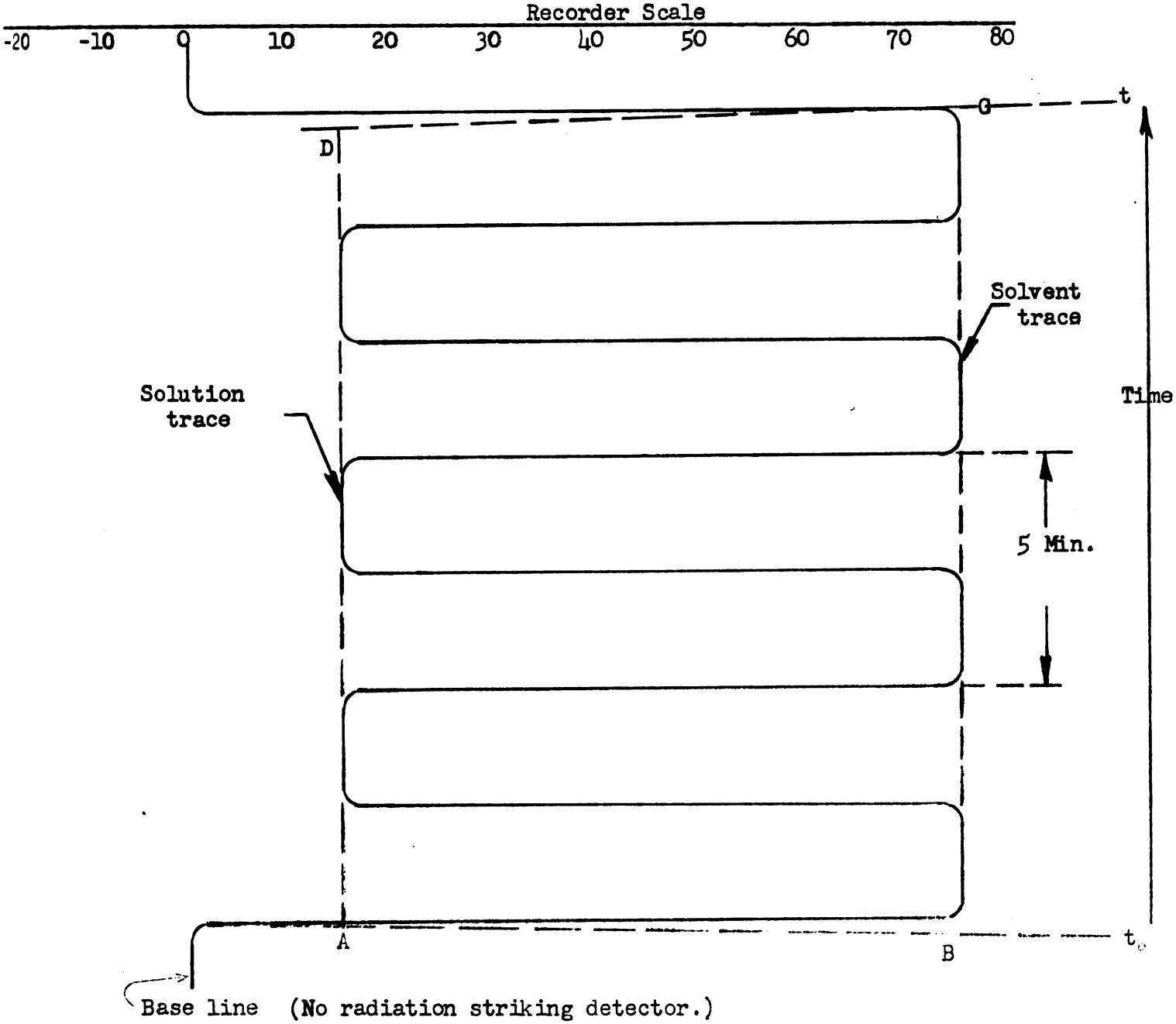

Area ABCD is a measure of the radiation absorbed by the solution during the interval $t-t_o$.

——— Actual trace of the recorder.
- - - - Interpolated trace.

(6) The Detector, Amplifier, and Recorder. The detector, amplifier, and recorder systems were assembled from components of The Farrand Electron Multiplier Photometer and the Leeds and Northrup Electro-Chemograph. The former consisted of a photomultiplier tube (1P28) and a power supply of 30 batteries of 30 volts each. The components of the Electro-Chemograph that were utilized were a Leeds and Northrup No. 7673 Thermionic Amplifier, the Polarizing Unit, and a Leeds and Northrup Micromax Recorder, Model S 40000 Series. The assembly of the components is shown schematically in Figure 6. The output of the photomultiplier system is passed on to the thermionic amplifier to amplify the current in order that it may be utilized in the measuring circuit of the recorder. The measuring circuit consists of a potentiometer which is automatically balanced by means of a mechanically operated slidewire which is calibrated for the range -40 to +160 millivolts. The recorder scale is divided into 100 equal divisions which cover the ranges -20 to 0 to +80. This arrangement provided for a current reversal which was useful for polarographic determinations. For this work the circuitry was arranged to employ the range 0 to +80. A portion of the circuitry of the Polarizer Unit was utilized to facilitate use of the recorder without further modification. The circuitry is shown in detail in Figure 7, and the details of operation of the electrical components are presented in the next section.

The apparatus was employed to obtain a plot of recorder scale deflection vs. wave length for the mercury arc used in the irradiation studies, cf. Figure 8. The slit width of the monochromator was set at 1.00 mm. for this determination.

Figure 6

Irradiation Apparatus for Kinetic Studies Schematic Representation of Assembly of Electrical Components

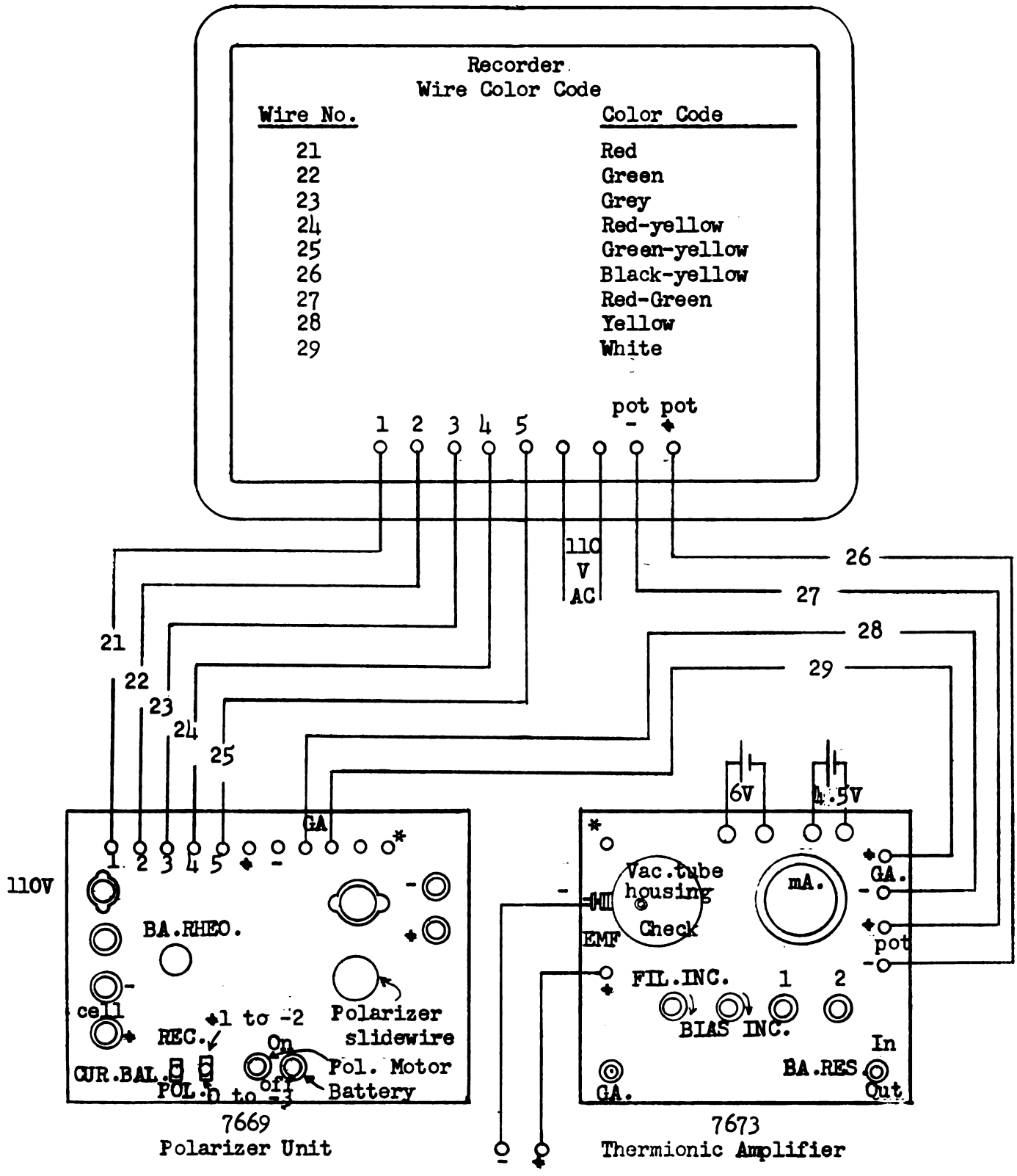

Figure 7

Irradiation Apparatus for Kinetic Studies--Electrical Circuitry

(cf. following page for legend)

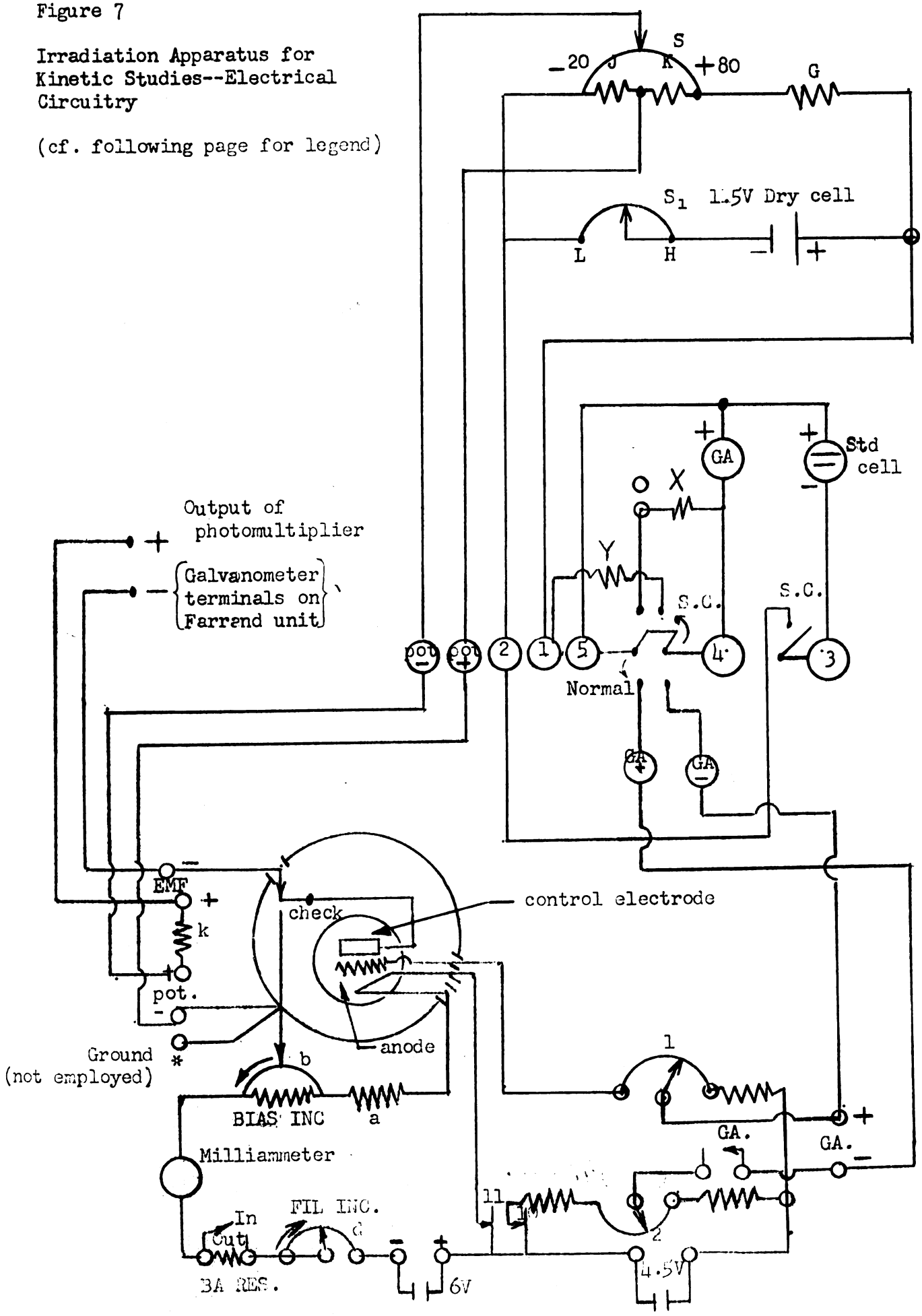

Figure 7

Data and Comments

G ✦ S (shunted) 101.9 Ω

J 0.2 (J ✦ K)

K 0.8 (J ✦ K)

X 15000 Ω

Y 20000 Ω

S (shunted) 40 Ω

S_1 75 Ω

S. C. - Position obtained with Curr. Bal. Switch in Rec. position

Amplifier

RH-507 Vacuum tube ("Inverted Triode")

Slidewires 1 and 2 - Coarse and fine adjustment for electrical zero of amplifier

a 10 Ω

b 40 Ω

c 15 Ω

BA RES. 20 Ω } Adjust filament current

k 5 Meg Ω

Figure 8

Ultraviolet Emission of Medium Pressure
Mercury Lamp - Slit Width = 1.00 mm.

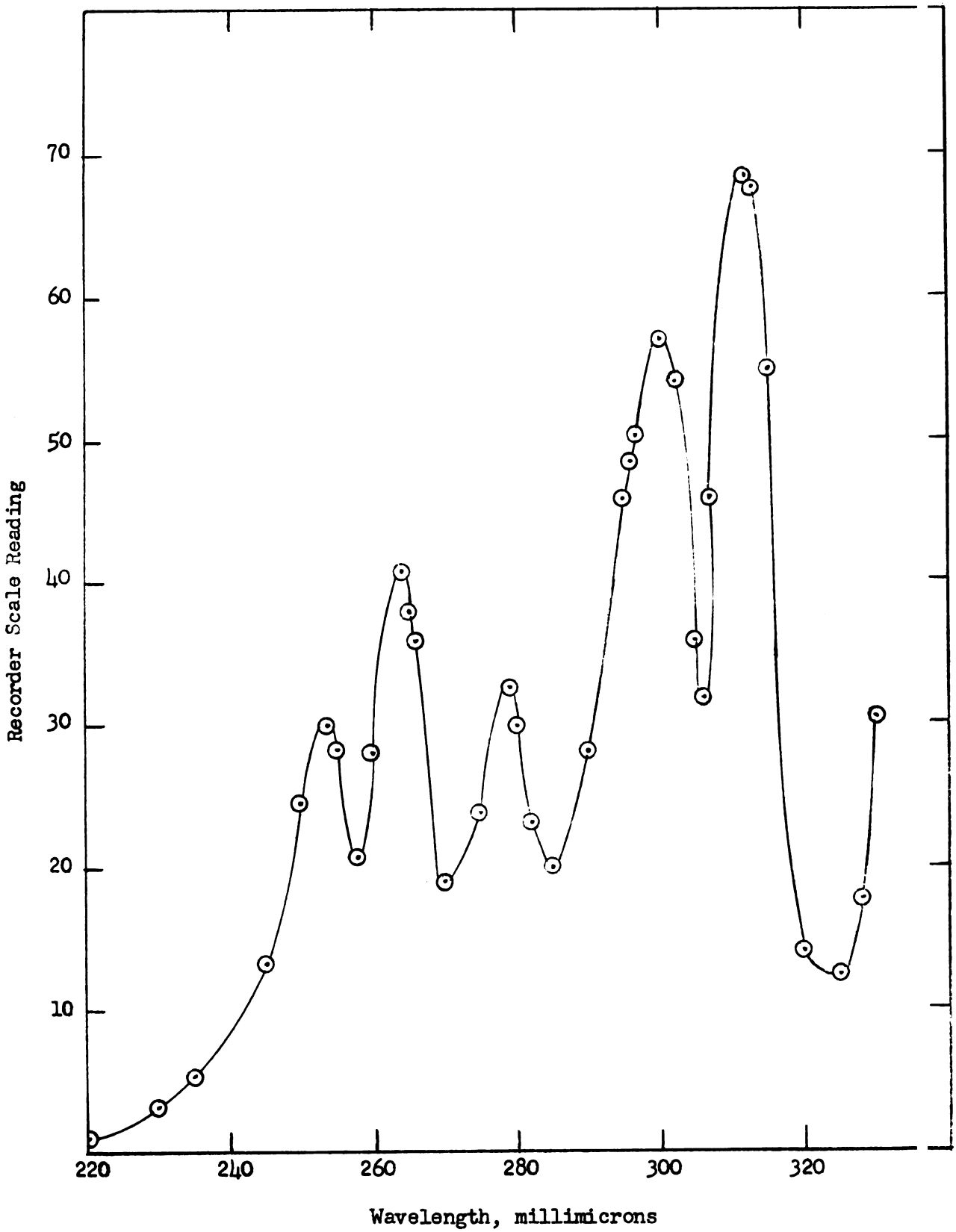

(7) Detector, Amplifier, and Recorder Operating Procedure. Refer to Figures 6 and 7 for the following discussion.

(a) On the amplifier: BA. RES. switch is snapped to the IN position and the check is pressed and locked in the down position. The latter operation brings the control electrode to the potential of its housing. BIAS INC. knob is turned in clockwise direction as far as it will go. The FIL. INC. knob is turned a slight distance in clockwise direction to snap switches "10" and "11" to the closed position. The instrument is allowed to warm up for about 30 minutes and then the FIL. INC. knob is adjusted until the milliammeter indicates 60 milliamperes.

(b) The current in the recorder-potentiometer circuit is standardized by holding the CUR. BAL. switch on the Polarizer Unit in REC. position and adjusting the rheostat S, until the galvanometer balances.

(c) The CUR. BAL. switch is placed in the normal position and the galvanometer key is depressed and locked on the amplifier. Knobs 1 and 2 on the amplifier unit are adjusted until the galvanometer is balanced. Since the check key is pressed down, the control electrode is at the potential of the housing; thus this procedure adjusts the electrical zero of the thermionic amplifier.

(d) The shutter on the phototube aperture is closed and the check key on the amplifier is released. The indicator on the recorder should rest at zero except for a small potential due to the dark current in the phototube. In general, adjustments for the

dark current were not necessary, since the indicator always came to rest within 1% of maximum scale deflection of the zero. In addition, the quantity measured in this work was the difference between two scale deflections, so that the position of the zero was not important. However, a dark current adjustment procedure was provided in the Farrand unit, and the adjustment was made at the beginning of the irradiation runs at a given wave length.

(e) The amount of scale deflection was controlled by the sensitivity dials on the Farrand unit. There were rheostats in the photomultiplier circuit which controlled the fraction of the total output of the tube which was fed to the external circuits. These dials were adjusted so that a convenient scale deflection was obtained with the radiation of a given wave length with distilled water in the solvent and solution beams. These settings were not disturbed during the irradiation work at a given wave length.

(f) The current in the potentiometer circuit was adjusted periodically during an irradiation run as described in (b). In addition, the electrical zero of the amplifier was also periodically adjusted as in (c).

2. Calibration of the Photometer

a. Principle of the Actinometric Procedure

In order to calibrate the photometer assembly, a photochemical reaction of known quantum yield is utilized. The amount of radiation

absorbed during a given interval of irradiation is determined from the extent of reaction and the quantum yield. The area on the recorder chart between the solvent and solution curves corresponding to the given interval of irradiation can be related to the amount of radiation absorbed, yielding essentially a value for the number of quanta per unit area on the recorder diagram. This value could be employed to compute the amount of radiation absorbed during a given interval of irradiation of another solution. Such a procedure would be valid only if the scale deflection on the recorder were directly proportional to the number of quanta striking the detector. However, this situation did not prevail. For example, a value for the number of quanta per unit area obtained from an area between scale deflections of 60 and 40 was larger than a value obtained from an area between scale deflections of 60 and 10. The varying scale deflections were obtained by altering the concentration of the actinometer compound; the scale deflection from the solvent beam remained fairly constant. It was possible to attribute this behavior largely to a non-linearity in the response of the photomultiplier tube with respect to the intensity of the radiation reaching the detector. The variance of the number of quanta per unit area with scale deflection was treated empirically by a simple calibration; a plot was made of quanta/unit area vs. the quantity, 1/2(solvent deflection + solution deflection). An approximate linear relation was obtained.

b. Causes of Non-Linearity of the Photometer

It was necessary to determine the major cause of non-linearity in order to establish the validity of the results. Several factors could contribute to the observed effect: non-linear response of the phototube with respect to incident intensity, non-linear amplification of the output of the

phototube, and effects due to the extent of monochromaticity of the radiation. It was the latter factor that was of greatest concern, since the first two factors could be treated by simple calibration methods without loss of validity of the results. The extent of monochromaticity contributes to the observed non-linear effect through the combined effects of dependence of phototube response upon wave length of the radiation and the shape of the absorption spectrum of the solution being irradiated. Since finite slit widths are employed, a band of radiation of varying wave length with the nominal wave length in the center of the band is obtained. The width of this band with respect to wave length is dependent on the slit width and the dispersion of the monochromator. The output of the phototube is represented by the value of a function which consists of the product of the slit function (the intensity as a function of wave length), the response of the phototube with respect to wave length, and the absorption spectrum of the material being irradiated; the value of the integral of this function over the wave length limits of the band represents the output of the phototube. It was necessary to establish that the non-linear effect observed (variation of the quanta absorbed per unit area with scale deflection) was not a result of a variation of the value of this integral with changes of any type in the absorption spectrum of the solution being irradiated; the absorption curve of the actinometer compound is altered by a change in concentration. The above condition must prevail if the calibration is to be employed in the determination of the number of quanta absorbed by a solution other than the actinometer compound; in such a case the general shape of the absorption curve would

be basically different in addition to differences caused by changes in concentration.

The maximum slit width employed in this study was 2.0 mm.; since the dispersion of the monochromator is 66A°/mm., the range of wave lengths present in the irradiating beam is the nominal wave length ± 132 A°, or a width of 264 A°. Values of the relative intensity of the output of the phototube were obtained from the spectral response curve for the 1P28 photomultiplier tube, and the values in the range of interest, 2300-3500 A°, are tabulated in Table II.

TABLE II

SPECTRAL RESPONSE OF 1P28 PHOTOMULTIPLIER TUBE

Wave Length, A°	Relative Response
2300	72.8
2400	74.2
2500	75.3
2600	76.2
2700	77.5
2800	79.5
2900	84.0
3000	89.0
3100	93.5
3200	96.0
3400	99.8
3500	100.0

Irradiation at a nominal wave length of 2804 A° was carried out with a slit width of 2.0 mm., which was the largest slit width employed in

this study. The range of wave lengths present would be 2672-2936 A^{o}; the amount of radiation from a given wave length would decrease on either side of the nominal wave length to zero at the limits. The range of spectral response over this wave length region is approximately 77-86% (on relative intensity scale). An estimate of the maximum possible effect on the value of the calibration ratio--quanta absorbed per unit area--as a result of variation of spectral response with wave length is about ten percent. However this effect is certainly much less than 10%, since this figure is based upon a uniform intensity distribution throughout the entire pass band of the monochromator.

c. Experimental Verification of Non-Linearity of Phototube Response

Although the above treatment of the spectral response data affords some justification for the belief that the non-linear effect is not due primarily to a variation of the value of the integral that determines the output of the phototube, more direct experimental evidence was deemed necessary. It was possible to attribute the non-linear effect on the calibration directly to a non-linear response of the phototube with respect to intensity of the radiation, by the following procedure. The scale deflections (on the recorder) of materials whose transmittancy of radiation was independent of wave length were determined by placing the materials in the solvent position of the irradiation apparatus. The materials utilized were air, 95% ethanol, a Monel metal 40 mesh wire screen, and a 16 mesh Nichrome wire screen of double thickness. To further insure wave length independence, the wire screens were coated with a layer of carbon black. In addition to the determination of the recorder scale

deflection, the output of the phototube was measured on a galvanometer which intercepted the signal which was fed to the amplifier. The percent transmission of the materials with air as a reference was also determined in a Beckman Model DU Spectrophotometer. These latter values were compared with percent transmission values obtained from the galvanometer and recorder scale deflections. The results which were obtained at 2804 A^{o} with a slit width of 2.0 mm. in the irradiation apparatus and 0.68 mm. in the DU Spectrophotometer are summarized in Table III.

TABLE III

NON-LINEARITY OF PHOTOMULTIPLIER RESPONSE

Sample	Scale Deflection		Percent Transmission, Air as Reference		
	Galvanometer	Recorder	DU	Galvanometer	Recorder
Air	4.44	57.3	--	--	--
95% Ethanol	4.24	54.1	88.2	95.5	94.4
Monel Screen[a]	2.26	28.3	27.2	50.9	49.4
Nichrome Screen[b]	1.46	18.0	13.0	32.9	31.3

[a] 40 mesh coated with carbon black.
[b] 16 mesh coated with carbon black.

The close agreement in the values of percent transmission calculated from the galvanometer and recorder scale deflections prove that linearity is not affected by the amplification. Since the transmissivities of the wire screens and the ethanol were shown to be wave length independent in this region, the differences in percent transmission determined by the spectrophotometer and the galvanometer or recorder scale deflections can only be due to a non-linear response of the photomultiplier tube with

respect to intensity of radiation. Further confirmation for this conclusion was afforded by the observation that when the intensity incident on the detector is reduced by placing a wire screen directly in front of the phototube, the ratio of quanta absorbed per unit area on the recorder diagram becomes almost independent of scale deflection. This observation will be discussed further in a later section.

d. Actinometer Compounds

(1) Uranyl Oxalate. An attempt was made to utilize the well-known uranyl oxalate photolysis as a chemical actinometer. A solution containing a uranyl salt such as the sulfate or nitrate together with oxalic acid is subjected to radiation, and the amount of unreacted oxalic acid is determined by titration with potassium permanganate. In order to circumvent the problems associated with the purification of uranyl sulfate or uranyl nitrate, Forbes and Heidt (13) have introduced the use of uranyl oxalate directly. The uranyl oxalate is prepared simply by mixing hot solutions of uranyl nitrate and oxalic acid, filtering the mixture, and allowing the filtrate to stand in an ice bath. The crystals are dried first in a vacuum desiccator and then at about 100° for several hours. However, the uranyl oxalate actinometer was not suitable for the comparatively low levels of radiation employed in this study.

(2) Malachite Green Leucocyanide Preparation. Since the photolysis of malachite green leucocyanide, p,p' didimethylaminotriphenylacetonitrile, may be followed spectrophotometrically, the reaction has been utilized as a chemical actinometer when the level of radiation has been low. The original work on the determination of the quantum yield of this reaction

was performed by Harris et al. (17). The results obtained by Harris were confirmed by Calvert and Rechen (7) who also developed a more convenient method of preparation for the compound; this method was employed to prepare the malachite green leucocyanide that was utilized as a chemical actinometer in this study.

A cold, saturated, aqueous solution containing 6 grams of potassium cyanide was added to a filtered 1% aqueous solution containing 9.3 grams of malachite green oxalate. In this work malachite green was used, but oxalic acid was added so that the solution was equivalent to that employed by Calvert and Rechen. The precipitate was filtered and washed with distilled water, and dissolved in cold 1% hydrochloric acid. The solution was stirred for one hour and carefully neutralized with cold 1% aqueous ammonia. The precipitate was filtered, washed with distilled water, and air dried.

The crude product was dissolved in 300 ml. of acetone, and the solution was filtered; 150 ml. of methanol were added, and the solution was acidified with several drops of acetic acid. About 350 ml. of solvent were removed rapidly by distillation; the remainder was cooled, and the crystals were filtered and washed with 10 ml. of cold methanol. The filtrate could be saved and more product recovered.

Reduced illumination (red safe-light) was employed in all subsequent treatment of the product. About 2 g. of the crystals were dissolved in 100 ml. of a 50% methanol-ethylacetate solution; 30 ml. of methanol, 1 ml. of acetone, and several drops of glacial acetic acid were added to the solution. About 105 ml. of the solvent mixture were removed by

rapid distillation; the remaining solution was cooled and the crystals were filtered and washed with a small amount of methanol. The filtrate may be saved for further recovery of product.

The previous step was repeated five times; the purified product had a melting point of 177-178° C. (Calvert and Rechen reported a melting point of 176-177° C.). The product was further characterized by its absorption spectrum in 95% ethanol and by its behavior on photolysis. The ultraviolet absorption spectrum determined on a Beckman DK-2 Spectrophotometer is shown in Figure 9. Ultraviolet absorption data were also determined on a Beckman DU Spectrophotometer in the range 2650-2750 A° with a slit width of 0.62 mm. The latter data indicated a maximum at 2725 A° with a molar absorptivity of 42,400 which was in agreement with data obtained from plots reported by Harris et al. (17). From the plots, the maximum was estimated to be in the range 2670-2700 A° with a molar absorptivity of 40,800.

(3) Photolysis of Malachite Green Leucocyanide. The ultraviolet irradiation of solutions of malachite green leucocyanide--which are colorless--yield intensely colored blue solutions; the colored ion formed is probably a carbonium ion with the indicated structural formula.

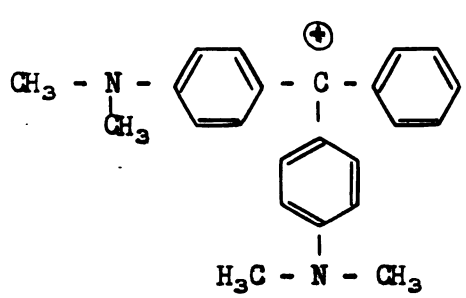

Figure 9

Ultraviolet Absorption Spectrum of Malachite Green Leucocyanide in 95% Ethanol

(Concentration 9.902×10^{-6} moles $liter^{-1}$
Determination on Beckman DK-2 spectrophotometer
Reference 95% Ethanol)

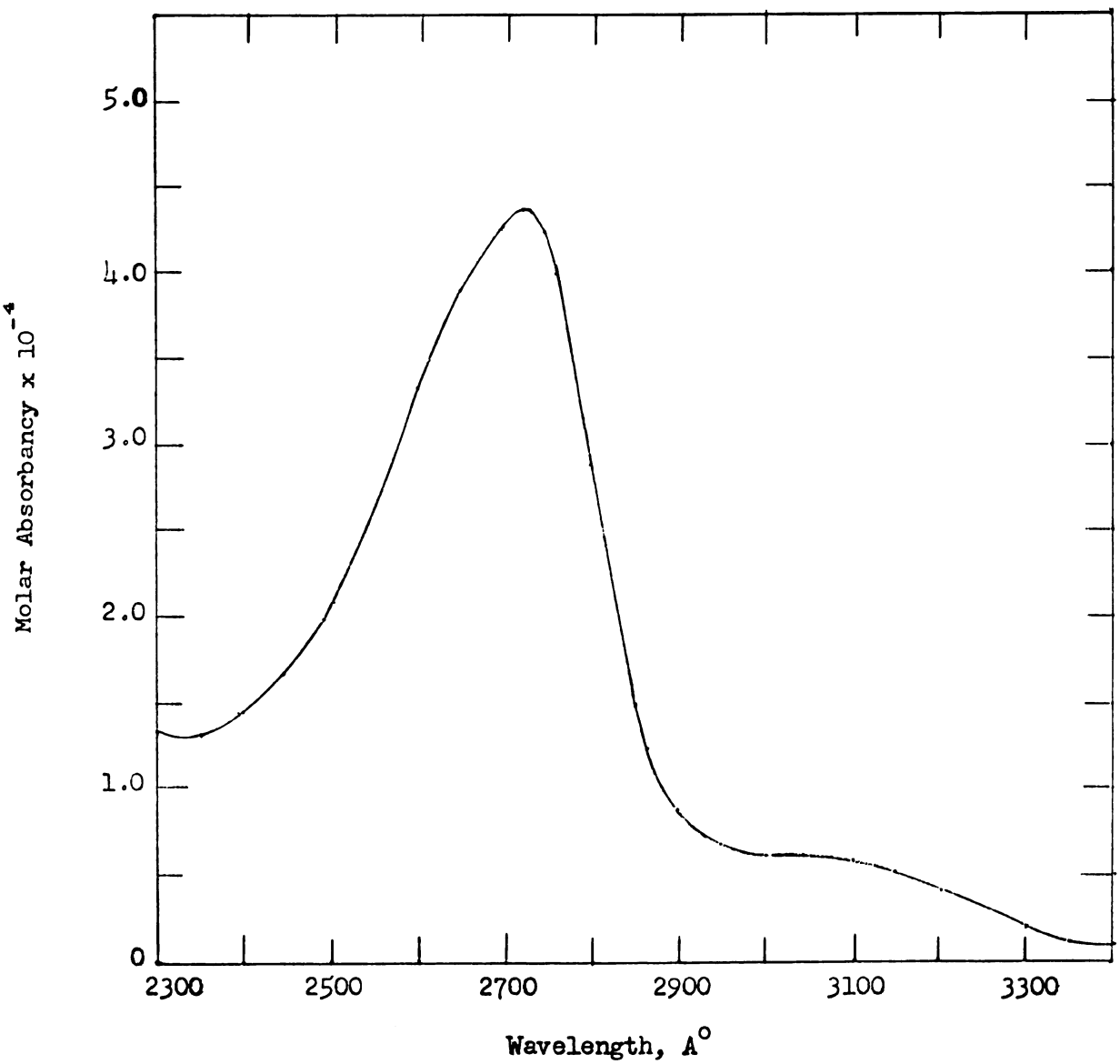

The irradiations have been carried out in 95% ethanol by Harris et al. (17) and in absolute ethanol by Calvert and Rechen (7) with similar results. However, in both cases, the color fades unless hydrochloric acid is added. The formation of the colored ion forms the basis for the spectrophotometric determination of the extent of the photolysis and, consequently, the determination of the number of quanta absorbed. The quantum yield of the photolysis is 1.00 and is independent of wave length of irradiation in the range characterized, i.e., 2480-3300 A° (7). Calvert and Rechen claim that these results are valid with the stipulation that the light intensities are not more than 3×10^{13} quanta/sec incident on an area of about 0.3 sq. cm.

A calibration curve of concentration vs. absorption was prepared by photolysis of solutions of known concentration of malachite green leucocyanide in 95% ethanol (acidified with hydrochloric acid), cf. Figure 10.

The procedure employed for the determination of the calibration curve was essentially that of Calvert and Rechen (7). Immediately prior to irradiation, 0.16 ml. of 0.3 M. hydrochloric acid were added to 3.0 ml. of a solution of malachite green leucocyanide in a Beckman quartz spectrophotometer cell with a path length of 1.00 cm. The solution was irradiated in the apparatus described in the preceding section employing a wave length of 2804 A° and a slit width of 2.0 mm. The irradiation was interrupted periodically to determine the absorbancy of the irradiated solution at 6200 A° with a slit width of 0.110 mm. in a Beckman DU Spectrophotometer. The reference cell solution employed for this determination was 95%

Figure 10

Calibration Curve--Absorbancy of Irradiated Malachite Green Leucocyanide in 95% Ethanol (Acidified)

(Reference 95% Ethanol (Acidified), Wavelength 6200 A°, Slit Width 0.110 mm.)

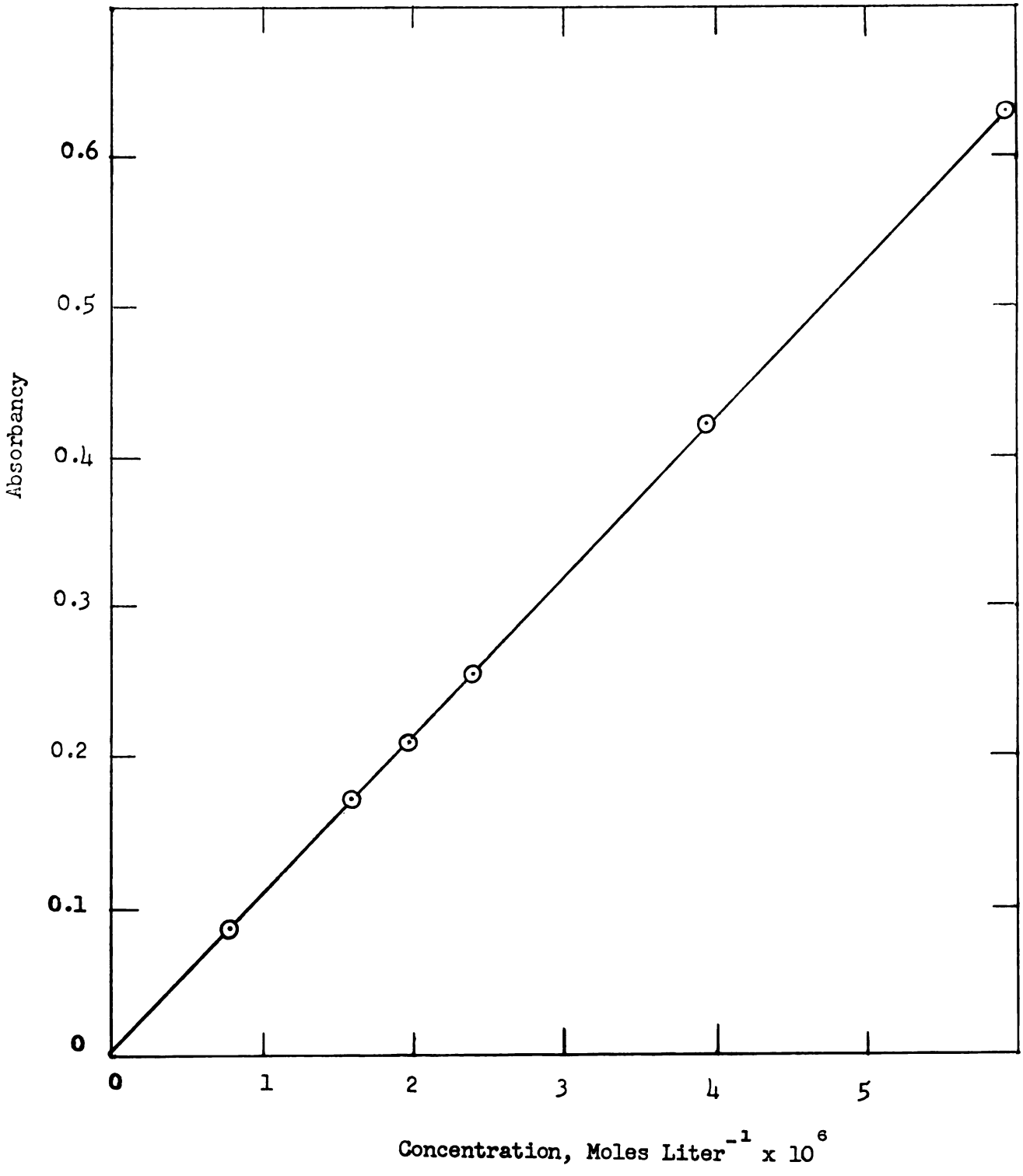

ethanol acidified with hydrochloric acid. Although Calvert and Rechen reported the maximum of the band to be at 6200 A^{o}, it actually occurred between 6150 and 6200 A^{o}. Since it was more convenient to employ a wave length that coincides with a calibrated scale division rather than interpolate between 6150 and 6200 A^{o}, the value of the absorbancy at 6200 A^{o} was utilized in this study. Irradiation was continued until the absorbancy of the irradiated solution was constant. This procedure was repeated for solutions of the actinometer compound at several concentrations. Additional values for the calibration curve were obtained by dilution of the irradiated solutions. The results are summarized in Table IV.

The average value for the molar absorptivity is $(10.67 \pm .09) \times 10^{4}$; the limits are the standard deviation of the data. It can be concluded that, within the limits of experimental error, the Beer-Lambert Law is obeyed. There is some discrepancy between the average value for the molar absorptivity as reported by Calvert and Rechen--9.49×10^{4}--and the value obtained in this work. However, the former value is based on data obtained from solutions of concentrations of 10^{-6} molar or less.

It is probable that the extent of complete photolysis of malachite green leucocyanide is less for the solutions at lower concentration and the non-photolyzed portion is a larger fraction of the total than those conducted at higher concentration. This explanation could account for the discrepancy. It is assumed that the actinometer compound has been completely converted to the irradiated compound in the calculation of the molar absorptivity on the basis that the absorbancy of the irradiated solution remains constant. However, at very dilute concentrations only

TABLE IV

ABSORBANCY OF IRRADIATED MALACHITE GREEN LEUCOCYANIDE IN 95% ETHANOL

Wave Length: 6200 A^{o}
Slit Width: 0.110 mm.
Reference: Acidified 95% Ethanol

Concentration Moles $Liter^{-1}$ x 10^{6}	Absorbancy	Molar Absorptivity x 10^{-4}
0.7920	0.085*	10.73
1.584	0.171*	10.80
1.980	0.209	10.56
2.376	0.255*	10.73
3.961	0.422	10.65
5.941	0.629	10.59
5.941	0.631	10.62

*Obtained by dilution.

a slight fraction of the radiation is absorbed and a large period of time of irradiation would be required to produce a detectable change in absorbancy. Essentially, the argument is made that photolysis is more complete in solutions of higher concentration if the criterion for complete photolysis is the constancy of absorbancy with irradiation time.

For calibration purposes a least squares fit of the absorbancy data was made employing the linear relation

$$A = A_o + \epsilon Cl$$

where

A = absorbancy

A_o = constant

ϵ = molar absorptivity

C = concentration, moles liter $^{-1}$

l = path length (1.00 cm.).

The constants determined by this treatment were a value of 0.002 for A_o and a value of 10.576×10^4 for ϵ; these values were employed to calculate the concentration of converted malachite green leucocyanide in the actinometric determinations.

e. Calibration Results

The value of the ratio of quanta absorbed per unit area of recorder pattern was determined as a function of average scale deflection, i.e., 1/2 (solvent scale deflection plus solution scale deflection) at the three irradiating wave lengths employed in this study--2537, 2804, and 2967 A°.

The irradiation procedure was identical to that employed for the determination of the absorbancy vs. concentration curve for irradiated malachite green leucocyanide. However, only a partial photolysis of the actinometer compound was effected; a cell containing 95% ethanol acidified with hydrochloric acid was placed in the solvent beam, and a recorder trace of solvent and solution beams was obtained while the irradiation was in progress. Prior to the calibration procedure, distilled water was placed in the cells in both the solvent and solution beams, and the mirrors and plates were adjusted slightly so that the radiation striking the detector from either beam yielded an equivalent scale deflection. The two beams were equivalent to about 1%; the apparatus was not disturbed during all irradiations at a given wave length, and the equivalence of the beams was checked periodically.

In order to obtain measurable areas between the solvent and solution recorder traces, it was necessary to convert appreciable amounts of the actinometer compound to the irradiation product, which also absorbs in the ultraviolet; an inner filter effect was obtained. In previous utilization of this actinometer compound less than one percent was converted, and it was possible to ignore the inner filter effect. A correction was made for the inner filter effect by obtaining the value of the ratio of quanta absorbed per unit area as a function of percent conversion and extrapolating to zero percent conversion.

The irradiation of a solution of malachite green leucocyanide at a given concentration was periodically interrupted and its absorbancy at 6200 A^{o} was determined in the Beckman DU Spectrophotometer with a slit width of 0.110 mm. The concentration of irradiated compound was determined from the absorbancy measurement and the calibration data of the previous section; a value of quanta absorbed per unit area was calculated--employing a value of 1.00 for the quantum yield. The areas between the solvent and solution curves were determined by means of the trapezoidal rule. This procedure yielded a series of values for quanta absorbed per unit area and percent conversion from which a linear extrapolation could be made to zero percent conversion by the linear least squares procedure. These data are summarized in Appendix I.

For a given irradiating wave length, the value of the ratio of quanta absorbed per unit area (the value extrapolated to zero percent conversion) was plotted as a function of the average scale deflection of solvent and solution beams. The latter was measured at the midpoint of the interval

of irradiation for which the ratio of quanta per unit area was determined. This procedure was adopted since there was a slight variance in the value of the scale readings as the irradiation progressed. The variance was due to a change in absorption as the actinometer compound was converted and to a slight change in incident intensity as the result of changes in the mercury arc. Since the extrapolated value of the ratio-quanta absorbed per unit area--was determined from a number of irradiation intervals whose average scale deflection of the solvent and solution beams varied slightly from interval to interval, an average value of the scale deflections of the various intervals was employed in the plots. The relation between the average scale deflection and quanta absorbed per unit area was linear within the limits of experimental error, cf. Figure 11. The data were fitted by the method of least squares to the linear relationship

$$\frac{q}{a} = \mu + \gamma T_{\frac{1}{2}}$$

where

$\frac{q}{a}$ = quanta absorbed per unit area on recorder trace

μ = constant

γ = constant

$T_{\frac{1}{2}}$ = average value of scale deflection.

The detailed data are presented in Appendix I and a summary of the results is tabulated in Table V.

Figure 11

Calibration of Photometer--2967 A°

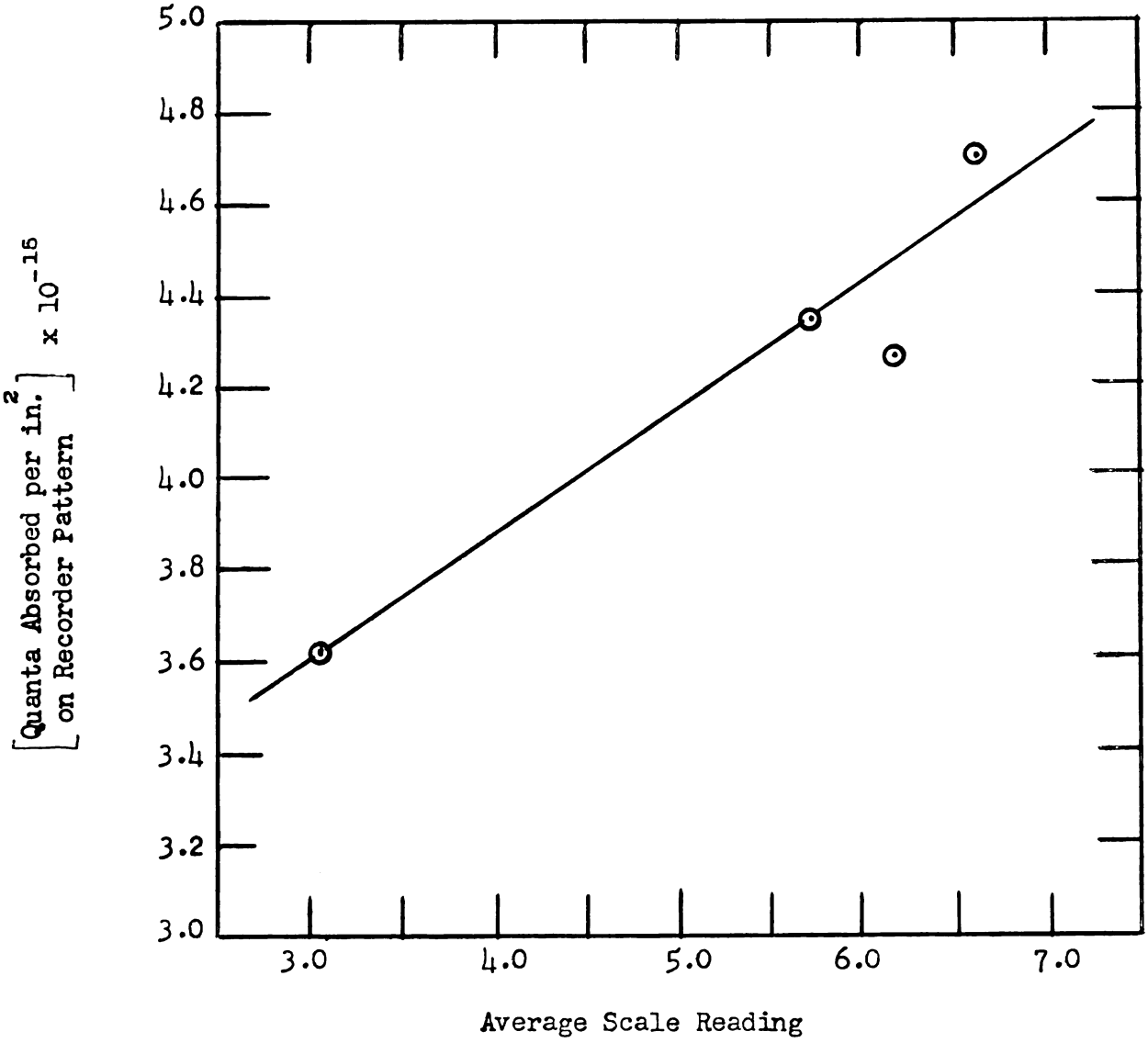

TABLE V

CALIBRATION OF DETECTOR ASSEMBLY

Wave Length A°	Slit Width mm.	$\mu \times 10^{-15}$ quanta $in.^{-2}$	$\gamma \times 10^{-15}$ quanta $in.^{-2}$
2537	1.50	1.27	0.0523
2804	2.00	-1.98	1.54
2967	1.50	2.80	0.268

The order of intensity of radiation striking the photomultiplier tube with respect to wave length is 2804 > 2967 > 2537 A°. This order is the result of the intensity of the source with respect to wave length, (cf., Figure 8), the slit widths, and the fact that two layers of 40 mesh Monel metal screen were placed immediately in front of the detector for the irradiation at 2967 and 2537 A°. The order of deviation--with respect to wave length of irradiation--of the constancy of $\frac{q}{a}$ for a variation of $T_{\frac{1}{2}}$ is also 2804 > 2967 > 2537 A° as evidenced by the value of the slope, γ. This is further proof that the deviation from a constant value for $\frac{q}{a}$ at a particular wave length is due to a non-linear response of the detector with respect to intensity of the radiation striking the detector.

The data of Table V were utilized to calculate the total quanta absorbed during an interval of irradiation of the ergosterol solutions from the area between the solution and solvent curves recorded during the irradiation.

3. Irradiation Procedure

a. Preparation of Solutions

Stock solutions of ergosterol in isopropyl alcohol and in n-hexane were prepared from a sample of purified ergosterol which was generously furnished by W. H. C. Shaw of Glaxo Laboratories, Ltd., Greenford, England. The stock solutions were prepared from about ten milligrams of ergosterol (weighed to 0.1 milligram) diluted to 100 ml. with the appropriate solvent which had been flushed with nitrogen for at least one hour immediately before preparation of the solution. Aliquots of the stock solutions were diluted with several solvents to produce a series of solutions of varying viscosity. The solutions were prepared as follows:

(a) 5 ml. of the isopropyl alcohol stock solution were diluted to 25 ml. with isopropyl alcohol.

(b) 5 ml. of isopropyl alcohol stock solution plus 15 ml. isopropyl alcohol were diluted to 25 ml. with glycerol; designated as 20% glycerol.

(c) 5 ml. of n-hexane stock solution were diluted to 25 ml. with n-hexane.

(d) 5 ml. of n-hexane stock solution plus 15 ml. of n-hexane were diluted to 25 ml. with mineral oil; designated as 20% mineral oil.

(e) 5 ml. of n-hexane stock solution plus 10 ml. of n-hexane were diluted to 25 ml. with mineral oil; designated as 40% mineral oil.

b. The Irradiation Process

Three ml. of a given solution were placed in the Beckman spectrophotometer cell and the cell was positioned in the irradiation apparatus.

A cell containing solvent was placed in the other beam of the apparatus. Stirring was effected during irradiation by the magnetic stirring device discussed in a previous section. Irradiations were conducted in an air-conditioned room which was maintained at about 22° C. The mercury arc was turned on, but a shutter was placed in the beam in front of the monochromator to allow the intensity of the beam to stabilize. The shutter was then removed and the irradiation of the cell was started. The light intensities transmitted by the solvent and solution cells were recorded by means of the photometer arrangement described in an earlier section. The irradiation was interrupted periodically for spectrophotometric analysis of the solution.

c. Spectrophotometric Analysis of the Samples

The ultraviolet absorption spectra of the irradiated materials were determined in the range 3400-2200 A° on the Beckman DK-2 spectrophotometer; three spectrophotometer cells were employed for the determination of the spectra. Two cells containing solvent were utilized to balance the two beams and to determine the zero absorption line. The cell in the sample beam of the spectrophotometer was replaced with the cell containing the irradiated solution, and the spectrum was determined. A small correction (less than .01 absorbancy unit) was applied to the spectrum to correct for the difference in transmission of the cells used in the solvent beam. A further correction was made for the error in calibration of the chart paper; the wave length on the instrument indicator dial differed (generally less than 10 A°) from the value on the chart. A corrected calibration scale was obtained by stopping the instrument when the wave

length indicator recorded the desired wave lengths and marking this position on the chart paper. This scale was aligned with a reference wave length on each spectral determination and the desired wave lengths were marked off on the spectrum. The spectrophotometric analysis yielded the concentrations of the components of the mixture as a function of time of irradiation.

d. Summary of Irradiation Conditions Employed

The conditions of irradiation were as follows:

Wave Length of Irradiation A°	Slit Width mm.
2537	1.50
2804	2.00
2967	1.50

The solvents employed are summarized below:

2537 A° - one run with each of the solvents, i.e., n-hexane, 20% mineral oil, isopropyl alcohol, and 20% glycerol.

2804 A° - same as 2537 A°

2967 A° - same as 2537 A° with the addition of a duplicate run with n-hexane and an additional run with 40% mineral oil.

4. Materials and Purification Procedures

Ergosterol, Lumisterol, Calciferol. Purified samples of ergosterol, lumisterol, and calciferol--which were generously furnished by W. H. C. Shaw of Glaxo Laboratories, Ltd., Greenford, England--were utilized for the kinetic studies and for the verification of the analytical procedure.

Isopropyl Alchol. Commercial grades of alcohol were purified by shaking with sodium hydroxide, separating the aqueous layer and fractionally distilling the alcohol layer. The ultraviolet absorption spectra of the fractions were determined in the range 3400-2200 A^{o} in the Beckman DK-2 spectrophotometer employing distilled water as the reference. The suitable fractions were transparent to about 2500 A^{o} (greater than 95% transmission); a general absorption began at 2500 A^{o}, but the transmission was still larger than 80% at 2300 A^{o}. During the latter stages of the preparative work, Analytical Reagent Grade material was obtained from Mallinckrodt; this material was almost as transparent as the purified alcohol and was employed without further treatment for the preparative work. However, for the kinetic studies and the verification of the analytical procedure, it was also purified as described above.

Ethanol. A commercial grade of 95% ethanol was refluxed for several hours with 10 grams of silver nitrate and 1 gram of potassium hydroxide per liter of solvent; the liquid was decanted and fractionally distilled. The ultraviolet absorption spectra of the fractions were determined as described for isopropyl alcohol; the transparency in the ultraviolet was similar to that of isopropyl alcohol.

Glycerol. Mallinckrodt Analytical Reagent Grade glycerol was employed without further purification. In the region 2500-3400 A^{o}, the material exhibits a minimum transmittancy of 75% with distilled water as reference. A large fraction of the apparent absorption may be attributed to the difference in refractive indices of water and glycerol. Attempted vacuum distillation of this product was not successful, as the transmittancy of

the distilled material was lower than that of the untreated glycerol.

n-Hexane. A commercial grade of n-hexane was passed through an activated silica gel column with an internal diameter of 4.0 cm. and a height of 75 cm. A flow rate of about 2 ml. per minute was employed. The silica gel was obtained from The Davison Chemical Co., Baltimore, Md., and was designated as a desiccant (activated) commercial grade. The purified n-hexane was completely transparent up to 2500 A° where a general absorption started; the transmittancy decreased to about 75-85% transmission at 2300 A°. Distilled water was employed as a reference.

Mineral Oil. U.S.P. grade mineral oil was passed through a silica gel column with a diameter of 4.0 cm. and a height of 110 cm. Nitrogen was employed to apply a pressure of about 15 lbs. per sq. in (gauge); a flow rate of about 20 ml. per hour was achieved under these conditions. The ultraviolet absorption spectra of the fractions were determined employing distilled water as a reference. In the range 2500-3400 A°, the minimum percent transmission decreased from about 85% for the first fractions to about 70% for the later fractions. The fractions were combined and passed through another silica gel column with a diameter of 3.0 cm. and a height of 75 cm. A flow rate of about 20 ml. per hour was again achieved by applying pressure with nitrogen at a pressure of 15 lbs. per sq. in. (gauge). In the range 2500-3400 A°, the minimum transparency of the fractions varied from 95-90% transmission. A general absorption began at 2500 A° and the transmittancy decreased to 20-35% transmission at 2300 A°. The purified material did not fluoresce when subjected to ultraviolet radiation.

Miscellaneous Materials. Solvents and other materials employed were of C.P., Spectral Grade, or Reagent Grade purity, and were used without further treatment.

Stability of Irradiation Solvents. The solvents employed in the irradiation work were examined for stability to ultraviolet radiation by subjecting each of the solvents to radiation at 2804 A^{o} with a slit width of 2.00 mm. for periods of at least one hour. The ultraviolet absorption spectra of the solvents were not altered by this treatment.

Storage and Handling Procedures. The ergosterol, lumisterol, and calciferol which were received from W. H. C. Shaw in sealed glass ampules were stored in a small desiccator which was refrigerated at temperatures lower than -40^{o} C. The necks of the ampules were cut and material was withdrawn; nitrogen was passed through the ampule before sealing with a tightly fitting rubber serum bottle cap. The opened ampules were immediately placed in the desiccator and refrigerated.

Stock solutions of the materials in glass stoppered reagent bottles were stored in a large desiccator which was refrigerated at 5^{o} C.; the desiccator was flushed with nitrogen before sealing. Solutions of ergosterol and lumisterol were stable for a period of at least three months when stored under these conditions; the ultraviolet absorption spectra were employed as the criteria of stability. Calciferol did not exhibit this stability over the three month period; the absorbancy of the stored solution increased appreciably in the range 2200-2600 A^{o}.

Spectrophotometric determinations employed for verification of the analytical procedure were conducted on solutions which had been stored

under the above conditions for not more than several days. The stock solutions of ergosterol employed for the kinetic studies were stored under the above conditions; the ultraviolet absorption spectrum was always determined prior to each irradiation run. Dilutions for the kinetic runs were made immediately prior to the run and the diluted solutions were not stored.

5. Viscometry

The viscosities of the solvent and solvent mixtures were determined with Ostwald viscometers in a thermostated bath maintained at 25 ± 0.1° C. Absolute viscosity was calculated from the two parameter equation

$$\eta = Rdt - S\frac{d}{t}$$

where η = absolute viscosity in centipoise

d = density of the liquid in grams cm^{-3}

t = time of flow of liquid between calibrated marks of the viscometer

R, S = empirically determined constants.

Densities of the liquids were determined with pycnometers calibrated with distilled water. The constants, R and S, were determined empirically by utilization of liquids of known viscosity--i.e., distilled water and a water-glycerol mixture. The composition of the latter was determined from its specific gravity and the composition—specific gravity data of aqueous glycerol mixtures which have been reported by Bosart and Snoddy (3). The viscosity data employed for the determination of the empirical constants were those of Sheely (38).

TABLE OF CONTENTS

III. DISCUSSION OF PREPARATIVE WORK

A. General

The objectives of the preparative work were to obtain the components of the irradiation mixture, to obtain preliminary kinetic data to check the qualitative conclusions of Sharpe (37), and to acquire a familiarity with the experimental techniques that have been employed in the investigation of the photochemical isomerization of ergosterol. The components of the irradiation mixture were desired in order to directly verify the analytical curve fitting technique developed by Sternberg and Sharpe (37), and to obtain the ultraviolet absorption spectra of the components. It was believed that the results obtained from the analytical curve fitting technique could be improved by more reliable spectral data. Another objective of the preparative work was to obtain verification that there were no specific interactions among the components of the irradiation mixture and that the mixtures obtained obeyed the Beer-Lambert-Bouger Law.

While the preparative work was in progress, W. H. C. Shaw of Glaxo Laboratories, Ltd., furnished us with tabulated spectral data and with purified samples of ergosterol, lumisterol, calciferol, and precalciferol 3,5 dinitrobenzoate. The preparative work was discontinued upon receipt of these materials and data, since the other objectives of the preparative work had by that time been achieved. Up to the time of receipt of the materials, the preparative runs were directed towards the preparation of precalciferol in a pure state.

The results obtained by Sharpe (37) indicated that precalciferol should be most suitably prepared in hydroxylic solvents with irradiation at comparatively long wave lengths. Although the results of Sharpe were invalidated, with respect to quantitative interpretation, by the omission of precalciferol from the calculations, it was believed that the qualitative conclusions with respect to precalciferol formation were valid. These conclusions were also rationalized on the basis of the ultraviolet absorption spectra of the components of the irradiation mixture and on previously reported data. These data have been summarized by Havinga and Bots (18) in the following manner:

Wavelength of Irradiation, A°	Product Composition
> 2840	Calciferol + lumisterol
< 2840	Calciferol + large amount of tachysterol + small amount of lumisterol
< 2540	Larger amounts of tachysterol + smaller amounts of calciferol
> 2900	Reduced yields of calciferol

Although precalciferol is not listed in the above tabulation, the indicated calciferol would actually be precalciferol if the temperature of the irradiation mixture were maintained at room temperature or below. On the basis of Sharpe's experimental results and his proposed mechanism, a hydroxylic solvent or a solvent of high viscosity should suppress the formation of lumisterol. Therefore, irradiation of ergosterol at low temperatures with radiation of wavelength greater than 2840 A° and in a hydroxylic solvent should yield a product consisting largely of

precalciferol and unreacted ergosterol. It was considered necessary to limit the extent of conversion of ergosterol in order to minimize the formation of overirradiation products.

In order to fulfill the wavelength requirements, the radiation of the low pressure mercury arc was filtered by aqueous copper sulfate solutions at concentrations of 5.00 grams/100 ml. water and 1.25 g./100 ml. water; the thickness of the filter solution chamber was 0.5 cm. Under these conditions, the more concentrated solution absorbed 90% of the radiation of wavelength less than 2900 A^{o}, while the more dilute solution absorbed 90% of the radiation of wavelength less than 2790 A^{o}. The more dilute solution was employed for the later preparative runs to decrease the reaction time and thus minimize the thermal conversion of precalciferol to calciferol.

Since the solubility of ergosterol in 95% ethanol is quite limited, this solvent is not suitable for the preparative work. Crude solubility determinations were made at room temperature to find a more suitable hydroxylic solvent. Saturated solutions of ergosterol in absolute ethanol and in isopropyl alcohol were prepared at room temperature. The solutions were filtered, aliquots of the filtrate were evaporated to dryness in vacuo, and the weights of the residues were obtained. The solubility of ergosterol in isopropyl alcohol was found to be 10.7 grams per liter as compared with 3.9 grams per liter found in absolute ethanol. The solubility in isopropyl alcohol is adequate and this solvent was employed in all of the preparative work.

B. Results

In general, observation of the ultraviolet absorption spectra of the irradiation mixture and of the chromatographic fractions indicated that precalciferol was the major product. On the basis of the intensity of the antimony trichloride color produced by the fractions from the chromatographic separation, one fairly narrow band was observed during the early portion of the elution procedure of the methanol soluble fraction of the irradiation product. However, during one run in which the ergosterol solution being irradiated was not cooled efficiently, two bands were clearly detected. The first band did not contain much product while the second band contained the bulk of the material. Apparently most of the precalciferol had been converted to calciferol during the irradiation and the "working up" of the resin.

A particular run will be discussed in detail. A solution containing 7.67 grams of ergosterol dissolved in 900 ml. of isopropyl alcohol was irradiated for 94 minutes. After evaporating the solvent in vacuo, the resin was taken up in methanol and 2.51 grams of precipitate (ergosterol) were separated by filtration. The ultraviolet absorption spectrum of the filtrate was determined after suitable dilution of a small aliquot of the filtrate with methanol; the reference solution consisted of methanol that was saturated with ergosterol at the same temperature as the sample solution, so that the contribution of ergosterol to the spectrum would be nullified. The reference solution was prepared by filtration of a saturated solution of ergosterol in methanol (at the

temperature of the methanol extraction of the irradiation resin) and dilution of the filtrate with methanol in the same manner as the sample solution. The absorption spectrum was very similar to that of precalciferol with an absorption maximum at 2600 A^{o}. However, the extinction coefficient, $E^{1\%}_{1\ cm.}$, at the maximum had a value of only 164 based on the total solute, while the extinction coefficient of precalciferol is equal to 230 at 2600 A^{o}. The discrepancy is partly due to the ergosterol that was in solution, which acted essentially as a spectroscopically inactive diluent, since its absorption was balanced by the ergosterol in the reference solution.

The methanol solution was evaporated in vacuo and about 4.5 grams of resin were recovered. The residue was taken up in the petroleum ether-acetone mixture and chromatographed on alumina employing petroleum ether as eluent. About 75 ml. of liquid that was first eluted was discarded; this liquid gave a negative test with antimony trichloride reagent. Ten ml. fractions were then collected at an elution rate of 3 ml./min. The fractions were immediately immersed in an ice bath, and the antimony trichloride reagent test was applied to each fraction. The results of the tests are summarized in Figure 12.

On the basis of the color test it is apparent that only one major band is present, and this band is quickly eluted from the column. The behavior is characteristic of precalciferol. Fractions 10-27 were combined (the upper limit of the band was somewhat arbitrary), and the solvent was evaporated in vacuo. About two grams of residue were recovered. The remaining fractions were arbitrarily combined and solvent was evaporated as follows:

Figure 12

"Chromatogram" of Methanol
Soluble Fraction

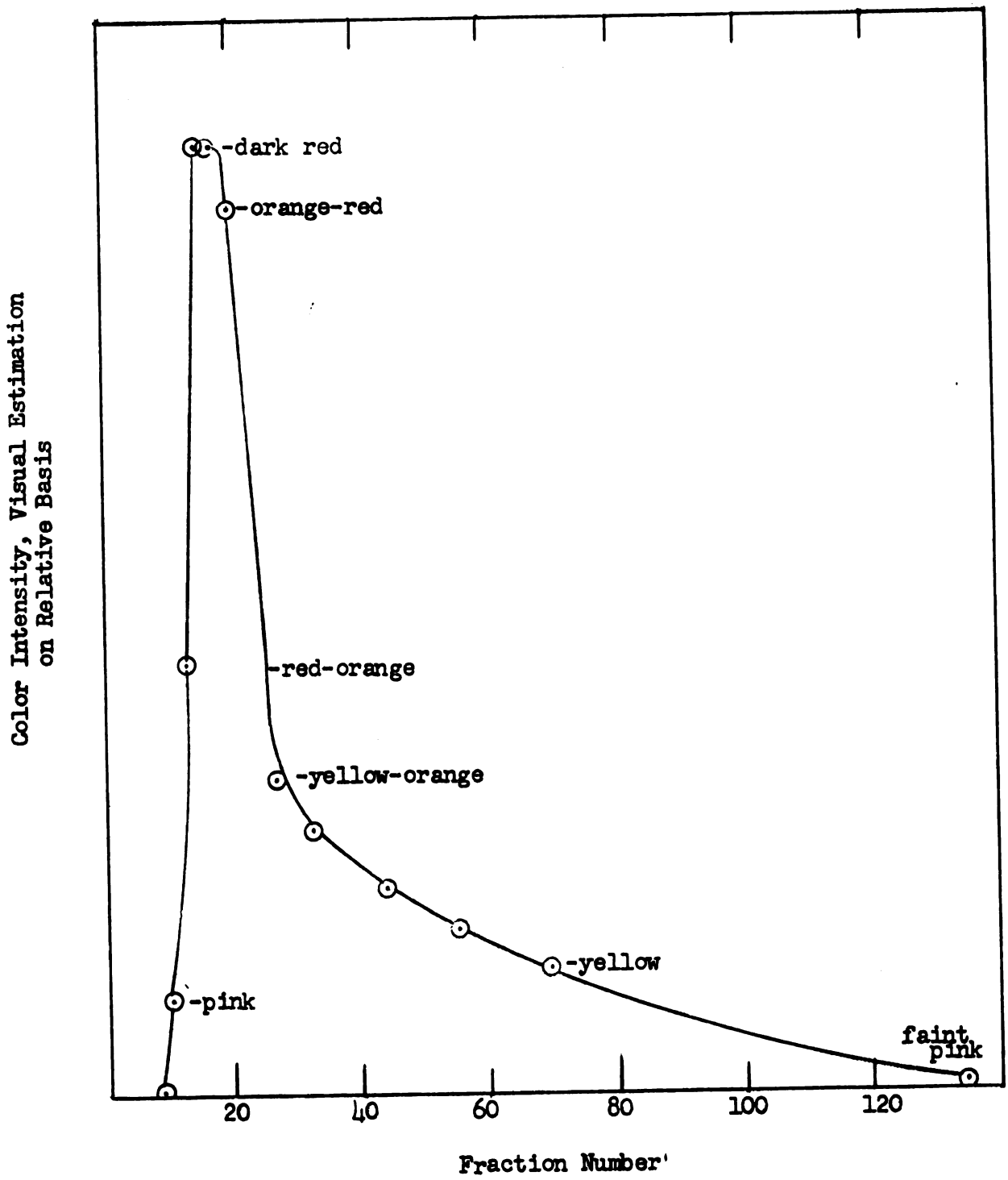

Fractions	Residue Recovered (Approximate)
28-47	2 grams
48-87	.4 grams
88-135	.3 grams

Weighed amounts of the crude residues were dissolved in isopropyl alcohol, and the ultraviolet absorption spectra were determined with isopropyl alcohol as the reference on the Beckman DK-2 Spectrophotometer. The spectrum of the "precalciferol band" fractions 10-27, was quite similar to that of precalciferol; the absorption maximum was at 2615 A° with $E^{1\%}_{1\ cm}$ equal to 202 as compared to a value of 230 for precalciferol (maximum at 2600 A°). The discrepancy could reasonably be attributed to small amounts of less absorbing contaminant, since the crude resins were employed for the spectral determination.

The spectrum of fractions 28-47 was quite similar to that of fractions 10-27, and it is reasonable to conclude that fractions 10-47 consisted largely of precalciferol. The spectrum of fractions 48-87 indicated that this portion consisted essentially of a mixture of precalciferol and calciferol; it should be noted that these fractions contained a very small amount of solute (about .4 grams). Ergosterol was clearly indicated by the spectrum of fractions 88-135 (maxima were obtained at about 2950, 2820, 2720, and 2620 A°), although an additional maximum at about 2520 A° indicated the presence of other irradiation products.

The above analysis confirms the belief that the prescribed conditions of irradiation should produce precalciferol relatively free of other irradiation products.

About 0.8 grams of the 3,5 dinitrobenzoate of precalciferol were prepared from the residue of fractions 10-27. The procedure of Velluz et al. (42), as described in the experimental section, was utilized. The preparative experimental work was discontinued at this point since W. H. C. Shaw furnished complete spectral data and purified samples of the required materials.

C. Miscellaneous Observations

1. Stability of the Irradiation Mixture

The ultraviolet absorption spectra of samples withdrawn at intervals from the irradiation apparatus were determined after storage for six days at 5° C. and compared with the spectra determined immediately at the time of withdrawal from the system. These data were obtained for the run that was described in detail in the preceding section and are summarized in Table VI.

The absorption spectrum of ergosterol (zero time of irradiation) does not change significantly during the storage period. However, the absorbancy of the stored irradiation mixtures consistently increases during storage. The change in absorbancy may be attributed to a slow thermal conversion of precalciferol to calciferol, since the absorption spectrum of the latter is more intense than that of precalciferol, cf. Figure 2.

TABLE VI

STABILITY OF THE IRRADIATION MIXTURES

Concentration of Irradiation Mixture 0.0026 g./100 ml.

Time of Irradiation (Minutes)	Wavelength A°	Absorbancy S	Absorbancy O
0	2940	.424	.420
	2900	.383	.378
	2820	.772	.769
	2765	.612	.605
	2715	.727	.730
	2635	.503	.497
26	2930	.358	.340
	2900	.347	.328
	2820	.636	.615
	2765	.543	.520
	2710	.632	.612
	2630	.489	.460
62	2920	.278	.259
	2820	.498	.463
	2765	.449	.413
	2710	.516	.475
	2630	.426	.390
94	2920	.279	.263
	2810	.500	.465
	2765	.469	.432
	2710	.533	.494
	2630	.428	.391

S = After storage for 6 days at 5° C.
O = Immediately after withdrawal from irradiation system

2. Yellow Component of Irradiation Product

The irradiated ergosterol solution sometimes took on a yellow color. Ergosterol itself becomes slightly yellow on standing. It has not been ascertained whether the yellow color is an oxidative degradation product or an irradiation product. This component appeared as a yellow band on the alumina chromatographic column and was eluted off the column during the last portion of the precalciferol band and the first portion of the calciferol band. These yellow chromatographic fractions were combined, the solvent was evaporated in vacuo, and a weighed amount of the residue was dissolved in isopropyl alcohol, and the ultraviolet absorption spectra was determined in the range 5000 to 2300 A°. Isopropyl alcohol was employed as a reference and the percent transmittancy scale of the Beckman DK-2 spectrophotometer was utilized.

The absorption due to the yellow component begins at about 5000 A° and appears to reach a maximum at about 3300 A°. However, the components of the irradiation mixture start to absorb in this region and the maximum of the yellow component is masked since the latter is probably present as a minor constituent of the mixture. The value of the extinction coefficient, $E^{1\%}_{1\ cm}$, at 3300 A° calculated on the basis of total solute is about 5.

D. Verification of Beer-Lambert-Bouger Law

Since the analytical method employed in the kinetic studies utilizes the Beer-Lambert-Bouger Law, it was first necessary to establish the applicability of this law to the ergosterol irradiation mixture.

The linearity of absorbancy vs. concentration for single components has been established for several components of the irradiation mixture (21,51). Because of the possibility of specific interactions among components, it was deemed necessary to obtain verification of the applicability of this law to solutions containing mixtures of the components. This further verification was obtained in two additional respects:

(1) for irradiation mixtures, the linearity of the absorbancy vs. overall concentration of the entire mixture was established, and

(2) for synthetic mixtures prepared from pure components, the additivity of absorbancies of the pure components to give the absorbancy of the mixture was verified.

The latter verification will be discussed in the next section; spectral data obtained during the preparative runs were utilized for (1).

The spectra of the irradiated solutions were determined periodically during the irradiation; in addition, several dilutions were made of the irradiated solutions and their spectra were determined. Plots of absorbancy at various wavelengths (in the region 3000-2300 A^{o}) were obtained from these spectra. A linear relationship was found between absorbancy and overall concentration of the irradiation mixture. The standard deviation from linearity was found to be only $\pm$ 0.012 absorbancy units. This value was obtained on the basis that the plots were constrained to pass through the origin; the standard deviation was calculated from 71 experimental values which comprised 19 separate plots. The absorbancies of the samples employed covered the complete range from about .025 to 1.50.

TABLE OF CONTENTS

IV. SPECTROPHOTOMETRIC ANALYSIS OF MULTICOMPONENT SYSTEMS USING THE LEAST SQUARES MATRIX METHOD

Because of the general applicability of the least squares matrix method to spectrophotometric data, the method will first be presented in general form, and then applied to the ergosterol irradiation system.

A. Least-Squares Treatment--Matrix Method

The calculation of concentrations of n components in spectrophotometric analyses has been generally regarded as a process of solving a set of n simultaneous linear equations (obtained by selecting absorbancies at n wavelengths) in the n unknowns (concentrations). As n becomes large, this method exhibits great sensitivity to small errors in the experimental data. An alternative viewpoint is to regard the calculation as a curve-fitting process, in which the experimental absorbancy curve is to be matched, as well as possible, by an absorbancy curve calculated by combining the extinction curves of the individual components with selected weighting factors (the concentrations); the best possible matching is to be determined by the usual least squares criterion. The curve fitting may be based on any desired number of wavelengths greater than n, and may be performed in a number of different ways. One method of curve fitting is to prepare a library of calculated curves for different compositions and select from the library the calculated curve most nearly matching the experimental curve. The same goal can be achieved, however, by an analytic method which can be conveniently developed in terms of a matrix notation. The application of the matrix analytic method to

spectral data was suggested by Professor Richard H. Schwendeman.

The treatment presented here assumes applicability of the Beer-Lambert-Bouger Law to the absorption spectrum of the system. For a system of n components, then, the absorbancy A_i at wavelength λ_i is given by

$$A_i = \sum_{j=1}^{n} a_{ij} c_j b \qquad \text{(IV-1)}$$

where a_{ij} is the absorptivity of component j at wavelength λ_i, c_j is the concentration of component j, and b is the cell thickness, usually in cm. The units of all of these quantities must be compatible, such that if c_j is the molar concentration, a_{ij} will be the molar absorptivity, while if c_j is the concentration of component j in gm./100 ml. of solution, a_{ij} will be the absorptivity of a 1% (w./v.) solution, usually designated $E^{1\%}_{1cm.}$.

Since the cell thickness is usually constant in an experimental application, it is convenient to work with

$$D_i = \frac{A_i}{b} = \sum_{j=1}^{n} a_{ij} c_j \qquad \text{(IV-2)}$$

where D_i is then the absorbancy per unit length of cell. In practice it sometimes proves convenient to work with equations of the form of (IV-2) in which the symbols D_i, a_{ij}, and c_j represent functions derived from the absorbancies per unit length, the absorptivities, and the concentrations; the relationships which follow apply to the mathematical form of equation (IV-2) and are not restricted to the usual definitions of the symbols.

If data are available at m different wavelengths, λ_1, $\lambda_2 \ldots$, λ_m, equation (IV-2) becomes a set of m simultaneous linear equations.

Such equations can be written in matrix notation as

$$\underline{D} = \underline{a}\,\underline{c} \qquad \text{(IV-3)}$$

where the underlined symbols represent the matrices appearing in expanded form as

$$\begin{bmatrix} D_1 \\ D_2 \\ D_3 \\ \cdot \\ \cdot \\ \cdot \\ \cdot \\ D_m \end{bmatrix} = \begin{bmatrix} a_{11} & a_{12} & a_{13} & \cdots & a_{1n} \\ a_{21} & a_{22} & \cdots & & a_{2n} \\ a_{31} & \cdot & \cdot & \cdot & a_{3n} \\ \cdot & \cdot & \cdot & \cdot & \cdot \\ \cdot & & & & \cdot \\ \cdot & & & & \cdot \\ \cdot & & & & \cdot \\ a_{m1} & a_{m2} & \cdots & & a_{mn} \end{bmatrix} \begin{bmatrix} c_1 \\ c_2 \\ c_3 \\ \cdot \\ \cdot \\ \cdot \\ \cdot \\ c_n \end{bmatrix} \qquad \text{(IV-4)}$$

Note that in the matrices it is not required that $m = n$--that is, the number of wavelengths need not be the same as the number of components. However, if $m = n$, the matrix $\underline{a}$ is square and has an inverse $\underline{a}^{-1}$ (unless its characteristic determinant is equal to zero). If the matrix $\underline{a}$ is known and non-singular, its inverse can be found (30), and we can obtain

$$\underline{a}^{-1}\,\underline{D} = \underline{a}^{-1}\,\underline{a}\,\underline{c} \qquad \text{(IV-5)}$$

or

$$\underline{c} = \underline{a}^{-1}\,\underline{D} \qquad \text{(IV-6)}$$

which is the solution for the concentrations (knowledge of the matrix $\underline{c}$ implies knowledge of each of its elements, the concentrations of the

individual components). This is the usual method of treatment of spectrophotometric data.

If $m < n$ (fewer wavelengths than components) no solutions for the $\underline{c}$ matrix can be obtained (fewer equations than unknowns). However, if $m > n$ (more wavelengths observed than the number of components), we have more equations than unknowns and can obtain a variety of solutions for the $\underline{c}$ matrix by using different sets of equations. In the presence of experimental errors in both the $\underline{a}$ and $\underline{D}$ matrices, it will not ordinarily be possible to satisfy equation (IV-3) or (IV-4) exactly. However, it is possible to obtain the matrix $\underline{c}$ which will minimize the quantity

$$\Delta^2 = \sum_{i=1}^{m} (D_i' - D_i)^2 \qquad \text{(IV-7)}$$

where the D_i come from the experimental absorbancies and the D_i' are values computed using equation (IV-3) with the $\underline{a}$ matrix and the $\underline{c}$ matrix obtained. Δ^2 is the sum of the squares of the individual deviations. Equation (7) can also be written in matrix notation as

$$\Delta^2 = \widetilde{(\underline{D'} - \underline{D})}\ (\underline{D'} - \underline{D}) \qquad \text{(IV-8)}$$

in which the matrix $\widetilde{(\underline{D'} - \underline{D})}$ is the transpose of the matrix $(\underline{D'} - \underline{D})$--i.e., it is obtained from the original matrix merely by interchange of rows and columns. Δ^2 is a single number, so is not underlined in the matrix equation (IV-8). Selection of $\underline{c}$ to minimize Δ^2 is the familiar least squares criterion for obtaining the best set of concentration values,

and can be seen to correspond to obtaining the closest fit of a calculated absorbancy curve to the experimental absorbancy curve.

It can be shown (12) that the least squares criterion is satisfied by solving equation (IV-3) in the following manner. First, multiply both sides of (IV-3) by the transpose of the matrix $\underline{a}$ (generally non-square). Then

$$\tilde{\underline{a}}\ \underline{D} = \tilde{\underline{a}}\ \underline{a}\ \underline{c} \qquad \text{(IV-9)}$$

The matrix $\tilde{\underline{a}}\ \underline{a}$ will be a square matrix, with dimensions n x n, since it results from multiplication of the n x m matrix $\tilde{\underline{a}}$ by the m x n matrix $\underline{a}$. The matrix $\tilde{\underline{a}}\ \underline{D}$ will be n x 1 since it results from multiplication of the n x m matrix $\tilde{\underline{a}}$ by the m x 1 matrix $\underline{D}$. The multiplication by the transpose matrix to obtain the best least squares fit is a consequence of the form of equation (IV-8), in which Δ^2 is itself a product of a matrix with its transpose.

The matrix equation (IV-9) may be regarded as a new set of n simultaneous linear equations in the n unknown concentrations. This may be solved by the usual methods of solution of simultaneous linear equations, where the number of equations is equal to the number of unknowns. Unfortunately, the solution of a set of simultaneous linear equations would be necessary for each sample analyzed if equation (IV-9) were to be used. The matrix inversion method described below requires a more difficult operation than solving a set of simultaneous linear equations, but the difficult step needs to be performed only once, and the result can be used in all subsequent analyses.

brea

Iran

This

to ob

squa

new m

where

compu

istic

tate

The t

In wh

the al

Since the square matrix $\underset{\sim}{a}^{T}\,\underset{\sim}{a}$ will (if non-singular) have an inverse, both sides of equation (IV-9) may be multiplied by this inverse, $(\underset{\sim}{a}^{T}\,\underset{\sim}{a})^{-1}$. Then

$$(\underset{\sim}{a}^{T}\,\underset{\sim}{a})^{-1}\,\underset{\sim}{a}^{T}\,\underset{\sim}{D} = (\underset{\sim}{a}^{T}\,\underset{\sim}{a})^{-1}\,(\underset{\sim}{a}^{T}\,\underset{\sim}{a})\,\underset{\sim}{c} = \underset{\sim}{c} \qquad \text{(IV-10)}$$

This is the solution to the matrix equation (IV-3), for it prescribes how to obtain from it the concentrations $\underset{\sim}{c}$ best satisfying (by the least squares criterion) the experimental data. It is convenient to define a new matrix, $\underset{\sim}{M}$, by

$$\underset{\sim}{M} = (\underset{\sim}{a}^{T}\,\underset{\sim}{a})^{-1}\,\underset{\sim}{a}^{T} \qquad \text{(IV-11)}$$

where $\underset{\sim}{M}$ is an n x m matrix which can be obtained directly, by suitable computations, from the known matrix $\underset{\sim}{a}$. $\underset{\sim}{M}$ will be a matrix characteristic of the system studied and the wavelengths selected, and will facilitate calculation of the concentrations $\underset{\sim}{c}$ by

$$\underset{\sim}{c} = \underset{\sim}{M}\,\underset{\sim}{D} \qquad \text{(IV-12)}$$

The individual concentrations then are given by

$$c_i = \sum_{j=1}^{m} M_{ij}\ D_j \qquad \text{(IV-13)}$$

in which each concentration is expressible as a linear combination of the absorbancy values at the set of wavelengths selected.

B. Application of the Method to the Ergosterol Irradiation System

1. Procedure

The matrix method was applied to solutions of known composition and the calculated values of the concentrations of the components were compared to the true values. The applicability of the Beer-Lambert-Bouger Law was verified further with respect to the additivity of the absorbancies of the components in a mixture.

Solutions of known composition consisting of ergosterol, lumisterol, and calciferol in varying proportions were prepared from the pure components employing purified isopropyl alcohol as the solvent. Stock solutions of each of the components were prepared as follows: about ten milligrams of material were weighed to 0.1 of a milligram and diluted to 100 ml. The solutions were then prepared by dilution of aliquots of the stock solutions--employing 1, 2, 3, and 5 ml. volumetric pipets--to 25 ml.

The ultraviolet absorption spectra of the synthetic mixtures and of the pure components were determined employing the Beckman Model DK-2 Spectrophotometer and a path length of 1.00 cm. In general, the spectra of the pure components in isopropyl alcohol were in good agreement with values reported by Shaw, Jefferies, and Holt (39,40).

2. Verification of the Beer-Lambert-Bouger Law

In addition to the verification for irradiation mixtures as described in the preparative section, the applicability of the Beer-Lambert-Bouger Law was verified for synthetic mixtures prepared from pure components;

the additivity of absorbancies of the pure components to give the absorbancy of the mixture was verified.

The spectra of synthetic mixtures of known compositions were compared with absorbancies calculated from the spectra of the individual components and the composition of the solution to establish the additivity of absorbancies of the pure components. This comparison was made at intervals of five millimicrons in the wavelength range 230 to 300 millimicrons and a standard deviation, S.D., was calculated for each synthetic mixture. The standard deviation was calculated on the following basis:

$$S.D. = \sqrt{\frac{(\text{Absorbancy of Mixture-Calculated Absorbancy})^2}{n}} \qquad \text{(IV-14)}$$

where n is the number of wavelengths at which the comparisons were made. The values of the absorbancies of the solutions were about 0.45 to 0.70 at the maxima. The data are presented in Table VII.

The data verify the additivity of absorbancies of components in a mixture within the limits of experimental error. It was believed that deviations from the Beer-Lambert-Bouger Law would be most likely to occur in solutions containing calciferol and lumisterol, since these compounds form a crystalline molecular addition compound--i.e., the old Vitamin D_1. However, the data indicate the absence of such an interaction in solution, at least at the concentrations employed.

3. Specific Modifications of the Method for the System Studied

In the ergosterol irradiation system, all four of the products are isomeric, so that the initial concentration of starting material (ergosterol)

TABLE VII

VERIFICATION OF THE BEER-LAMBERT-BOUGER LAW--ADDITIVITY OF ABSORBANCIES OF PURE COMPONENTS IN SYNTHETIC MIXTURES

Composition of Solution (g. per 100 ml. of solution)			S.D.* Absorbancy Units
Ergosterol	Lumisterol	Calciferol	
0.001380	0.000444	0	± 0.006
0.000920	0.000888	0	± 0.009
0.000460	0.001332	0	± 0.009
0.001380	0	0.000392	± 0.005
0.000920	0	0.000784	± 0.005
0.000460	0	0.001176	± 0.008
0	0.000444	0.001176	± 0.008
0	0.000888	0.000784	± 0.010
0	0.001332	0.000392	± 0.007
0.001380	0.000444	0.000392	± 0.015
0.000920	0.000888	0.000784	± 0.006

*

$$S.D. = \sqrt{\frac{(\text{Absorbancy of Mixture} - \text{Calculated Absorbancy})^2}{n}}$$

is always the total concentration of the five species present in the system. Designating ergosterol as component 1, we have

$$c_1^{\,o} = \sum_{j=1}^{5} c_j = c_1 + \sum_{j=2}^{5} c_j \qquad \text{(IV-15)}$$

or

$$c_1 = c_1^{\,o} - \sum_{j=2}^{5} c_j \qquad \text{(IV-16)}$$

Substitution of the value for c_1 from equation (IV-16) into equation (IV-1) gives

$$A_i = a_{i1}\, c_1^{\,o}\, b - a_{i1} b \sum_{j=2}^{5} c_j + \sum_{j=2}^{5} a_{ij} c_j b \qquad \text{(IV-17)}$$

or

$$A_i = a_{i1} c_1^{\,o} b + \sum_{j=2}^{5} (a_{ij} - a_{i1})\, c_j\, b \qquad \text{(IV-18)}$$

Because of the practical difficulty in making dilute solutions accurately up to known concentration by weighing, it is convenient to normalize the results to put them on the basis of the initially observed ergosterol concentration, as determined spectrophotometrically. Equation (IV-18) is therefore divided by equation (IV-19), which applies to the initial condition, before irradiation.

$$A_i^{\,o} = a_{i1}\, c_1^{\,o}\, b \qquad \text{(IV-19)}$$

The division gives

$$\frac{A_i}{A_i^o} = 1 + \sum_{j=2}^{5} \frac{a_{ij} - a_{i1}}{a_{i1}} \frac{c_j}{c_1^o} \qquad \text{(IV-20)}$$

or

$$\frac{A_i}{A_i^o} - 1 = \sum_{j=2}^{5} \left(\frac{a_{ij}}{a_{i1}} - 1 \right) \frac{c_j}{c_1^o} \qquad \text{(IV-21)}$$

Equation (IV-21) is put into the form of equation (IV-2) by defining

$$D_i = \frac{A_i}{A_i^o} - 1 \qquad \text{(IV-22)}$$

$$E_{ij} = \frac{a_{ij}}{a_{i1}} - 1 \qquad \text{(IV-23)}$$

and

$$C_j = \frac{c_j}{c_1^o} = \frac{c_j}{\sum_{j=1}^{5} c_j} \qquad \text{(IV-24)}$$

C_j is seen to be the fraction of component j in the irradiation products. Then

$$D_i = \sum_{j=2}^{5} E_{ij} C_j \qquad \text{(IV-25)}$$

When m wavelengths are considered, we obtain a set of m simultaneous equations in the four unknown concentrations. The resultant set of equations has the matrix form of equation (IV-3)

$$\underline{D} = \underline{E}\ \underline{C} \qquad \text{(IV-26)}$$

The best values for the concentrations by the least squares criterion are then given by equation (IV-10) or (IV-12), which here have the form

$$\underline{C} = (\underline{\tilde{E}}\,\underline{E})^{-1}\,\underline{\tilde{E}}\,\underline{D} \qquad \text{(IV-27)}$$

or

$$\underline{C} = \underline{M}\,\underline{D} \qquad \text{(IV-28)}$$

with

$$\underline{M} = (\underline{\tilde{E}}\,\underline{E})^{-1}\,\underline{\tilde{E}}. \qquad \text{(IV-29)}$$

The matrix $\underline{M}$ can now be calculated from available data on the absorptivities of the components at whatever set of wavelengths is selected for the analysis. This calculation requires setting up the $\underline{E}$ matrix, elements of which are defined by equation (IV-23), multiplying this matrix by its transpose $\underline{\tilde{E}}$, obtained by interchanging the rows and columns of $\underline{E}$, and then finding the inverse $(\underline{\tilde{E}}\,\underline{E})^{-1}$, of the square product matrix, $\underline{\tilde{E}}\,\underline{E}$. The matrix inversion is the only tedious step, and here involves inversion of a 4 x 4 matrix. When the inverse matrix, $(\underline{\tilde{E}}\,\underline{E})^{-1}$, is obtained, it is to be multiplied by $\underline{\tilde{E}}$ to give the desired $\underline{M}$ matrix.

4. Calculations of the Matrix $\underline{M} = [(\underline{\tilde{E}}\,\underline{E})^{-1}\,\underline{\tilde{E}}]$.

The data used were those of Shaw *et al.* (39,40) and are tabulated in Table VIII.

The matrix inversion was performed for several different combinations of wavelengths in an attempt to find the matrix $[(\underline{\tilde{E}}\,\underline{E})^{-1}\,\underline{\tilde{E}}] = \underline{M}$ which would give the best results in the calculation of the compositions of synthetic mixtures. The following choices of wavelength were carried through the matrix inversion: (continued on p. 81)

TABLE VIII

ULTRAVIOLET ABSORPTION OF ERGOSTEROL AND IRRADIATION PRODUCTS

	$E^{1\%}_{1cm}$ Values in Absolute Ethanol				
λ, Å	Ergosterol	Lumisterol	Tachysterol	Calciferol	Precalciferol
2300	44.7	32.3		247	156
2320		33.1		260	
2340		34.8			
2350	45.2			282	154
2360		37.7			
2370				298	
2380		41.4			
2400	51.4	46.4	136	324	169
2420		53.0		339	
2440		60.4			
2450	65.8		172	361	189
2460		69.5			
2470				377	
2480		80.3			
2490	88.8				
2500	97.1	96.9	229	399	210
2510	104.8				
2520	111.0	107.6	258.2	412	217
2530	116.2				
2540	121.8	121.3			
2550	128.5	128.3	303	434	225
2560	136.6	136.2	320.0	439.5	226.7
2570	148.0			445	
2580		152.4			
2590	175.8				
2600	189.5	169.7	396	463	230
2610	197.4				
2620	202.5	184.3		470	
2630	203.5	189.0	451.5	472.3	227.3
2640	204.5	194.9	469.6	474.0	225.8
2650	208.2	200.2	494	475	224
2660	216.7	205.3			
2663	220.5	207.5	525	473.8	220.5
2670			551		
2680	246.1	218.5	583.6	469	214.9
2690			590		

Continued

TABLE VIII - Continued

λ, Å	Ergosterol	Lumisterol	Tachysterol	Calciferol	Precalciferol
2700	281.5	232.3	602	458	207
2710	290.2	235.6	609		
2715	290.5	237.0	611	447.1	199.5
2720	289.2	238.0	614	444	197.1
2730	280.0	236.4	620		
2740	265.5	233.1	631		
2750	252.7	231.0		412	182
2760	245.6	226.9	668	397.5	176.8
2770	247.0	224.7		384	
2780	258.4	223.7	718		
2790	272.2	223.7	737	353	158.8
2800	288.2	223.7	745	340	152
2810	301.5	222.5	742		
2820	306.0	219.3	728	306.0	137.2
2830	296.4	213.5		290	
2839	275.5	203.7	679.5	275.5	124.2
2840	271.7	202.5	677	273.9	123.6
2850	240.3			258	117.
2860	209.0	177.9	631		
2870			617	227	
2880	165.9	152.4	609	210.1	98.1
2890	157.7		608		
2895	157.2	137.2	608	188.7	89.0
2900	158.3	133.3	608	181	86
2910	162.9		607		
2912	164.0	125.8	606	164.0	79
2920	168.4	121.3	599	153.5	74.3
2930	172.6				
2935	174.0	112.8	572.5	134.6	66.0
2940	173.6	110.1	561		
2950	167.0			119	58.5
2960	148.4	92.3	481	107.7	53.2
2980	89.3	69.1	386		
3000	42.5	46.4	307	70	37.5
3010	29.8				
3030	8.2				
3050		12.0	177	38	22
3070	2.6				
3100	0.8	4.1	118	18	12.5
3125		3.3	98		
3150		2.9	82		

The above values were obtained from large scale plots drawn from tabulated data that were kindly furnished by Shaw (40), and were used for the calculation of the matrix M in cases 1-4.

Continued

TABLE VIII - Continued

λ, Å	Ergosterol	Lumisterol	Tachysterol	Calciferol	Precalciferol
2500	97.0	95.0	225.0	399.0	209.0
2600	186.0	170.0	394.0	461.0	230.0
2650	213.0	200.0	492.5	475.0	223.0
2700	276.0	231.0	601.0	459.0	208.0
2750	257.5	228.5	655.0	408.0	181.0
2800	282.5	224.5	743.0	340.0	153.0
2850	250.0	189.0	657.5	257.5	118.0
2900	159.0	133.5	607.0	182.5	85.0

The values listed above were obtained from enlarged plots of the figures presented in the paper by Shaw et al. (39) and were utilized for the calculation of the matrix M in Case (0).

(0) Eight wavelengths - 2500, 2600, 2650, 2700, 2750, 2800, 2850, and 2900 Å. Data for this case were taken directly from enlarged plots of the figures from Shaw et al. (39). For Cases 1-4, data were taken from large scale plots drawn from tabulated data furnished by Shaw (40).

(1) Twelve wavelengths at intervals of 40 Å from 2520 to 2960 Å.

(2) Twelve wavelengths including the maxima and minima of the components of the mixture, i.e., 2500, 2600, 2630, 2650, 2715, 2720, 2760, 2790, 2800, 2820, 2895, and 2935 Å.

(3) Twelve wavelengths including points of intersection of the ergosterol curve with those of the other components and maxima and minima of the other components, i.e., 2500, 2550, 2600, 2650, 2663, 2720, 2790, 2800, 2820, 2839, 2895, and 3000 Å.

(4) Twelve wavelengths including the maxima and minima of ergosterol and points of intersection of the ergosterol absorption curve with curves of the other components, i.e., 2500, 2550, 2630, 2663, 2715, 2760, 2820, 2839, 2895, 2912, 2935, and 3000 Å.

The matrices $\underline{M}$ and the determinants $(\underline{\tilde{E}}\,\underline{E})^{-1}$ are presented in Table IX.*

5. Applicability of the Calculated Matrices

The calculated matrices $\underline{M}$ were checked by applying them to spectral data obtained on synthetic mixtures consisting of ergosterol, lumisterol,

---

*The matrix inversions were, with the exception of case (0), carried out on the MISTIC Computer at Michigan State University; the author is indebted to Miss Susann Brimmer for carrying out the calculations on the computer.

TABLE IX

MATRICES $\underline{M}$ AND DETERMINANTS $(\tilde{\underline{E}}\,\underline{E})^{-1}$

Case (0)

Wavelength Å / Component	2500	2600	2650	2700	2750	2800	2850	2900
Lumisterol	-2.15720	0.25981	4.39502	-1.06662	3.45070	-2.49132	-5.06356	1.78503
Tachysterol	0.14277	-0.13675	-0.08807	-0.27276	-0.04675	-0.06464	-0.08429	0.60911
Precalciferol	1.41332	-0.59016	-1.87141	-0.77855	-1.57408	0.24349	0.99577	0.91496
Calciferol	-0.30395	0.35248	0.76416	0.38767	0.58333	-0.09036	-0.36590	-0.57103

Determinant of $(\tilde{\underline{E}}\ \underline{E})^{-1}$ = 1.78552

Case (1)

	2520	2560	2600	2640	2680	2720	2760	2800	2840	2880	2920	2960
Lumisterol	-1.09061	0.09074	-0.49285	0.83306	0.44371	-0.24479	1.54837	-0.39920	-0.78587	2.19901	-0.60393	-2.11446
Tachysterol	0.10887	0.07848	-0.12889	-0.07160	-0.11208	-0.24357	0.01170	-0.09913	-0.13848	0.36520	0.23470	0.07976
Precalciferol	0.95585	0.30044	-0.29380	-0.66351	-0.71135	-0.93205	-0.77416	-0.42189	-0.41728	0.13128	0.76610	0.82304
Calciferol	-0.17494	0.00137	-0.22892	0.30070	0.30737	0.41409	0.24542	0.16800	0.17546	-0.22128	-0.36750	-0.31914

Determinant of $(\tilde{\underline{E}}\ \underline{E})^{-1}$ = 6.46265

Case (2)

	2500	2600	2630	2650	2715	2720	2760	2790	2800	2820	2895	2935
Lumisterol	-1.23881	-0.41003	0.61060	1.44397	-0.27563	-0.11357	1.86769	0.25902	-0.48815	-1.48899	1.55699	-2.38290
Tachysterol	0.12221	-0.09184	-0.06895	-0.02746	-0.17810	-0.17214	0.04079	0.01718	-0.03461	-0.11037	0.40579	0.16999
Precalciferol	1.05645	-0.16504	-0.51241	-0.71629	-0.62479	-0.66987	-0.76721	-0.26278	-0.15088	-0.01979	0.41711	1.14956
Calciferol	-0.17267	0.17850	0.26483	0.30471	0.29165	0.30239	0.23873	0.07100	0.05213	0.03429	-0.32738	-0.47392

Determinant of $(\tilde{\underline{E}}\ \underline{E})^{-1}$ = -1.66057

Continued

TABLE IX - Continued

Wavelength Å	Case (3)											
Component	2500	2550	2600	2650	2663	2720	2790	2800	2820	2839	2895	3000
Lumisterol	-2.28876	-0.06854	-0.00265	2.92668	2.68300	0.70997	0.10587	-0.98194	-2.40058	-1.82839	-0.02015	0.33906
Tachysterol	0.09387	-0.00215	-0.02591	-0.14020	-0.13158	-0.06491	-0.01538	0.02363	0.07371	0.05454	0.03890	0.16818
Precalciferol	1.29747	0.09732	-0.16421	-1.59898	-1.50876	-0.69685	-0.33901	0.14949	0.78411	0.52596	-0.10107	0.34138
Calciferol	-0.30301	0.08833	0.13107	0.63766	0.59663	0.26860	0.11351	-0.06901	-0.30702	-0.21478	0.00045	-0.19273
Determinant of $(\tilde{E}\ E)^{-1}$ = .03010												

	Case (4)											
	2500	2550	2630	2663	2715	2760	2820	2839	2895	2912	2935	3000
Lumisterol	-1.37645	-0.22086	0.80301	1.31106	0.42123	1.60395	-0.73383	-0.47318	0.39287	-0.90434	-2.20839	0.67990
Tachysterol	0.05197	0.00180	-0.05984	-0.07665	-0.06039	-0.07812	-0.00699	-0.01225	0.01533	0.05521	0.08543	0.15197
Precalciferol	0.86806	0.14323	-0.64144	-0.92793	-0.60520	-1.10500	-0.01046	-0.12611	-0.30492	0.31700	0.89763	0.22835
Calciferol	-0.12930	0.07969	0.29619	0.38278	0.24308	0.40695	0.00095	0.03876	0.08239	-0.13980	-0.34436	-0.14769
Determinant of $(\tilde{E}\ E)^{-1}$ = 0.01283												

and calciferol in isopropyl alcohol in varying proportions. These were the same solutions employed to verify the Beer-Lambert-Bouger Law. Each of the matrices described above was applied to six synthetic mixtures, and the calculated compositions were compared with the known values for the composition. The application of the matrices $\underline{M}$ to spectral data of the synthetic mixtures requires the value A_i^o (cf. Equations IV-19 to IV-25); this is the value of the absorbancy of an ergosterol solution of concentration equivalent to the sum of the concentrations of the individual components of the given synthetic mixture. A value of A_i^o was calculated from the sum of the concentrations of the given synthetic mixture and the $E_{1cm}^{1\%}$ values for ergosterol that were furnished by Shaw et al., cf. Table VIII. The results are summarized in Table X.

It is to be noted that although all five components were not present in the synthetic mixtures, the matrix $\underline{M}$ was calculated from ultraviolet absorption data for the five components. Therefore, compositions for components at zero concentration also serve to establish the validity of the computational procedure.

An "over all" standard deviation defined as

$$\pm \sqrt{\frac{\sum_c \sum_i [(\text{Calculated fraction of component i in mixture}) - (\text{known fraction of component i in mixture})]^2}{30}}$$

--where the index i refers to a summation over the five components, c refers to a summation over the six mixtures and the value 30 is the total number of "determinations"--was employed as a basis for selecting the best matrix $\underline{M}$. The values for the standard deviation are given in Table XI.

TABLE X

CALCULATED COMPOSITIONS OF SYNTHETIC MIXTURES

Component	Calculated Percent Composition of Synthetic Mixture (0)	(1)	(2)	(3)	(4)	Known Percent Composition
Matrix M						
Mixture 1						
Lumisterol	80.5	79.3	83.4	80.0	81.3	77.3
Tachysterol	-0.9	-0.4	-0.2	-0.7	-0.8	0
Precalciferol	-8.1	-5.7	-7.2	-7.8	-8.3	0
Calciferol	26.7	25.7	25.7	26.2	26.4	22.7
Ergosterol	1.7	1.2	-1.7	2.3	1.4	0
Mixture 2						
Lumisterol	61.0	56.4	57.4	60.1	50.9	53.1
Tachysterol	2.5	-2.1	2.0	-4.4	-3.9	0
Precalciferol	-7.1	-4.9	-4.0	-12.6	-7.7	0
Calciferol	50.0	49.4	48.1	52.1	50.1	46.9
Ergosterol	-1.1	1.2	0.5	3.9	10.5	0
Mixture 3						
Lumisterol	45.3	32.6	35.0	51.4	33.0	27.4
Tachysterol	-1.7	0.1	-0.8	-2.2	-1.5	0
Precalciferol	-15.1	-4.3	-8.7	-18.1	-10.4	0
Calciferol	80.2	76.5	77.0	81.3	78.2	72.6
Ergosterol	-8.7	-5.0	-2.6	-12.4	0.7	0
Mixture 4						
Lumisterol	73.9	78.8	82.5	84.3	81.8	74.3
Tachysterol	-2.2	-1.0	-1.1	-1.1	-1.0	0
Precalciferol	-8.2	-6.5	-8.2	-9.1	-8.0	0
Calciferol	3.0	2.1	2.2	2.6	2.2	0
Ergosterol	33.5	26.5	24.6	23.2	25.0	25.7
Mixture 5						
Lumisterol	42.2	53.8	50.2	47.6	50.2	49.1
Tachysterol	-0.7	-1.6	-0.8	-0.5	-0.6	0
Precalciferol	1.0	-4.5	-2.2	-0.4	-1.5	0
Calciferol	-0.5	2.1	-0.5	-0.3	0.2	0
Ergosterol	58.0	50.2	53.3	53.3	51.7	50.9
Mixture 6						
Lumisterol	8.3	31.6	31.1	24.6	31.2	24.3
Tachysterol	-1.7	-0.6	-0.7	-0.1	-0.5	0
Precalciferol	-2.7	-9.1	-7.6	-4.9	-7.5	0
Calciferol	1.9	3.2	3.0	1.8	2.9	0
Ergosterol	94.3	75.0	74.2	78.7	73.9	75.7

TABLE XI

STANDARD DEVIATIONS OBTAINED FOR EACH M MATRIX

Matrix M	(Standard deviation in percent of component in mixture)
0	± 7.7
1	± 3.8
2	± 4.4
3	± 7.7
4	± 4.9

The results demonstrate the effectiveness of employing a larger number of wavelengths, (i.e., utilizing more experimental data), since with the exception of the results obtained from matrix 3, the results obtained from the matrices based on twelve wavelengths were superior to those obtained from the eight wavelength matrix. Of the twelve wavelength matrices, matrix 1--which was based on equally spaced wavelength intervals--yielded the best results.

It was originally believed that more significant information would be obtained by use of wavelengths at which the absorptivities of other components intersected that of ergosterol, since at these intersections the difference from the initial ergosterol absorption is attributable entirely to the non-intersecting components. However, matrices 3 and 4, which were based on the intersection points (plus other wavelengths) yielded results inferior to those obtained from matrix 1 (equal wavelength intervals) and matrix 2 (based on the maxima and minima of components). Apparently, any advantage gained by the elimination of a

given component at the point of intersection with the ergosterol curve was offset by the zero value introduced into the calculations.

Matrix 1, which was based on equal intervals of wavelength in the significant region of the spectrum was selected as the matrix capable of yielding the best results on the basis of the above comparison. This matrix was applied to five more synthetic mixtures to further establish the validity of the procedure. Results obtained with matrix 0 are also included for comparison purposes and the results are presented in Table XII.

An "overall" standard deviation was calculated for matrices 0 and 1 utilizing the data for eleven mixtures or 55 determinations. The values for the standard deviation are:

Matrix M	(Standard Deviation in Percent of Component in Mixture)
(0)	7.6
(1)	4.0

These results are comparable to those obtained by the use of the values from only six mixtures. In addition, a standard deviation for individual components defined as

$$\pm\sqrt{\frac{\sum_{c}(\text{Calculated fraction of component in mixture} - \text{Known fraction of component in mixture})^2}{11}}$$

--where the index c refers to a summation over the eleven mixtures for a given component--was calculated for matrices 0 and 1. The data are summarized in Table XIII.

TABLE XII

CALCULATED COMPOSITIONS OF SYNTHETIC MIXTURES

Component	Calculated Percent Composition				
Matrix M	Lumisterol	Tachysterol	Precalciferol	Calciferol	Ergosterol
Mixture 7					
True Comp.	0	0	0	22.1	77.9
(0)	-8.9	-0.6	1.7	22.3	85.6
(1)	8.2	-1.0	-5.7	25.1	73.4
Mixture 8					
True Comp.	0	0	0	46.0	54.0
(0)	1.8	-1.2	-4.8	48.9	55.2
(1)	0.9	-0.5	-3.2	48.4	54.5
Mixture 9					
True Comp.	0	0	0	71.9	28.1
(0)	14.3	-2.4	-13.0	79.1	22.1
(1)	4.1	-1.5	-6.4	77.4	26.5
Mixture 10					
True Comp.	34.3	0	0	30.2	35.5
(0)	22.2	-3.0	-6.9	34.3	53.4
(1)	37.2	-1.8	-7.7	34.3	37.9
Mixture 11					
True Comp.	20.0	0	0	17.7	62.3
(0)	14.3	-2.3	-6.2	19.0	75.2
(1)	15.6	-0.8	-3.1	17.6	70.8

TABLE XIII

STANDARD DEVIATION OF INDIVIDUAL COMPONENTS

Matrix M Component	Standard Deviation in Percent of Component in Mixture	
	(0)	(1)
Lumisterol	± 10.3	± 4.8
Tachysterol	± 1.9	± 1.2
Precalciferol	± 8.0	± 5.8
Calciferol	± 4.0	± 3.2
Ergosterol	± 10.1	± 3.4

The data presented in Table XIII demonstrate further the improvement effected by the utilization of data from a large number of wavelengths. As one would expect, higher deviations were obtained for lumisterol, precalciferol, and ergosterol than for tachysterol and calciferol, since the absorption curves of the former are quite similar. It would not be reasonable to attribute the low deviation obtained for tachysterol to the absence of tachysterol in the synthetic mixtures, since precalciferol was also absent and it shows a high deviation which may more reasonably be attributed to similarity in spectra.

Matrix 1--the twelve wavelength matrix which was based on equally spaced wavelength intervals--was employed in the kinetic studies.

TABLE OF CONTENTS

V. IRRADIATION RESULTS

A. Application of the Matrix Method to Sharpe's Data

Neglect of precalciferol as a component of the irradiation mixture in the original treatment of Sharpe's data invalidated the results of his calculations. The matrix method, employing matrix (0), was applied to Sharpe's data to obtain further verification for the computational analytical procedure on actual irradiation mixtures and to re-evaluate the irradiation data. Matrix (0) is based on absorbancy data at the same wavelengths employed by Sharpe in his curve fitting treatment. Several calculations were also made from the utilization of matrix (1), but the results were inferior to those obtained with matrix (0) since it was necessary to use interpolated values of the absorbancy data. Sharpe had not reported absorbancy data at wavelengths which coincided with the wavelengths employed by matrix (1).

Compositions were calculated as functions of time of irradiation from Sharpe's data for irradiated solutions at five wavelengths of irradiation--2537, 2654, 2804, 2967, and 3132 A^{o}--and employing four solvents--n-hexane, cyclohexane, diethyl ether, and 95% ethanol. The source and monochromator employed by Sharpe were identical to the components employed in this investigation; a slit width of 2.50 mm. was used for all his irradiation runs. The thickness of the irradiation cell was 0.57 mm. and the initial concentrations of ergosterol were approximately equal in the various solvents (about 0.02 gm./100 ml.,

so that the absorbancy was roughly 0.3 at 2710 A^{o}). The results are reported as weight percentages and are summarized in Tables XIVa-XIVe. Plots of concentration vs. time were made for the recalculated compositions, cf. Figures 13a-1 to 13e-4.

Any evaluation of the recalculated results was necessarily limited to qualitative interpretation because of the absence of sufficient actinometric data and the high standard deviation of the results obtained with matrix (0). The application of the matrix method to Sharpe's data demonstrated that the computational procedure could be applied to actual irradiation mixtures as well as synthetic mixtures. Reasonable values were obtained for the decay of ergosterol and build-up of irradiation products. The compositions obtained by the matrix method are in general accord with other analyses of irradiation mixtures as will be discussed below.

Negative values which consistently became more negative with increasing irradiation time were obtained for the concentration of calciferol. However, the differences between the negative concentrations of calciferol and a value of zero were generally less than the value of the standard deviation for calciferol, except for irradiation mixtures for which the percent conversion of ergosterol was quite high. The consistent growth of negative values might be attributed to the formation of a spectroscopically active substance which was neglected in the matrix formulation. It is evident from the results that under Sharpe's experimental conditions, ergosterol was converted at a rapid rate and over-irradiation products may have been formed; his use of very thin unstirred cells would tend to

TABLE XIVa*

COMPOSITION OF IRRADIATION MIXTURES--2537 A°

Time, Min.	Calculated Composition, Percent E	L	T	P	D
		Ethyl Ether--Run Code 211			
5	76.5	5.4	2.8	15.2	-1.0
10	60.6	4.9	8.4	26.1	-3.5
20	38.0	14.4	19.4	34.7	-6.4
30	23.9	14.1	27.7	44.1	-9.8
		95% Ethanol--Run Code 221			
5	81.8	-3.6	4.1	19.3	-1.7
10	61.5	3.6	12.1	25.5	-2.7
20	45.3	0.8	27.3	31.2	-4.6
30	29.2	6.8	39.7	29.3	-5.1
45	15.4	7.8	52.6	32.4	-8.2
60	7.7	10.5	58.6	33.0	-9.8
90	6.9	3.2	63.0	40.2	-13.3
		n-Hexane--Run Code 231			
5	74.8	5.9	3.8	18.4	-3.0
10	58.1	6.6	11.0	27.8	-3.4
20	32.5	10.4	23.8	39.9	-6.6
30	23.3	1.6	30.1	58.6	-13.5
		Cyclohexane--Run Code 241			
5	79.9	5.4	1.4	14.2	-0.9
10	66.4	6.8	7.4	20.9	-1.4
20	50.7	2.3	18.9	32.7	-4.6
30	36.9	-0.3	27.4	43.8	-8.1

*Glossary of Symbols in Table: E = Ergosterol; L = Lumisterol; T = Tachysterol; P = Precalciferol; D = Calciferol (Vitamin D_2).

TABLE XIVb

COMPOSITION OF IRRADIATION MIXTURES--2654 A°

Time, Min.	Calculated Composition, Per cent E	L	T	P	D
		Ethyl Ether--Run Code 311			
5	71.8	4.5	3.5	22.9	-2.7
10	54.1	5.5	11.5	31.2	-2.3
20	29.3	17.6	19.2	39.8	-5.9
30	17.7	11.8	38.0	38.1	-5.5
60	5.8	29.0	23.8	40.1	1.4
		95% Ethanol--Run Code 321			
5	73.0	2.5	4.0	21.8	-1.4
10	54.1	5.5	11.5	31.2	-2.3
20	28.0	5.5	26.7	39.8	-5.3
30	17.7	11.8	38.0	38.1	-5.5
		n-Hexane--Run Code 331			
5	68.7	6.5	4.3	22.3	-1.8
10	45.5	14.1	11.8	31.2	-2.6
20	20.4	18.7	24.9	40.7	-4.7
30	15.5	2.1	30.8	63.9	-12.3
		Cyclohexane--Run Code 341			
5	76.5	0.6	3.4	21.2	-1.8
10	59.8	2.8	9.7	29.9	-2.2
20	39.5	0.8	22.9	41.4	-4.6
30	30.8	-10.2	32.2	56.9	-9.7

TABLE XIVc

COMPOSITION OF IRRADIATION MIXTURES--2804 A°

Time, Min.	Calculated Composition, Percent E	L	T	P	D
		Ethyl Ether--Run Code 411			
5	83.1	-0.3	1.0	15.5	0.8
10	79.8	-3.8	-3.4	28.1	-0.7
20	50.2	-0.6	9.5	43.2	-2.2
30	33.2	3.0	15.8	50.8	-2.8
60	12.9	-1.9	28.4	67.0	-6.4
		95% Ethanol--Run Code 421			
5	84.4	-0.2	0.9	16.6	-0.8
10	70.2	1.0	3.1	26.8	-1.1
20	42.3	13.3	8.6	37.3	-1.6
30	36.9	5.6	13.6	46.6	-2.7
60	16.3	9.9	25.5	51.9	-3.6
90	9.3	4.0	34.8	57.5	-5.6
120	6.4	0.0	40.2	60.4	-7.0
		n-Hexane--Run Code 431			
5	81.8	1.9	0.6	16.2	-0.5
10	63.5	6.9	3.1	27.2	-0.7
20	40.9	11.3	9.1	39.6	-1.0
30	26.4	11.7	15.7	48.3	-2.1
60	11.0	-1.0	27.6	69.3	-5.9
		Cyclohexane--Run Code 441			
5	82.0	6.2	0.1	10.9	0.8
10	68.1	8.2	2.0	21.3	0.4
20	48.4	8.7	7.3	36.6	-1.1
30	33.0	10.6	13.1	44.7	-1.4
60	16.2	1.8	25.7	60.9	-4.5

TABLE XIVd

COMPOSITION OF IRRADIATION MIXTURES--2967 A°

Time, Min.	Calculated Composition, Percent E	L	T	P	D
		Ethyl Ether--Run Code 511			
5	84.4	2.6	0.5	13.4	-0.9
10	80.7	-16.9	4.1	37.5	-5.4
20	55.2	8.1	4.5	33.8	-1.7
30	43.3	8.2	7.7	44.7	-4.0
45	31.9	6.8	10.9	54.0	-3.6
60	16.6	13.2	13.9	60.8	-4.5
75	15.1	6.9	15.6	68.3	-5.9
90	9.6	-4.5	19.4	86.5	-11.1
		95% Ethanol--Run Code 521			
5	88.0	-4.9	1.1	17.8	-1.9
10	77.4	-4.0	2.0	26.4	-1.8
20	59.5	-3.5	6.0	41.1	-3.0
30	38.7	4.7	10.4	50.1	-3.9
45	29.7	-2.1	15.3	62.5	-5.4
60	18.9	2.2	18.3	66.9	-6.3
90	10.1	-1.0	22.0	77.4	-8.6
		n-Hexane--Run Code 531			
5	78.5	10.7	0.6	10.5	-0.2
10	64.8	11.4	2.1	22.5	-0.9
20	43.1	19.6	4.9	32.3	0.1
30	29.9	20.0	8.6	42.1	-0.6
45	17.2	18.0	13.1	53.8	-2.1
60	7.4	14.7	16.7	65.2	-4.1
75	4.4	8.6	18.6	74.0	-5.6
90	3.8	0.5	19.7	83.5	-7.4
		Cyclohexane--Run Code 541			
5	85.9	0.1	0.5	14.2	-0.8
10	71.3	3.8	2.0	24.0	-1.0
20	57.3	1.3	4.8	37.6	-1.0
30	39.1	5.7	9.4	48.4	-2.6
45	22.0	7.7	14.6	59.2	3.6
60	16.5	4.6	17.6	65.7	-4.4
75	10.2	4.3	19.8	70.8	-5.1
90	9.5	-1.9	21.2	78.1	-6.9

TABLE XIVe

COMPOSITION OF IRRADIATION MIXTURES--3132 A°

Time, Min.	Calculated Composition, Percent E	L	T	P	D
		Ethyl Ether--Run Code 611			
10	94.1	4.2	0.0	2.6	-1.0
30	96.4	-3.1	0.2	9.3	-2.8
60	85.3	4.1	0.4	14.4	-4.2
120	73.3	9.3	-0.4	25.0	-7.5
		95% Ethanol--Run Code 621			
5	101.6	-4.5	0.1	3.4	-0.8
20	96.5	-0.8	0.4	4.7	-0.7
60	86.5	-3.2	6.8	11.4	-1.5
90	88.4	-3.5	1.5	15.4	-1.7
120	83.9	-2.7	2.1	18.7	-2.1
180	78.8	-2.5	2.6	23.9	-2.7
240	72.0	-1.3	3.5	29.5	-3.7
300	67.2	1.8	3.2	31.1	-3.3
360	64.1	-1.2	4.1	38.1	-5.2
480	59.9	-3.5	4.5	46.1	-7.0
		n-Hexane--Run Code 631			
15	93.5	3.8	0.3	3.0	-0.6
30	94.8	-0.6	0.3	7.0	-1.5
60	86.4	2.1	0.7	13.8	-3.0
90	81.7	1.8	0.9	20.0	-4.5
120	77.1	1.5	1.2	26.2	-6.0
180	65.3	3.7	2.1	38.6	-9.8
		Cyclohexane--Run Code 641			
5	98.8	0.5	-0.1	1.3	-0.4
10	97.3	1.8	-0.4	1.2	0.0
20	95.1	1.0	0.0	4.8	-0.9
30	95.2	0.3	-0.3	5.5	-0.6
45	92.7	-0.1	-0.1	8.9	-1.4
60	89.5	-0.2	0.7	13.7	-2.6
90	80.2	3.5	1.0	19.0	-3.7
120	79.6	-0.8	1.3	24.6	-4.7
150	70.7	3.0	1.9	30.9	-6.6
180	68.4	0.2	2.6	36.7	-7.9
240	57.6	2.7	3.2	47.7	-11.2

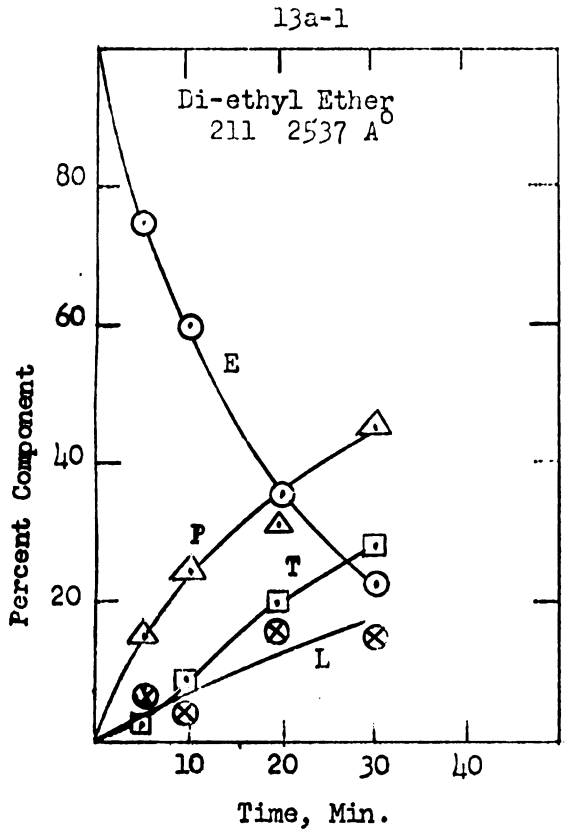

Figures 13a-1 and 13a-2

Composition of Irradiation Mixtures--
Sharpe's Data

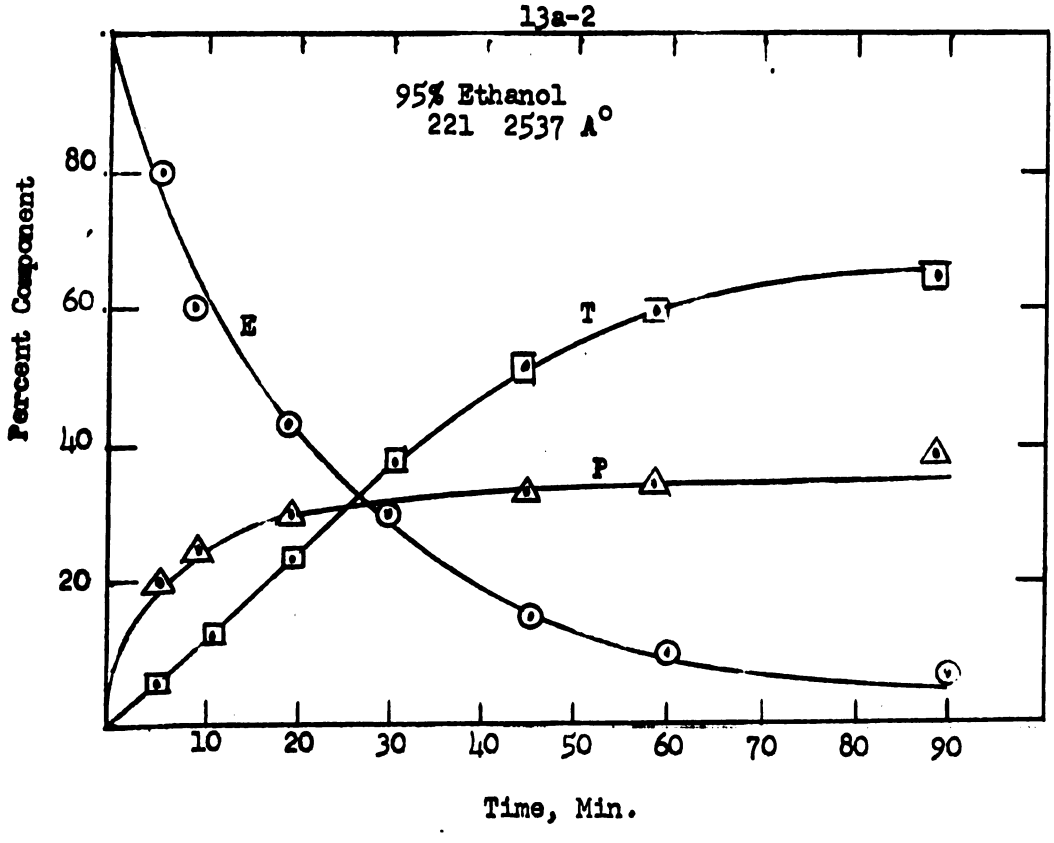

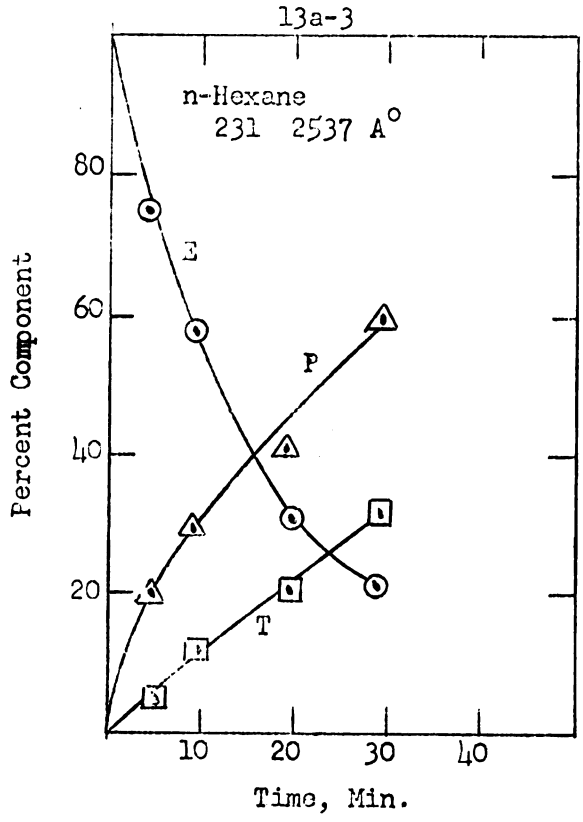

Figures 13a-3 and 13a-4

Composition of Irradiation Mixtures--
Sharpe's Data

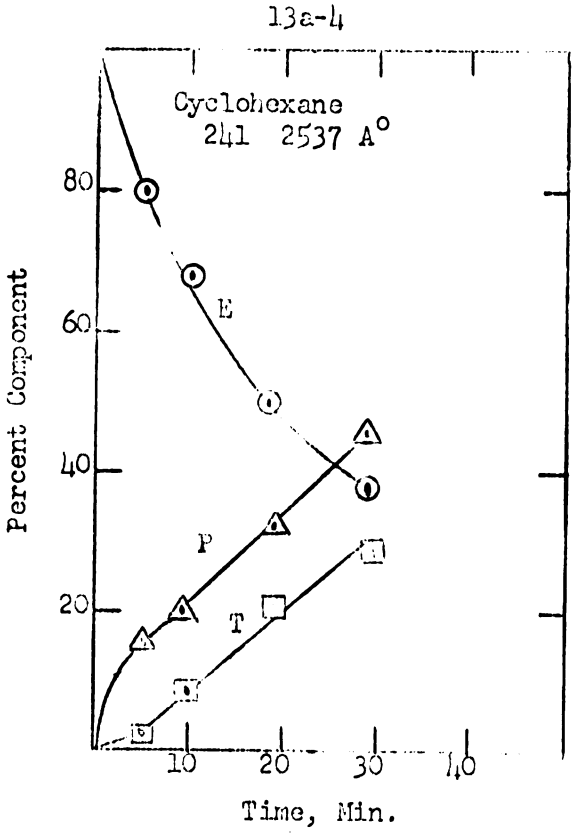

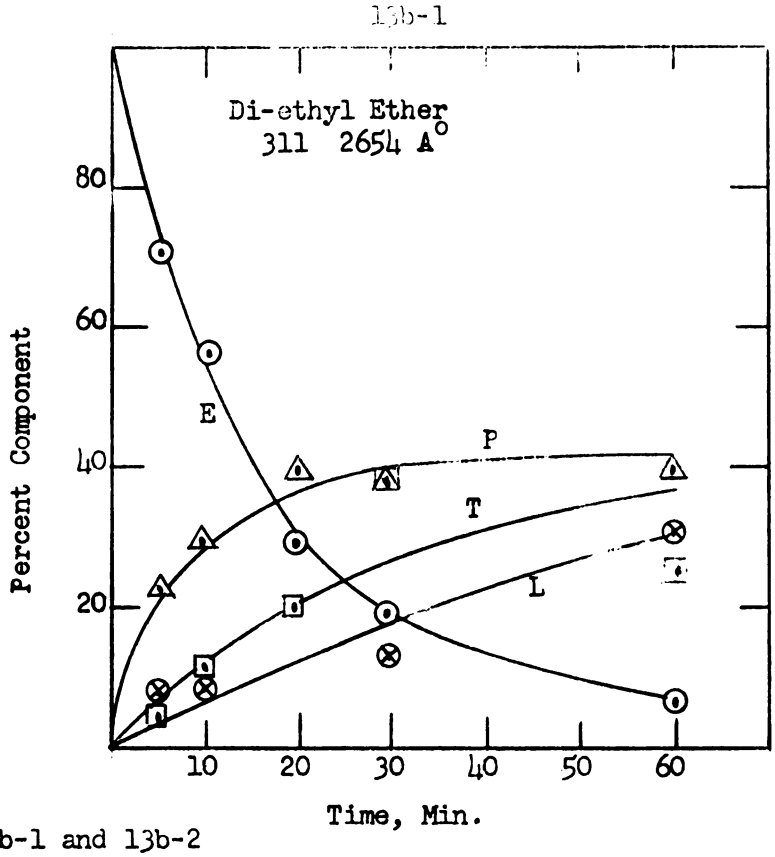

Figures 13b-1 and 13b-2

Composition of Irradiation Mixtures--Sharpe's Data

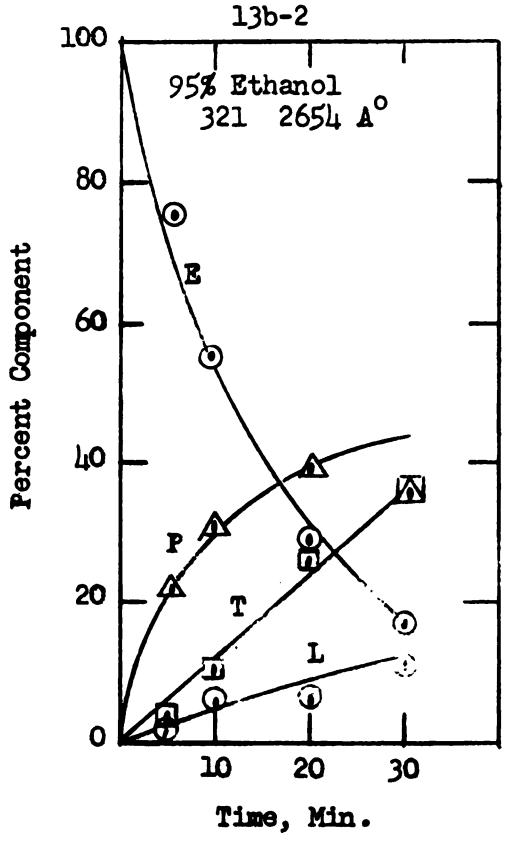

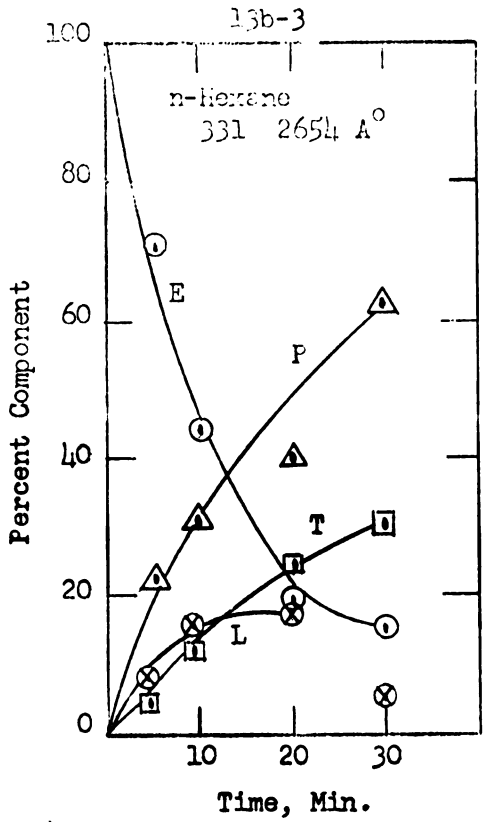

Figures 13b-3 and 13b-4

Composition of Irradiation Mixtures--Sharpe's Data

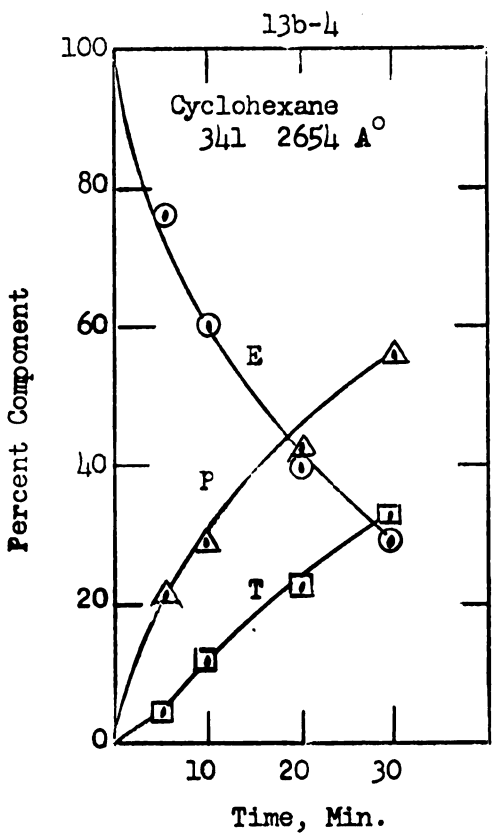

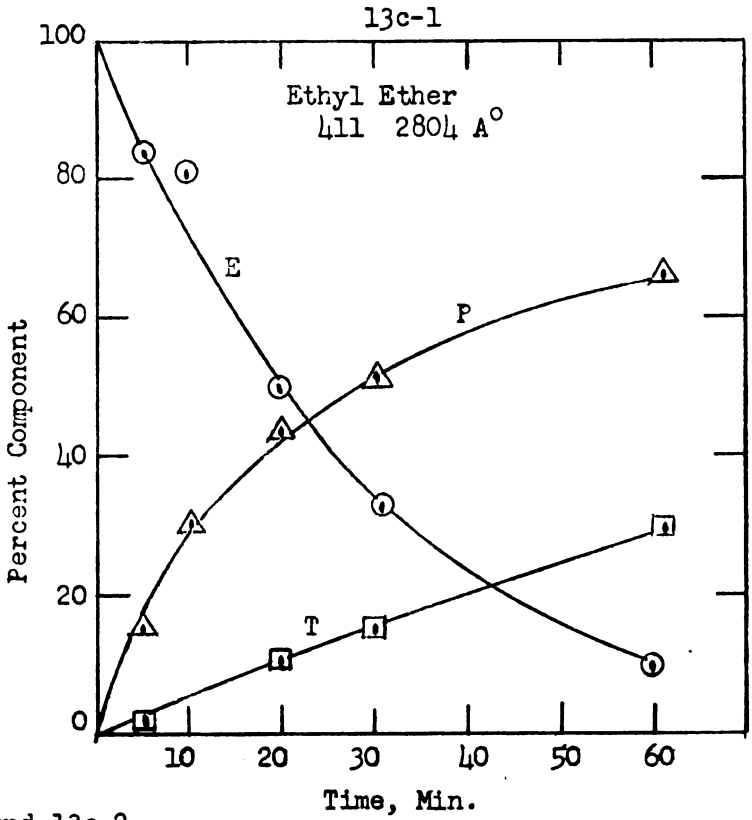

Figures 13c-1 and 13c-2

Composition of Irradiation Mixtures--Sharpe's Data

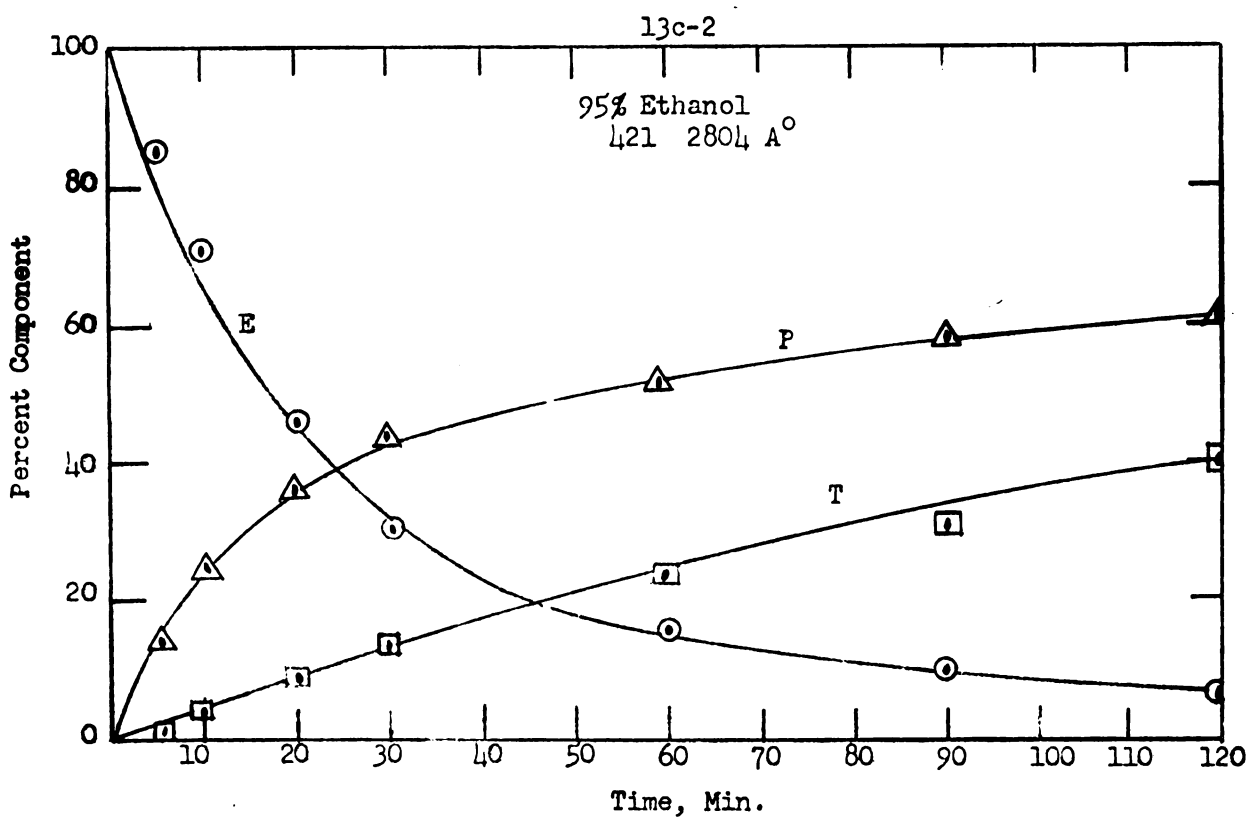

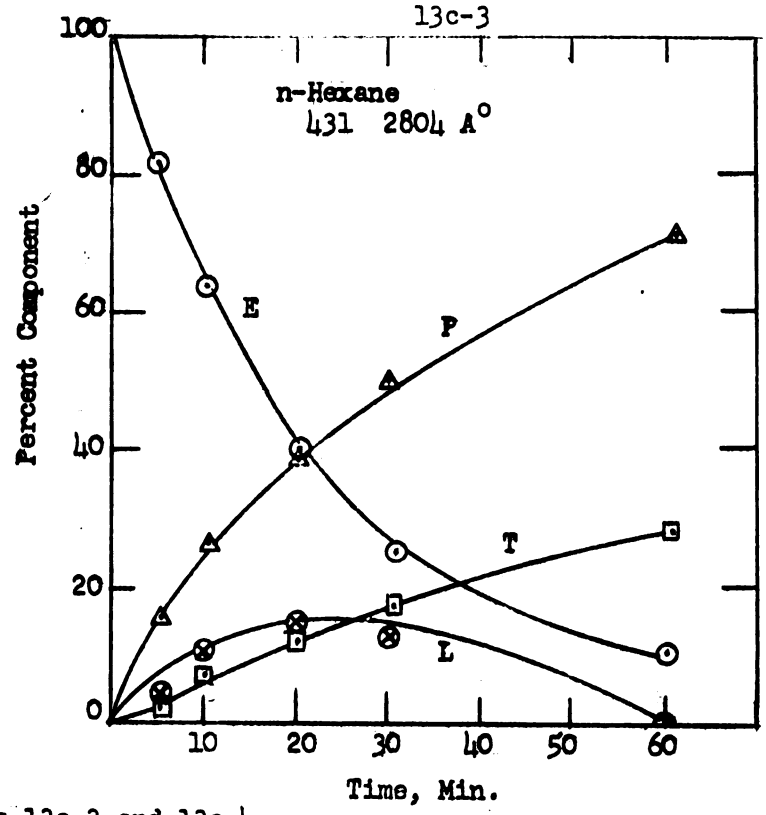

Figures 13c-3 and 13c-4

Composition of Irradiation Mixtures--Sharpe's Data

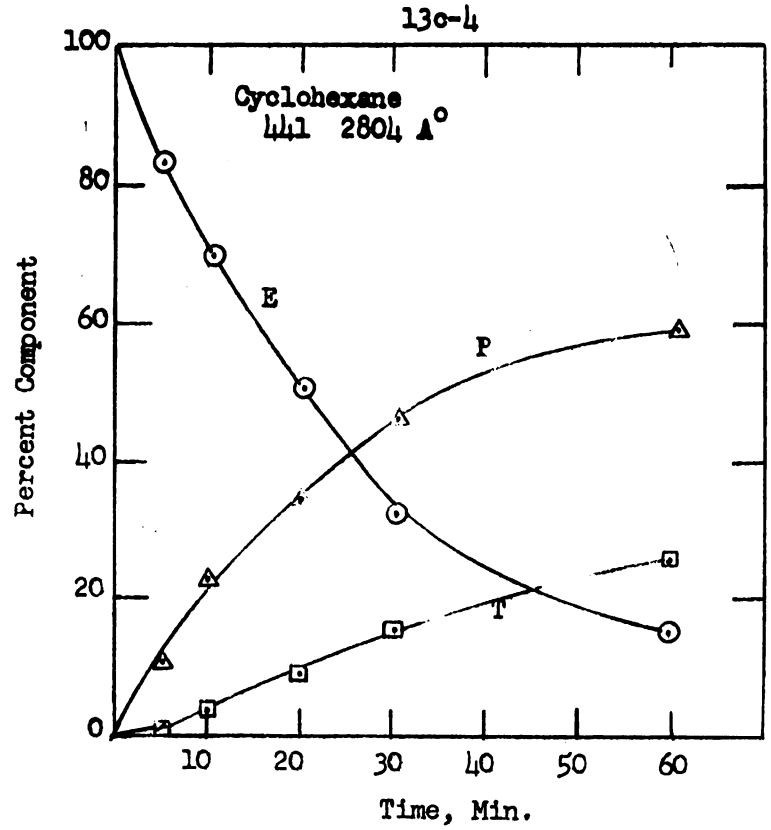

13d-1

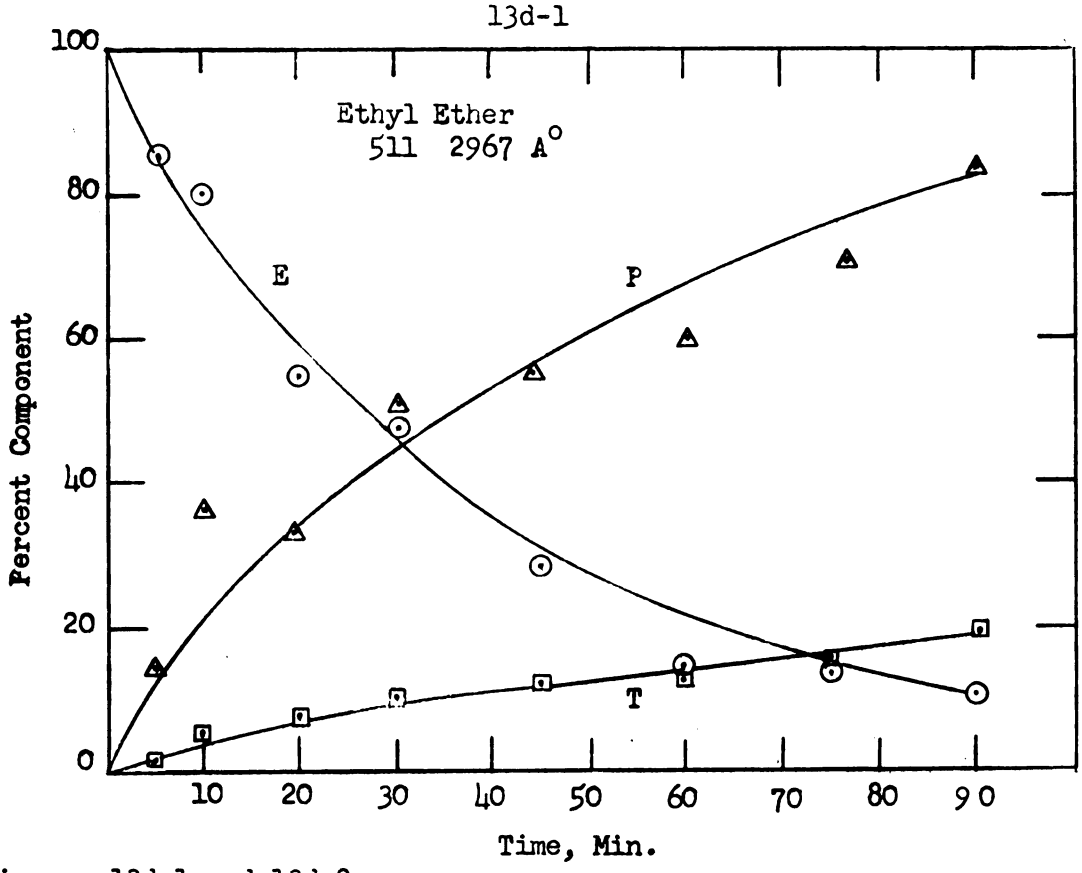

Figures 13d-1 and 13d-2

Composition of Irradiation Mixtures--Sharpe's Data

13d-2

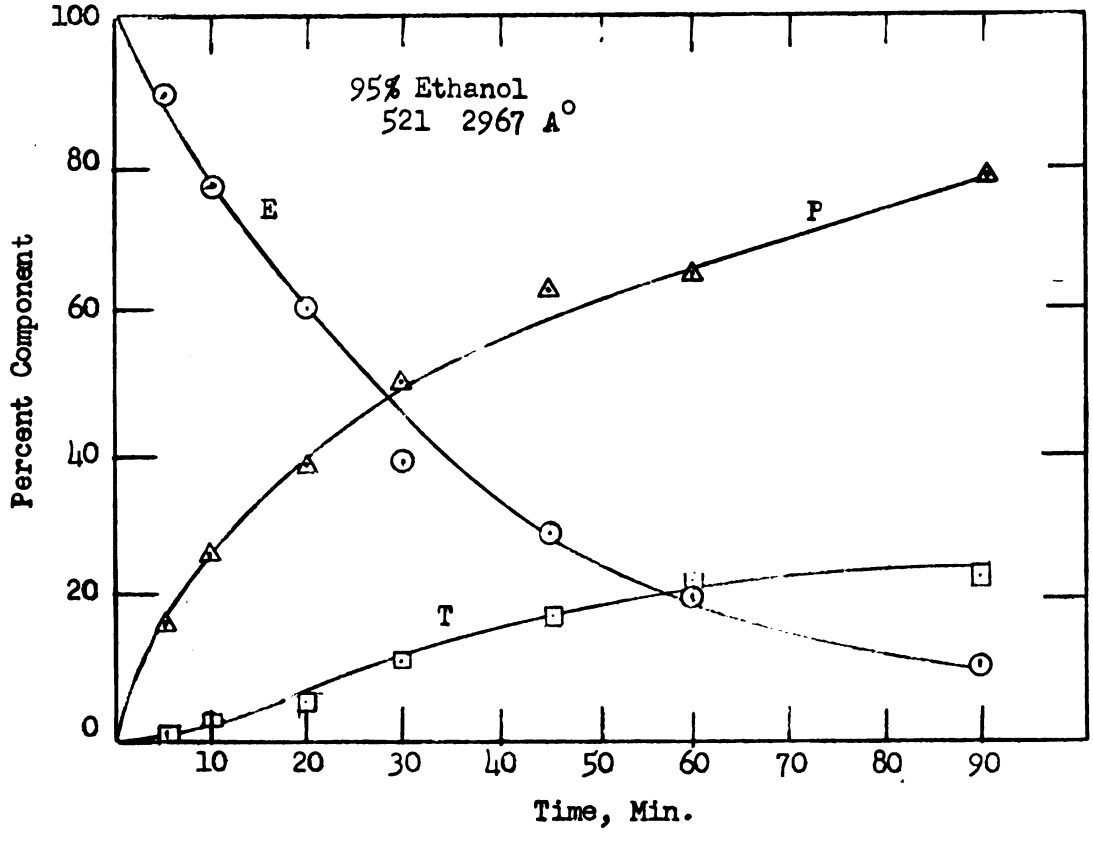

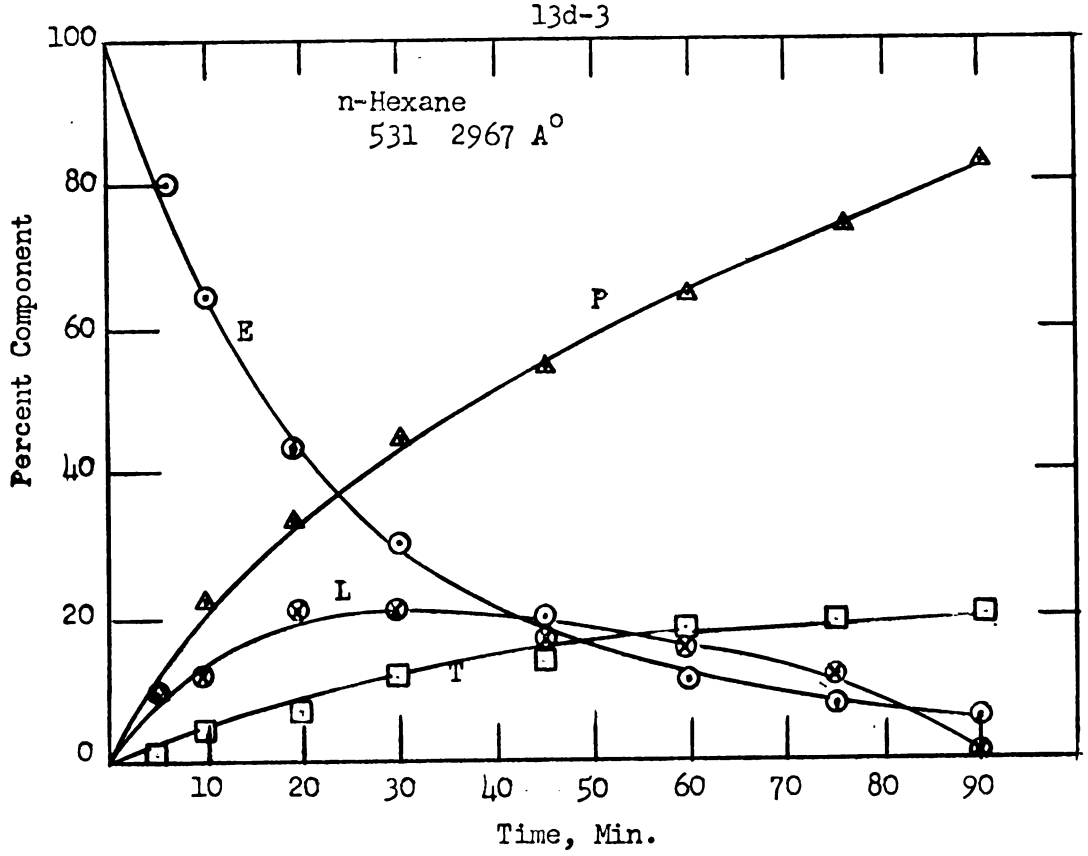

Figures 13d-3 and 13d-4

Composition of Irradiation Mixtures--Sharpe's Data

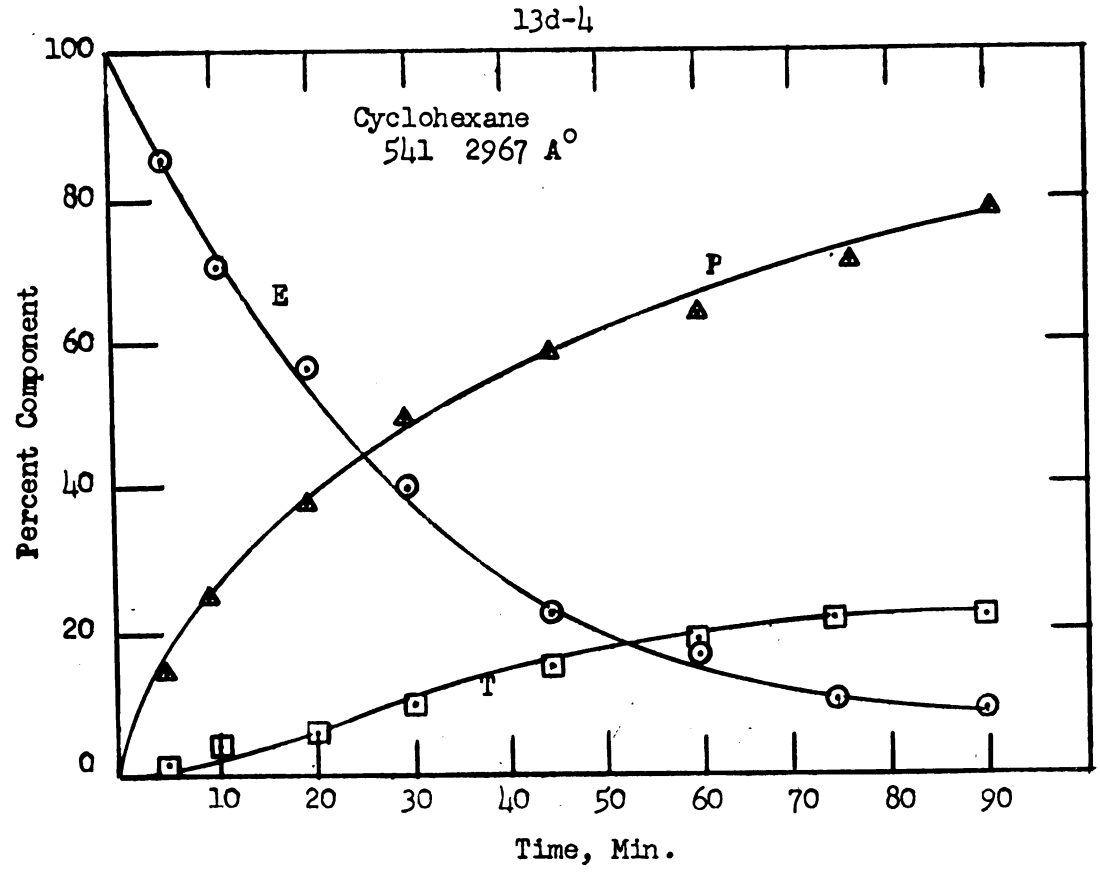

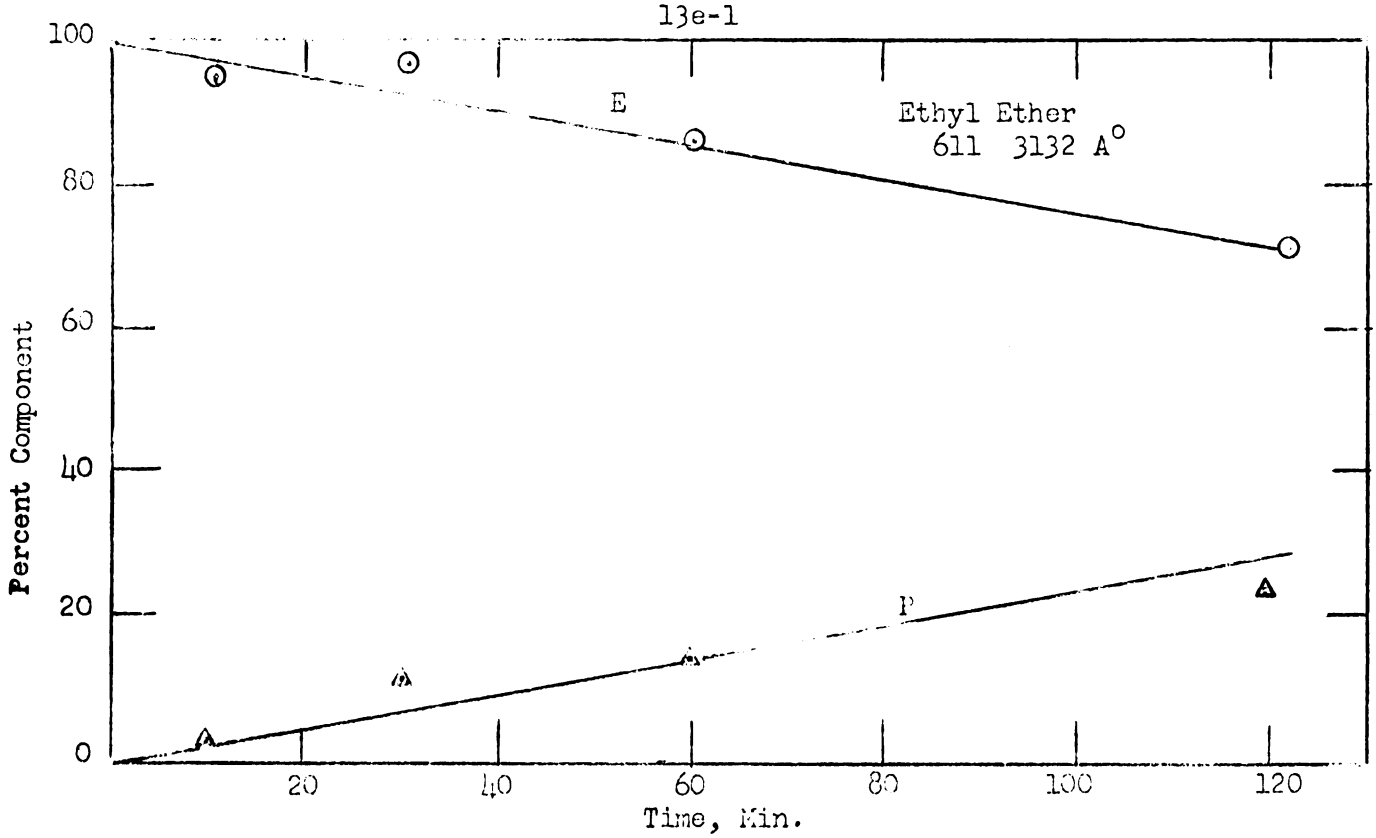

Figures 13e-1 and 13e-2

Composition of Irradiation Mixtures--Sharpe's Data

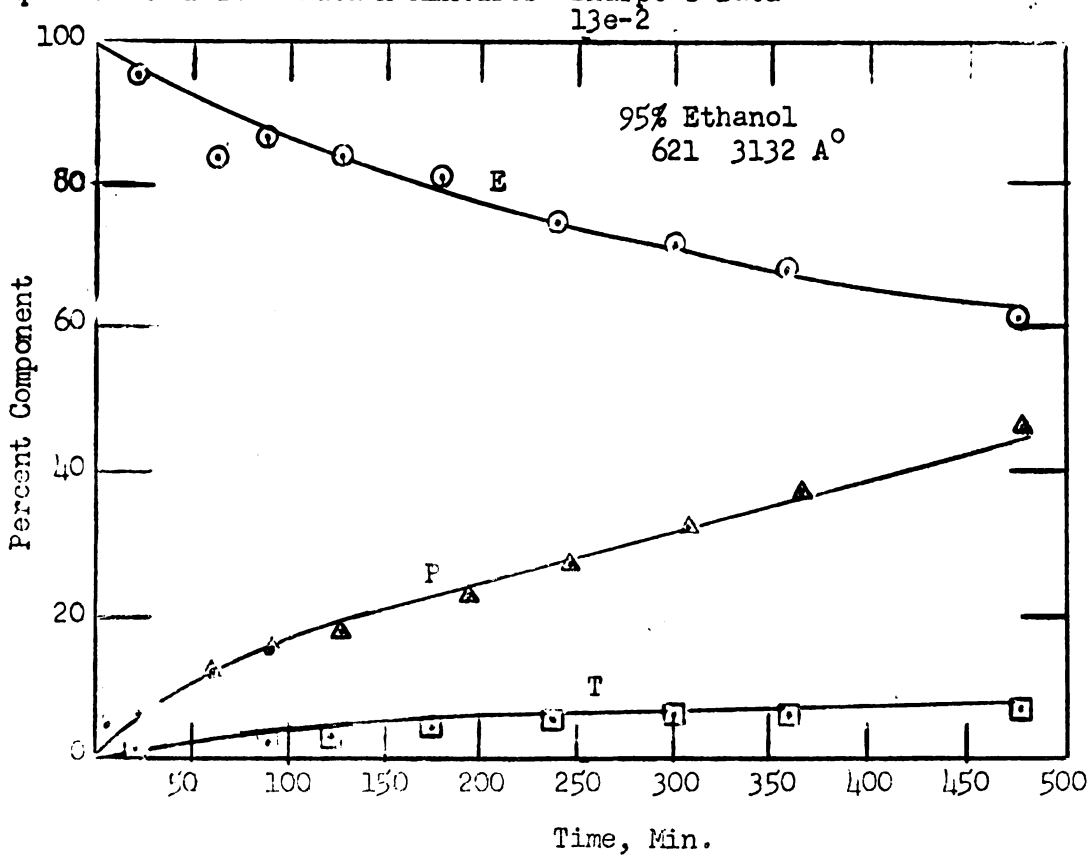

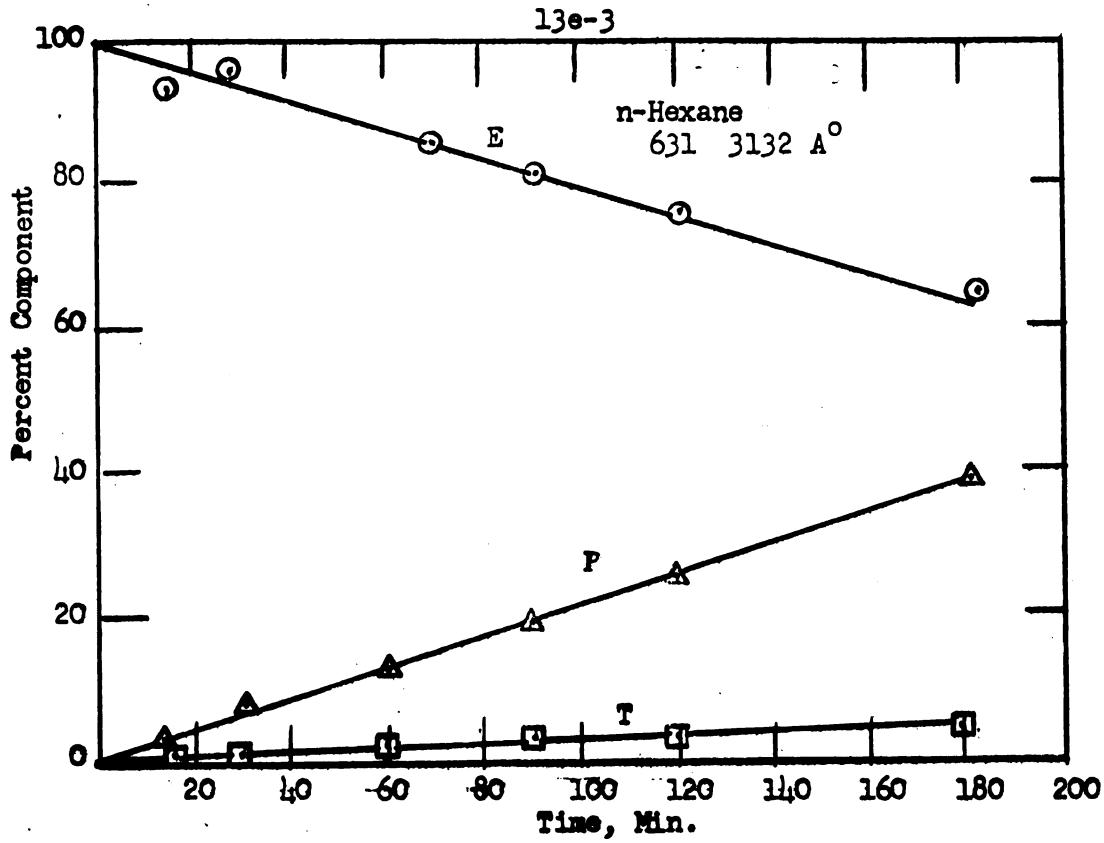

Figures 13e-3 and 13e-4

Composition of Irradiation Mixtures--Sharpe's Data

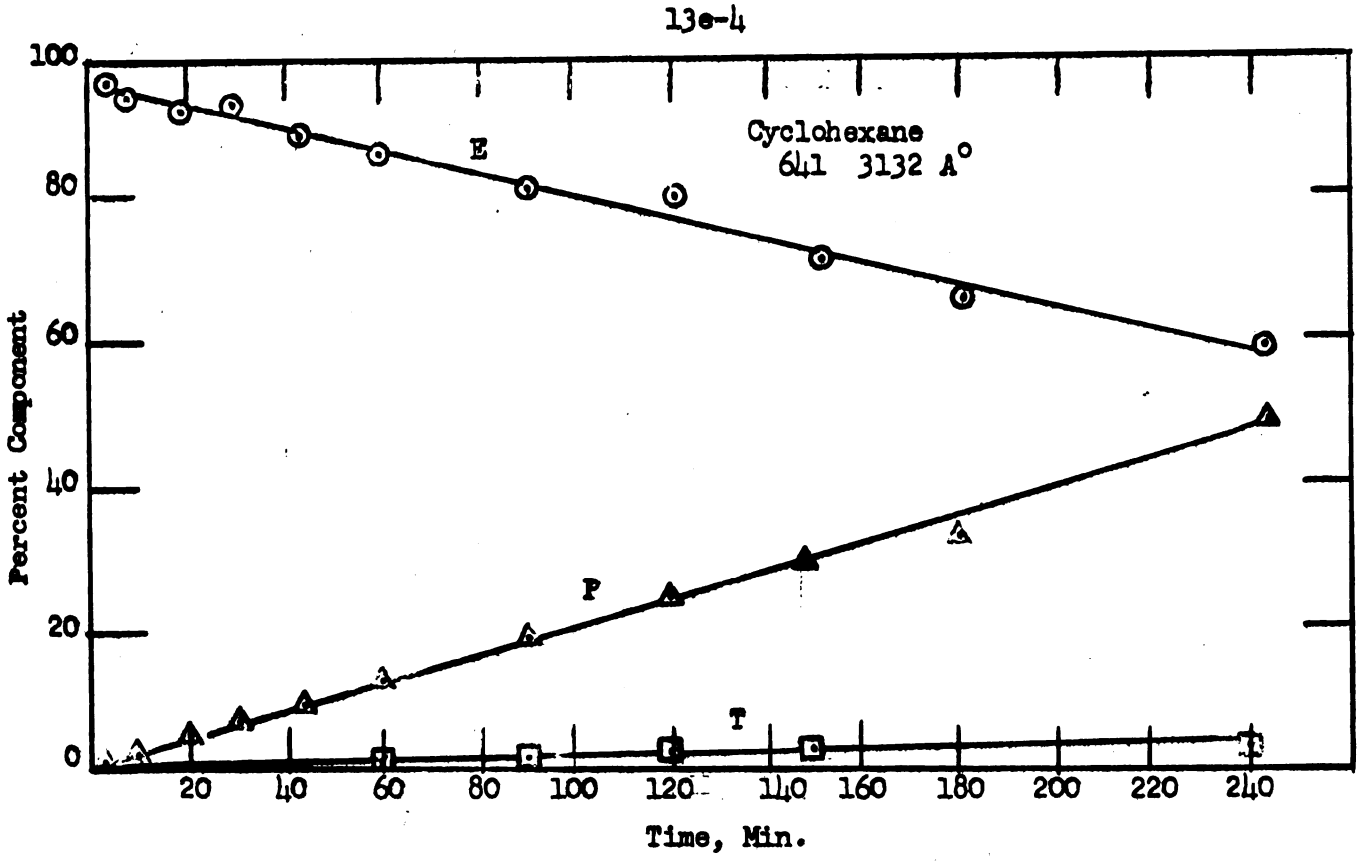

maximize over-irradiation effects. However, regardless of the cause of the build up of apparent negative concentrations, the occurrence of such values does not detract from the validity of the results, since the negative values were generally less than the value of the standard deviation except for very high percentages of conversion of ergosterol. Small negative values were also obtained for tachysterol in a few instances. In all such cases the concentration of the component was considered to be zero.

A remarkable result indicated by the calculations is that calciferol is not formed in appreciable quantities during the irradiation, although precalciferol is always the predominant product, except in some instances of high percentage conversion of ergosterol. The other products of the irradiation mixture, tachysterol and lumisterol, are formed in minor amounts and their relative abundancies are dependent on the conditions of irradiation. It would appear that nature has designed a reaction, which is remarkably free of major side reactions, to produce the desired physiologically active material, calciferol.

The absence of calciferol in irradiation mixtures which have been formed at room temperature may be attributed to the slowness of the thermal conversion of precalciferol to calciferol at room temperature. This observation with respect to calciferol formation substantiates the hypothesis that calciferol is not a primary photochemical product of the irradiation of ergosterol. Further substantiation of this hypothesis is afforded by evidence reported by Havinga and co-workers (47); they have observed that calciferol was not formed during irradiation of ergosterol at -180° C.

At this low temperature, the thermal reaction undoubtedly would have been suppressed.

The recalculated Sharpe data are also in accord with compositions of irradiation mixtures which have been reported by Havinga's group (33,34). In more limited kinetic studies, they have irradiated ergosterol in ethanol at 2537 A°. The concentrations of ergosterol, tachysterol, and precalciferol were obtained as functions of time of irradiation. Ergosterol was determined by digitonin precipitation; tachysterol and precalciferol were determined by the antimony trichloride colorimetric procedure (29). They have reported that ergosterol is converted to precalciferol in a yield of 85% and the remainder of the conversion product consists of tachysterol. In addition they report that irradiation of precalciferol results in the formation of tachysterol in almost quantitative yield. The latter observation is in accord with Sharpe's data obtained at low irradiating wavelength, i.e., 2537 and 2654 A°, in which tachysterol was obtained in relatively high abundance during the latter stages of the irradiation, after a build up of precalciferol had occurred.

The compositions of the irradiation mixtures obtained by the application of the matrix method of spectral data are also in general accord with data reported by Shaw and co-workers (39), which were obtained by application of the antimony trichloride colorimetric procedure and a direct spectrophotometric technique to the chromatographic fractions of irradiation mixtures. They chromatographed the irradiated mixture on alumina employing the procedure described in the experimental section.

Qualitative conclusions have been drawn with respect to the effect of wavelength of irradiation and solvent on the relative abundances of the products of the reaction and the rate of disappearance of starting material. Since lumisterol was formed only in minor amounts and the standard deviation for lumisterol was ± 10.3%, it was not possible to determine the effect of solvent and wavelength on lumisterol formation with any degree of certainty, except in the case of long wavelength irradiation-- i.e., 2967 A^{o}-- when appreciable amounts of the compound were formed. Because of the above consideration and the scatter of the calculated lumisterol concentration, plots of concentration vs. time were only drawn for lumisterol when appreciable amounts of the compound were found or when the scatter was not present.

In order to facilitate the deduction of solvent and wavelength effect, comparison of the compositions of the irradiated solutions were made at 50% conversion of ergosterol. The results are summarized in Tables XV and XVI.

In general, for a given wavelength of irradiation (with the exception of the very longest wavelength of 3132 A^{o}) the reaction proceeds most rapidly in n-hexane. It is not possible to draw further conclusions from the data of Table XV, since the time for 50% conversion does not vary significantly for the other solvents. Precalciferol abundance was relatively independent of solvent at a given wavelength of irradiation, with the exception of irradiation at 2967 A^{o}; there is a particularly large difference between the amounts of precalciferol in 95% ethanol (47.5%) and in n-hexane

TABLE XV

SOLVENT EFFECT ON RATE OF DISAPPEARANCE OF ERGOSTEROL

Wavelength / Solvent	Relative Time for 50% Conversion* 2537 A°	2654 A°	2804 A°	2967 A°	3132 A°**
Diethyl Ether	1.00	1.00	1.00	1.00	1.00
95% Ethanol	1.25	1.04	0.87	1.06	2.54
n-Hexane	0.89	0.76	0.74	0.63	1.10
Cyclohexane	1.36	1.21	0.87	0.91	1.23

*Based on a value of 1.00 for the 50% conversion of ergosterol in diethyl ether at the given wavelength.

**Time for 40% conversion; extrapolated in some cases.

(28.2%). At the shorter wavelengths of irradiation, 2537 and 2654 A°, the formation of tachysterol is clearly greater in 95% ethanol and cyclohexane than in diethyl ether or n-hexane. The latter distinction is not as discernible at the longer wavelengths. Because of the limitations of the analytical data with respect to the concentration of lumisterol, the effect of solvent on the abundance of this component cannot be deduced with a reasonable degree of certainty. However it should be noted that lumisterol was formed in significant amounts only in n-hexane and diethyl ether.

The detailed interpretation of these results will be presented in a later section. However, it should be pointed out that, as reported by Sharpe (37), the solvent effect appears to correlate with solvent viscosity. The viscosities of the solvents employed in Sharpe's work are listed on p. 112 (53):

TABLE XVI

SOLVENT AND WAVELENGTH EFFECT ON PRODUCT COMPOSITION

Wavelength / Product	Composition, Percent* 2537 A°	2654 A°	2804 A°	2967 A°	3132 A°
			Diethyl Ether		
L	9.5	7.0	--	--	--
T	11.9	11.3	10.5	6.0	--
P	31.2	32.1	43.9	38.0	42.4
			95% Ethanol		
L	--	5.2	--	--	--
T	22.2	13.1	7.2	8.6	5.9
P	30.5	32.0	36.2	47.5	43.7
			n-Hexane		
L	--	12.0	9.8	17.2	--
T	13.7	10.7	7.8	4.0	2.2
P	31.1	29.5	34.5	28.2	43.0
			Cyclohexane		
L	--	--	--	--	--
T	17.0	15.6	6.9	6.0	3.0
P	31.7	35.9	33.9	40.5	45.0

*Composition at 50% conversion of ergosterol except for irradiations at 3132 A° in which case the compositions are given for 40% conversion of ergosterol.

Solvent	Temperature, °C.	Viscosity, Centipoise
Diethyl ether	25	0.222
n-Hexane	25	0.294
Cyclohexane	17	1.02
95% Ethanol	25	2.35

The rate of disappearance of ergosterol was generally most rapid in n-hexane and in diethyl ether, solvents of low viscosity; however, the data are not consistent for diethyl ether, showing good agreement at 2537, 2654, and 3132 A°., but slower disappearance of ergosterol than in higher viscosity solvents at 2804 and 2967 A°. Lumisterol was formed in significant quantities only in the solvents of low viscosity, n-hexane and diethyl ether, while tachysterol abundance was greatest in solvents of high viscosity, cyclohexane and 95% ethanol. Attributing the solvent effect in Sharpe's results exclusively to viscosity is open to criticism, however, since the solvents used also differed structurally. Functional groups such as the hydroxyl group of ethanol may have caused certain specific effects by interaction with the components of the irradiation mixture.

The observed wavelength effect can be attributed largely to the relative wavelength variations of the absorption spectra of the components, leading to operation of the "inner-filter effect." This effect can be evaluated and the results compared independently of it by means of quantum yield calculations based on a kinetic study, as reported in a later section of the present work.

B. Irradiation Results--Kinetic Study

The present investigation of the photochemical isomerization of ergosterol was undertaken to obtain data from which a quantitative kinetic analysis could be made. Sharpe's recalculated results were utilized in the planning of this experimental work. Before presentation of the quantitative treatment, the results of this investigation will be discussed in a qualitative manner.

Sharpe's results indicated the occurrence of a solvent effect which might be attributed to the viscosity of the solvents, but the observed effect could also be attributed to a specific polar interaction, since the solvent of highest viscosity, 95% ethanol, was also a polar solvent. Still another possible explanation of the solvent effect in Sharpe's results is that the use of thin, unstirred cells may have led to a diffusion controlled process, in which the same molecules tended to remain in the more intense portion of the beam to undergo successive radiational changes. This would lead to greater tachysterol build-up in more viscous solvents, where the initially formed precalciferol would absorb another quantum of light to undergo the next step without diffusing out of the most intense portion of the beam. It was noted by Sharpe, however, that the solvent effect can not be attributed solely to such factors, since it has been observed by other investigators irradiating refluxing solutions.

The uncertainty of interpretation of the solvent effect was resolved in this study by employing structurally similar solvents to obtain a variation of viscosity, and by carrying out the kinetic studies in stirred

cells of 1.0 cm. thickness. Under Sharpe's conditions of irradiation, the reaction proceeded rapidly and the probability of occurrence of over-irradiation products was increased. The rate of the reaction was decreased in this study by employing narrower slit widths and a larger volume of solution in the cell. The use of narrow slit widths also increased the degree of monochromaticity of the radiation, which yielded more definitive results on the effect of wavelength.

Concentrations of the irradiation mixtures of the current study were calculated by application of matrix (1) to the ultraviolet absorption spectra of the irradiated mixtures.* The data are presented in Tables XVIIa-XVIIc, and in Figures 14a-1 to 14c-5. The results are expressed as weight percentages; although results are presented to the third decimal place, the figures do not possess this significance. It was convenient in the computational work to carry out the calculations as presented in the tables; the values employed in the kinetic calculations are those tabulated. Results were appropriately rounded off at later stages of the calculations.

The application of matrix (1) to the data of this investigation yielded results quite similar to those obtained by application of matrix (0) to Sharpe's data. However, in the calculations based on the present study, the consistent growth of negative values for calciferol was not observed. The negative values that were obtained were generally of smaller magnitude, and the values were more uniformly scattered about the zero concentration level.

---

*The absorbancies of the irradiated solutions are tabulated in Appendix II.

TABLE XVIIa

COMPOSITION OF IRRADIATION MIXTURES--KINETIC STUDY--2537 A°
(Slit Width 1.50 mm.)

Time, Min.	Calculated Composition, Percent E	L	T	P	D
Isopropyl alcohol--Run No. III-10					
Initial Conc. of Ergosterol 0.00242 gms./100 ml.					
20	92.518	2.555	0.710	5.310	-1.093
40	89.887	1.748	1.082	8.647	-1.364
60	83.400	4.230	1.892	12.634	-2.156
90	80.430	4.645	2.499	14.917	-2.491
120	76.655	4.922	2.983	16.578	-1.138
185	74.233	1.012	5.487	20.797	-1.529
245	62.614	4.749	9.042	26.158	-2.563
305	58.802	5.413	11.356	25.845	-1.416
365	55.186	3.072	14.752	29.136	-2.146
410	48.884	5.585	17.386	30.789	-2.644
20% Glycerol--Run No. III-14					
Initial Conc. of Ergosterol 0.00242 gms./100 ml.					
20	92.908	1.948	0.549	5.975	-1.380
40	90.805	1.559	1.071	7.413	-0.848
60	89.843	-2.774	1.876	12.476	-1.421
90	85.700	-1.166	2.356	13.819	-0.709
120	81.557	-0.266	3.094	16.968	-1.353
180	76.395	-0.550	5.095	20.269	-1.209
240	64.048	1.608	9.712	28.539	-3.907
330	59.865	1.421	12.849	29.066	-3.201
420	57.465	-3.703	16.890	31.370	-2.022
n-Hexane--Run III-22					
Initial Conc. of Ergosterol 0.00216 gms./100 ml.					
20	92.476	5.222	-0.372	2.730	-0.056
40	90.446	3.694	-0.309	7.587	-1.418
60	88.165	2.891	0.276	10.621	-1.953
90	84.206	2.250	1.038	15.087	-2.581
120	81.904	1.932	1.479	17.369	-2.684
185	74.562	1.782	3.702	23.528	-3.574
240	67.128	2.262	6.797	28.539	-4.726
330	57.742	4.101	10.164	33.520	-5.527
420	47.752	5.205	15.261	38.395	-6.613

Continued

TABLE XVIIa - Continued

Time, Min.	Calculated Composition, Percent E	L	T	P	D
20% Mineral Oil--Run III-18 Initial Conc. of Ergosterol 0.00216 gms./100 ml.					
20	95.714	0.646	-0.313	5.616	-1.663
40	93.773	-1.388	0.535	9.007	-1.927
60	88.661	0.707	0.832	12.188	-2.388
90	85.753	-0.977	1.716	15.633	-2.125
120	80.078	2.106	2.315	17.472	-1.971
185	75.397	-4.948	5.540	27.194	-3.183
240	67.822	-3.741	8.209	32.255	-4.545
330	60.247	-4.426	12.623	38.753	-7.197
404	51.300	-0.724	15.911	40.742	-7.229

TABLE XVIIb

COMPOSITION OF IRRADIATION MIXTURES--KINETIC STUDY--2804 A°
(Slit Width 2.00 mm.)

Time, Min.	Calculated Composition, Percent E	L	T	P	D
Isopropyl alcohol--Run No. II-14					
Initial Conc. of Ergosterol 0.00242 gms./100 ml.					
14	93.156	0.819	0.558	7.650	-2.183
29	91.051	-1.402	0.519	11.431	-1.499
49	84.698	0.330	0.016	15.733	-0.777
58	78.528	0.540	1.580	21.143	-1.791
88	71.398	-2.315	3.470	30.422	-2.975
118	67.989	-5.637	5.455	34.206	-2.013
213	51.396	-7.070	10.488	47.010	-1.824
273	39.782	-3.314	14.946	50.547	-1.961
318	35.749	-1.816	16.993	51.190	-2.116
20% Glycerol--Run No. II-9					
Initial Conc. of Ergosterol 0.00242 gms./100 ml.					
15	92.806	-0.852	1.234	9.848	-3.036
30	84.627	2.646	0.763	13.389	-1.425
45	83.653	-1.524	1.177	18.370	-1.676
60	72.629	3.918	2.523	23.402	-2.472
90	73.372	-3.753	3.082	28.794	-1.495
120	65.843	-2.474	3.702	33.350	-0.421
150	58.432	-4.218	6.550	40.633	-1.397
240	45.490	-6.468	12.943	50.592	-2.557
305	38.730	-9.038	16.038	53.372	0.898
365	38.157	-10.959	16.384	58.533	-2.115
n-Hexane--Run No. II-18					
Initial Conc. of Ergosterol 0.00216 gms./100 ml.					
15	97.185	-2.034	-0.614	5.346	0.117
30	88.917	1.544	-0.545	0.930	9.154
45	74.764	9.544	0.188	9.041	6.463
60	77.792	4.196	-0.124	11.434	6.702
90	62.559	7.958	-0.863	23.678	6.668
120	60.394	-3.172	4.665	32.671	5.442
150	55.042	-3.733	6.082	37.508	5.101
230	38.240	-1.817	11.101	43.566	8.910
290	25.970	2.070	16.062	48.776	7.122
350	19.289	1.341	19.464	54.257	5.649

Continued

TABLE XVIIb - Continued

Time, Min.	Calculated Composition, Percent E	L	T	P	D
20% Mineral Oil--Run No. II-24 Initial Conc. of Ergosterol 0.00216 gms./100 ml.					
15	89.968	2.373	1.146	7.983	-1.470
30	86.054	1.146	1.091	12.863	-1.154
44	81.969	1.941	1.897	21.271	-3.196
59	77.892	-4.912	2.952	26.548	-2.480
89	64.939	1.697	3.940	31.883	-2.459
119	60.600	-2.315	5.382	39.647	-3.314
189	48.133	-3.337	9.552	48.174	-2.522
249	42.924	-7.962	13.781	56.338	-5.081
324	26.249	4.237	17.833	56.447	-4.766

TABLE XVIIc

COMPOSITION OF IRRADIATION MIXTURES--KINETIC STUDY--2967 A°
(Slit Width 1.50 mm.)

Time, Min.	Calculated Composition, Percent E	L	T	P	D
Isopropyl Alcohol--Run No. II-61					
Initial Conc. of Ergosterol 0.00242 gms./100 ml.					
30	92.485	-0.650	0.975	9.628	-2.438
60	89.640	2.887	0.705	14.487	-1.945
90	79.750	3.513	0.274	16.641	-0.178
120	75.518	1.523	1.419	23.604	-2.064
195	62.853	2.084	3.429	33.318	-1.684
285	54.086	-1.956	6.274	43.817	-2.221
375	41.699	2.297	8.760	48.916	-1.672
20% Glycerol--Run No. II-64					
Initial Conc. of Ergosterol 0.00242 gms./100 ml.					
30	89.691	0.768	1.247	10.164	-1.870
60	86.890	-2.749	2.073	16.771	-2.985
90	82.933	-4.071	2.115	22.010	-2.987
120	72.932	0.797	3.005	25.281	-2.015
200	64.931	-2.935	4.536	35.245	-1.777
290	53.780	-2.720	7.397	43.926	-2.383
380	44.807	-4.241	10.488	51.857	-2.911
n-Hexane--Run No. II-53					
Initial Conc. of Ergosterol 0.00216 gms./100 ml.					
30	92.776	1.298	0.233	8.657	-2.974
60	85.702	1.680	0.886	15.389	-3.657
90	76.854	6.030	1.169	19.540	-3.593
120	73.855	4.340	1.500	24.414	-4.109
180	62.840	8.127	2.469	29.151	-2.587
270	50.034	10.450	4.847	36.812	-2.143
330	40.798	14.638	6.584	40.258	-2.278
375	39.796	9.844	7.980	44.781	-2.401
n-Hexane--Run No. II-67					
Initial Conc. of Ergosterol 0.00216 gms./100 ml.					
330	43.939	10.345	6.290	38.071	1.355
330*	42.368	12.492	6.437	39.164	--
375	40.993	6.132	7.884	44.270	0.721
375*	40.394	7.988	7.932	44.526	--
435	33.783	9.886	8.985	45.822	1.524
495	25.432	14.613	10.558	47.177	2.220
560	22.626	11.469	11.863	52.444	1.598

*Average compositions, II-53, II-67.

TABLE XVIIc - Continued

Time, Min.	Calculated Composition, Percent E	L	T	P	D
20% Mineral Oil--Run II-57 Initial Conc. of Ergosterol 0.00216 gms./100 ml.					
30	94.141	3.175	-0.741	6.156	-2.731
60	89.528	-1.719	-0.036	14.872	-2.645
90	80.134	2.733	0.858	19.742	-3.467
120	74.658	2.309	1.167	24.582	-2.716
180	63.755	3.703	2.989	32.896	-3.343
285	51.076	3.018	6.074	43.949	-4.117
360	44.216	4.616	7.698	46.378	-2.908
420	37.184	3.567	10.214	54.019	-4.984
40% Mineral Oil--Run No. II-70 Initial Conc. of Ergosterol 0.00216 gms./100 ml.					
31	89.956	1.897	0.834	8.554	-1.241
61	80.994	3.246	1.572	16.735	-2.547
91	76.026	3.596	1.709	20.071	-1.402
121	73.004	-0.409	2.591	26.917	-2.103
211	56.920	2.224	5.139	38.126	-2.409
301	46.318	0.950	8.205	47.549	-3.022
391	36.658	3.322	10.614	51.809	-2.403

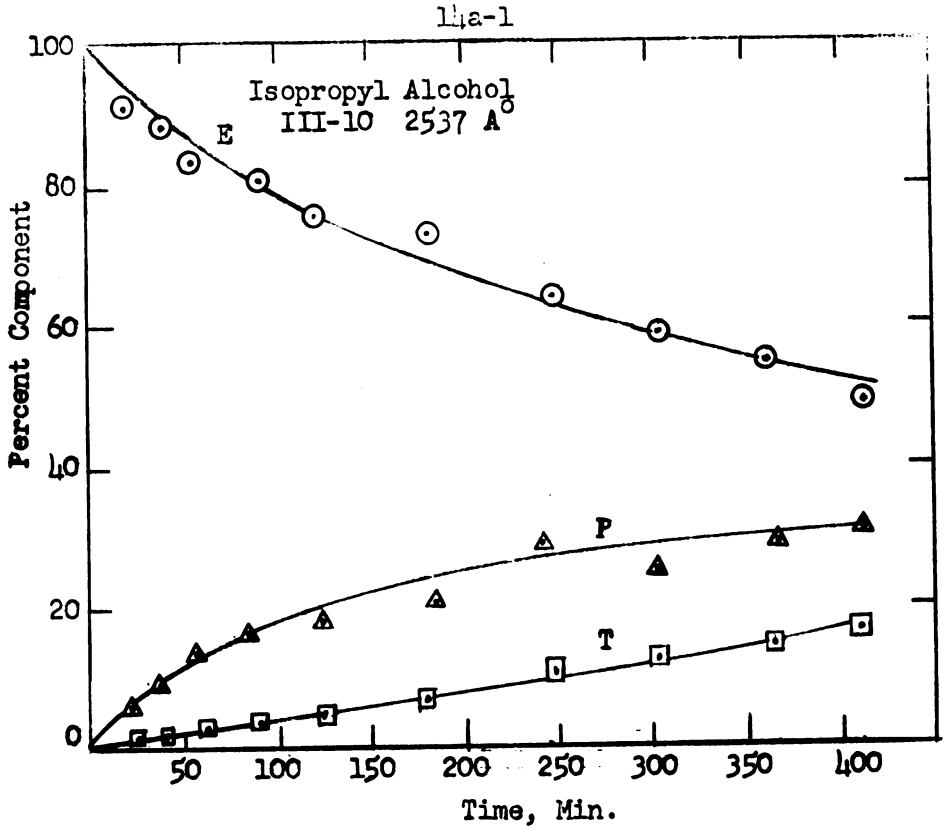

Figures 14a-1 and 14a-2

Composition of Irradiation Mixtures--Kinetic Study

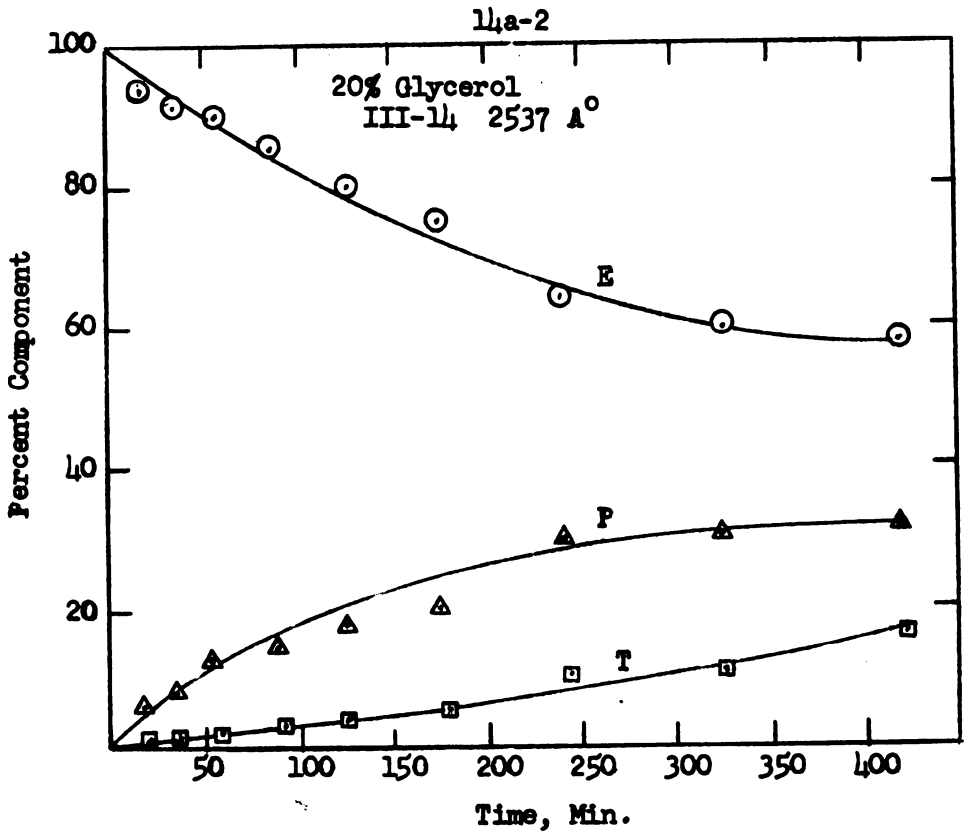

14a-3

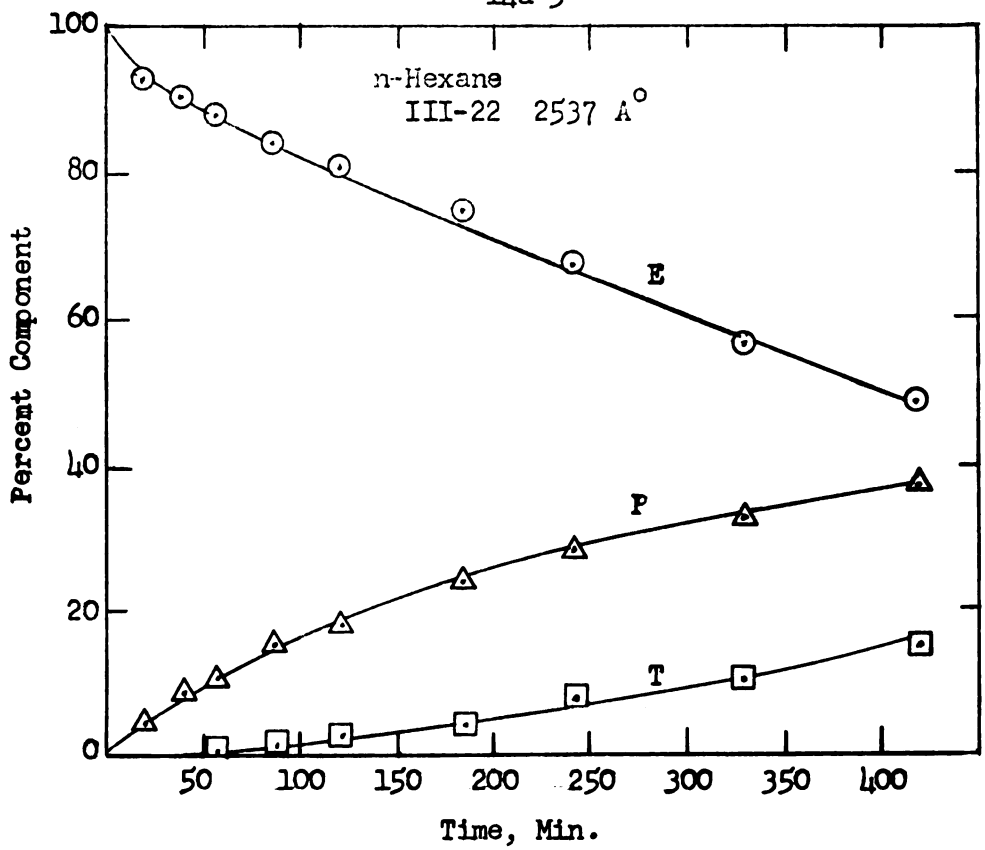

Figures 14a-3 and 14a-4

Composition of Irradiation Mixtures--Kinetic Study

14a-4

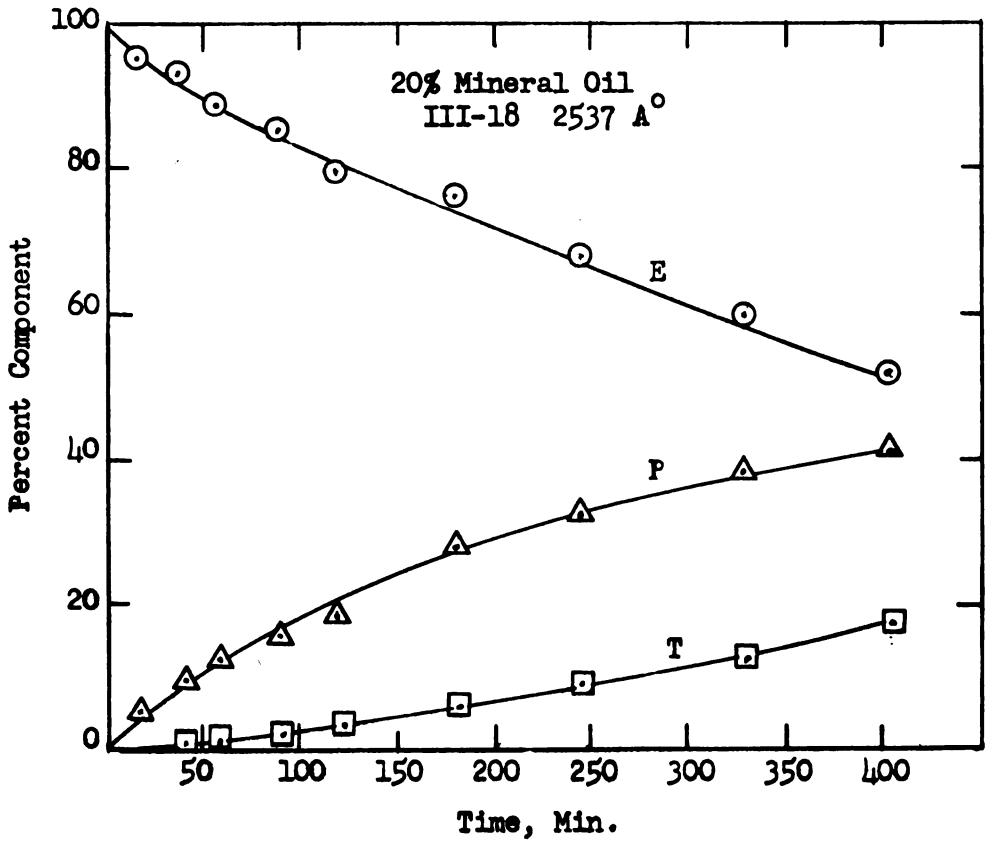

14b-1

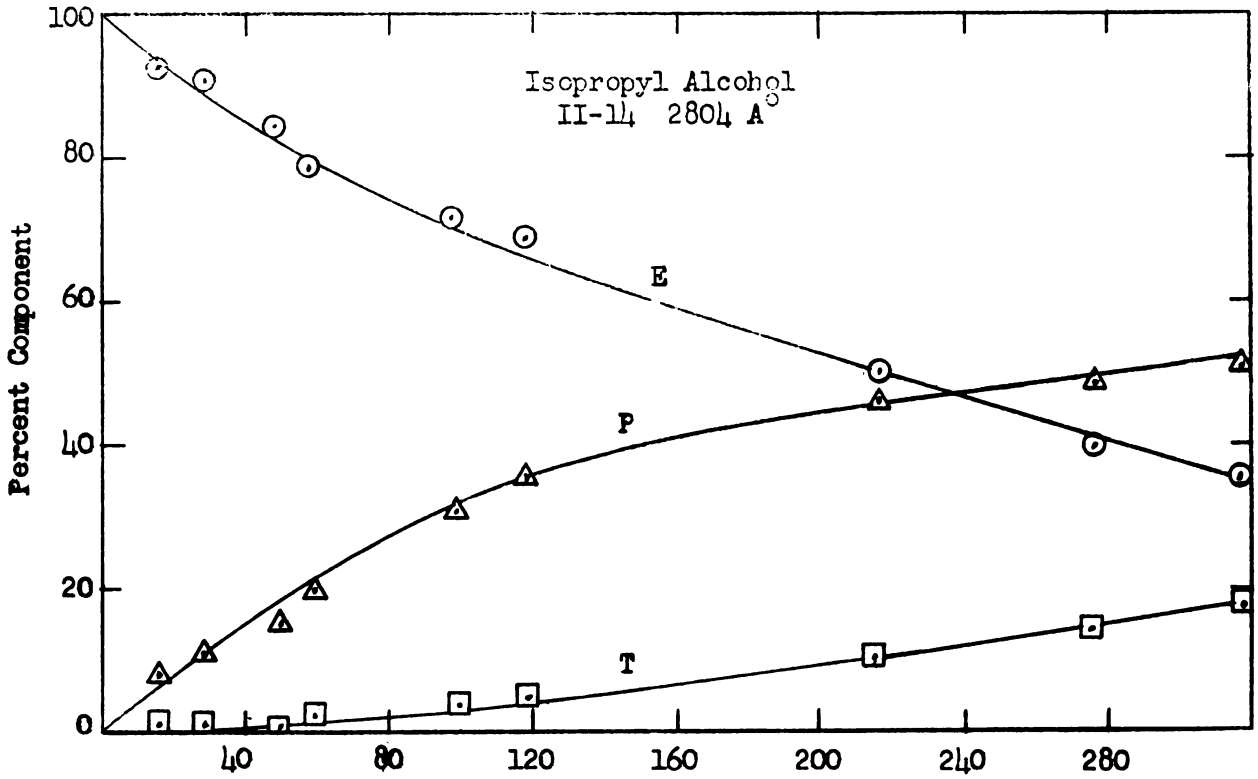

Figures 14b-1 and 14b-2

Composition of Irradiation Mixtures--Kinetic Study

14b-2

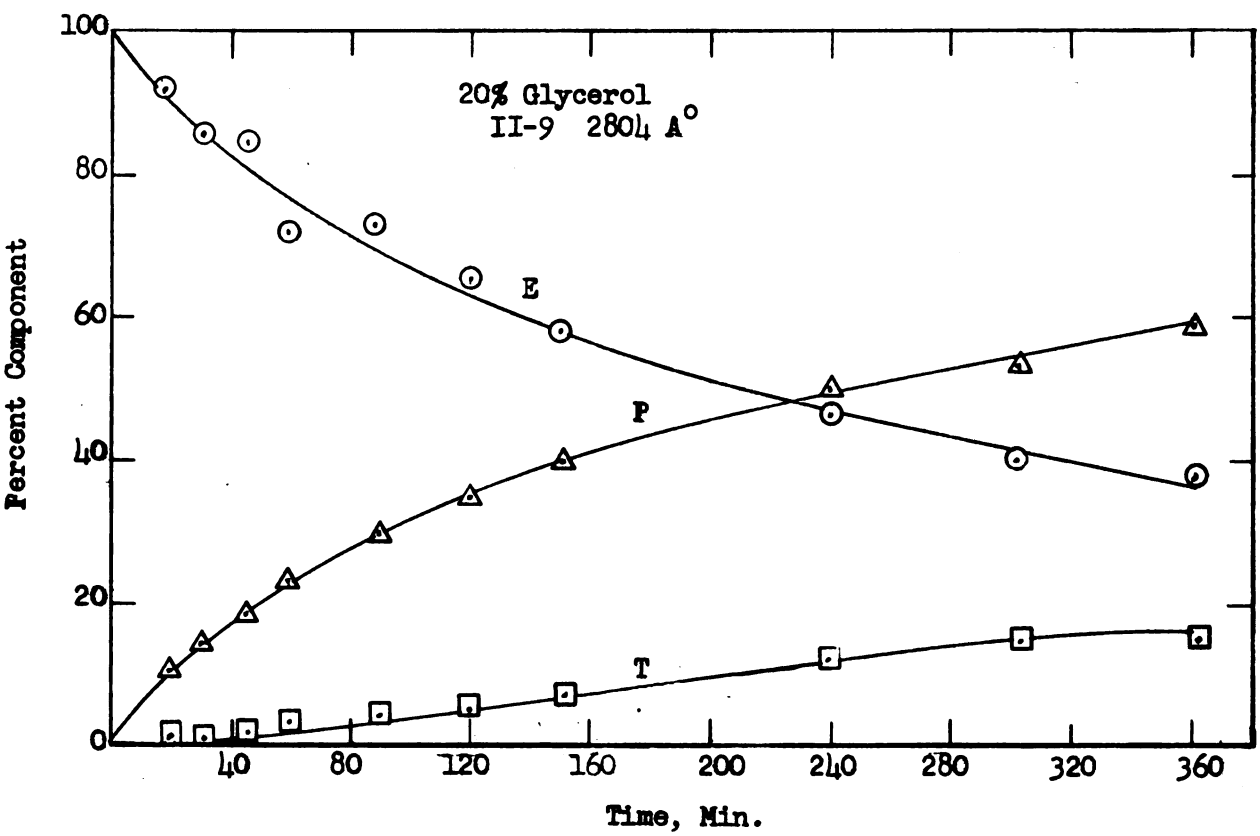

14b-3

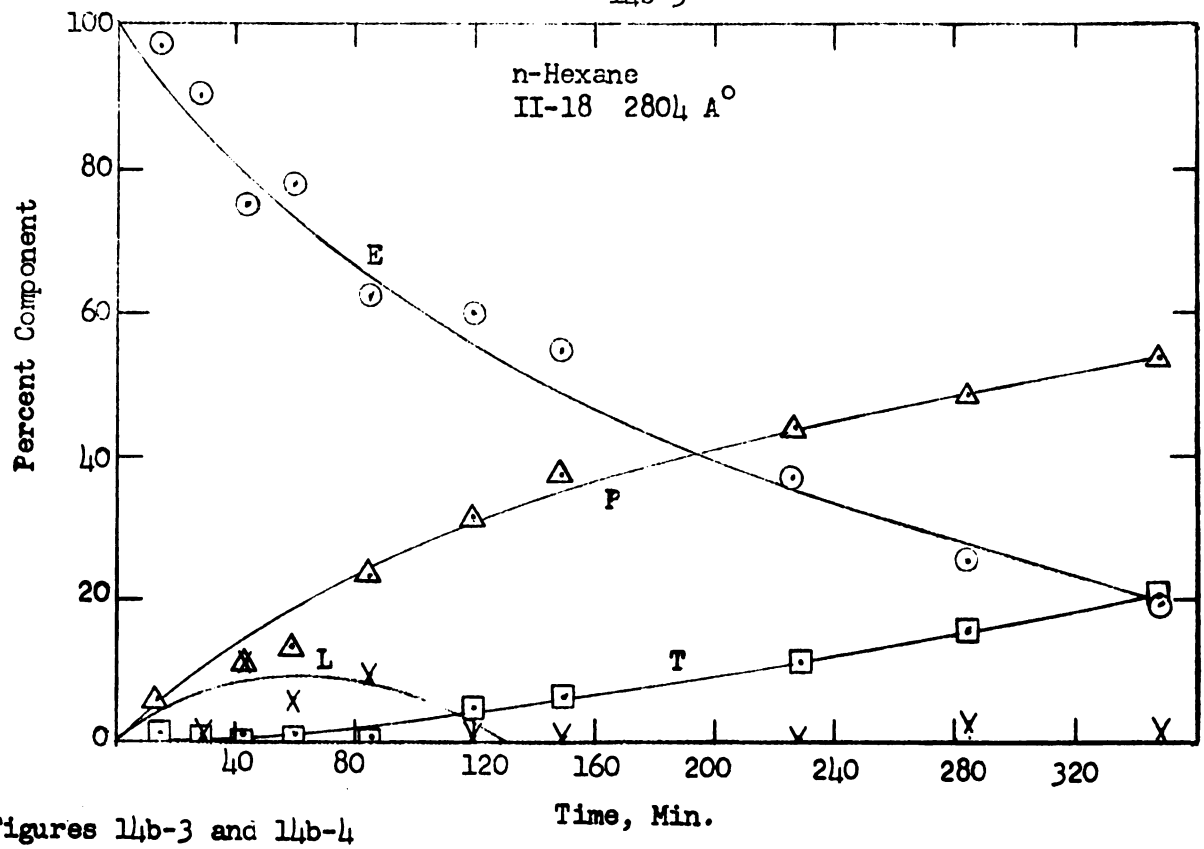

Figures 14b-3 and 14b-4

Composition of Irradiation Mixtures--Kinetic Study

14b-4

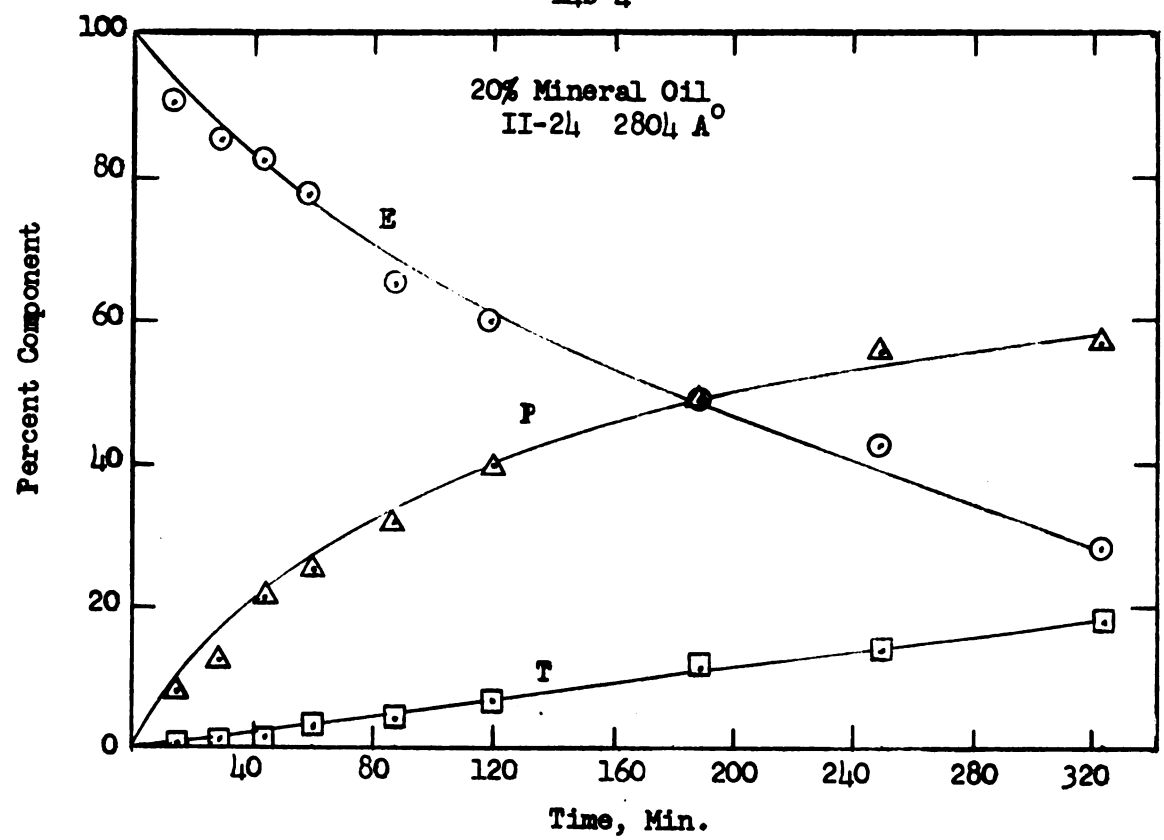

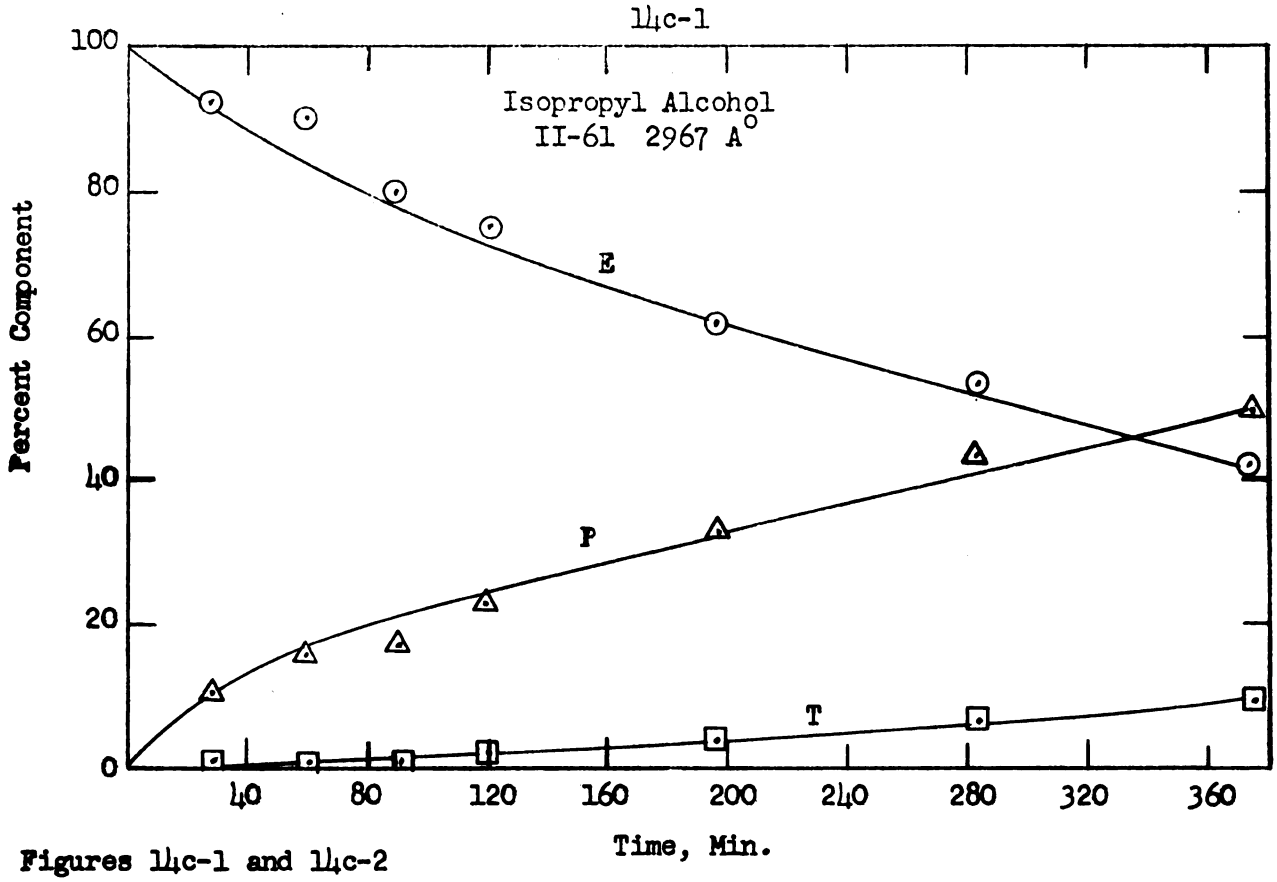

Figures 14c-1 and 14c-2

Composition of Irradiation Mixtures--Kinetic Study

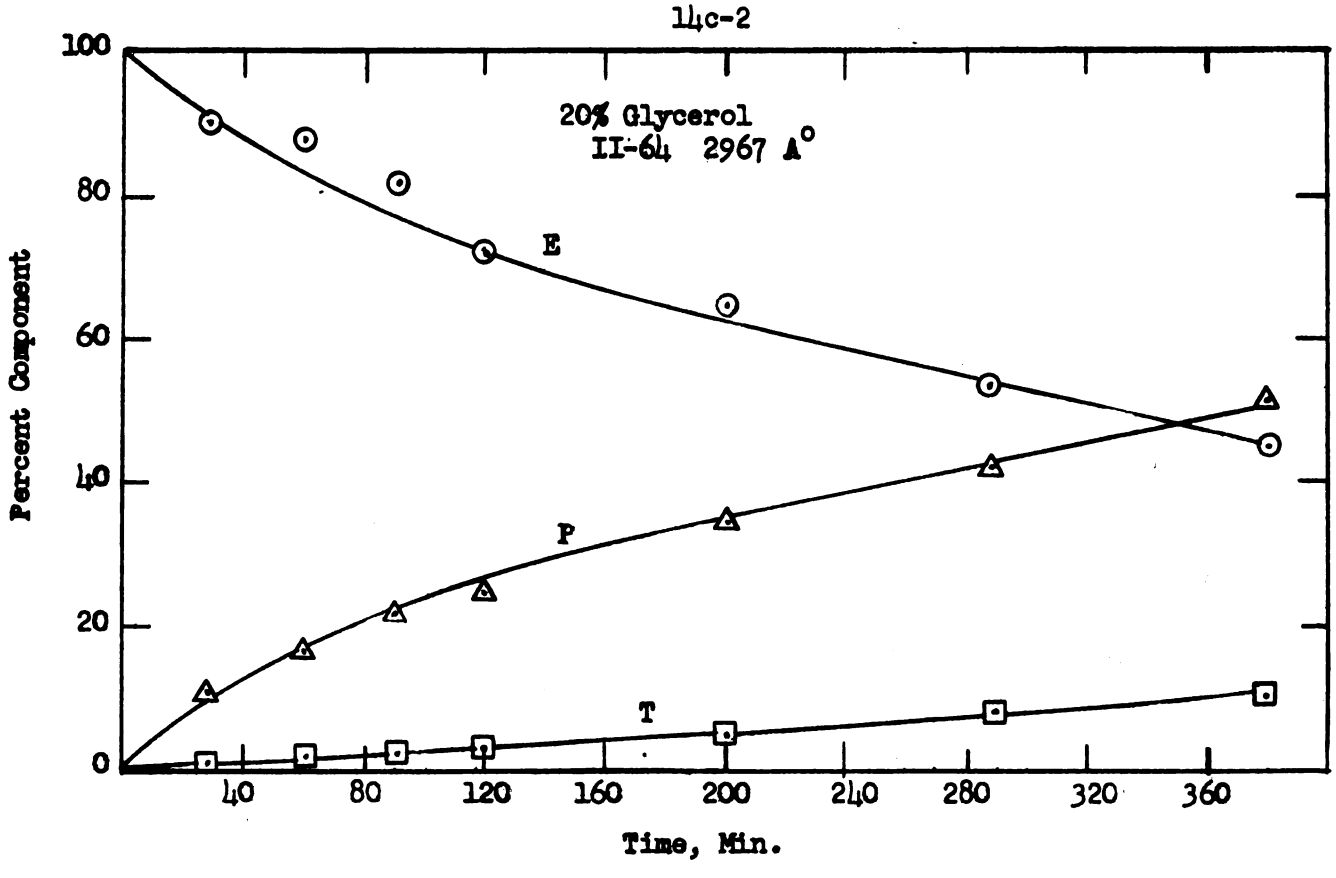

14c-3

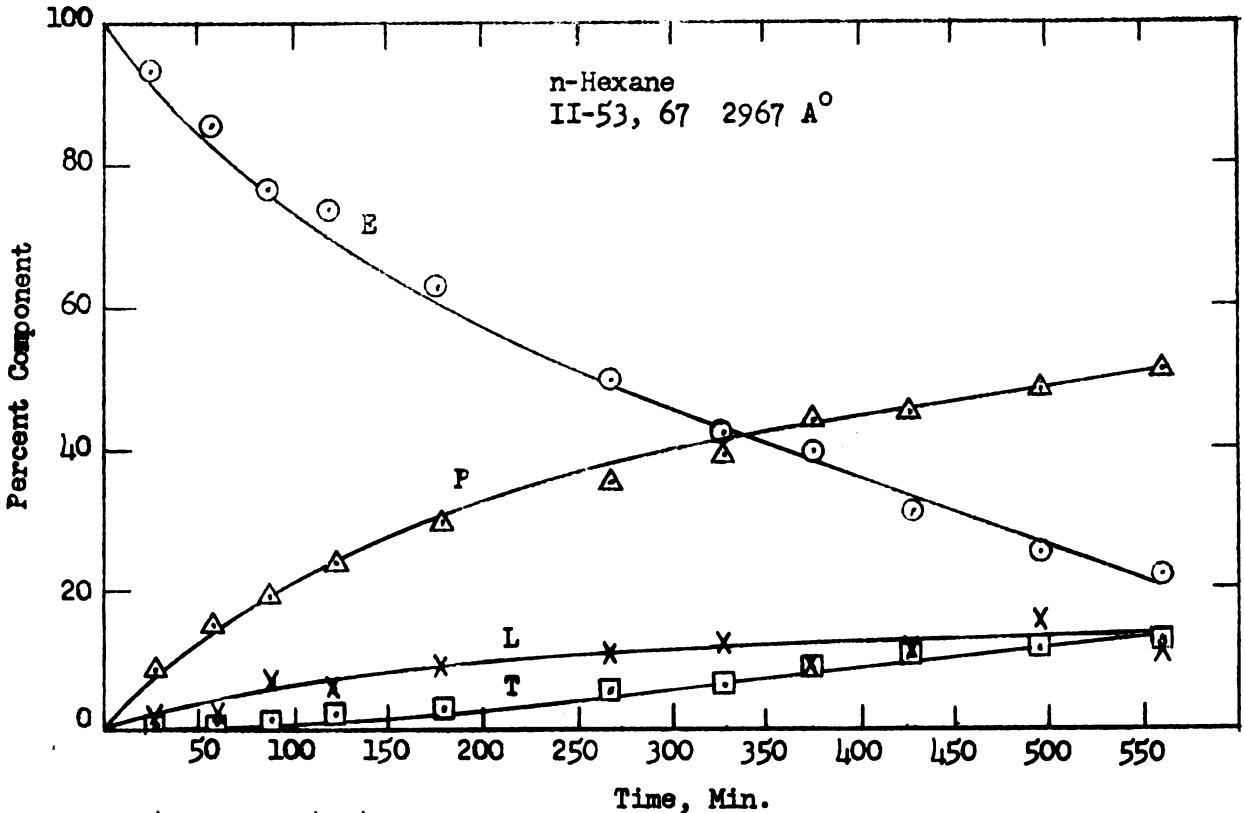

Figures 14c-3 and 14c-4

Composition of Irradiation Mixtures--Kinetic Study

14c-4

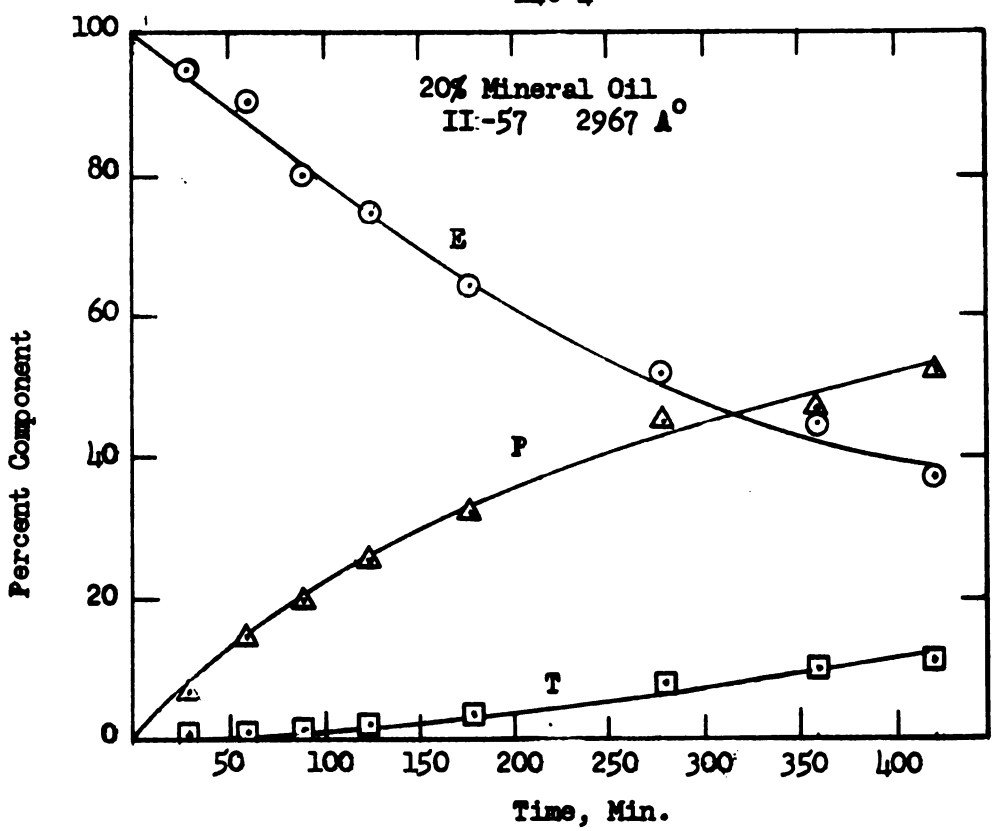

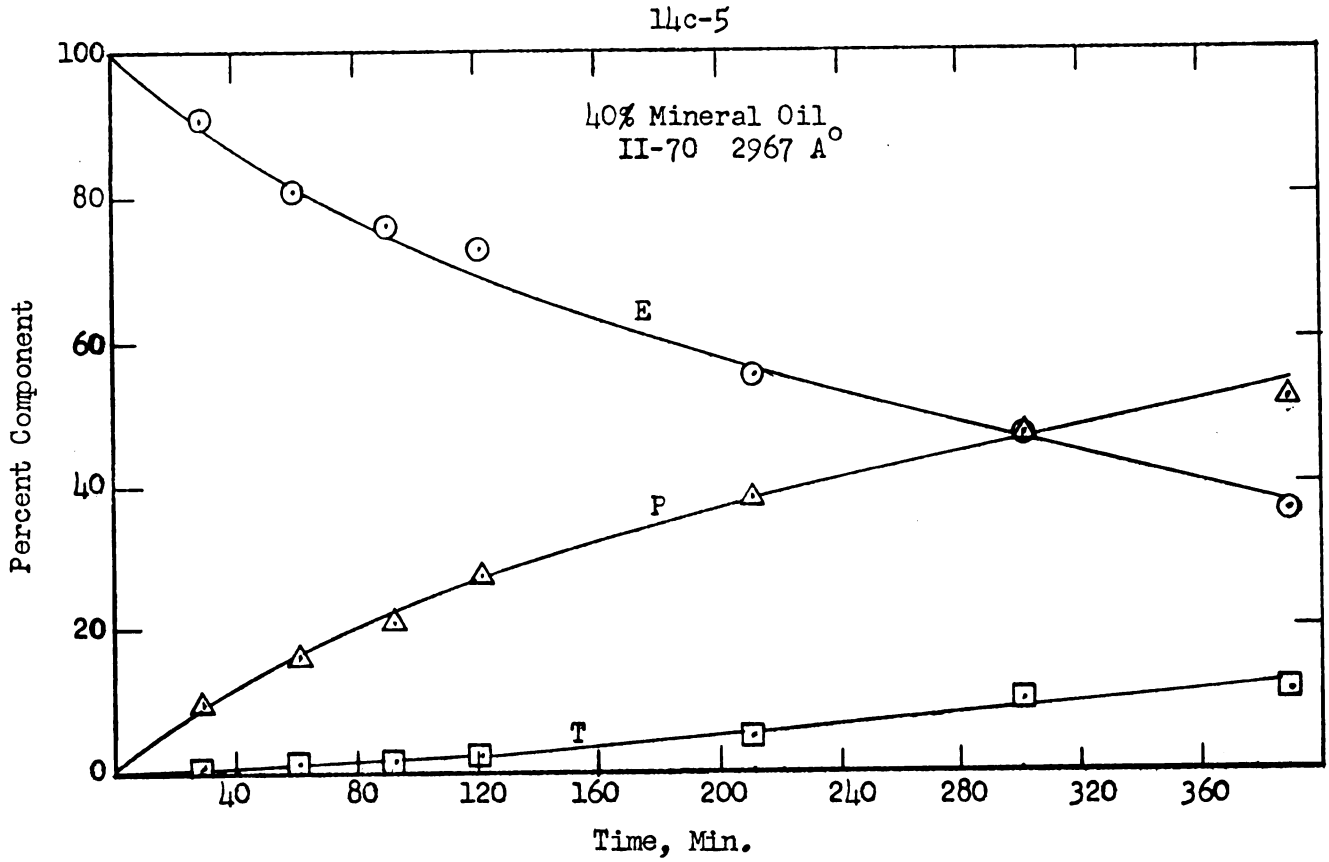

Figure 14c-5

Composition of Irradiation Mixtures--Kinetic Study

A quantitative kinetic treatment of these data was made, and will be presented in a later section. However, it is appropriate to point out certain facts revealed by qualitative examination of the data. In general, there are no gross differences between the results of this investigation and the recalculated Sharpe data. Again, calciferol was not formed in significant quantities throughout any of the irradiation runs, and lumisterol was found in significant quantities only when n-hexane was employed as a solvent. Although lumisterol was found in significant quantities in n-hexane at 2804 A°, the data are not too conclusive, since there are only a few values that are larger than the standard deviation for lumisterol by matrix (1), $\pm$ 4.8%. However, the formation of lumisterol was definitely established in n-hexane at 2967 A°; a consistent build-up (although scatter was present) of the compound was obtained, cf. Figure 14c-3. In addition, the run was repeated without interruption during the first 330 minutes of irradiation, and continued in the usual manner with periodic interruption for the determination of the absorption spectra until about 80% of the ergosterol was converted. The two runs were coupled at the common points, 330 and 375 minutes, and one plot was made of the two runs employing the average values at the common points. The calculated compositions were well within the standard deviations for all components at the common points, the quanta absorbed up to 330 and 375 minutes were equivalent within experimental error in both runs. The repetition of the irradiations in n-hexane at 2967 A° also established the general reproducibility of the results. In addition, the uninterrupted run served to prove that interruption of the irradiation did not appreciably affect the course of the reaction.

The results of the present investigation lend further support to the hypothesis that the solvent effect is primarily due to a variance of viscosity rather than the polarity differences, for in a structurally similar solvent of viscosity higher than n-hexane (20% mineral oil in n-hexane) lumisterol was not found in significant quantities. The viscosities of the solvents employed in this study were determined as described in the experimental section and are tabulated in Table XVIII.

TABLE XVIII

SOLVENT VISCOSITIES
(Temperature 25 ± 0.1 °C.)

Solvent	Viscosity, Centipoise
Isopropyl alcohol	2.068
20% Glycerol	7.135
n-Hexane	0.304
20% Mineral Oil	0.561
40% Mineral Oil	1.192

It is apparent that the viscosity effect is quite sensitive, since only a two-fold increase in viscosity (from n-hexane to 20% mineral oil) is sufficient to prevent the formation of lumisterol within the limits of detection of the analytical procedure--i.e., about 5%.

TABLE OF CONTENTS

VI. DEVELOPMENT OF KINETIC EXPRESSIONS

A quantitative kinetic treatment has been made of the data obtained in this investigation. The kinetic expressions have been developed on the bases of recent considerations of the reaction mechanism, stereochemical aspects of the components of the irradiation mixture, and the electronic changes that occur during the photochemical reaction. The kinetic treatment is also to a large part based on the qualitative conclusions drawn from the recalculated irradiation results of Sharpe's thesis and the calculations of the irradiation results of this study, both presented in Section V. The derivation of the kinetic expressions will be presented after a survey of pertinent material.

A. Survey of Recent Considerations on the Reaction Mechanism

The early mechanism postulated for the irradiation of ergosterol, i.e.,

$$\text{ergosterol} \xrightarrow{h\nu} \text{lumisterol} \xrightarrow{h\nu} \text{tachysterol}$$
$$\xrightarrow{h\nu} \text{calciferol} \xrightarrow{h\nu} \text{over-irradiation products}$$

has been modified during the past decade. After the discovery of precalciferol by Velluz and his co-workers (42), the traditional mechanism was re-examined by Havinga's group (19,20). They have concluded from the results of experiments with ergosterol and 7-dehydrocholesterol which were labeled with carbon-14 that lumisterol and tachysterol are not necessary intermediates in the sequence leading to calciferol.

Their tracer experiments involved the irradiation of mixtures containing approximately equal amounts of labelled ergosterol and inactive lumisterol; similar experiments were performed with mixtures of labelled 7-dehydrocholesterol and inactive lumisterol$_3$. The irradiation resin was treated with digitonin to precipitate the provitamin; the rest of the products were separated on the basis of their reactivities with maleic anhydride--i.e., tachysterol > calciferol > lumisterol. From the specific radio-activities of the separated products, it was concluded that neither lumisterol nor tachysterol play a part in the main route of the conversion of provitamin D to calciferol. However, the authors stated that this conclusion was less definite with respect to tachysterol than lumisterol.

Other reasons for discarding the traditional reaction sequence were also cited by Havinga's group. They have reasoned that it is difficult to explain the magnitude of the quantum yield of calciferol formation which they state is about 0.3, even at the beginning of the irradiation when the percentage of provitamin that is converted is quite small and the concentrations of lumisterol and tachysterol are quite low. In addition, Havinga states that the angular methyl group, $C^{19}H_3$, is not likely to move into another position without the bond between C_9 and C_{10} or C_{10} and C_5 being broken.

In order to overcome these objections, Havinga's group had proposed the following reaction scheme:

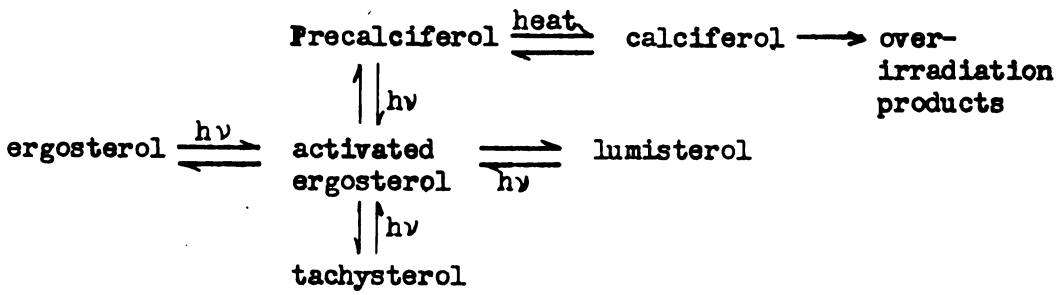

More recent work of Havinga's group (33) has yielded results from which it was concluded that precalciferol is a direct product of the irradiation and that lumisterol and tachysterol are secondary products. In addition, they have shown that the irradiation of precalciferol yields tachysterol almost quantitatively; only about one percent of the precalciferol is converted to ergosterol and over-irradiation products. On the basis of their observed quantum yield of 0.4 for the conversion of precalciferol to tachysterol and the observations previously cited, they concluded that the excited states of ergosterol and precalciferol cannot be equivalent. They argue that since 85% of the conversion product in the irradiation of ergosterol consists of precalciferol, the quantum yield for the conversion of precalciferol to tachysterol should be less than 0.15 if the excited states of ergosterol and precalciferol are identical; this is not compatible with the experimental quantum yield of 0.4. Independently of the latter conclusion, the experimental facts of the conversion of ergosterol primarily to precalciferol and the almost quantitative conversion of precalciferol to tachysterol appear quite definite. These experimental facts are in complete accord with the results of this investigation.

B. Stereochemical Considerations

The structural formulae showing stereochemical details that are most generally accepted (with the exception of precalciferol) are presented in Figure 1. Most structural and stereochemical details have been established for quite some time for ergosterol and lumisterol. The steroid structure

is preserved for these materials, and the rigidity of the fused ring system excludes many complicating stereochemical configurations and conformations. However, such is not the case for tachysterol, precalciferol, and calciferol; these compounds possess structures in which the B ring is broken.

1. Tachysterol

Important contributions to the determination of the structural formula and stereochemical details of tachysterol were made by Grundmann (15), and the groups under the direction of Havinga (27,47) and Inhoffen (24,25). Tachysterol is represented as a structure which permits a planar relationship to exist between all three double bonds, with a trans configuration of the Δ-6, 7 bond. The evidence for this configuration is based on infrared spectra, relative reactivity with maleic anhydride, and the observation of an iodine catalyzed cis-trans isomerization of precalciferol to tachysterol. The latter point will be discussed in conjunction with the structure of precalciferol. A strong absorption band is found for tachysterol at 957 cm^{-1}; this band is ascribed to a trans configuration of the Δ-6, 7 bond. The deduction of a trans configuration on the basis of reactivity toward maleic anhydride is based on the existence of an inverse relationship between the rate of reaction and the number of cis substituents of the most reactive dienoic system of calciferol and related compounds in the s-cisoid conformation (1,8,27).

2. Precalciferol

The structure for precalciferol that is presented in Figure 1 is based on evidence similar to that given for establishing the tachysterol structure, some stereochemical relations, and consideration of the ultraviolet absorption spectra of the components of the irradiation mixture. The infrared spectrum of precalciferol does not possess the trans band at 957 cm^{-1} which has been interpreted by Havinga's group as evidence for a cis Δ -6, 7 relationship. The reactivity of precalciferol with maleic anhydride indicates a sterically interfering system which is consistent with the assignment of a cis Δ -6, 7 structure. The transformation of precalciferol into tachysterol by iodine--a reagent which is known to effect cis to trans isomerization--proceeds quite readily. The structure is further substantiated by the absence of an absorption band at 900 cm^{-1}; this band characterizes a terminal methylene group.

Precalciferol could exist in various rotational conformations derivable from rotation about the S-5, 6 or S-7, 8 bonds. Two planar conformations formed by rotation about the S-5, 6 bond are shown in Figure 15. Both of the planar conformations are sterically hindered, but the cis S-5, 6 conformer is much more hindered. However, even the trans S-5, 6 conformation will be hindered by the mutual repulsion of the hydrogen atoms on C_4 and C_9. The structure in Figure 1 was proposed by Sharpe on the basis of the inability of all three double bonds to exist in one plane and still satisfy the evidence that indicates that precalciferol is a Δ -6, 7 cis isomer of tachysterol. According to Sharpe, the favored conformation is one in which Δ -6, 7 and Δ -8, 9 exist in a

Figure 15

Planar Rotational Conformers
of Precalciferol

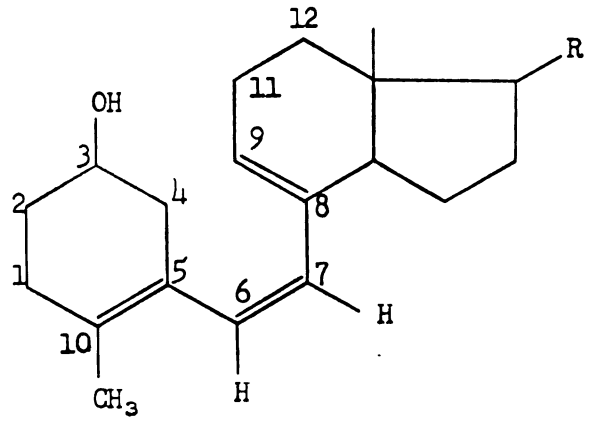

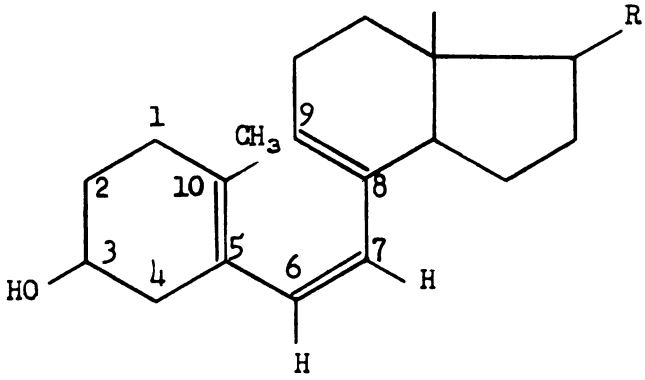

cisoid relation in a plane perpendicular to the plane of the substituents on Δ -5, 10. Since this structure has only two conjugated double bonds capable of resonance, and these are in a constrained cisoid relationship, the ultraviolet extinctions are much lower for precalciferol than for tachysterol, because of the shorter length of the chromophoric group. In general the spectrum of precalciferol is much like that of the closed ring structures of ergosterol and lumisterol.

A very important feature of this proposed structure is that it is the first sterically favorable conformation which would result upon rupture of the C_9-C_{10} bond. This is consistent with the experimental fact that precalciferol is the most abundant product of the irradiation of ergosterol.

At this point it is pertinent to bring out another feature of the structure postulated for precalciferol by Sharpe. The structure has C_9 and the hydrogens on C_{19} in close proximity making the thermal transfer of a proton or hydrogen atom (which is presumed to be necessary to form calciferol) sterically plausible.

3. Calciferol

Although calciferol was not formed in significant quantities during the irradiation of ergosterol and was not included in the kinetic treatment, its structural features will be surveyed for the sake of completeness. As stated by Havinga (47) the only controversial point is the question of the most favorable conformation at the S-6, 7 bond. Evidence for the S-6, 7 form is supplied by Crowfoot and Dunitz (9),

who found that, in the solid state, calciferol 3-nitro 4-iodobenzoate has the S-6, 7 trans form. Additional evidence for the trans S-6, 7 conformation is afforded by the stereochemical consideration that the planar cis-6, 7 conformation would have strong steric interference. Inhoffen (23,26) had argued for the cis-6, 7 structure on the basis of the low extinction of the ultraviolet absorption band and on the stabilization that would occur (as the result of a 6 π-electron system) if the molecule possessed the planar cis S-6, 7 conformation. However, Havinga's group (47) has presented the results of approximate quantum mechanical calculations that are consistent with the assumption of the trans S-6, 7 conformation for calciferol. However, it should be noted that even the trans S-6, 7 conformation will prevent the molecule from achieving a completely planar structure. The results of these calculations are also consistent with the accepted assumption of a trans S-5, 6; trans Δ-6, 7; and cis S-7, 8 structure for tachysterol.

C. Electronic Changes During the Reaction

From an examination of the components of the irradiation mixture it is apparent that all changes that take place during the irradiation of ergosterol occur in ring B. A detailed mechanism must explain how the changes are effected. The interpretation of the reaction in terms of changes in the excited states of the components as presented by Sharpe will be utilized as a working hypothesis for the development of the kinetic expressions.

The initial step surely involves absorption of radiant energy by ergosterol, since the reaction is initiated by light. A detailed description of the excited state of the ergosterol molecule that has absorbed ultraviolet radiation cannot be given at the present time. However, plausible arguments are given in Sharpe's thesis for considering that the excited molecule is best described as an ionic excited state. These arguments, together with the interpretation of changes in the excited state that could lead to the products of the irradiation, will be only briefly surveyed in view of the extensive discussion available in Sharpe's thesis.

The seat of the absorption of radiation of maxima between 2400 and 2900 A^{o} by all of the components is undoubtedly in the conjugated double bond network in ring B. The excited molecule must initially be in a singlet excited state, since the high value of the molar absorbancy indicates an allowed transition from the singlet ground state. Several possibilities exist, however, with regard to the detailed nature of this singlet state and the subsequent processes it may undergo within its normally expected lifetime of about 10^{-8} seconds.

Excited states in conjugated systems often can be described best by the language of valence bond theory, in which ionic resonance forms make a principal contribution to the lowest lying excited states; application of this description leads to the suggestion that the excited state of ergosterol can best be described as an "ionic" excited state, with charge separation in ring B. Some of the structures contributing to this state

are represented in Figure 16. Contributing structures include several in which the C_9-C_{10} bond is cleaved heterolytically. Such structures facilitate the necessary rearrangements to the irradiation products, since the chain composed of C_6, C_7, C_8, and C_9 can undergo rotational motion, the energy barrier to which has been lowered considerably by the absorption of radiation. As shown in Sharpe's thesis, the products can all be derived readily from rotations possible with the labile bond system in the "ionic" excited state.

Alternatively, a description of the excited state based primarily on molecular orbital consideration, would not suggest charge separation, but would, rather, suggest a general "loosening" of the bond structure and an enhanced chemical reactivity associated with two electrons in different molecular orbitals but with spins paired. Such a state is, in a sense, a "diradical," since the electrons are in different orbitals, although the total spin is zero. A set of diradical structures, analogous to the ionic structures shown in Figure 16, can be written to describe the excited state. Rearrangements are again facilitated by the lability of the double bond network, and plausible routes to products can be postulated, again analogous to those described for the "ionic" excited state.

In either case, it would appear that the rearrangements must take place within the approximately 10^{-8} sec. lifetime expected for an excited singlet state. It is also probable that the rearrangements require longer than 10^{-13}-10^{-14} sec. (the period of a molecular vibration), since vibrational fine structure is clearly evident in the absorption spectrum

Figure 16

Valence Bond Structures of the Ionic Excited State of Ergosterol (37)

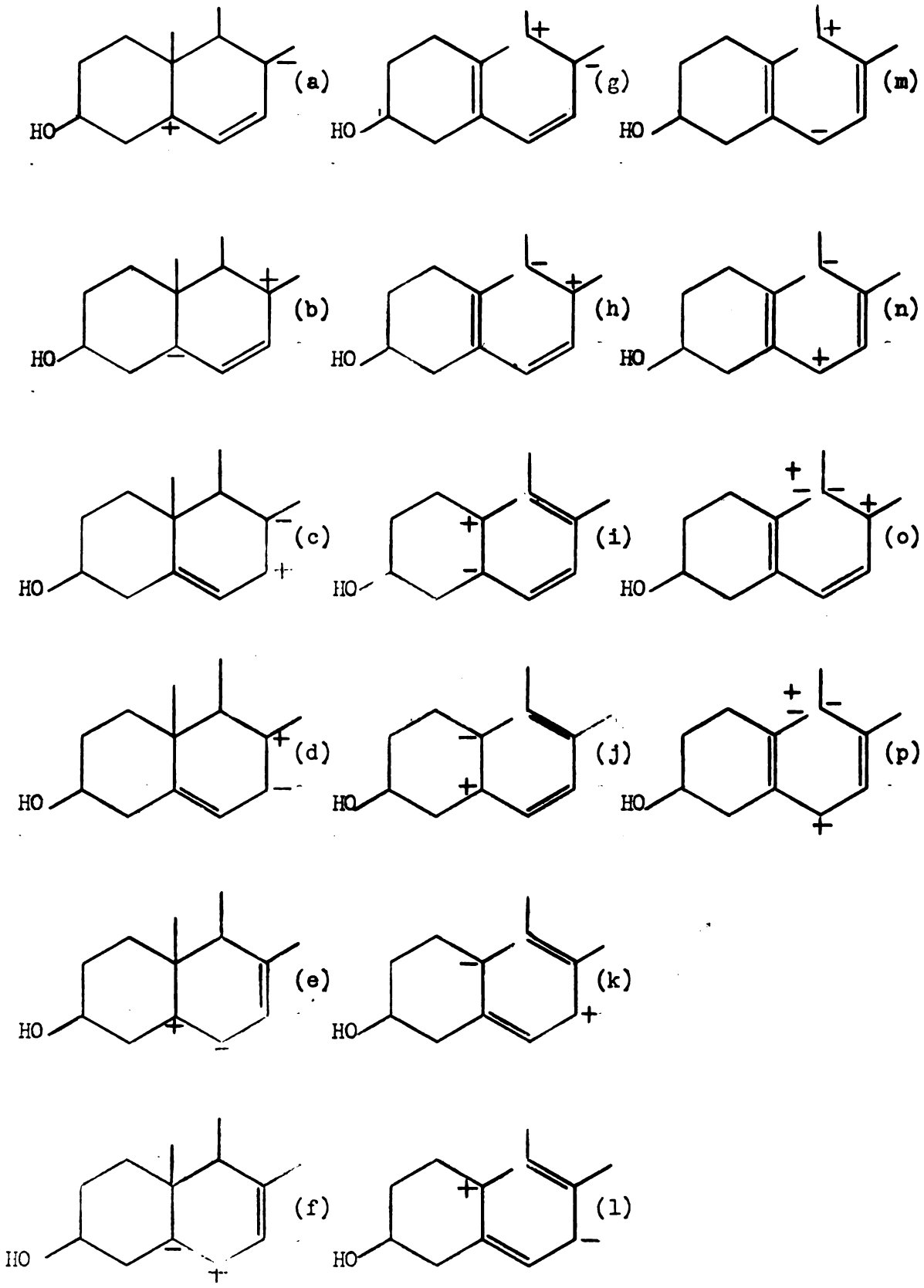

of ergosterol. There seems to be little basis for choice between the two descriptions of the excited state, the differences between which are largely the property of the attempt to approach the description from the two extreme views of valence-bond and molecular-orbital theory. However, one shred of evidence seems to favor the "ionic" excited state; the lack of formation of calciferol in the photochemical sequence suggests that a diradical state is not involved in this sequence, since the later thermal isomerization of precalciferol to calciferol can plausibly be attributed to the presence of a low-lying thermally-accessible diradical triplet state of precalciferol (41).

The other alternatives seem more clearly ruled out. A transition to an excited singlet state above the dissociation limit of the C_9-C_{10} bond (leading to dissociation in 10^{-13}-10^{-14} sec.) appears unlikely in view of the vibrational fine structure on the spectrum. A transition directly to a diradical triplet excited state is ruled out by the high value of the molar absorbancy. A transition directly to an excited singlet state followed by a radiationless transition to an excited triplet state seems improbable in view of the high quantum yield (of the order of magnitude of unity) of the conversion from ergosterol to precalciferol.

It seems fairly definite, then, that an excited singlet state is formed and rearranges within perhaps 10^{-9}-10^{-12} seconds to the structure characteristic of precalciferol and possibly other products. The rearrangement can be pictured as a cross-over from a potential energy surface of the optically excited state of ergosterol to a potential

energy surface of some state of the product.

The cross-over involves rotational motion of bulky portions of the large steroid molecules through the solvent, and may well be expected to be influenced by the viscosity of the medium, in accord with the qualitative results presented in Section III. The period of rotational motion is of the order of 10^{-9}-10^{-10} sec. and will be viscosity dependent, so that the probability of rearrangement within the lifetime of the excited species(prior to fluorescence or collisional deactivation), and hence quantum yields of products, may be solvent dependent. Furthermore, the heights of rotational barriers will be somewhat altered by viscosity.

These concepts have guided the interpretation of the kinetic data. They focus interest on the effect of solvent and irradiating wavelength on the various quantum yields of individual steps. They also suggest a question as to whether the excited state of a given product that results from rotational movements of the excited ergosterol molecule is identical to the excited state that is attained by direct irradiation of the particular product of the irradiation mixture. It was initially believed that the optically attained excited state was equivalent to that derived from the excited ergosterol molecule. However, as will be shown, application of kinetic expressions derived on the assumption of equivalence of the excited states leads to a discrepancy which can be resolved only by abandoning this assumption. As was discussed earlier, this conclusion is in agreement with the recent work of the Havinga group.

D. Derivation of Kinetic Expressions

1. Introductory Discussion

One cannot deduce the order of the formation of the products from the qualitative considerations that are described above. However, this treatment has been utilized as a working hypothesis which has served as a basis for the choice of reaction sequences in the kinetic treatment. Appropriate kinetic expressions have been derived and applied to the data. Compliance of the data with the kinetic expressions then substantiated the original hypothesis.

As discussed above, the kinetic expressions are dependent on the relationship between the optically attained excited states of the irradiation products and those derived from the excited ergosterol molecule. Kinetic expressions were first derived on the basis that the two types of excited state were equivalent. Application of these expressions to the data of the runs in which lumisterol was not formed yielded seemingly satisfactory results. However, a discrepancy between certain quantum yields obtained from this treatment and other reported values led to a re-examination of the kinetic derivation. A second treatment was developed in which the assumption of equivalence of excited states was abandoned. The discrepancy in regard to quantum yields was resolved by the latter treatment. In addition, it was also possible to apply the treatment based on non-equivalent excited states to runs in which lumisterol was formed. Attempts to extend the first kinetic treatment to such runs had not been successful. Both kinetic treatments will be

presented, since the discrepancy brought out by equivalent excited state treatment affords evidence that the optically excited states of the irradiation products are not identical to the excited state derived from excited ergosterol.

During the application of these kinetic treatments--which were based on certain simplifying assumptions--to the kinetic data, it became apparent that a general mathematical pattern existed for the system. It is pertinent to present these general kinetic concepts before proceeding with the derivation of the kinetic expressions which are specifically designed for application to the available data.

2. Some General Considerations of the Reaction Mechanism and Kinetic Treatment

Many types of information point to the fact that the normal reaction in ergosterol irradiation consists of a sequence of steps including optical excitation, and molecular rearrangement and deactivation of excited species. There is no indication that any reactions between pairs of molecules are important; each step of the mechanism must be considered to be first-order. Certain generalizations can be made for any combination of series or parallel first-order reactions (14). In this case the mathematics becomes further simplified by the fact that the stable components can be formed only from short-lived intermediates. Furthermore, analytical concentration-time data are available on all of the long-lived components of the irradiation mixture; these data, coupled with the actinometric and spectrophotometric data, make possible the calculation also of the quanta absorbed by each component during each time interval.

With these data available, it will be shown that any proposed mechanism can be reduced to solutions of the form

$$C_i = \sum_j \beta_{ij} \tilde{I}_j \qquad \text{(VI-1)}$$

where C_i is the concentration of component i at time t and $\tilde{I}_j$ is the integrated absorption for the j^{th} component from time 0 to t

$$\tilde{I}_j = \int_0^t I_a A_j dt \qquad \text{(VI-2)}$$

Experimental data on all of the C_i and $\tilde{I}_j$ are available as functions of time. The β_{ij} are constants which are collections of ratios of rate constants and may be expressed as products of "quantum yields" for particular conversions, where each "quantum yield" represents the fraction of a particular excited species converted to a particular component.

Since each of the components of the irradiation mixture absorbs light in the same wavelength region, it seems plausible to consider a general mechanism with the following features:

a) Each of the components can exist either in its ground state or in an excited state.

b) The excited state of any component can be reached by optical excitation of its ground state, or by rearrangement of the excited state of any of the other components.

c) The ground state of any component can be altered only by optical excitation, and can be formed from the excited state of any component.

This set of conditions can be restricted to special cases of interest by limiting the transformations which can occur among the excited species,

and limiting the formation of particular ground state components from excited states of other components. Furthermore, this general case includes situations in which an additional excited state exists for each component, accessible only from excited states of certain other components, and capable only of passing on to its own corresponding ground state, since any process $A \longrightarrow B \longrightarrow C$, where B is short-lived, is kinetically indistinguishable from the direct process $A \longrightarrow C$. The only type of situation not included within this mechanism which seems at all plausible at the present time might be one in which optically non-accessible excited states exist for each of the components and can be reached from both optically accessible and non-accessible excited states of the other components. The addition of these possibilities will not invalidate the conclusions reached from the mechanism considered, and incorporation of such steps could be made with only slight additional complication of the algebra.

The number of steps included in the mechanism makes it inconvenient to write out the reaction scheme on a single diagram with arrows indicating the individual steps. It is more convenient to systematize the designation of the components and the writing of kinetic steps as follows:

	Long-lived Component	Designation	Short-lived Component	Designation
Ergosterol	E	1	E^*	1'
Precalciferol	P	2	P^*	2'
Lumisterol	L	3	L^*	3'
Tachysterol	T	4	T^*	4'

Rate constants for individual steps will be designated K_{ij} where the step is $i \longrightarrow j$. For each intermediate, i, the summation of rate constants for disappearance is designated σ_i.

$$\sigma_i = \sum_{j \neq i} K_{ij} \qquad \text{(VI-3)}$$

The ratio of the rate constant for a particular step to the summation of rate constants of the disappearing species is formally similar to a quantum yield and is designated ϕ_{ij} where

$$\phi_{ij} = K_{ij}/\sigma_i \quad \text{or} \quad K_{ij} = \sigma_i \phi_{ij} \qquad \text{(VI-4)}$$

The complete mechanism is

(VI-5)

$$E \xrightarrow{h\nu} E^* \; ; \; \text{Rate} = I_a A_E = I_E$$

$$E^* \xrightarrow{K_{1'1}} E \; ; \; E^* \xrightarrow{K_{1'2}} P \; ; \; E^* \xrightarrow{K_{1'3}} L \; ; \; E^* \xrightarrow{K_{1'4}} T$$

$$E^* \xrightarrow{K_{1'2'}} P^* \; ; \; E^* \xrightarrow{K_{1'3'}} L^* \; ; \; E^* \xrightarrow{K_{1'4'}} T^*$$

$$P \xrightarrow{h\nu} P^* \; ; \; \text{Rate} = I_a A_P = I_P$$

$$P^* \xrightarrow{K_{2'1}} E \; ; \; P^* \xrightarrow{K_{2'2}} P \; ; \; P^* \xrightarrow{K_{2'3}} L \; ; \; P^* \xrightarrow{K_{2'4}} T$$

$$P^* \xrightarrow{K_{2'1'}} E^* \; ; \quad ; \; P^* \xrightarrow{K_{2'3'}} L^* \; ; \; P^* \xrightarrow{K_{2'4'}} T^*$$

$$L \xrightarrow{h\nu} L^* \; ; \; \text{Rate} = I_a A_L = I_L$$

$$L^* \xrightarrow{K_{3'1}} E \; ; \; L^* \xrightarrow{K_{3'2}} P \; ; \; L^* \xrightarrow{K_{3'3}} L \; ; \; L^* \xrightarrow{K_{3'4}} T$$

$$L^* \xrightarrow{K_{3'1'}} E^* \; ; \; L^* \xrightarrow{K_{3'2'}} P^* \; ; \quad ; \; L^* \xrightarrow{K_{3'4'}} T^*$$

$$T \xrightarrow{h\nu} T^* \; ; \; \text{Rate} = I_a A_T = I_T$$

$$T^* \xrightarrow{K_{4'1}} E \; ; \; T^* \xrightarrow{K_{4'2}} P \; ; \; T^* \xrightarrow{K_{4'3}} L \; ; \; T^* \xrightarrow{K_{4'4}} T$$

$$T^* \xrightarrow{K_{4'1'}} E^* \; ; \; T^* \xrightarrow{K_{4'2'}} P^* \; ; \; T^* \xrightarrow{K_{4'3'}} L^* \; ;$$

From the mechanism, application of the steady state approximation to the short-lived intermediates leads to the following set of simultaneous

linear equations:

$$\frac{d(E^*)}{dt} = 0 = I_E - \sigma_{1,1}(E^*) + K_{2,1}(P^*) + K_{3,1}(L^*) + K_{4,1}(T^*) \qquad \text{(VI-6)}$$

$$= I_E - \sigma_{1,1}(E^*) + \phi_{2,1}\,\sigma_{2,1}(P^*) + \phi_{3,1}\,\sigma_{3,1}(L^*) + \phi_{4,1}\,\sigma_{4,1}(T^*)$$

$$\frac{d(P^*)}{dt} = 0 = I_P + K_{1,2}(E^*) - \sigma_{2,1}(P^*) + K_{3,2}(L^*) + K_{4,2}(T^*) \qquad \text{(VI-7)}$$

$$= I_P + \phi_{1,2}\sigma_{1,1}(E^*) - \sigma_{2,1}(P^*) + \phi_{3,2}\,\sigma_{3,1}(L^*) + \phi_{4,2}\,\sigma_{4,1}(T^*)$$

$$\frac{d(L^*)}{dt} = 0 = I_L + K_{1,3}(E^*) + K_{2,3}(P^*) - \sigma_{3,1}(L^*) + K_{4,3}(T^*) \qquad \text{(VI-8)}$$

$$= I_L + \phi_{1,3}\sigma_{1}(E^*) + \phi_{2,3}\sigma_{2,1}(P^*) - \sigma_{3,1}(L^*) + \phi_{4,3}\,\sigma_{4,1}(T^*)$$

$$\frac{d(T^*)}{dt} = 0 = I_T + K_{1,4}(E^*) + K_{2,4}(P^*) + K_{3,4}(L^*) - \sigma_{4,1}(T^*) \qquad \text{(VI-9)}$$

$$= I_T + \phi_{1,4}\sigma_{1,1}(E^*) + \phi_{2,4}\sigma_{2,1}(P^*) + \phi_{3,4}\sigma_{3,1}(L^*) - \sigma_{4,1}(T^*).$$

Rewriting these in matrix form,

$$\begin{bmatrix} 1 & -\phi_{2,1} & -\phi_{3,1} & -\phi_{4,1} \\ -\phi_{1,2} & 1 & -\phi_{3,2} & -\phi_{4,2} \\ -\phi_{1,3}-\phi_{2,3} & 1 & -\phi_{4,3} \\ -\phi_{1,4}-\phi_{2,4} & -\phi_{3,4} & 1 \end{bmatrix} \begin{bmatrix} \sigma_{1,1}(E^*) \\ \sigma_{2,1}(P^*) \\ \sigma_{3,1}(L^*) \\ \sigma_{4,1}(T^*) \end{bmatrix} = \begin{bmatrix} I_E \\ I_P \\ I_L \\ I_T \end{bmatrix} \qquad \text{(VI-10)}$$

It is readily seen that these equations can be solved for $\sigma_{1,1}(E^*)$, $\sigma_{2,1}(P^*)$, $\sigma_{3,1}(L^*)$ and $\sigma_{4,1}(T^*)$ in terms of constants and the absorbed light

quantities I_E, I_P, I_L, I_T. Each expression will be a linear combination, such that

$$\sigma_{i'}(C_{i'}) = \sum_j \alpha_{i'j} \; I_j \qquad \text{(VI-11)}$$

where the $\alpha_{i'j}$ are each ratios of sums of products of ϕ's.

The expressions for rate of change of stable species can now be expressed as follows:

$$\frac{d(E)}{dt} = - I_E + K_{1'1}(E^*) + K_{2'1}(P^*) + K_{3'1}(L^*) + K_{4'1}(T^*) \qquad \text{(VI-12)}$$

$$= \left(\sum_{i'=1'}^{4'} \phi_{i'1}\,\alpha_{i'1} - 1\right) I_E + \sum_{K=2}^{4} \sum_{i'=1'}^{4'} \phi_{i'1}\,\alpha_{i'K}\, I_K \qquad \text{(VI-13)}$$

Integrating between t = 0 and t = t,

$$(E)^\circ - (E) = \left(1 - \sum_{i'=1'}^{4'} \phi_{i'1}\,\alpha_{i'1}\right) \tilde{I}_E - \sum_{K=2}^{4} \sum_{i'=1'}^{4'} \phi_{i'1}\, \alpha_{i'K}\, \tilde{I}_K \qquad \text{(VI-14)}$$

Similarly,

$$(P) = \left(\sum_{i'=1'}^{4'} \phi_{i'2}\,\alpha_{i'2} - 1\right) \tilde{I}_P + \sum_{K \neq 2}^{1,3,4} \sum_{i'=1'}^{4'} \phi_{i'2}\,\alpha_{i'K}\, \tilde{I}_K \qquad \text{(VI-15)}$$

$$(L) = \sum_{i'=1'}^{4'} \left(\phi_{i'3}\,\alpha_{i'3} - 1\right) \tilde{I}_L + \sum_{K \neq 3}^{1,2,4} \sum_{i'=1'}^{4'} \phi_{i'3}\, \alpha_{i'K}\, \tilde{I}_K \qquad \text{(VI-16)}$$

$$(T) = \sum_{i'=1'}^{4'} \left(\phi_{i'4}\,\alpha_{i'4} - 1\right) \tilde{I}_T + \sum_{K=1}^{3} \sum_{i'=1'}^{4'} \phi_{i'4}\, \alpha_{i'K}\, \tilde{I}_K \qquad \text{(VI-17)}$$

or, in general,

$$(C_j)-(C_j)^{\circ} = \sum_{i'=1'}^{4'} (\phi_{i',j}\, a_{i',j} - 1)\, \tilde{I}_j + \sum_{K \neq j} \sum_{i'=1'}^{4'} \phi_{i',j}\, a_{i',K}\, \tilde{I}_K \qquad \text{(VI-18)}$$

where (C_j) is the concentration of component j at time t and $(C_j)^{\circ}$ is the initial concentration of component j. Thus each concentration is seen to be expressible as a linear combination of the integrated absorbed quanta.

The complexity is considerably reduced when certain less general cases are treated. Two such cases of interest are:

(1) formation of products only through their corresponding excited states (equivalent to optically excited states, and

(2) non-interconversion of optically excited states, with products formed in ground states (or optically inaccessible excited states) from optically excited states of other species.

The first case mathematically is expressed by

$$\phi_{i',j} = 0 \text{ except for } i = j$$

Hence (VI-19)

$$(\phi_{1',1}, \phi_{2',2}, \phi_{3',3}, \phi_{4',4} \neq 0, \text{ all others zero}).$$

This leads to simplified concentration expressions as follows:

$$(C_j)-(C_j)^{\circ} = (\phi_{j',j} a_{j',j} - 1)\, \tilde{I}_j + \sum_{K \neq j} \phi_{j',j}\, a_{j',K}\, \tilde{I}_K \qquad \text{(VI-20)}$$

The second case mathematically is expressed by

$$\phi_{i,j} = 0, \quad \phi_{i,j} \neq 0 \qquad \text{(VI-21)}$$

This eliminates all off-diagonal terms in the matrix (VI-10), and leads simply to

$$\begin{aligned} \sigma_1(E^*) &= I_E \; ; \quad \alpha_{1,1} = 1 \; ; \; \alpha_{1,j} = 0 \text{ for } j \neq 1. \\ \sigma_2(P^*) &= I_P \; ; \quad \alpha_{2,2} = 1 \; ; \; \alpha_{2,j} = 0 \text{ for } j \neq 2. \\ \sigma_3(L^*) &= I_L \; ; \quad \alpha_{3,3} = 1 \; ; \; \alpha_{3,j} = 0 \text{ for } j \neq 3. \\ \sigma_4(T^*) &= I_T \; ; \quad \alpha_{4,4} = 1 \; ; \; \alpha_{4,j} = 0 \text{ for } j \neq 4. \end{aligned} \qquad \text{(VI-22)}$$

The concentration expressions then become:

$$(C_j)-(C_j)^\circ = (\phi_{j,j}-1)\,\tilde{I}_j + \sum_{K \neq j} \phi_{K,j}\,\tilde{I}_K \qquad \text{(VI-23)}$$

Further simplification can result from specific assumptions about relative magnitudes of particular rate constants or "quantum yields." Two particularly pertinent special cases related to the two just discussed will be presented in detail. Because of the simplicity in obtaining the kinetic expressions directly in these cases, their treatment will be individually derived, rather than developed from this general derivation.

3. Glossary of Symbols Used in Specific Kinetic Derivations

The symbols employed in the derivation are defined as follows:

E, T, P. L = ergosterol, tachysterol, precalciferol, and lumisterol, respectively.

(E), (T), (P), (L) = concentration of the indicated component; in this study, moles per liter of solution.

$(E)^{\circ}$, $(P)^{\circ}$, $(T)^{\circ}$, $(L)^{\circ}$ = initial (zero time) concentration of the indicated component; in this study, all components but ergosterol were initially at zero concentration.

E^*, T^*, P^*, L^* = indicated component in its optically accessible excited state.

(E^*), (T^*), (P^*), (L^*) = concentration of the indicated component in its excited state.

$P^{*'}$ = an excited state of precalciferol which is optically inaccessible and is derived from E^*.

t = time of irradiation.

k_j = kinetic rate constant, j denoting the reaction step considered.

I_a = rate of absorption of radiation per unit volume by all of the components of the irradiation mixture, i.e., total moles of quanta (Einsteins) absorbed per unit time per liter.

A_E, A_P, A_T, A_L = fraction of the radiation that is absorbed by the component indicated by the subscript.

$\tilde{I}_E$, $\tilde{I}_P$, $\tilde{I}_T$, $\tilde{I}_L$ = the value of the definite integral, $\int_0^t I_a A_i dt$, where the subscript i denotes a given component. The value of this integral is the total number of moles of quanta per liter that are absorbed by the indicated component during the interval of irradiation 0 to t.

4. Case of Equivalence of Optical and Derived Excited States

In the following development it is assumed that lumisterol and calciferol are not formed in significant quantities during the irradiation. The stereochemical and electronic considerations suggest the following sequence for the irradiation of ergosterol:

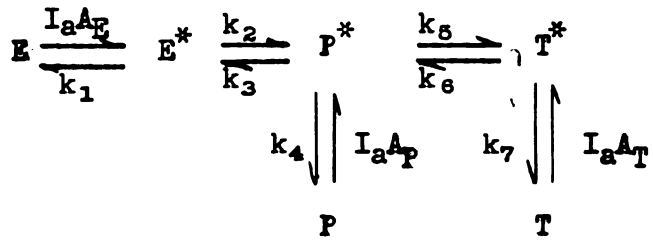

(VI-24)

This reaction scheme may be considerably simplified by certain assumptions that are based on experimental observation. The rate constants k_3 and k_6 must be very small, since the irradiation of precalciferol results in the almost quantitative conversion of precalciferol to tachysterol (33). It is therefore assumed that k_3 and k_6 are essentially equal to zero.

In the kinetic development the excited states of the components of the irradiation mixture are considered to be reactive intermediates, and the steady state approximation is applied to these species, i.e., the rate of change of the concentration of the active species is set equal to zero. The law of photochemical equivalence is applied to the absorption of radiant energy for each of the components. From the steady state relations, expressions are obtained for the concentrations of the active species in terms of experimental quantities; these expressions are substituted into the appropriate rate equations, and the differential equations are integrated.

The modified reaction scheme may be written as:

$$E \underset{k_1}{\overset{I_a A_E}{\rightleftharpoons}} E^* \xrightarrow{k_2} P^* \xrightarrow{k_5} T^* \qquad \text{(VI-25)}$$

$$k_4 \downarrow\uparrow I_a A_P \qquad k_7 \downarrow\uparrow I_a A_T$$

$$P \qquad\qquad T$$

The rate equations for the reactive intermediates, applying the steady state approximation, are:

$$\frac{d(E^*)}{dt} = 0 = I_a A_E - (k_1 + k_2)(E^*) \qquad \text{(VI-26)}$$

$$\frac{d(P^*)}{dt} = 0 = I_a A_P + k_2(E^*) - (k_4 + k_5) P^* \qquad \text{(VI-27)}$$

$$\frac{d(T^*)}{dt} = 0 = I_a A_T + k_5(P^*) - k_7(T^*) \qquad \text{(VI-28)}$$

The concentrations of the active species are obtained by solution of the resulting three simultaneous equations (VI-26, VI-27, and VI-28). The results are:

$$(E^*) = \frac{I_a A_E}{k_1 + k_2} \qquad \text{(VI-29)}$$

$$(P^*) = \frac{I_a A_P + \left(\frac{k_2}{k_1 + k_2}\right) I_a A_E}{k_4 + k_5} \qquad \text{(VI-30)}$$

$$(T^*) = \frac{I_a A_T + \left(\frac{k_5}{k_4 + k_5}\right) I_a A_P + \left(\frac{k_2}{k_1 + k_2}\right)\left(\frac{k_5}{k_4 + k_5}\right) I_a A_E}{k_7} \qquad \text{(VI-31)}$$

The rate expressions for the components of the irradiation mixture in their normal ground states may be written:

$$\frac{d(E)}{dt} = k_1(E^*) - I_a A_E \qquad \text{(VI-32)}$$

Substituting the value of (E^*) from equation (VI-29):

$$\frac{d(E)}{dt} = - \frac{k_2}{k_1 + k_2} I_a A_E = - \phi_E I_a A_E \qquad \text{(VI-33)}$$

where the quantity $\phi_E = \frac{k_2}{k_1 + k_2}$ has been introduced. This is the quantum yield for ergosterol conversion, since it represents the fraction of the excited ergosterol converted to other products.

$$\frac{d(P)}{dt} = k_4(P^*) - I_a A_P \qquad \text{(VI-34)}$$

Substituting the value of (P^*) from equation (VI-30):

$$\frac{dP}{dt} = \frac{k_4}{k_4 + k_5} \phi_E I_a A_E - \frac{k_5}{k_4 + k_5} I_a A_P \qquad \text{(VI-35)}$$

$$= (1 - \phi_P) \phi_E I_a A_E - \phi_P I_a A_P \qquad \text{(VI-36)}$$

Where the quantity $\phi_P = \frac{k_5}{k_4 + k_5}$ has been introduced. This is the quantum yield for precalciferol conversion, since it represents the fraction of the excited precalciferol converted to other products. The quantity $1 - \phi_P = 1 - \frac{k_5}{k_4 + k_5} = \frac{k_4}{k_4 + k_5}$ is the fraction of excited precalciferol returning to the ground state. It is important to note here that there is a fundamental difference in the nature of ϕ_E and ϕ_P, since E^* is formed only through optical excitation of ergosterol, while P^* is formed both by optical excitation of precalciferol and by rearrangement of excited ergosterol, E^*. Equation (VI-36) was left in this form for future algebraic manipulation.

$$\frac{d(T)}{dt} = k_7(T^*) - I_a A_T \qquad \text{(VI-37)}$$

Substituting the value of (T^*) from equation (VI-31):

$$\frac{d(T)}{dt} = \phi_P (I_a A_P + \phi_E I_a A_E) \qquad \text{(VI-38)}$$

Integration of equation (VI-33) between the limits of 0 and t yields a linear relationship between the amount of ergosterol that has reacted and the amount of radiation absorbed by ergosterol, with a slope equal to the quantum yield, ϕ_E; the integrated form of (VI-33) is written:

$$(E)^\circ - (E) = \phi_E \int_0^t I_a A_E dt = \phi_E \tilde{I}_E \qquad \text{(VI-39)}$$

Integration of equation (VI-36) between the limits of 0 and t yields

$$(P)-(P)^\circ = (1 - \phi_P)\ \phi_E \tilde{I}_E - \phi_P \tilde{I}_P \qquad \text{(VI-40)}$$

Since $(P)^\circ = 0$ at $t = 0$, and $\phi_E \tilde{I}_E = (E)^\circ - (E)$, equation (VI-40) becomes

$$(P) = (1 - \phi_P)\ [(E)^\circ - (E)] - \phi_P\ \tilde{I}_P \qquad \text{(VI-41)}$$

In runs where no lumisterol or calciferol is formed, we may substitute (T) for the quantity $(E)^\circ - (E) - (P)$. The following relationship is obtained after this substitution and rearrangement of terms.

$$(T) = \frac{k_5}{k_4}\ [(P) + \tilde{I}_P] \qquad \text{(VI-42)}$$

Equation (VI-42) shows that a plot of the indicated experimental quantities should be linear with a slope equal to the ratio of two rate constants.

Again, an integration of (VI-38) between the limits of 0 and t yields a linear relation between experimental quantities,

$$(T) - (T)^{\circ} = \phi_P (\tilde{I}_P + \phi_E \tilde{I}_E) \qquad \text{(VI-43)}$$

Since $(T)^{\circ} = 0$ and $\phi_E \tilde{I}_E = (E)^{\circ} - (E)$, equation (VI-43) becomes

$$T = \phi_P [(E)^{\circ} - (E) + \tilde{I}_P] \qquad \text{(VI-44)}$$

The slope of a plot of the appropriate experimental quantities is equal to ϕ_P, the quantum yield for the process $P \longrightarrow T$.

5. Case of Non-Equivalent Optical and Derived Excited States

Incorporation of the non-equivalency of P^* and $P^{*'}$ results in the following modification of expression (VI-24):

$$\begin{array}{ccccc} E & \underset{k_1}{\overset{I_a A_E}{\rightleftharpoons}} & E^* & \xrightarrow{k_a} & L \\ & & \downarrow k_2 & & \\ & & P^{*'} & & \\ & & \downarrow k_2' & & \\ & & P & \underset{k_4}{\overset{I_a A_P}{\rightleftharpoons}} & P^* \xrightarrow{k_5} T \end{array} \qquad \text{(VI-45)}$$

Excited states of tachysterol and lumisterol which might be considered as derived from P^* and E^* are not shown in expression (VI-45), since inclusion of such excited states results in kinetic expressions which incorporate effects that the experimental data are not capable of detecting. Many additional steps could also be included showing that the products of the irradiation could be converted to ergosterol; however, such steps again lead to expressions which require more accurate data than are available. These considerations will be discussed further.

The rate equations for the reactive intermediates, incorporating the steady state approximation, are:

$$\frac{d(E^*)}{dt} = I_a A_E - (k_1 + k_2 + k_8)(E^*) = 0 \qquad \text{(VI-46)}$$

$$\frac{d(P^*)}{dt} = I_a A_P - (k_4 + k_5)(P^*) = 0 \qquad \text{(VI-47)}$$

$$\frac{d(P^{*\prime})}{dt} = k_2(E^*) - k_2'(P^{*\prime}) = 0 \qquad \text{(VI-48)}$$

These equations can be solved directly for (E^*), (P^*), and $(P^{*\prime})$, giving:

$$(E^*) = \frac{I_a A_E}{k_1 + k_2 + k_8} \qquad \text{(VI-49)}$$

$$(P^*) = \frac{I_a A_P}{k_4 + k_5} \qquad \text{(VI-50)}$$

$$(P^{*\prime}) = \frac{k_2}{k_2'}(E^*) = \frac{k_2 I_a A_E}{k_2'(k_1 + k_2 + k_8)} \qquad \text{(VI-51)}$$

The rate expressions for the components in their normal ground states may be written:

$$\frac{d(E)}{dt} = -\frac{k_2 + k_8}{k_1 + k_2 + k_8} I_a A_E = -\phi_E I_a A_E \qquad \text{(VI-52)}$$

The quantum yield ϕ_E is defined as $(k_2 + k_8)/(k_1 + k_2 + k_8)$; this definition is consistent with the expression for ϕ_E in the previous section, and represents the fraction of excited ergosterol which is converted to other products.

$$\frac{d(P)}{dt} = \frac{k_2 I_a A_E}{k_1 + k_2 + k_8} - \frac{k_5 I_a A_P}{k_4 + k_5} \qquad \text{(VI-53)}$$

$$\frac{d(P)}{dt} = \phi_{EP} I_a A_E + \phi_{PT} I_a A_P \qquad \text{(VI-54)}$$

where ϕ_{EP} is defined as $\frac{k_2}{k_1 + k_2 + k_3}$ and represents the fraction of excited ergosterol which is converted to precalciferol, and ϕ_{PT} is defined as $\frac{k_5}{k_4 + k_5}$ and represents the fraction of optically excited precalciferol converted to tachysterol.

$$\frac{d(T)}{dt} = \phi_{PT} I_a A_P \qquad \text{(VI-55)}$$

$$\frac{dL}{dt} = \frac{k_3 I_a A_E}{k_1 + k_2 + k_3} \qquad \text{(VI-56)}$$

$$\frac{dL}{dt} = \phi_{EL} I_a A_E \qquad \text{(VI-57)}$$

where ϕ_{EL} is defined as $\frac{k_3}{k_1 + k_2 + k_3}$ and represents the fraction of excited ergosterol converted to lumisterol.

Integration of equations (VI-52, VI-54, VI-55, and VI-57) between the limits of zero and t yields:

$$(E)^\circ - (E) = \phi_E \tilde{I}_E = (\phi_{EL} + \phi_{EP})\tilde{I}_E \qquad \text{(VI-58)}$$

$$(P) = \phi_{EP}\tilde{I}_E - \phi_{PT}\tilde{I}_P \qquad \text{(VI-59)}$$

$$(T) = \phi_{PT}\tilde{I}_P \qquad \text{(VI-60)}$$

$$(L) = \phi_{EL}\tilde{I}_E \qquad \text{(VI-61)}$$

Equations (VI-59, VI-60, and VI-61) are derived on the basis that the concentrations of P, T, and L are zero at t equal to zero.

The equations (VI-58, VI-59, VI-60, and VI-61) are linearly related through the material balance equation $(E)^{\circ} = (E) + (L) + (P) + (T)$. Since the material balance equation has been used in obtaining the concentrations in the analytical procedure, only equations (VI-58, VI-60 and VI-61) are used in the kinetic treatment.

The reaction scheme (VI-45) is mathematically identical to the simplified reaction scheme in which $P^{*'}$ is deleted, i.e.,

$$\begin{array}{ccccc} E & \underset{k_1}{\overset{I_a A_E}{\rightleftharpoons}} & E^* & \xrightarrow{k_a} & L \\ & & \downarrow k_2 & & \\ & & P & \underset{k_4}{\overset{I_a A_P}{\rightleftharpoons}} P^* & \xrightarrow{k_5} T \end{array} \qquad \text{(VI-62)}$$

The expressions derived from reaction scheme (VI-62) are identical to equations (VI-58, VI-59, VI-60 and VI-61).

As in the case of equivalent excited states, simple linear relationships are obtained. In general, considerations of other reaction steps in (VI-45) or (VI-62) will lead to expressions in which a quantity such as (P) is a linear combination of products of quantum yields and the integrals $\tilde{I}_1$. These would introduce a curvature to the linear relations (VI-58, VI-60, and VI-61). However, the values of the secondary terms are quite small, and more accurate data than are available would be required to detect the curvature. The equations derived from reaction schemes (VI-45 and VI-62) were found to yield the most plausible fit of the data within the experimental limits of accuracy of the data.

TABLE OF CONTENTS

VII. RESULTS OF THE KINETIC STUDY

A. Treatment of the Data

It is evident from the kinetic equations that in addition to the concentrations of the components, the kinetic procedure requires the knowledge of the number of moles of quanta per liter absorbed by a given component during the interval of irradiation from time 0 to t, i.e., the value of the integral $\int_0^t I_a A_i dt$.

The total numbers of quanta absorbed by all of the components of the irradiation mixture were directly available from the experimental data for any interval of irradiation. The average rate of absorption of radiation, $\bar{I}_a$, was calculated from these data for small intervals of irradiation and covering the entire irradiation run; these data are tabulated in Appendix III. It was assumed that the average value $\bar{I}_a$ could be substituted for the instantaneous rate I_a for small intervals of irradiation. By means of this assumption, the definite integral whose value is equal to the number of quanta absorbed by the i^{th} component during the interval $t = 0$ to $t = t_1$ can be written as

$$\int_0^t I_a A_i dt = \bar{I}a_{(1)} \int_0^{t_{(1)}} A_i dt + \bar{I}a_{(2)} \int_{t_{(1)}}^{t_{(2)}} A_i dt + \cdots + \bar{I}a_{(n)} \int_{t_{(n-1)}}^{t_n \text{ or } t_1} A_i dt \qquad \text{(VII-1)}$$

where the numerical subscripts in parentheses denote the subdivisions of the irradiation intervals for which the values of $\bar{I}_a$ have been calculated. The use of an average value of the rate of absorption of radiation is justified, since the rate of absorption changes gradually during the irradiation.

The integral $\int A_i dt$ was evaluated (between the limits corresponding to the intervals for which $\bar{I}_a$ was calculated) from the concentration-time data, using the known ultraviolet molar absorbancies of the components of the irradiation mixture. The fraction of radiation absorbed by a given component of a mixture for which the Beer-Lambert-Bouger Law is valid is given by the following expression (32):

$$A_i = \frac{C_i \epsilon_i}{C_1 \epsilon_1 + C_2 \epsilon_2 + \cdots + C_m \epsilon_m} \qquad \text{(VII-2)}$$

where C_i = concentration of the indicated component i, and

ϵ_i = molar absorbancy of component i.

Since the radiation emanating from the monochromator was not purely monochromatic, average values of the molar absorbancies were employed to evaluate A_i.

The calculations involved the assumption that the distribution of intensity of radiation with respect to wavelength was that afforded by a triangular slit function. An expression for the average molar absorbancy was derived on the basis of this assumption and the dispersion of the monochromator, i.e., 66 A° (or 6.6 mμ.) per mm. The derivation for a slit width of 1.00 mm. is presented below.

The average molar absorbancy is given by

$$\epsilon_i = \frac{\int_{-6.6}^{0} \epsilon_{\lambda i} S_1(\lambda) d(\lambda - \lambda_0) + \int_{0}^{6.6} \epsilon_{\lambda i} S_2(\lambda) d(\lambda - \lambda_0)}{\int_{-6.6}^{0} S_1(\lambda) d(\lambda - \lambda_0) + \int_{0}^{6.6} S_2(\lambda) d(\lambda - \lambda_0)} \qquad \text{(VII-3)}$$

where ϵ_λ = molar absorbancy at wavelength λ, mμ, for component i

λ_0 = nominal wavelength, mμ, and the slit functions S_1 and S_2 are given by

$$S_1(\lambda) = \frac{\lambda - \lambda_0}{6.6} + 1 \qquad \text{(VII-4a)}$$

$$S_2(\lambda) = -\frac{\lambda - \lambda_0}{6.6} + 1 \qquad \text{(VII-4b)}$$

Substitution of the values of $S_1(\lambda)$ and $S_2(\lambda)$ given by equations (VII-4a) and (VII-4b) into equation (VII-3) and evaluation of the denominator of the latter equation yields

$$\bar{\epsilon} = \frac{1}{6.6}\left[\int_{-6.6}^{6.6} \epsilon_{\lambda_i} d(\lambda - \lambda_0) + \int_{-6.6}^{0} \epsilon_{\lambda_i} \frac{(\lambda - \lambda_0)}{6.6} d(\lambda - \lambda_0) - \int_{0}^{6.6} \epsilon_{\lambda_i} \frac{(\lambda - \lambda_0)}{6.6} d(\lambda - \lambda_0)\right] \qquad \text{(VII-5)}$$

The spectral data furnished by W. H. C. Shaw (40) were utilized in the evaluation of the three definite integrals of equation (VII-5).

The integral $\int_{-6.6}^{6.6} \epsilon_{\lambda_i} \, d(\lambda - \lambda_o)$ was evaluated with a planimeter from plots of molar absorbancy vs. wavelength. The other two integrals of equation (VII-5) were evaluated by numerical integration, employing the trapezoidal rule; intervals of 10 A° were employed in the integration.

Equation (VII-5) has been derived on the basis of a slit width of 1.00 mm.; slit widths of 1.50 and 2.00 mm. were employed in the irradiation studies. The limits for the value of $\lambda - \lambda_o$ are given by twice the product of the dispersion of the monochromator (66 A° per mm.) and the slit width. Accordingly, equation (VII-5) is modified to incorporate the appropriate value of the limits of $\lambda - \lambda_o$. Values of the nominal wavelengths and the limits of $\lambda - \lambda_o$ were rounded off as follows: 2537 A° to 2540 ± 100 A°, slit width = 1.50 mm.; 2804 A° to 2800 ± 130 A°, slit width=2.00 mm.; 2967 A° to 2970 ± 100 A°, slit width=1.50 mm. The values of the average molar absorbancies calculated by this procedure are given in Table XIX, together with the molar absorbancy at a wavelength corresponding to the "rounded off" nominal wavelength.

The fraction of radiation absorbed by a given component, A_i, was computed for all experimental points by means of equation VII-2, utilizing average values for the molar absorbancies. Plots of A_i vs. time of irradiation were made and the value of the integral $\int A_i dt$ (over the limits corresponding to the irradiation interval for which $\bar{I}_a$ was calculated) was determined by numerical integration of the data obtained from the smooth curves drawn through the experimental points.

TABLE XIX

MOLAR ABSORBANCIES AT IRRADIATING WAVELENGTHS

Components	Molar Absorbancies	
	Average, $\bar{\epsilon}$	ϵ
2540 A° (2537 A°)		
Ergosterol	5981	4831
Lumisterol	4886	4811
Tachysterol	11570	11340
Precalciferol	8770	8837
2800 A° (2804 A°)		
Ergosterol	10320	11430
Lumisterol	8365	8873
Tachysterol	26830	29550
Precalciferol	5922	6029
2970 A° (2967 A°)		
Ergosterol	4188	4597
Lumisterol	3162	3280
Tachysterol	16800	17240
Precalciferol	2058	1940

The trapezoidal rule was employed in the numerical integration process. These data are presented in Appendix III together with the values of $\bar{I}_a$.

The data required to compute the value of the integral $\int_0^t I_a A_i dt$ from equation (VII-1) are made available by the procedure described above. The calculated values of this integral are also presented in Appendix III. Since I_a was measured in quanta per minute, the calculated integrals were divided by Avogadro's number and multiplied by 1000/(volume of solution in ml. in sample cell) to give the reported integrals in units of moles of quanta absorbed by the component per liter of solution.

In performing the computations described above, the concentration of calciferol was taken to be zero; the calculated concentration of calciferol was generally less than the standard deviation. A value of zero was also employed for the concentration of lumisterol in all cases except in n-hexane at 2804 and 2967 A°. The few small negative values that were obtained for the concentration of tachysterol were also considered as zero in the calculations.

B. Results of Kinetic Treatment

Using the concentration-time data calculated in section VB and the irradiation data processed as described in section VIIA, the relationships predicted from the kinetic derivations have been checked.

1. Case of Equivalence of Optical and Derived Excited States

The derivation based on the mechanism

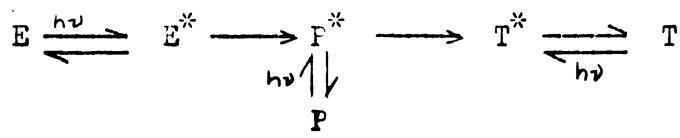

(VI-24)

was found to yield the equations

$$(E)^{\circ} - (E) = \phi_E[\tilde{I}_E] \qquad \text{(VI-39)}$$

$$(T) = \frac{K_5}{K_4}[(P) + \tilde{I}_P] \qquad \text{(VI-42)}$$

$$(T) = \phi_P[(E)^{\circ} - (E) + \tilde{I}_P]. \qquad \text{(VI-44)}$$

In each case a linear dependence of the experimental quantity on the left hand side of the equation is predicted. The data used are presented in Table XX. Typical plots of each of the three equations are shown in Figure 17.

A linear least squares procedure was applied to the data to obtain the values of ϕ_E, k_5/k_4, and ϕ_P. The usual least squares procedure, which is based on the assumption that one variable is known exactly, was not employed, since both of the variables in the kinetic equations are subject to error. The procedure employed yielded a straight line for which the sum of the squares of the perpendicular distances from the experimental points to the line was minimized (35). Essentially, the data were fitted to the linear relation

$$y = -\frac{a}{b} - \frac{1}{b}x \qquad \text{(VII-6)}$$

where y and x are the variables and a and b are constants from which the slope and intercept are calculated. The relationship presented by

Figure 17

Typical Kinetic Plots, Case of Equivalent Optical and Derived Excited States

2537 A° 20% Mineral Oil Run III-18

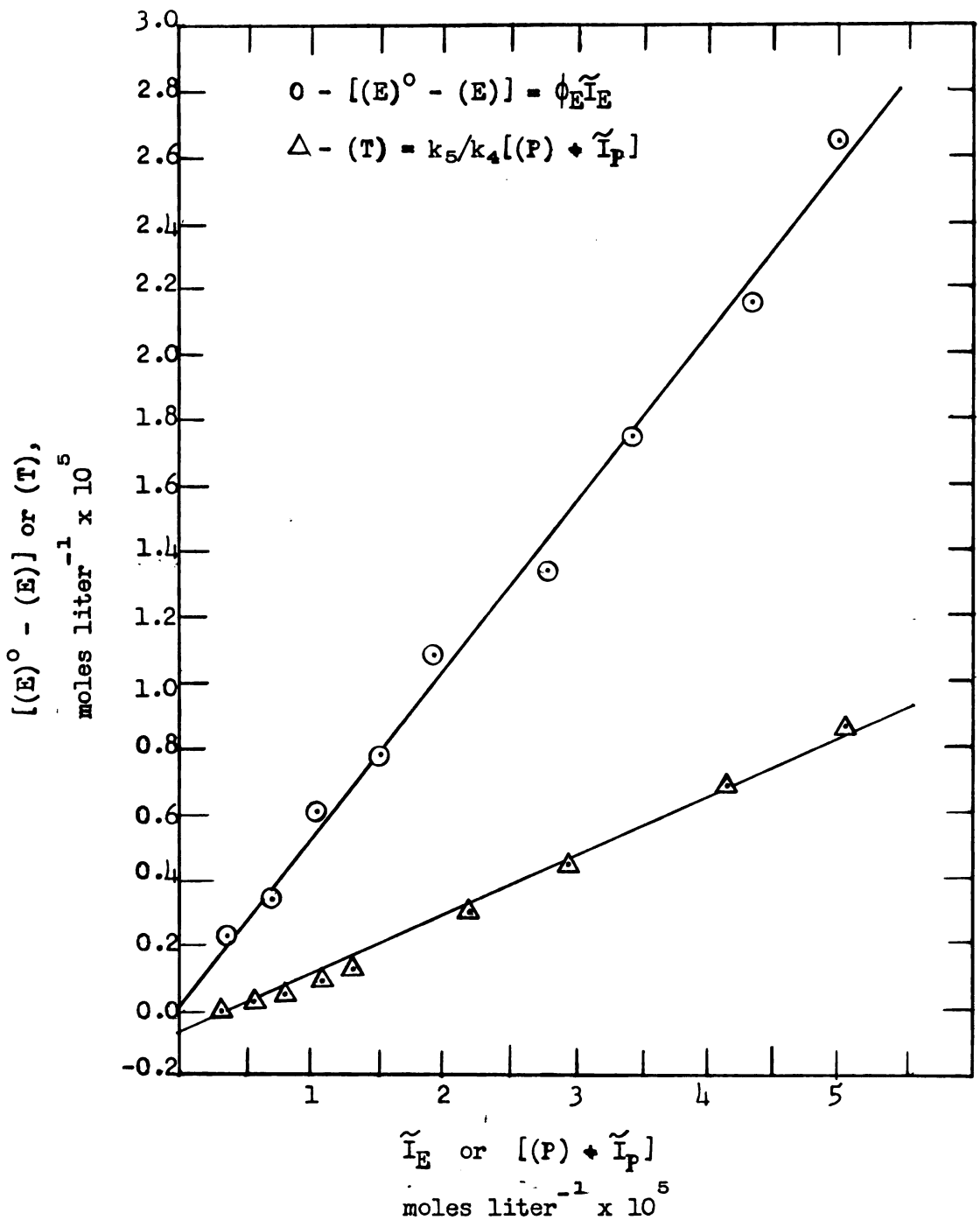

TABLE XX

KINETIC DATA

Interval, Min.	Component Concentrations at End of Interval, moles liter^{-1} x 10^5 (E)	(T)	(P)	Converted Ergosterol, moles liter^{-1} x 10^5 $(E)^o - (E)$	Kinetic Quantities, moles liter^{-1} x 10^5 $\tilde{I}_E$	$(P) \div \tilde{I}_p$	$(E)^o - (E) \div \tilde{I}_p$
2537 A° Isopropyl Alcohol Run III-10 $(E)^o = 6.101 \times 10^{-5}$ moles liter^{-1}							
0-20	5.644	0.043	0.324	0.457	0.453	0.343	0.476
0-40	5.484	0.066	0.528	0.617	0.861	0.601	0.690
0-60	5.088	0.115	0.771	1.013	1.236	0.924	1.166
0-90	4.907	0.152	0.910	1.194	1.757	1.212	1.496
0-120	4.677	0.182	1.011	1.424	2.234	1.481	1.894
0.185	4.529	0.335	1.269	1.572	3.192	2.182	2.485
0.245	3.820	0.552	1.596	2.281	3.991	2.986	3.671
0.305	3.588	0.693	1.577	2.513	4.717	3.489	4.425
0.365	3.367	0.900	1.778	2.734	5.395	4.271	5.227
0.410	2.982	1.061	1.878	3.119	5.863	4.833	6.074
2537 A° 20% Glycerol Run III-14 $(E)^o = 6.101 \times 10^{-5}$ moles liter^{-1}							
0-20	5.668	0.034	0.364	0.433	0.402	0.380	0.449
0-40	5.540	0.065	0.452	0.561	0.764	0.510	0.619
0-60	5.481	0.114	0.761	0.620	1.106	0.884	0.743
0-90	5.228	0.144	0.843	0.873	1.612	1.100	1.130
0-120	4.976	0.189	1.035	1.125	2.056	1.442	1.532
0-180	4.661	0.311	1.237	1.440	2.911	2.020	2.223
0-240	3.908	0.592	1.741	2.193	3.654	2.963	3.415
0-330	3.652	0.784	1.773	2.449	4.654	3.768	4.444
0-420	3.506	1.030	1.914	2.595	5.598	4.744	5.425

Continued

TABLE XX - Continued

Interval, Min.	Component Concentrations at End of Interval, moles liter^{-1} x 10^5 (E)	(T)	(P)	Converted Ergosterol, moles liter^{-1} x 10^5 $(E)^o - (E)$	Kinetic Quantities, moles liter^{-1} x 10^5 $\bar{I}_E$	$(P) + \bar{I}_P$	$(E)^o - (E) + \bar{I}_P$
2537 A° n-Hexane Run III-22 $(E)^o = 5.446 \times 10^{-5}$ moles liter^{-1}							
0-20	5.036	0.000	0.149	0.410	0.384	0.161	0.422
0-40	4.926	0.000	0.413	0.520	0.741	0.459	0.566
0-60	4.801	0.015	0.578	0.645	1.077	0.680	0.747
0-90	4.586	0.056	0.822	0.860	1.550	1.046	1.084
0-120	4.460	0.080	0.946	0.986	1.976	1.316	1.356
0-185	4.061	0.202	1.281	1.385	2.758	2.011	2.115
0-240	3.656	0.370	1.554	1.790	3.348	2.659	2.895
0-330	3.145	0.554	1.825	2.301	4.216	3.671	4.147
0-420	2.600	0.831	2.091	2.846	4.980	4.838	5.593
2537 A° 20% Mineral Oil Run III-18 $(E)^o = 5.446 \times 10^{-5}$ moles liter^{-1}							
0-20	5.212	0.000	0.306	0.234	0.375	0.326	0.254
0-40	5.107	0.029	0.490	0.339	0.720	0.558	0.407
0-60	4.828	0.045	0.664	0.618	1.046	0.798	0.752
0-90	4.670	0.093	0.851	0.776	1.516	1.090	1.015
0-120	4.361	0.126	0.952	1.085	1.949	1.316	1.449
0-185	4.106	0.302	1.481	1.340	2.789	2.224	2.083
0-240	3.694	0.447	1.757	1.752	3.438	2.949	2.944
0-330	3.281	0.687	2.110	2.165	4.346	4.146	4.201
0-404	2.794	0.866	2.219	2.652	4.979	5.054	5.487

Continued

TABLE XX - Continued

Interval, Min.	Component Concentrations at End of Interval, moles liter^{-1} x 10^5 (E)	(T)	(P)	Converted Ergosterol, moles liter^{-1} x 10^5 $(E)^o - (E)$	Kinetic Quantities, moles liter^{-1} x 10^5 $\tilde{I}_E$	$(P) \div \tilde{I}_p$	$(E)^o - (E) \div \tilde{I}_p$
2804 A° Isopropyl Alcohol Run II-14 $(E)^o = 6.101 \times 10^{-5}$ moles liter^{-1}							
0-14	5.683	0.034	0.467	0.418	1.092	0.485	0.436
0-29	5.555	0.026	0.697	0.546	2.159	0.771	0.620
0-49	5.167	0.001	0.960	0.934	3.469	1.165	1.139
0-58	4.791	0.096	1.290	1.310	4.031	1.576	1.596
0-88	4.356	0.212	1.856	1.745	5.734	2.474	2.363
0-118	4.148	0.333	2.087	1.953	7.286	3.110	2.976
0-213	3.136	0.640	2.868	2.965	11.273	5.464	5.561
0-273	2.427	0.912	3.084	3.674	13.159	6.841	7.431
0-318	2.181	1.037	3.123	3.920	14.384	7.825	8.622
2804 A° 20% Glycerol Run II-9 $(E)^o = 6.101 \times 10^{-5}$ moles liter^{-1}							
0-15	5.662	0.075	0.601	0.439	1.124	0.630	0.468
0-30	5.163	0.047	0.817	0.938	2.136	0.919	1.040
0-45	5.104	0.072	1.121	0.997	3.087	1.327	1.203
0-60	4.431	0.154	1.428	1.670	3.969	1.762	2.004
0-90	4.476	0.188	1.757	1.625	5.622	2.423	2.291
0-120	4.017	0.226	2.035	2.084	7.096	3.110	3.159
0-150	3.565	0.400	2.479	2.536	8.462	4.035	4.092
0-240	2.775	0.790	3.087	3.326	11.781	6.176	6.415
0-305	2.363	0.978	3.256	3.738	13.568	7.640	8.122
0-365	2.328	1.000	3.571	3.773	15.060	9.218	9.420

Continued

TABLE XX - Continued

Interval, Min.	Component Concentrations at End of Interval, moles liter^{-1} x 10^5 (E)	(T)	(P)	Converted Ergosterol, moles liter^{-1} x 10^5 $(E)^o - (E)$	Kinetic Quantities, moles liter^{-1} x 10^5 $\widetilde{I}_E$	$(P) + \widetilde{I}_P$	$(E)^o - (E) + \widetilde{I}_P$
2804 A° 20% Mineral Oil Run II-24 $(E)^o = 5.446 \times 10^{-5}$ moles liter^{-1}							
0-15	4.900	0.062	0.435	0.546	0.915	0.456	0.567
0-30	4.686	0.059	0.700	0.760	1.763	0.781	0.841
0-44	4.464	0.103	1.158	0.982	2.483	1.325	1.149
0-59	4.242	0.161	1.446	1.204	3.228	1.738	1.496
0-89	3.536	0.214	1.736	1.910	4.584	2.348	2.522
0-119	3.300	0.293	2.159	2.146	5.775	3.161	3.148
0-189	2.621	0.520	2.624	2.825	8.116	4.720	4.921
0-249	2.338	0.750	3.068	3.108	9.751	6.236	6.276
0.324	1.430	0.971	3.074	4.016	11.195	7.616	8.558
2967 A° Isopropyl Alcohol Run II-61 $(E)^o = 6.101 \times 10^{-5}$ moles liter^{-1}							
0-30	5.642	0.060	0.587	0.459	1.025	0.613	0.485
0-60	5.469	0.043	0.884	1.091	1.975	0.971	1.178
0-90	4.866	0.017	1.015	1.235	2.876	1.190	1.410
0-120	4.607	0.087	1.440	1.494	3.720	1.726	1.780
0-195	3.835	0.209	2.033	2.266	5.718	2.721	2.954
0-285	3.300	0.383	2.673	2.801	7.801	4.041	4.169
0-375	2.544	0.534	2.984	3.557	9.595	5.208	5.781

Continued

TABLE XX - Continued

Interval, Min.	Component Concentrations at End of Interval, moles liter^{-1} x 10^5 (E)	(T)	(P)	Converted Ergosterol, moles liter^{-1} x 10^5 (E)° - (E)	Kinetic Quantities, moles liter^{-1} x 10^5 $\tilde{I}_E$	(P) ÷ $\tilde{I}_P$	(E)° - (E) ÷ $\tilde{I}_P$
2967 A° 20% Glycerol Run II-64 (E)° = 6.101 x 10^{-5} moles liter^{-1}							
0-30	5.472	0.076	0.620	0.629	0.956	0.647	0.656
0-60	5.301	0.126	1.023	0.800	1.845	1.117	0.894
0-90	5.060	0.129	1.343	1.041	2.708	1.535	1.233
0-120	4.450	0.183	1.542	1.651	3.524	1.858	1.967
0-200	3.961	0.277	2.150	2.140	5.528	2.902	2.892
0-290	3.281	0.451	2.680	2.820	7.530	4.087	4.227
0-380	2.734	0.640	3.164	3.367	9.281	5.410	5.613
2967 A° 20% Mineral Oil Run II-57 (E)° = 5.446 x 10^{-5} moles liter^{-1}							
0-30	5.127	0.0	0.335	0.319	0.918	0.352	0.336
0-60	4.876	0.0	0.810	0.570	1.810	0.877	0.637
0-90	4.364	0.047	1.075	1.082	2.662	1.225	1.232
0-120	4.066	0.064	1.339	1.380	3.448	1.601	1.642
0-180	3.472	0.163	1.792	1.974	4.952	2.367	2.549
0-285	2.782	0.331	2.393	2.664	7.200	3.697	3.968
0-360	2.408	0.419	2.526	3.038	8.600	4.492	5.004
0-420	2.025	0.556	2.942	3.421	9.557	5.502	5.981

Continued

TABLE XX - Continued

Interval, Min.	Component Concentrations at End of Interval, moles liter^{-1} x 10^5 (E)	(T)	(P)	Converted Ergosterol, moles liter^{-1} x 10^5 $(E)^o - (E)$	Kinetic Quantities, moles liter^{-1} x 10^5 $\tilde{I}_E$	$(P) \div \tilde{I}_P$	$(E)^o - (E) \div \tilde{I}_P$
2967 A° 40% Mineral Oil Run II-70 $(E)^o = 5.446 \times 10^{-5}$ moles liter^{-1}							
0-31	4.889	0.045	0.466	0.547	0.944	0.491	0.572
0-61	4.411	0.086	0.911	1.035	1.810	1.003	1.127
0-91	4.140	0.093	1.093	1.306	2.576	1.274	1.487
0-121	3.976	0.141	1.466	1.470	3.310	1.760	1.764
0-211	3.100	0.280	2.076	2.346	5.310	2.853	3.123
0-301	2.522	0.447	2.590	2.924	6.990	4.060	4.394
0-391	1.996	0.578	2.822	3.450	8.403	5.135	5.763

Continued

TABLE XX - Continued

Interval, Min.	Component Concentrations at End of Interval, moles liter^{-1} x 10^5 (L)	(T)	Converted Ergosterol, moles liter^{-1} x 10^5 $(E)^o - (E)$	Kinetic Quantities, moles liter^{-1} x 10^5 $\bar{Y}_E$	$\bar{Y}_P$
2804 A° n-Hexane Run II-18 $(E)^o = 5.446 \times 10^{-5}$ moles liter^{-1}					
0-15	0.000	0.000	0.153	0.862	0.009
0-30	0.084	0.000	0.604	1.536	0.032
0-45	0.520	0.010	1.374	2.353	0.084
0-60	0.228	0.000	1.210	3.078	0.156
0-90	0.433	0.000	2.039	4.429	0.370
0-120	0.000	0.254	2.157	5.649	0.670
0-150	0.000	0.331	2.448	6.783	1.054
0-230	0.000	0.604	3.364	9.163	2.226
0-290	0.113	0.875	4.032	10.422	3.239
0-350	0.073	1.060	4.396	11.264	4.324
2967 A° n-Hexane Run II-53,67 $(E)^o = 5.446 \times 10^{-5}$ moles liter^{-1}					
0.30	0.071	0.013	0.394	0.922	0.023
0-60	0.092	0.048	0.779	1.768	0.079
0-90	0.328	0.064	1.261	2.550	0.162
0-120	0.236	0.082	1.424	3.289	0.270
0-180	0.442	0.134	2.024	4.623	0.528
0-270	0.569	0.264	2.721	6.324	1.021
0-330	0.680	0.350	3.138	7.286	1.424
0-375	0.435	0.432	3.246	7.957	1.766
0-435	0.538	0.489	3.606	8.776	2.270
0-495	0.796	0.575	4.061	9.481	2.822
0-560	0.625	0.646	4.214	10.123	3.454

Scarborough (35) to calculate the constant a was altered algebraically to the following to facilitate the computations:

$$a^3 \left[\left[xy \left[1 - \frac{(\Sigma x)^2}{(\Sigma y)^2} \right] + \frac{\Sigma x}{\Sigma y} \left[\Sigma x^2 - \Sigma y^2 \right] \right]\right]$$

$$+ a^2 \left[\left[\Sigma y - \frac{2n \Sigma x \; \Sigma xy}{(\Sigma y)^2} + \frac{1}{\Sigma y} \left[(\Sigma x)^2 + n (\Sigma x^2 - \Sigma y^2) \right] \right]\right]$$

$$+ a \left[\frac{n}{\Sigma y} \left(\Sigma x - \frac{n \Sigma xy}{\Sigma y} \right) \right] = 0 \qquad \text{(VII-7)}$$

The constant b was calculated from the value of a from VII-7 and the relationship

$$a\left(\frac{\Sigma x}{n}\right) + b \left(\frac{\Sigma y}{n}\right) + 1 = 0 \qquad \text{(VII-8)}$$

The origin, i.e., the point at zero time of irradiation was weighted as one experimental point in the calculations. During the course of these calculations it became evident that the least squares procedure described above yielded values of the quantum yields that were generally within 0.01 of the values obtained from graphical plots. The values of the quantum yields for the case of equivalent excited states were all calculated by the above procedure, but subsequent calculations were made with the more simple usual least squares procedure.

The results of the application of the kinetic equations are presented in Table XXI.

TABLE XXI

THE RESULTS OF THE KINETIC TREATMENT, EQUIVALENT EXCITED STATES

Solvent	Visc. Cps. 25°C.	Wavelength 2537 A° ϕ_E	ϕ_P	$\frac{k_5}{k_4}$	2804 A° ϕ_E	ϕ_P	$\frac{k_5}{k_4}$	2967 A° ϕ_E	ϕ_P	$\frac{k_5}{k_4}$
n-Hexane	0.304	.54	.15	.18	Lumisterol formed					
20% Min. Oil	0.561	.51	.17	.18	.33	.12	.12	.36	.10	.11
40% Min. Oil	1.192	--	--	--	--	--	--	.40	.10	.11
i-Pr. Alcohol	2.068	.49	.18	.23	.27	.12	.14	.38	.10	.11
20% Glycerol	7.135	.48	.19	.22	.25	.12	.12	.35	.11	.11

The values of ϕ_E, ϕ_P, and k_5/k_4 are found to be dependent on both solvent and irradiating wavelength. A detailed interpretation of these effects will be presented in a later section. However, it is interesting to note at this point that the values of ϕ_E are in approximate agreement with the quantum yield of calciferol formation as inferred from bioassay results. For example, a value of about 0.3 is obtained from the bioassay results of Steenbock and Hamans (16). The values of ϕ_E (from the present study) are based on the conversion per excited ergosterol molecule; since the major product of the irradiation is precalciferol (which would be detected as calciferol in a bioassay), values of ϕ_E should be at least in rough agreement with the quantum yield of calciferol formation as derived from bioassay results.

2. Case of Non-Equivalent Optical and Derived Excited States

The derivation based on the mechanism

$$\begin{array}{ccccc} E & \underset{\longleftarrow}{\overset{h\nu}{\rightleftharpoons}} & E^* & \longrightarrow & L \\ & & \downarrow & & \\ & & P & \underset{\longleftarrow}{\overset{h\nu}{\rightleftharpoons}} & P^* \longrightarrow T \end{array} \qquad \text{(VI-62)}$$

was found to yield the equations

$$(E)^\circ - (E) = \phi_E [\, \tilde{I}_E \,] \qquad \text{(VI-58)}$$

$$T = \phi_{PT} [\, \tilde{I}_P \,] \qquad \text{(VI-60)}$$

$$L = \phi_{EL} [\, \tilde{I}_E \,] \qquad \text{(VI-61)}$$

In each case a linear dependence of the experimental quantity on the left hand side of the equation upon the experimental quantity in square brackets on the right hand side of the equation is predicted. In comparing the experimental data with these equations, the irradiation data presented in Table XX and the $\tilde{I}_P$ values tabulated in Appendix III were used. Since the relationship (VI-58) is identical to that obtained in Case 1, it was necessary only to perform the additional calculations employing equations (VI-60) and (VI-61).

The predicted linear plots were again obtained, cf. Figures 18-30. It is not surprising that a plot of (T) vs. $\tilde{I}_P$ will be linear as well as a plot of (T) vs. the quantity (P) $\cdot$ $\tilde{I}_P$, since (P) and (T) both increase proportionately. The usual least squares procedure was utilized to obtain values for ϕ_{PT} and ϕ_{EL}; the point at zero time of irradiation was again weighted as one experimental point. The results are presented in Table XXII.

Figure 18

Kinetic Plots, Case of Non-Equivalent Optical and Derived Excited States

2537 A° Isopropyl Alcohol Run III-10

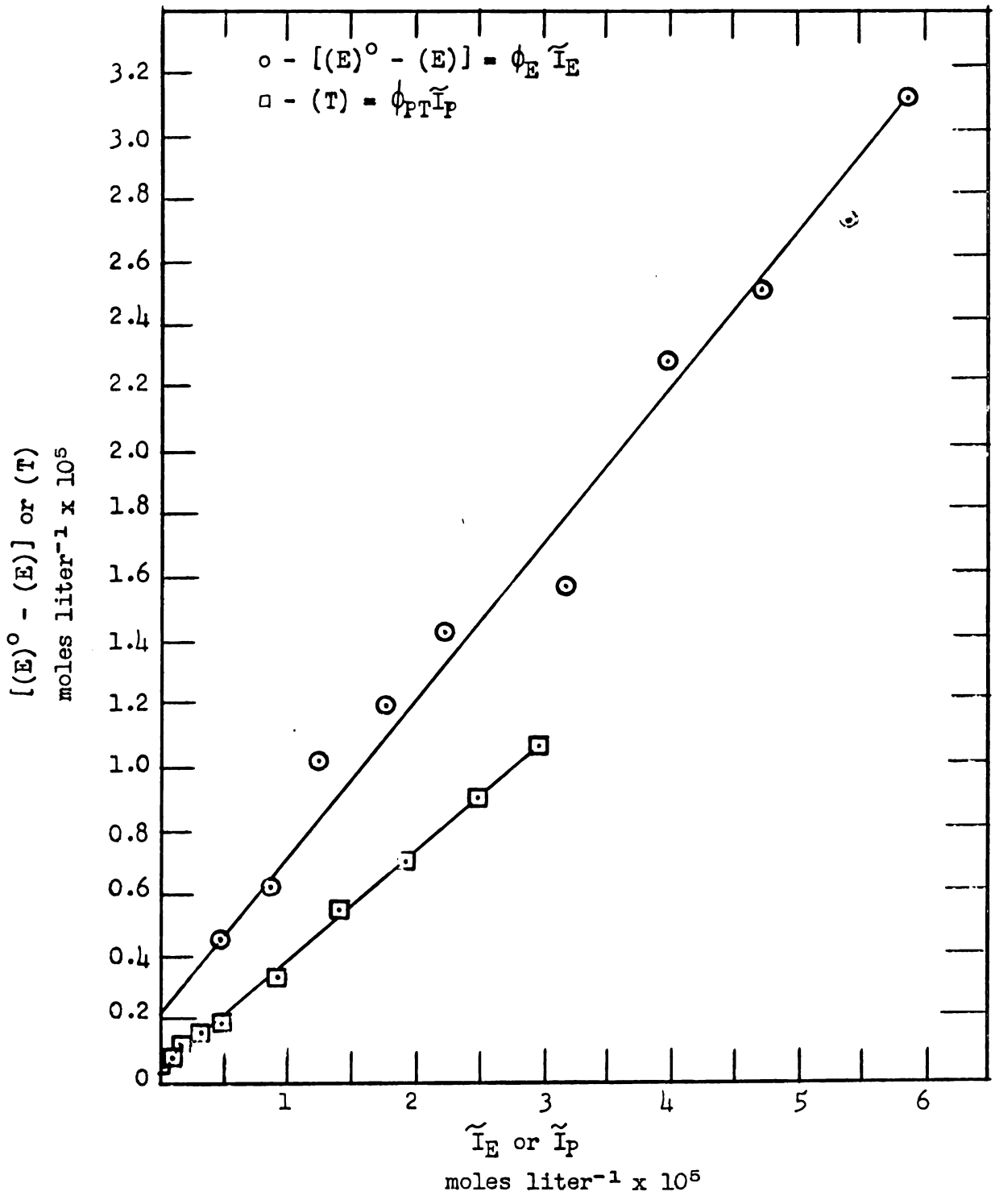

Figure 19

Kinetic Plots, Case of Non-Equivalent Optical and Derived Excited States

2537 A° 20% Glycerol Run III-14

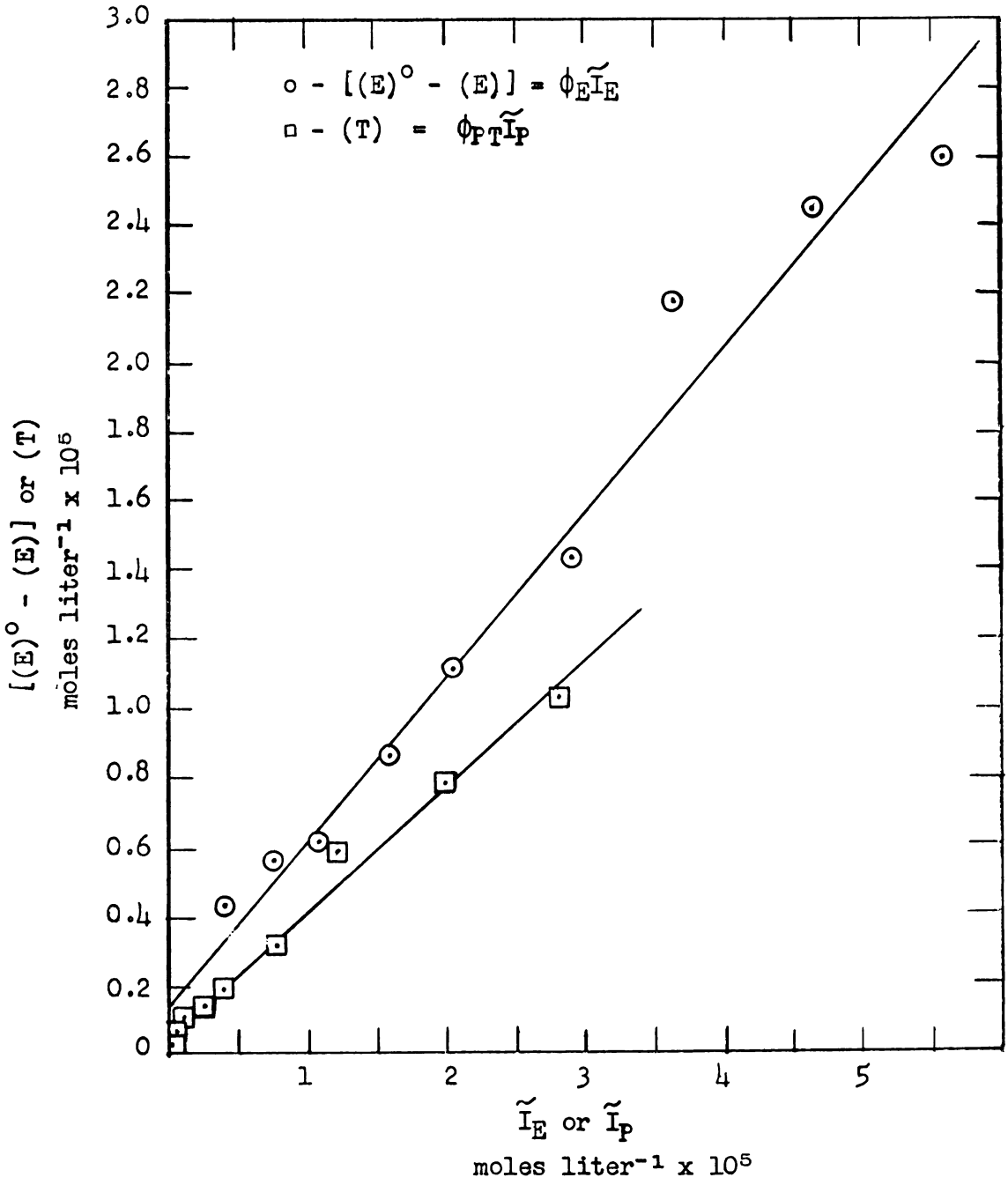

Figure 20

Kinetic Plots, Case of Non-Equivalent Optical and Derived Excited States

2537 A° n-Hexane Run III-22

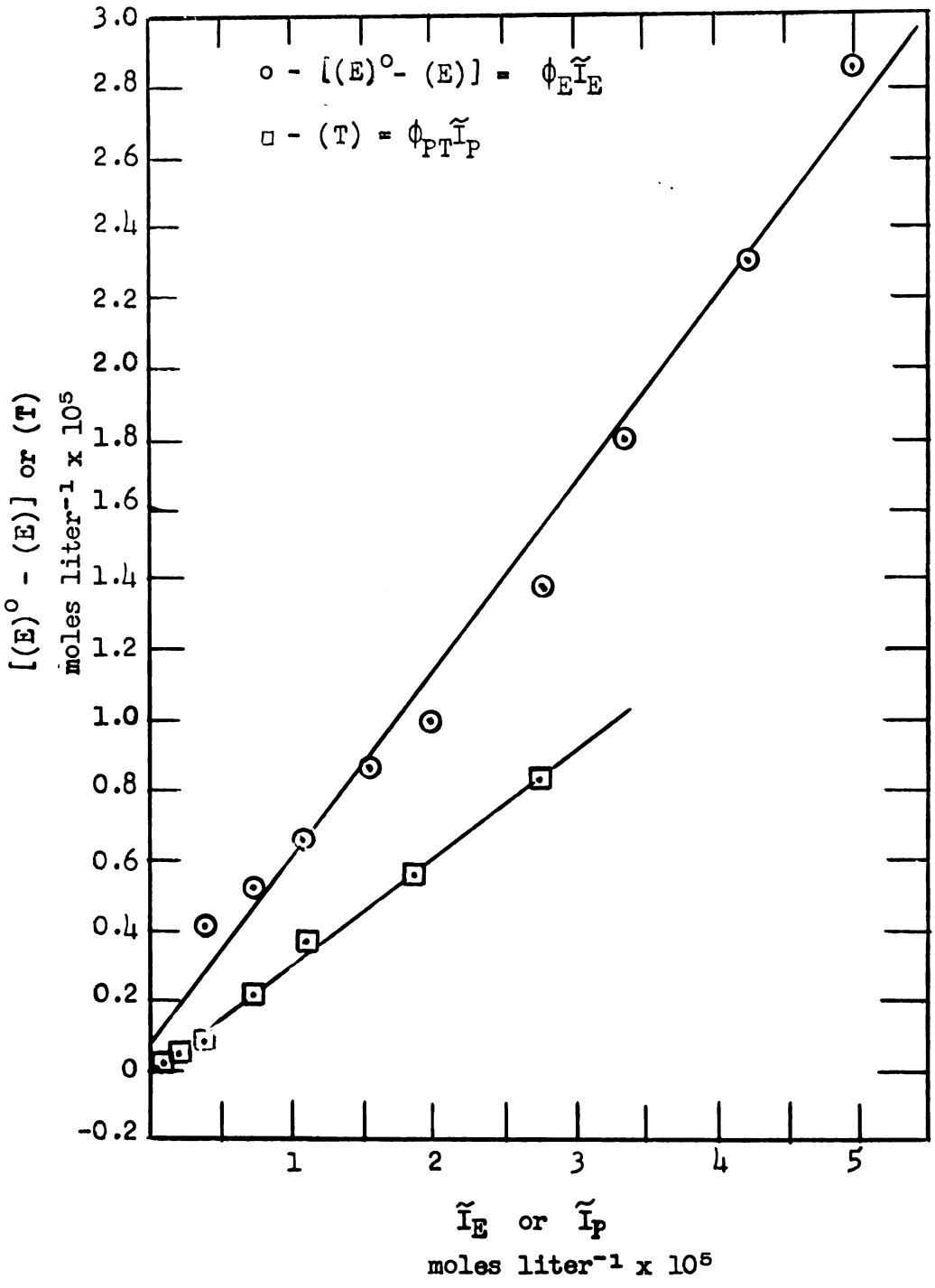

Figure 21

Kinetic Plots, Case of Non-Equivalent Optical and Derived Excited States

2537 A^{o} 20% Mineral Oil Run III-18

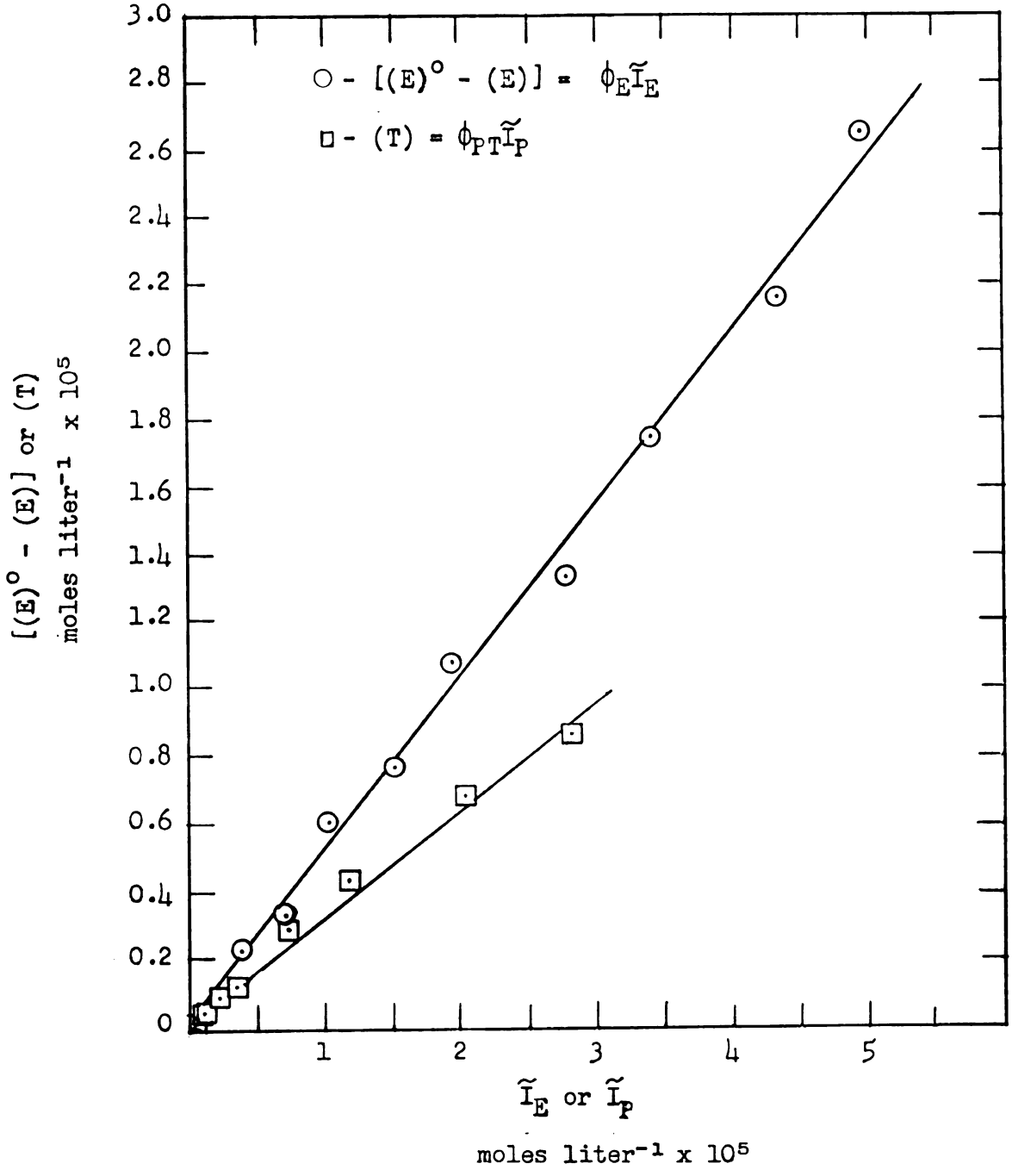

Figure 22

Kinetic Plots, Case of Non-Equivalent Optical and Derived Excited States

2804 A° Isopropyl Alcohol Run II-14

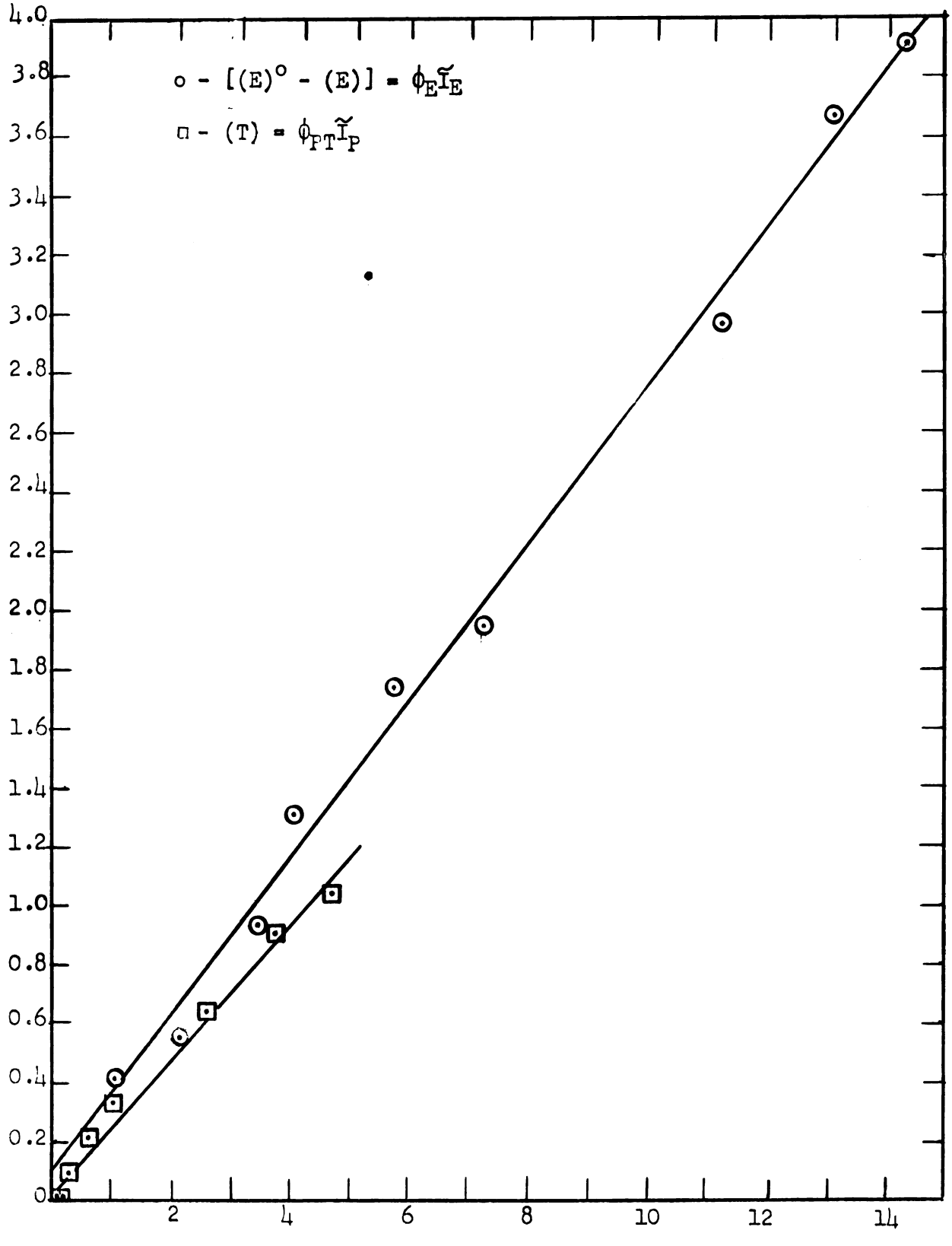

Figure 23

Kinetic Plots, Case of Non-Equivalent Optical and Derived Excited States

2804 A° 20% Glycerol Run II-9

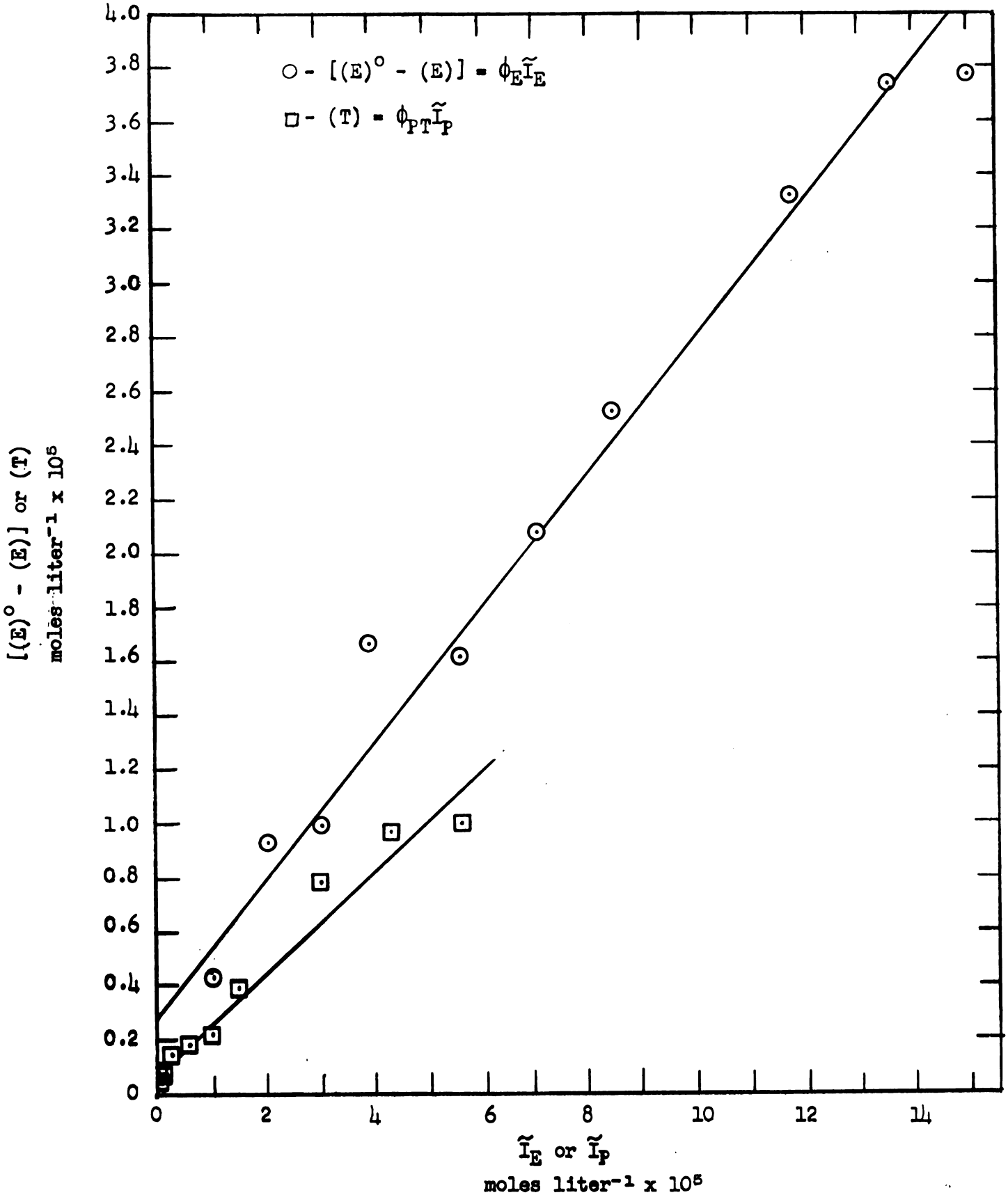

Figure 24

Kinetic Plots, Case of Non-Equivalent Optical and Derived Excited States

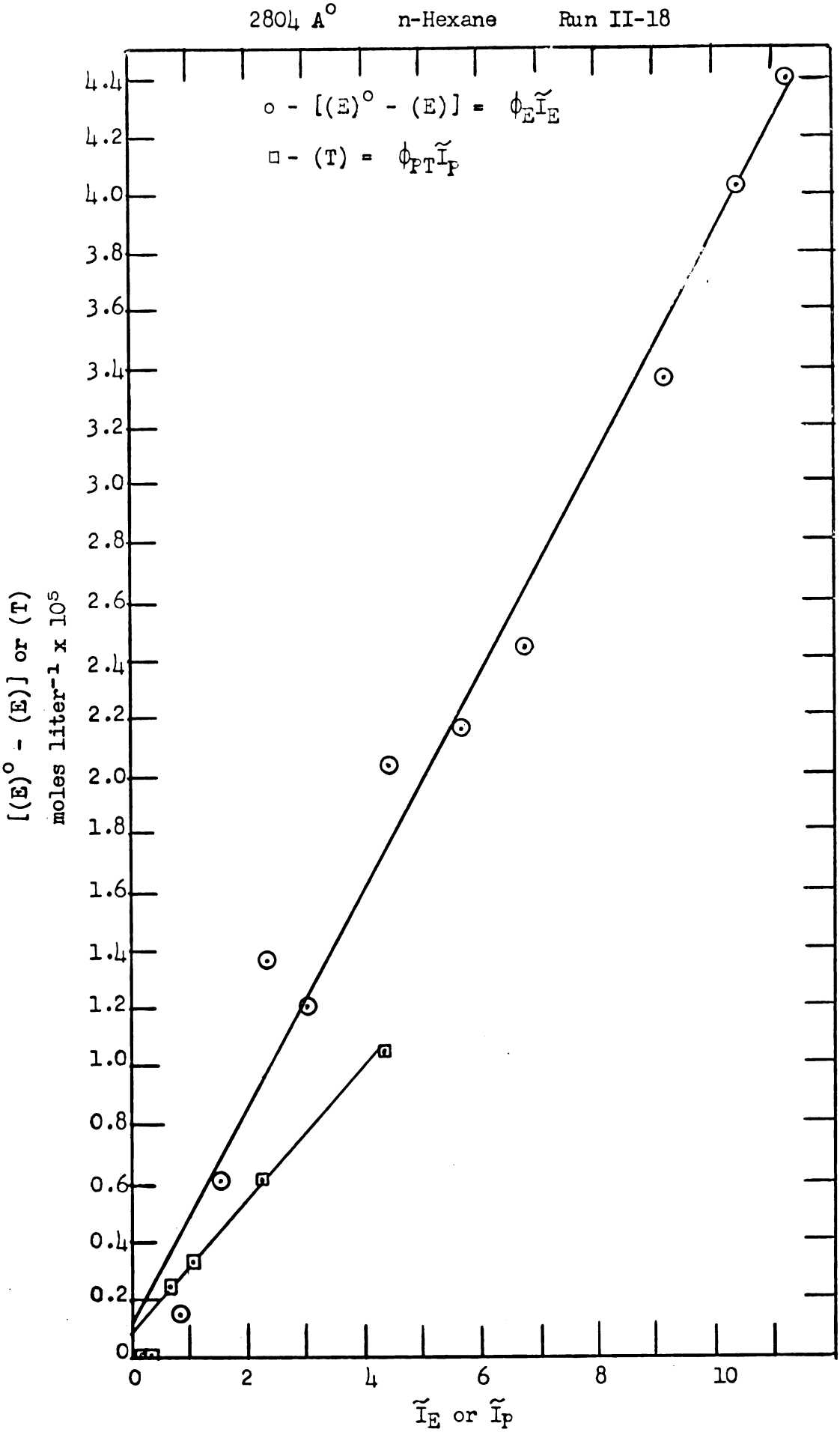

Figure 25

Kinetic Plots, Case of Non-Equivalent Optical and Derived Excited States

2804 A° 20% Mineral Oil Run II-24

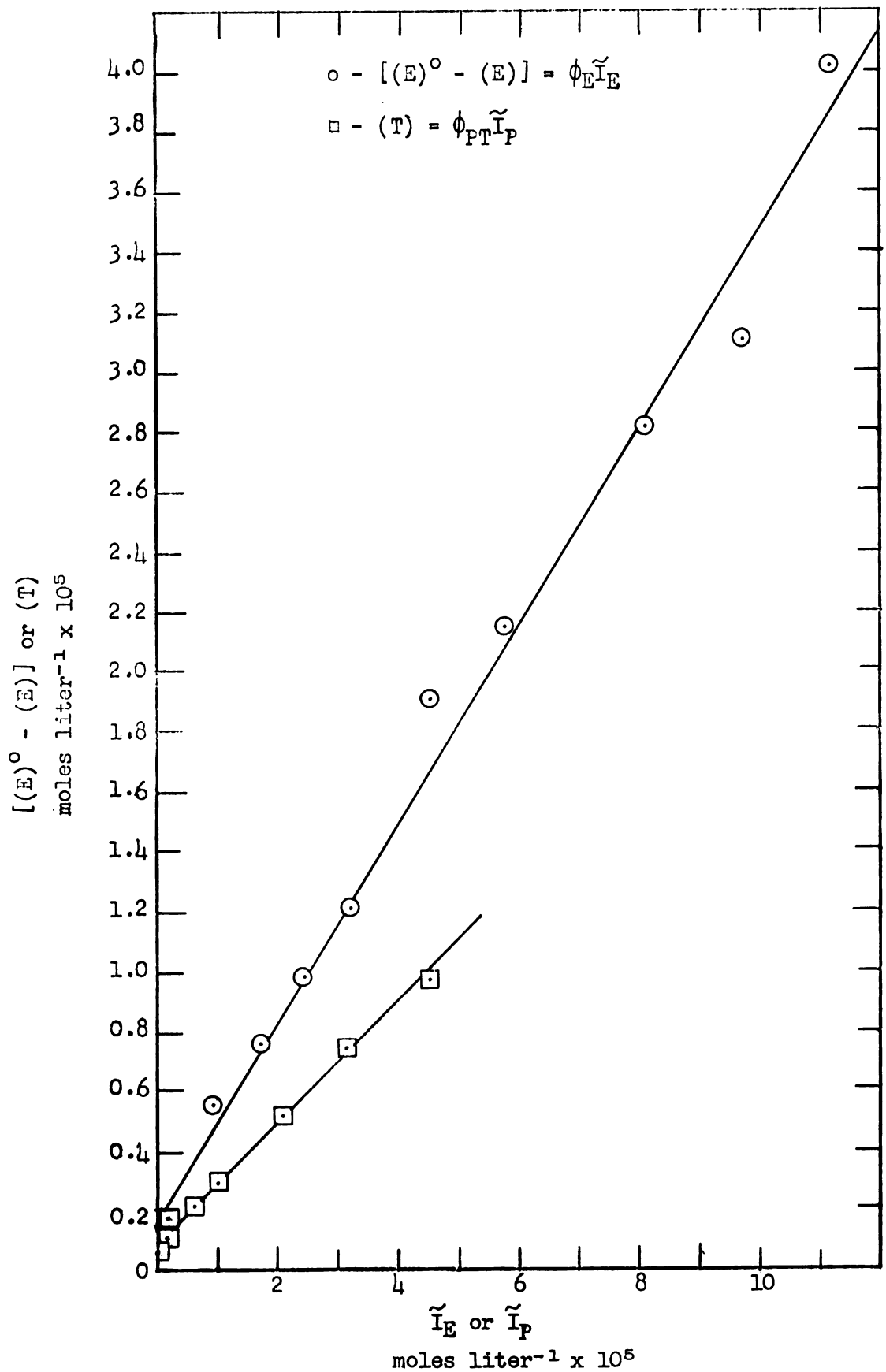

Figure 26

Kinetic Plots, Case of Non-Equivalent Optical and Derived Excited States

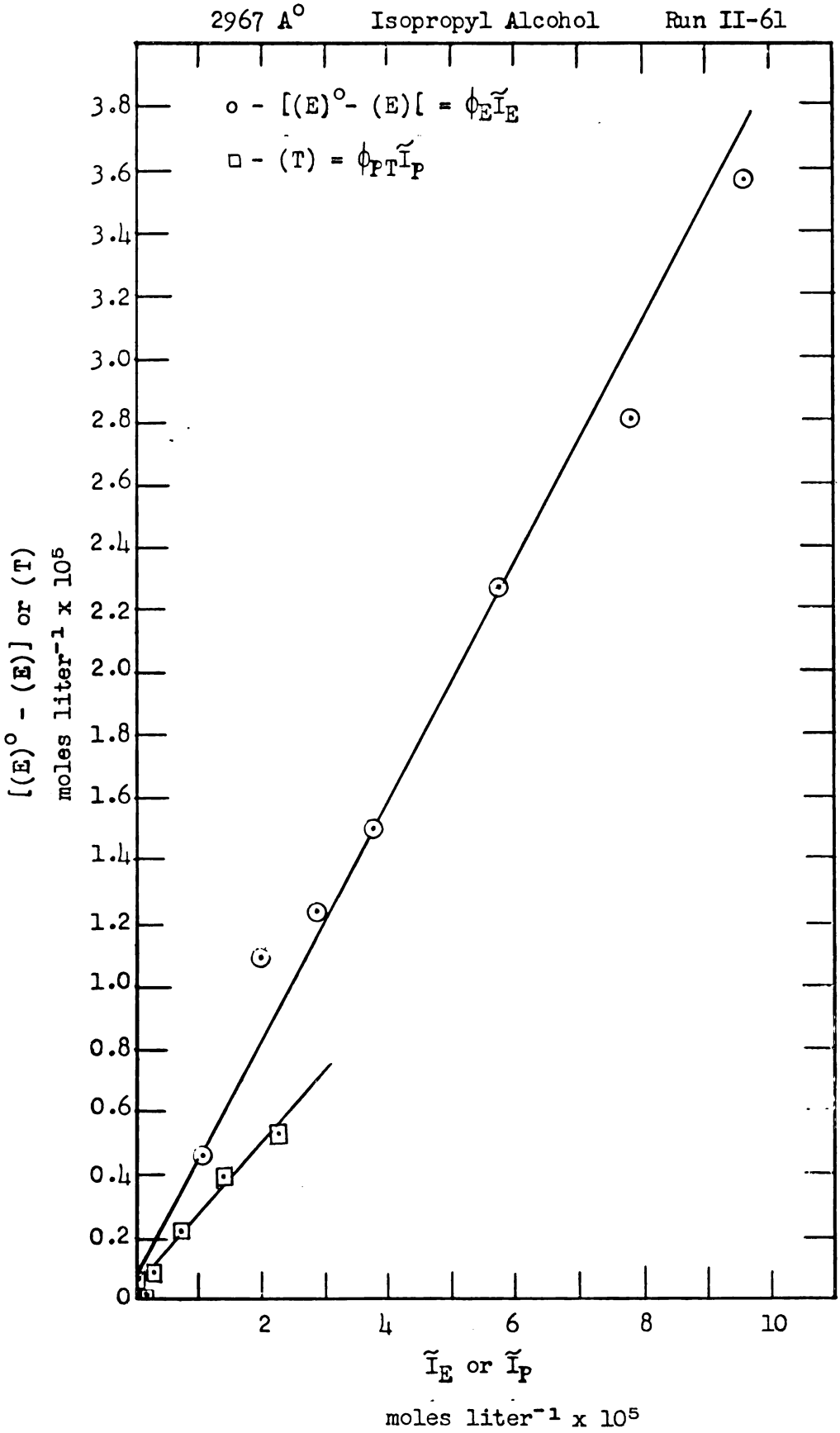

Figure 27

Kinetic Plots, Case of Non-Equivalent Optical and Derived Excited States

2967 A° 20% Glycerol Run II-64

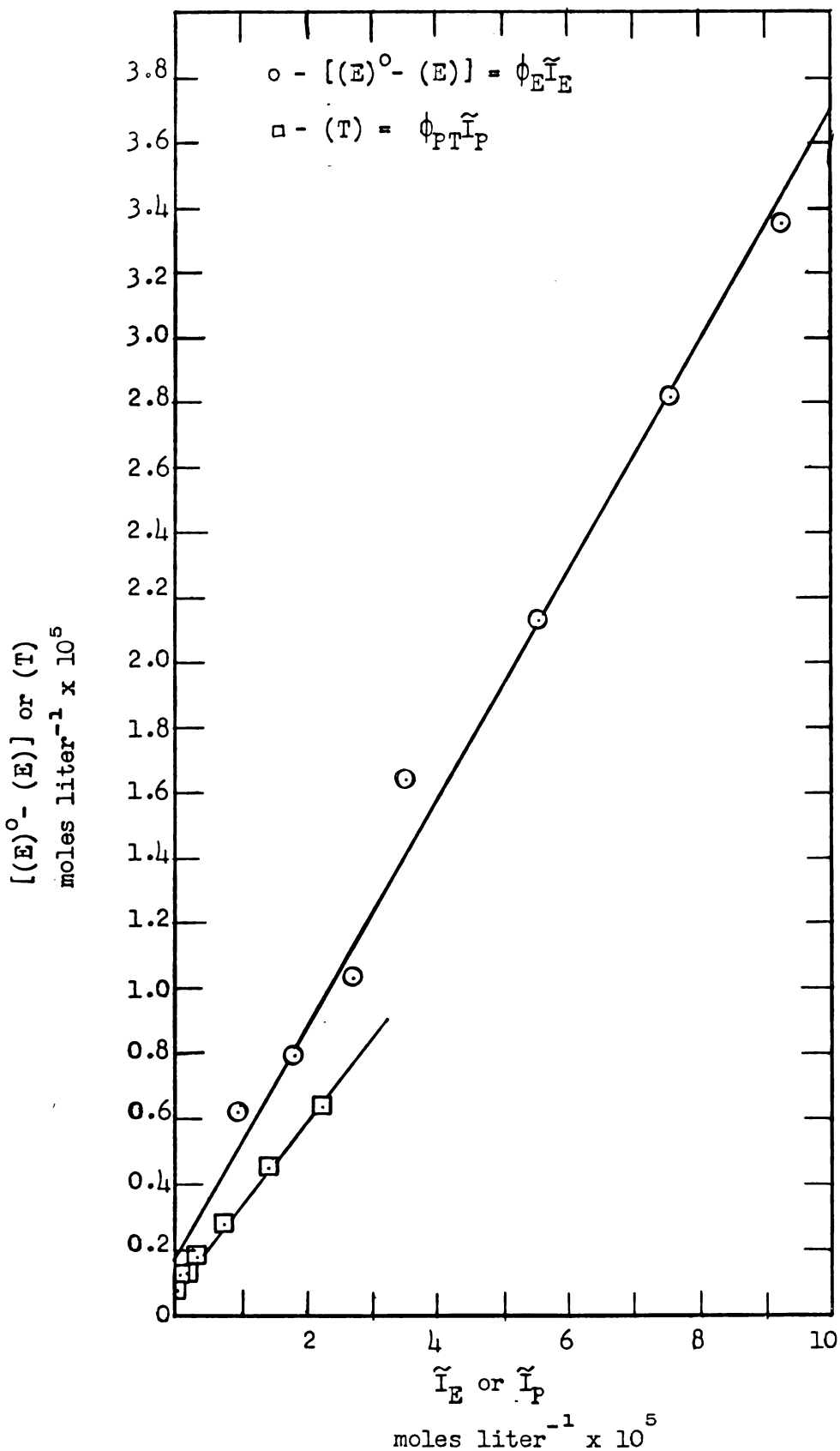

Figure 28

Kinetic Plots, Case of Non-Equivalent Optical and Derived Excited States

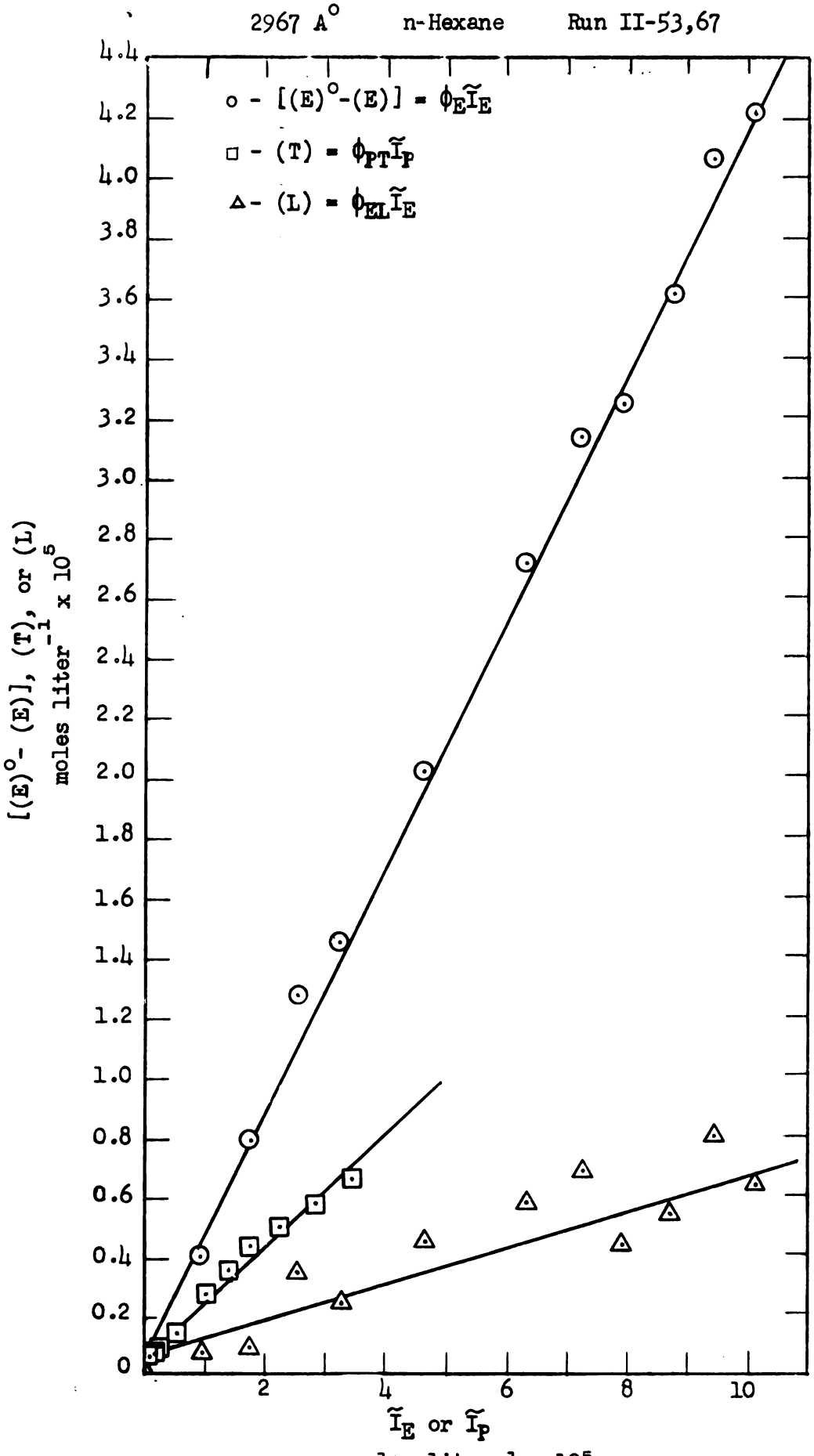

Figure 29

Kinetic Plots, Case of Non-Equivalent Optical and and Derived Excited States

2967 A° 20% Mineral Oil Run II-67

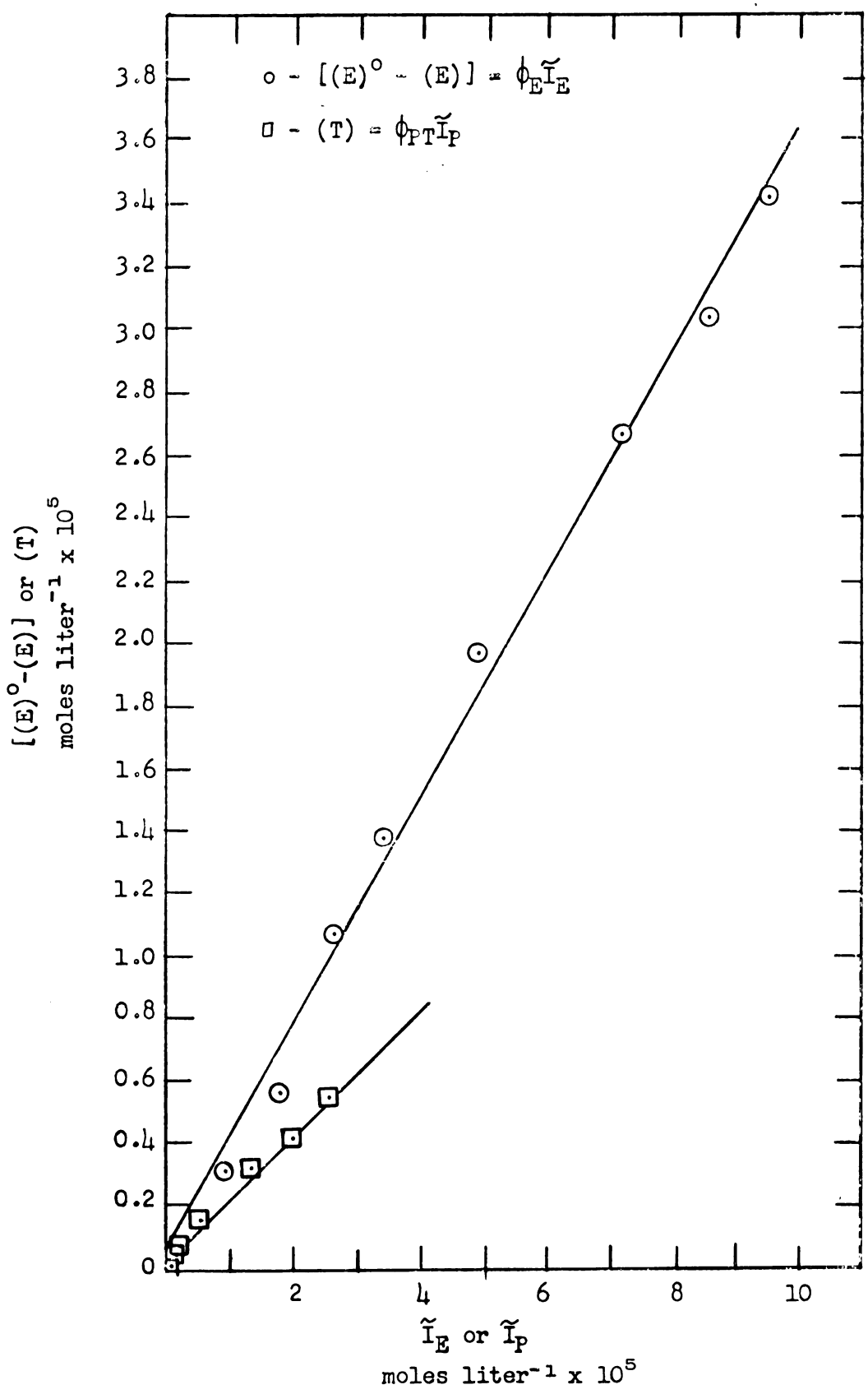

Figure 30

Kinetic Plots, Case of Non-Equivalent Optical and Derived Excited States

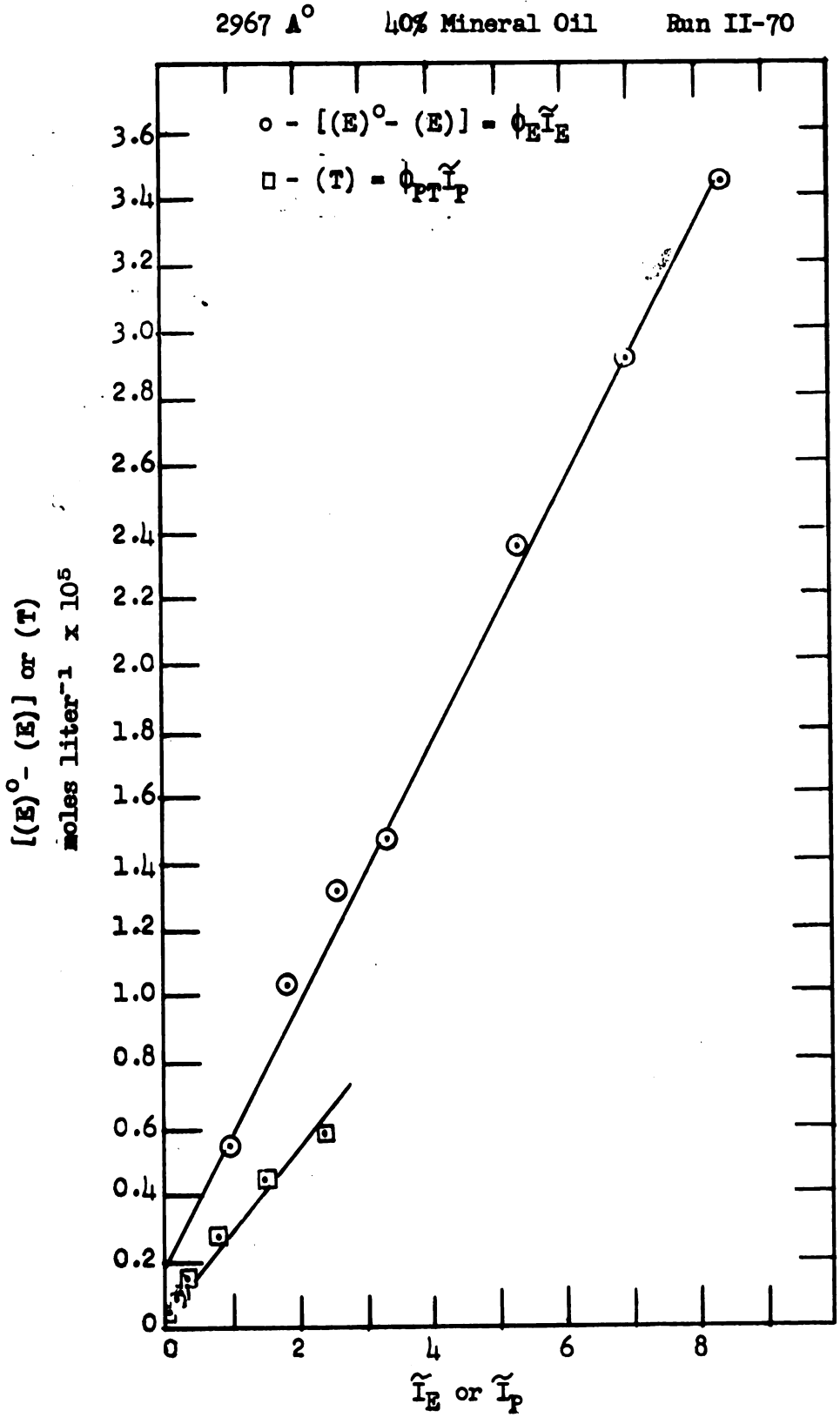

TABLE XXII

RESULTS OF THE KINETIC TREATMENT, NON-EQUIVALENT EXCITED STATES

Solvent	Visc. Cps. 25°C.	Wavelength 2527 A° ϕ_E	2527 A° ϕ_{PT}	2804 A° ϕ_E	2804 A° ϕ_{PT}	2967 A° ϕ_E	2967 A° ϕ_{PT}	2967 A° ϕ_{EL}
n-Hexane	0.304	0.54	0.31	0.38	0.24	0.41	0.19	0.06
20% Min. Oil	0.561	0.51	0.32	0.33	0.21	0.36	0.22	--
40% Min. Oil	1.192	--	--	--	--	0.40	0.24	--
i-Pr. Alcohol	2.068	0.49	0.35	0.27	0.23	0.38	0.24	--
20% Glycerol	7.135	0.48	0.36	0.25	0.19	0.35	0.26	--

Application of equation (VI-61) to the data at 2804 A° in n-hexane was not successful; lumisterol was not formed in sufficiently significant quantities.

It is apparent that the values of ϕ_{PT} obtained by the above treatment differ appreciably from the values of the equivalent quantity, ϕ_P, obtained for the case of the equivalent excited states. The significance of these differences will be discussed in detail in the next section.

VIII. INTERPRETATION OF KINETIC RESULTS

It is evident from the typical plots of Figure 17 that the kinetic expressions derived on the basis of the equivalence of optical and derived excited states fit the kinetic data rather well. The values for ϕ_E are in approximate agreement with the quantum yield of calciferol formation based on bioassay results. The quantities ϕ_P and k_5/k_4 appear to have values of reasonable magnitude, and the values of the two quantities are internally consistent. In general, the results yielded by the kinetic treatment based on equivalent optical and derived excited states appear to be capable of reasonable interpretation.

Attempts to extend the first kinetic treatment--expression (VI-24)--to the case in which lumisterol was formed were unsuccessful. In addition, an important discrepancy existed between the values of ϕ_P derived from the kinetic treatment and the result reported by Havinga's group for the value of the quantum yield for the process P $\longrightarrow$ T (33). They reported a value of 0.4 for the conversion of precalciferol to tachysterol; this value was obtained by direct irradiation of precalciferol at 2537 A^o in ethanol. A value comparable to Havinga's result derived from the kinetic treatment of this study is the value of ϕ_P at 2537 A^o in isopropyl alcohol; this value of ϕ_P is about one-half of the reported quantum yield, cf. Table XXI.

On the basis of the mechanism formulated by expression (VI-24), a value of 0.4 for ϕ_P would mean that the build up of tachysterol should be almost as great as that of precalciferol. It is evident from a

qualitative inspection of the concentration-time data, cf. Figures 14a-1 to 14c-5, that precalciferol is present in much larger quantities than tachysterol. Proceeding on the assumption that the value reported by Havinga's group is correct, and considering the resultant deduction with regard to tachysterol build up, one comes to the conclusion that precalciferol in its normal ground electronic state is a necessary intermediate for the formation of tachysterol by the irradiation of ergosterol. In effect, the data indicate that tachysterol is derived from the irradiation of precalciferol that is formed in the irradiation mixture.

In order to resolve the discrepancy in quantum yields, the mechanism was modified to incorporate the inference that normal precalciferol is a necessary intermediate in the formation of tachysterol, cf. expression (VI-62). The kinetic equations derived from expression (VI-62) fit the data equally as well as the equations derived from mechanism (VI-24), as is evident from Figures 17-30. The value of 0.36 for ϕ_{PT} at 2537 A° in isopropyl alcohol (Table XXII) is in good agreement with Havinga's value of 0.4 for the quantum yield of the process P $\longrightarrow$ T. The quantum yield ϕ_E is calculated from the same kinetic expression--equations (VI-39, VI-58)--for both reaction mechanisms, and, as previously stated, the values of ϕ_E are in accord with other reported data. In addition reaction scheme (VI-62) was capable of extension to yield a value for ϕ_{KL}; it should be noted that other reaction sequences, in which lumisterol was derived from precalciferol or tachysterol, were not consistent with the data.

In general, the kinetic relationships derived from the case termed non-equivalent optical and derived excited states satisfy the data of this investigation, and are in accord with data reported by other investigators. The combined results of the two reaction mechanisms--in particular, the apparent requirement that normal precalciferol is a necessary intermediate in the formation of tachysterol--suggest that the optical excited states of the irradiation products are not identical to the reactive intermediates that are derived through internal rotational movements of the segments of the optically excited ergosterol molecule.

Several qualitative conclusions regarding solvent and wavelength dependence are apparent from the results of the kinetic treatment, cf. Table XXII. As previously discussed, the solvent dependence may be attributed in large measure to a viscosity effect while the wavelength dependence is distinct from an inner filter effect. The obvious and important conclusion regarding the formation of lumisterol only in a solvent of low viscosity has been discussed in Section V.

The effects of viscosity on ϕ_E and ϕ_{PT} are fairly consistent, but quite small. The values of ϕ_E and ϕ_{PT} are considered to be reliable to ± 10%, estimating that the actinometric data are accurate to ± 10% and the analytical results are reliable to ± 5%. In general, the differences among the values of ϕ_E and ϕ_{PT} in different solvents and at a given wavelength are only slightly greater than the estimated limits of reliability. However, the fairly consistent variance of ϕ_E and ϕ_{PT} with viscosity suggests that the small viscosity effects are real. The quantum yield ϕ_E

decreases with increasing solvent viscosity in a consistent manner at 2537 and 2804 A°. The results exhibit some irregularity at 2967 A°, but even at this wavelength, the results do establish the stated trend of variance of ϕ_E with viscosity. The value of ϕ_{PT} varies directly as the solvent viscosity at each irradiating wavelength.

A rather marked wavelength dependence is shown by both ϕ_E and ϕ_{PT}. For a given solvent, ϕ_E and ϕ_{PT} are appreciably larger at the short wavelength (2537 A°) than at the longer wavelengths (2804 and 2967 A°). There is some discrepancy in the wavelength dependence exhibited at 2804 A°, since the values of ϕ_E and ϕ_{PT} are slightly larger (in most solvents) at 2804 A° than at 2967 A°. However, as a result of the experimental conditions employed, errors in the values at 2804 A° are considered to be somewhat greater than the results obtained at 2537 and 2967 A°. A larger slit width (2.00 mm.) was employed in irradiations at 2804 A° than at 2537 and 2967 A° (1.50 mm.). Consequently, the band width was greater and approximations introduced into the treatment of the actinometric data are of more limited validity. Examples of the approximations are the assumption of a triangular slit function and the utilization of average molar absorbancies over the band width. In addition, the larger slit width resulted in a stronger incident beam and the reaction proceeded more rapidly with the possible formation of over-irradiation products. The non-linearity of response of the photomultiplier tube was also greatest at 2804 A° because of the relatively high incident intensity and lack of screening of the photomultiplier, (cf. experimental section).

In any event, the wavelength effect on ϕ_E and ϕ_{PT} is quite marked and indicates that the energies of the quanta absorbed play an important role in the isomerization reaction.

It was possible to obtain a value of ϕ_{EL} only at 2967 A°, and the concentration-time data (Tables XVIIa-XVIIc) indicate that lumisterol is formed in significant quantities only when the wavelength of irradiation is greater than about 2800 A°. The value of ϕ_{EL} cannot be considered determined with any degree of precision; however, the appearance of significant amounts of lumisterol only in the least viscous solvent suggests that ϕ_{EL} is strongly viscosity dependent and favored by low viscosity. The appearance of lumisterol only at the longer wavelengths suggests further that ϕ_{EL} is wavelength dependent, but, because of the lack of precision in determination of lumisterol at low concentration, it is likely that lumisterol builds up to a low concentration at other wavelengths but is only clearly distinguishable from experimental error where the level of build-up is sufficiently high. The very low molar absorbancy of lumisterol relative to ergosterol and other components at 2967 A° probably permits its build-up there to a detectable concentration under the most favorable conditions of low viscosity.

It remains now to present a description of the photochemical isomerization, using the concepts presented as a basis for the kinetic derivation, that is consistent with conclusions drawn above. As suggested in Section VI, a contributing type of reaction step may be pictured as a cross-over from the potential energy surface of an excited state of a precursor to a potential energy surface of some state of the given product.

Ergosterol and its irradiation products may be regarded as minima in the multi-dimensional potential energy hyper-surface of the ground states of the system. The relative energies of the minima in the potential energy diagram must, of course, be drawn arbitrarily, but it seems reasonable that the energies of lumisterol and ergosterol should be approximately equal, while that of precalciferol should be slightly higher, because of the substitution of one π-bond for one σ-bond (even though the σ-bond was weakened by steric repulsions), and because of the fact that steric repulsions do not permit conjugation of the added π-bond of precalciferol with the other two π-bonds. Tachysterol is probably the component of lowest energy, based on its extended trans configuration, which minimizes steric repulsions and permits conjugation of the entire π-network of three double bonds. Similar considerations apply to the optical excited states and suggest that excited precalciferol, with the C_5-C_{10} double bond present in most of its contributing structures, but not conjugated with the excited π-network, is higher in energy than excited ergosterol, which has contributing structures with the C_9-C_{10} single bond or with two conjugated double bonds (see Figure 16).

Because of the complex nature of the reaction, it seems to be impossible to represent the important transformations by means of a single reaction coordinate. The transformations of ergosterol to precalciferol and lumisterol can, however, be described in terms of a single coordinate, which is essentially the angle of rotation about the bond C_5-C_6. The subsequent transformation of precalciferol to tachysterol cannot be

pictured through a simple coordinate, since this step involves rotation about the bonds C_5-C_6 and C_6-C_7.

In Figure 31 an attempt is made to represent the energetic relationships. The solid curve in Figure 31a shows potential energy vs. rotation about the bond C_5-C_6 for ground state ergosterol and lumisterol as represented by their valence bond structures shown in Figure 1; since the rotation is about a double bond and requires rupture of the C_9-C_{10} bond, this motion is strongly unfavorable for these structures. The solid curve in Figure 31b shows the corresponding potential energy relationship for precalciferol, as represented by its valence bond structure shown in Figure 1. Here a double minimum appears, with a barrier too low to permit isolation of the two separate forms (perhaps 5-10 K.cal./mole); the two minima correspond to the structures that would be obtained directly by rupture of the C_9-C_{10} bond and slight rotation from ergosterol and lumisterol, respectively. The positions corresponding to ergosterol and lumisterol are marked on the diagram.

One dashed curve in Figure 31c is an attempt to represent the potential energy of the species E^* obtained by optical excitation of ergosterol; its valence bond structure is assumed to be a composite of those shown in Figure 16. The other dashed curve in Figure 31c is a similar representation of P^*, the optically excited state of precalciferol; its valence bond structure is assumed to be a composite of corresponding ionic structures obtained from precalciferol, but with the C_5-C_9 double bond preserved and the excitation involving only the conjugated electrons in the opened ring B.

Figure 31a. Potential Energy Curves, E and L

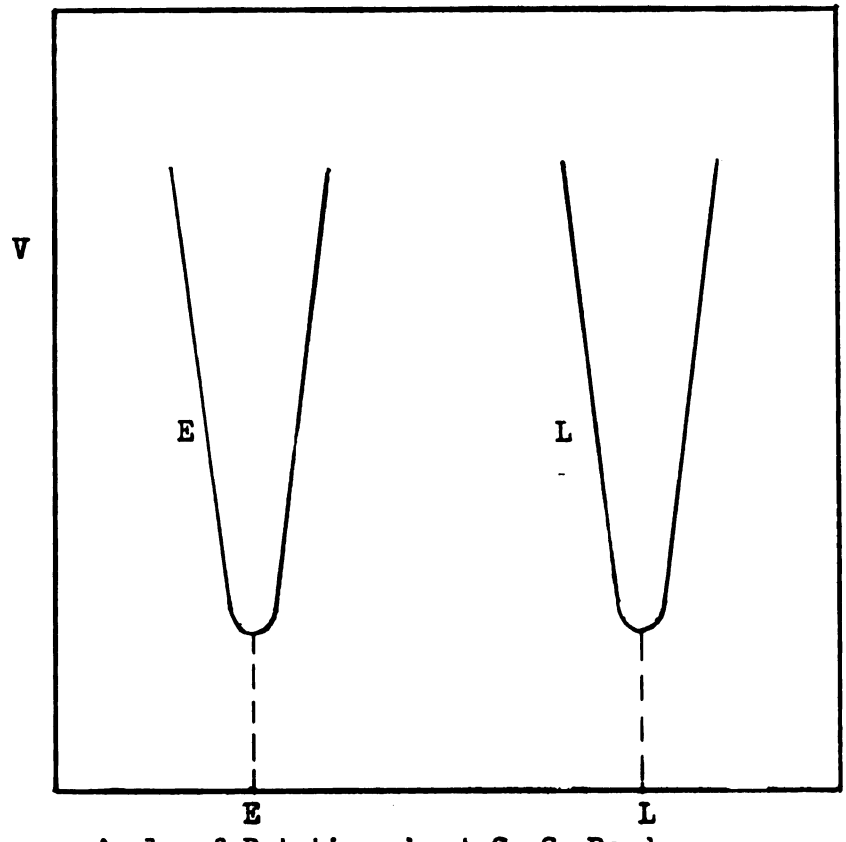

Figure 31b. Potential Energy Curves, P

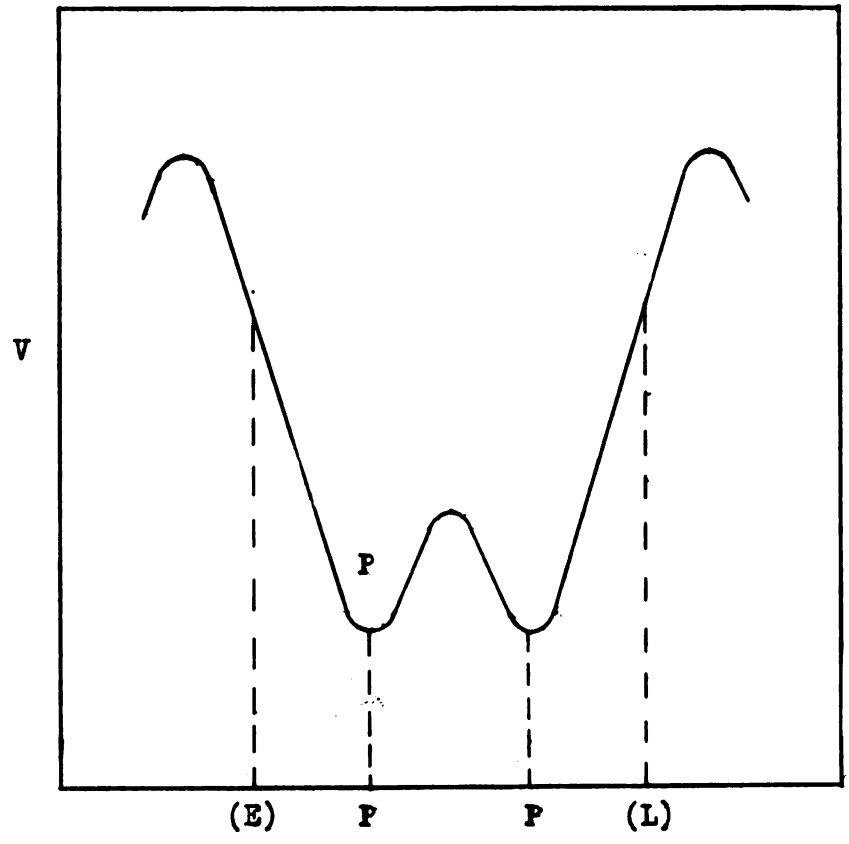

Figure 31c. Potential Energy Curves--
E, P. L, E^* and P^*

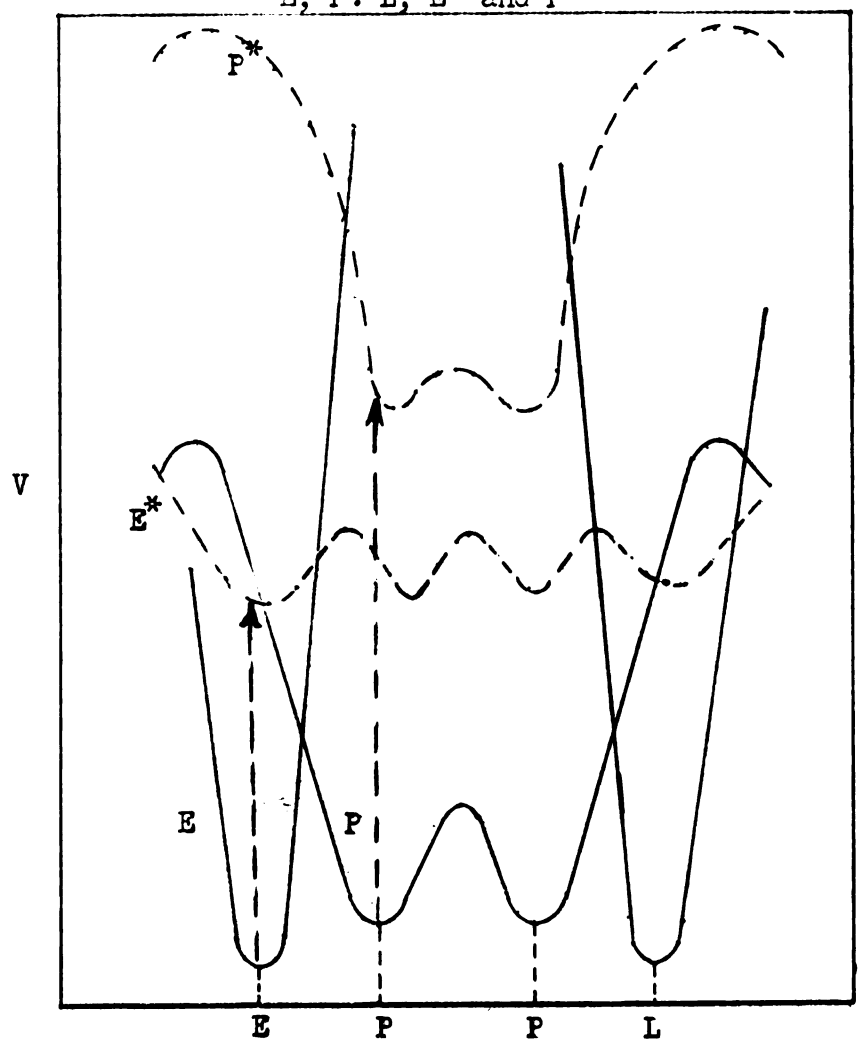

Figure 31d. Potential Energy Curves, P, T, P^* and T^*

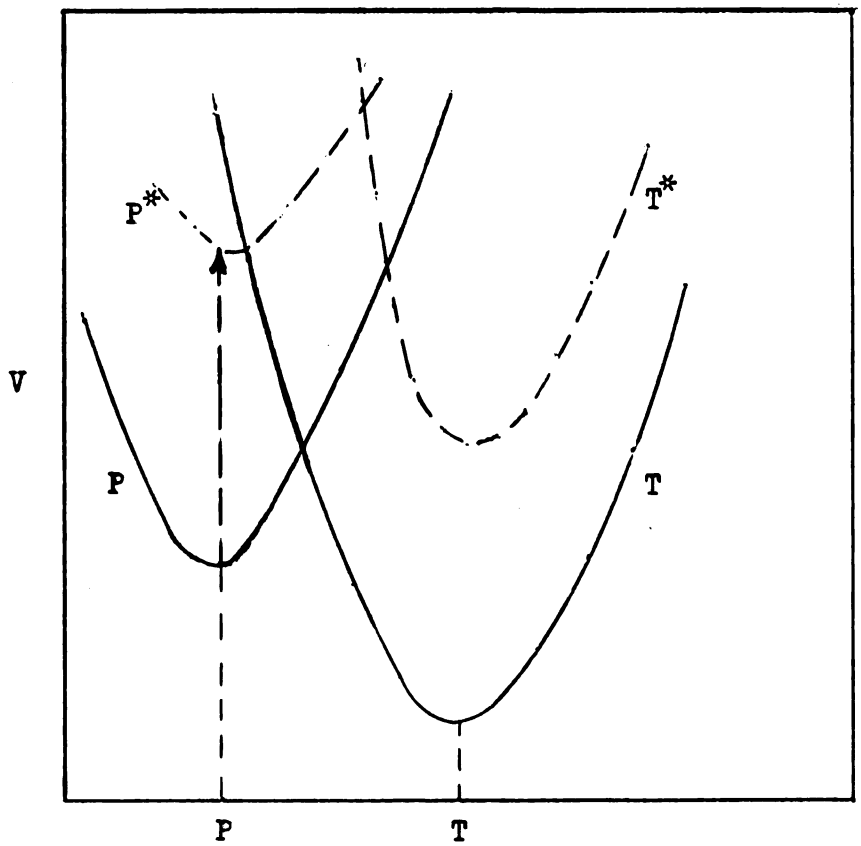

Figure 31c is the composite energy diagram, including all the states shown in Figures 31a and 31b. Also shown is a vertical line corresponding to optical excitation of ergosterol and another corresponding to optical excitation of precalciferol.

It is apparent that excited ergosterol could cross over to give normal precalciferol (in a vibrationally excited level of the ground electronic state). However, in a viscous medium the necessary rotational motion would be impeded (the rotational diffusion constant varies inversely with viscosity--Stokes-Einstein Law), and this would enhance the possibility of collisional or fluorescent deactivation to the ground state of ergosterol. Thus ϕ_E, the fraction of E^* going to products, would be expected to vary roughly inversely with viscosity, as observed.

It is possible that some of the excited ergosterol continues past the cross-over and is later deactivated to precalciferol or even to lumisterol. The latter possibility requires considerable motion of bulky parts of the molecule against the viscous resistance of the solvent, so is feasible only in solvents of particularly low viscosity.

The wavelength effect is not apparent from the diagram, since the excess energy of shorter wavelength may go into other vibrational modes. Since this excess vibrational energy does redistribute, before it is removed by collisions, some of it may help with the motion required to form precalciferol and lumisterol. The increase of ϕ_E at shorter wavelength bears this out. However, ϕ_{EL} was found significant only at the longest wavelength; it is felt that this is an artifice caused by (a) the impossibility of detecting with certainty low concentrations of lumisterol,

which made it unfeasible to include, in the mechanism, steps related to the subsequent fate of lumisterol, and (b) the aforementioned spectrum of lumisterol, which would permit its build-up much more strongly at the longest wavelength. Thus ϕ_{EL} probably increases somewhat with decreasing wavelength, but the concentration of lumisterol did not build up to detectable amounts in the kinetic study because of its many times more rapid consumption at shorter wavelengths.

From this diagram, it looks as though excitation of precalciferol should lead to ergosterol and lumisterol. This probably occurs to a small extent (Havinga (34) reported some ergosterol formed upon irradiation of precalciferol, with nearly quantitative formation of tachysterol), but return to precalciferol is relatively more favorable here than was return to ergosterol after absorption of light by ergosterol. More important, an alternative reaction coordinate is available for excited precalciferol involving successive or simultaneous rotation about the C_5-C_6 and C_6-C_7 bonds to form tachysterol. The relationship between precalciferol and tachysterol is shown schematically in Figure 31d. Here, again, ground states are shown by solid curves and excited states by dashed curves. The figure shows how, for that fraction of the excited precalciferol which executes motion along this combinational coordinate, formation of tachysterol (ϕ_{PT}) is very favorable and favored by an <u>increase</u> of viscosity, since deactivation over a large portion of the motion will lead preferentially to tachysterol rather than back to precalciferol. The wavelength dependence, again, can not be illustrated, but excess energy should make excitation of the combined rotations relatively more favorable than the

simple rotation about the C_5-C_6 bond, and should lead to increased quantum yield of tachysterol at shorter wavelengths, as observed.

There is, however, an alternative explanation of the results which must be given serious consideration. It has been clearly demonstrated that there is a wavelength dependence apart from the inner filter effect and also a solvent effect which may now definitely be said to be associated with viscosity. The mechanistic interpretation ascribes the wavelength dependence to the usefulness of excess energy per quantum in contributing to the isomerizations, and attributes the viscosity effect to a viscous barrier to the internal rotation necessary at the molecular level for the isomerizations. Both conclusions are based upon the assumption of homogeneity of the solution in the irradiation cell, which has been aided in these experiments by stirring and by the use of dilute solutions in thicker cells to give a diminished gradient of light intensity through the cell.

If it be now assumed that the effect of viscosity is on bulk diffusion within the cell, and that there is a measurably greater probability of absorption of a quantum of light by a molecule which has just been formed in an absorption act, the apportionment of the total light absorption among the absorbing species will be altered, but the spectrophotometrically determined concentrations of the individual species will be unaffected. Starting with a uniform distribution of ergosterol in the cell, the initial absorption act will create some precalciferol and, perhaps, some lumisterol. These species as formed will be non-uniformly distributed, each with a concentration gradient through the cell paralleling the incident intensity

gradient, with a preponderance in the front portion of the cell where the radiation intensity is greatest.

This natural "orienting" influence of the incident intensity gradient will be in competition with the disorienting effects of diffusion and stirring, which will tend towards re-establishing a uniform concentration distribution. The effect of viscosity will be upon the disorienting effects, with diffusion coefficients varying inversely with bulk viscosity, and a higher viscosity favoring a laminar flow upon stirring, providing relatively little mixing. The resultant concentration gradients will reflect the outcome of the competition between the orienting and disorienting factors, and will clearly be the greater the more viscous the solvent medium--although with adequate stirring they <u>may</u> prove negligible throughout the viscosity range employed.

If some concentration gradient remains, an apportionment of the absorbed light intensity at the next stage of the irradiation based on uniform concentrations throughout the cell will then ascribe too much absorption to ergosterol and not enough to precalciferol and lumisterol. As tachysterol builds up through conversion of precalciferol, it will, to even a greater extent (because of both light intensity and precalciferol concentration gradients), be concentrated in the front portion of the cell.

The calculated quantum yields according to equations (VI-58) and (VI-60) were given by

$$\phi_E = \frac{(E)^o - (E)}{\int_o^t A_E I_a dt}$$

and

$$\phi_{PT} = \frac{(T)}{\int_0^t A_P I_a dt}.$$

Here $\int_0^t A_E I_a dt$ represents the light absorbed by ergosterol and $\int_0^t A_P I_a dt$ represents the light absorbed by precalciferol, each during the time interval from t = 0 to t = t. But the calculated $\int_0^t A_E I_a dt$ will be too large and the calculated $\int_0^t A_P I_a dt$ will be too small, based on uniform concentration distribution. Hence the calculated value of ϕ_E will tend to be smaller than the correct value, and the calculated value of ϕ_{PT} will tend to be larger than the correct value. The effect of viscosity will be to enhance the discrepancies, so that ϕ_E will apparently tend to decrease and ϕ_{PT} will tend to increase with increasing viscosity; this prediction proves to be consistent with the experimental results.

The appearance of significant amounts of lumisterol only at the longest wavelength and in the least viscous solvent is also consistent with this type of viscosity effect, since lumisterol, whether it be formed from ergosterol or precalciferol, will tend to be formed primarily in the most intense portion of the beam where it will be readily converted to products (probably precalciferol), unless it is removed to a less intense portion of the beam, as at lower viscosity, or unless its light absorption is relatively low, as at the longest wavelengths used.

Fortunately the experimental data make it possible to choose between these two explanations. In the kinetic runs the absorbed light intensity varied between 3 and 15 x 10^{14} quanta per minute in the irradiation cell.

The sample concentration in the 3 ml. irradiation cell ranged from 5.4 to 6.1 x 10^{-5} moles/liter, which means there were about 10^{17} molecules in the irradiation cell. A given molecule would, on the average, be "hit" with one quantum every $\frac{10^{17}}{15 \times 10^{14}}$ min. or about 67 minutes or 4000 sec. The probability of a given molecule absorbing a quantum of light in one second is $\frac{1}{4000}$; the probability of a given molecule capturing two quanta in one second is $(\frac{1}{4000})^2$. With stirring, the mixing time is of the order of one or two seconds, as observed by allowing a drop of dye to fall into the stirred solution. Even making allowance for the fact that the beam of light occupies only about 20% of the volume of the solution in the cell, and allowing for the fact that the incident intensity in the front part of the cell is approximately double the value at the back, it seems necessary to rule out the possibility of reabsorption as a source of the observed viscosity dependence. A mechanistic interpretation thus appears justified.

The interpretation in terms of a potential energy diagram is necessarily highly speculative at this state of our knowledge. However, it provides a framework for discussion of the mechanism of a reaction of this type, clearly involving electronically excited species, and it suggests the types of further information which we must obtain to gain additional insight into the behaviour of excited molecules and into the detailed mechanism of ergosterol irradiation.

The speculative nature of some of the discussions must not be permitted to obscure certain more clearly defined conclusions from this study. First, it has been found possible to devise a purely

spectrophotometric procedure giving reasonably accurate analysis of the ergosterol irradiation mixture. Second, there is clearly a wavelength dependence apart from inner filter effects. The wavelength dependence appears to indicate a usefulness of the excess energy per quantum in producing the isomerizations. Third, the solvent effect is primarily associated with viscosity; the effect almost certainly can be attributed to viscous resistance to rotational diffusion associated with certain internal rotations necessary to the isomerization. Fourth, the optical excited state of ergosterol must differ from that of precalciferol. Fifth, the position of lumisterol in the reaction sequence is most probably as an alternative product to precalciferol resulting from excited ergosterol.

IX. SUGGESTIONS FOR FURTHER WORK

The present study, with its definite indications of viscosity and wavelength effects, points the way towards further related studies. The other components in the photochemical sequence--precalciferol, tachysterol, and lumisterol--should be irradiated directly at several wavelengths and in several solvents. The irradiation of precalciferol in alcohol at 2537 A° has been reported by Havinga's group, and their results have been very important in the development of the kinetic treatment of this thesis. In order to further establish the viscosity effect on the precalciferol irradiation step (on ϕ_{PT}) irradiation of precalciferol should be conducted as a function of solvent viscosity. It is possible that significant formation of ergosterol and lumisterol might be observed at lower viscosity and at longer wavelengths.

In this investigation it was assumed that neither lumisterol nor tachysterol underwent further reaction in the irradiation mixture. The agreement of the data with the kinetic expressions indicates that further reaction of these components (including the reverse reactions to form their precursors) can occur only to a minor extent. However, both lumisterol and tachysterol were present in only small amounts and their irradiation products would not have been perceptible. It is necessary to establish the fate of irradiated lumisterol and tachysterol for a more complete understanding of the reaction.

An inspection of the structures of ergosterol, lumisterol, and precalciferol suggests a question: are there two forms of precalciferol

differing in the relative orientation of the hydroxyl group on carbon-3 in the A ring? One of the suggested forms would be derived from ergosterol while the other would be formed from lumisterol. It has been assumed that the two forms are not separable. The irradiation of lumisterol would help answer such a question.

In order to more effectively utilize the available information on the ergosterol irradiation reaction, the energy relationships among the components of the irradiation sequence are required in both the ground and excited states. Possible studies that would contribute to this end are fluorescence and phosphorescence studies, very accurate determination of heats of combustion of the compounds, and a suggested study which may be termed "photothermochemistry." In the latter study a calorimetric measurement would be made of the fraction of absorbed radiant energy that is not utilized in the photochemical reaction and is dissipated as heat energy. The calorimetric data would be combined with determinations of the total radiation absorbed and quantum yields to furnish information on the differences in energy among the components of the irradiation mixture. This more direct measurement of energy differences could, like heats of hydrogenation, circumvent the problem of small differences in large quantities which makes heat of combustion data impracticable here.

In order to extend the usefulness of the computational analytical method, it is suggested that the matrix procedure be reformulated so that the stoichiometric relationship among the components is not utilized. The reformulation would involve the inversion of a 5 x 5 matrix rather than a 4 x 4 matrix. The resultant expression would enable the

calculation of the ergosterol concentration directly rather than by difference, and the analytical method could be applied to any mixture which contained the components of the irradiation sequence along with spectroscopically inert materials. Still an alternative procedure would be a similar treatment of the four-component mixture of ergosterol, lumisterol, tachysterol, and precalciferol. Elimination of calciferol appears entirely justified where the analysis is to be applied to irradiation mixtures, since calciferol is formed only in the subsequent thermal rearrangement.

A complete kinetic study of the thermal conversion of precalciferol to calciferol should be made, with study of the influence of medium to attempt to ascertain whether a hydrogen atom or proton is transferred.

X. SUMMARY

A kinetic study has been made of the photochemical isomerization of ergosterol in several solvents--isopropyl alcohol, 20% glycerol in isopropyl alcohol, n-hexane, 20% mineral oil in n-hexane, and 40% mineral oil in n-hexane--and employing three irradiating wavelengths (2537, 2804 and 2967 A^{o}).

In order to carry out this study, an analytical curve-fitting technique, the least squares matrix method, was applied to the ultraviolet absorption spectra of the mixture obtained upon irradiation of ergosterol. The method provided a rapid analysis of the complex mixture, and the components were determined within an average standard deviation of ± 4% in the weight percent of component. The analytical procedure was applied to the ultraviolet spectrum of the irradiation mixture, which was determined periodically during the irradiation; the concentration of each of the components was obtained as a function of time of irradiation. The analytical procedure was verified by application to synthetic mixtures of known composition, and in addition, the procedure was also applied to the spectral data of irradiated ergosterol solutions that were reported by Sharpe (37) in order to verify the applicability of the method to actual irradiation mixtures.

For the kinetic studies, a novel recording photometric apparatus was developed to continuously monitor the radiation absorbed by the solution undergoing irradiation.

A kinetic mechanism which could be expressed in general and specific forms was formulated, based upon stereochemical information, considerations of the excited states of the components of the irradiation mixture, and qualitative interpretation of the concentration-time data. The most general plausible mechanism led to relationships in which the concentrations of the components were expressed as linear combinations of terms consisting of definite integrals representing the amounts of radiation absorbed by individual components during the given irradiation interval. The particular mechanism best capable of describing the experimental results was found to be

$$\begin{array}{ccccc} E & \underset{\longleftarrow}{\overset{h\nu}{\longrightarrow}} & E^* & \longrightarrow & L \\ & & \downarrow & & \\ & & P & \underset{\longleftarrow}{\overset{h\nu}{\longrightarrow}} & P^* \longrightarrow T \end{array}$$

where E, P, T, and L represent ergosterol, precalciferol, tachysterol, and lumisterol, respectively, and E^* and P^* represent optically accessible electronic excited states of ergosterol and precalciferol, respectively. This mechanism reduced the relationships to the simple linear expressions (VI-58,60,61) which could be compared with the experimental data

$$\begin{aligned} (E)^{\circ}-(E) &= \phi_E \tilde{I}_E \\ (T) &= \phi_{PT} \tilde{I}_P \\ (L) &= \phi_{EL} \tilde{I}_E \end{aligned} \qquad \text{(VI-58,60,61)}$$

The kinetic treatment yielded values for quantum yields for the "over-all" conversion of ergosterol (ϕ_E), the conversion of ergosterol to

lumisterol (ϕ_{EL}), and the conversion of precalciferol to tachysterol (ϕ_{PT}). The kinetic runs were carried out in solvents with a range of viscosity, but fixed chemical nature, in a stirred reaction cell, so that any solvent effect may be ascribed to viscosity. The use of the integrated light absorption data in the kinetic treatment corrects for the inner filter effect, so that any observed wavelength dependence must be ascribed to other factors. The kinetic analysis disclosed both a solvent and wavelength dependence (the latter beyond inner filter effects) on the individual reaction steps of the photochemical isomerization. The values obtained are given in Table XXII.

TABLE XXII

RESULTS OF THE KINETIC TREATMENT, NON-EQUIVALENT EXCITED STATES

Solvent	Visc. Cps. 25°C.	Wavelength 2537 A° ϕ_E	2537 A° ϕ_{PT}	2804 A° ϕ_E	2804 A° ϕ_{PT}	2967 A° ϕ_E	2967 A° ϕ_{PT}	ϕ_{EL}
n-Hexane	0.304	0.54	0.31	0.38	0.24	0.41	0.19	0.06
20% Min. Oil	0.561	0.51	0.32	0.33	0.21	0.36	0.22	--
40% Min. Oil	1.192	--	--	--	--	0.40	0.24	--
i-Pr. Alcohol	2.068	0.49	0.35	0.27	0.23	0.38	0.24	--
20% Glycerol	7.135	0.48	0.36	0.25	0.19	0.35	0.26	--

The values of ϕ_E are in qualitative agreement with the quantum yield of calciferol formation as inferred from bioassay results. In addition the value of ϕ_{PT} is in good agreement with the quantum yield for the conversion of precalciferol to tachysterol determined by Havinga and his associates (33).

by the direct irradiation of precalciferol at 2537 A° in ethanol. These results further substantiate the validity of the analytical scheme as applied to the actual irradiation mixtures.

The quantum yield values obtained show individual variations with both wavelength and solvent. ϕ_E shows a definite trend of decreasing with increasing viscosity and with increasing wavelength. ϕ_{PT} also displays a trend towards lower values at longer wavelength, but shows a viscosity dependence in opposite direction to that observed for ϕ_E. ϕ_{EL} could be determined only in the least viscous solvent and at the longest wavelength; the value of this quantum yield is believed to be strongly viscosity dependent, but the wavelength dependence is probably an artifice associated with the low absorptivity of lumisterol at that wavelength.

The data thus far accumulated on the ergosterol irradiation reaction are not yet adequate to permit a complete description of the process. However, the new quantum yield data as functions of viscosity and wavelength, coupled with the recent results of the Havinga group, suggest a new framework for describing the behaviour of the system and point to certain information which would be particularly pertinent for extending our knowledge further.

The photoinitiation of the reaction may be considered as proceeding through the optically accessible singlet excited state of ergosterol. This excited state, which may be pictured as either ionic or diradical, almost surely has some major contributing structures with no bond between C_9 and C_{10}, and, accordingly, has an appreciably reduced barrier to

rupture of this bond and rotation about the C_5-C_6 bond as compared with ground state ergosterol. The excited ergosterol molecule could undergo rearrangement to another structure or collisional or fluorescent deactivation to normal ergosterol. The motion required for formation of the proposed precalciferol structure (see figure 1), constitutes an internal rotation, and would be governed by the viscosity-controlled rotational diffusion constant, so that viscosity of the medium should influence the possible fate of the excited ergosterol molecule. A small fraction of the excited ergosterol may, particularly in media of low viscosity, undergo a more extensive rotation to form lumisterol. The motions have been conveniently pictured in terms of a potential energy diagram.

Precalciferol which has been formed from excited ergosterol is itself capable of absorbing light and going to an excited structure. The quantum yield data of Havinga on the conversion of precalciferol to tachysterol are incompatible with the possibility that the excited states of ergosterol and precalciferol are the same, and a consideration of the important contributing structures suggests the nature of the difference. The excited precalciferol has two principal modes of motion accessible, one leading primarily back to precalciferol, the other to tachysterol. Higher viscosity favors the path to tachysterol.

In both photochemical steps, the excess energy available at shorter irradiating wavelengths is useful in promoting the isomerizations.

Considerable further information is needed before our understanding of the mechanism is complete. It is particularly desirable to study

irradiation of each of the intermediates with respect to wavelength and solvent effects. Any information leading to a clearer picture of the relative energies of states of the isomers would also be very valuable.

LITERATURE CITED

(1) Alder, K., and Schumacher, M. Fortschr. Chem. Org. Naturstoffe, 10, 1 (1953).

(2) Barton, D. H. R., and Kende, A. S. J. Chem. Soc., 688 (1958).

(3) Bosart, L. W., and Snoddy, A. O. Ind. Eng. Chem., 20, 1377 (1928).

(4) Braude, E. A., and Wheeler, O. H. J. Chem. Soc., 320 (1955).

(5) Brockman, H., and Schodder, H. Ber., 74, 73 (1941).

(6) Buchi, G., and Yang, N. C. J. Am. Chem. Soc., 79, 2318 (1957).

(7) Calvert, J. G., and Rechen, H. L. J. Am. Chem. Soc., 74, 2101 (1952).

(8) Crombie, L. Quart. Revs., 6, 101 (1952).

(9) Crowfoot, D. E., and Dunitz, J. D. Nature, 162, 608 (1948).

(10) Dasler, W. Ph. D. Thesis, University of Wisconsin, 1938.

(11) Dauben, W. G., Bell, I., Hutton, T. W., Laws, G. F., Rheiner, A. Jr., and Urscheler, H. J. Am. Chem. Soc., 80, 4116 (1958).

(12) Dwyer, P. S. Annals of Math. Stat., 15, 82 (1944).

(13) Forbes, G. S., and Heidt, L. J. J. Am. Chem. Soc., 56, 2363 (1934).

(14) Frost, A. A., and Pearson, R. G. "Kinetics and Mechanism," John Wiley & Sons, Inc., New York, 1953.

(15) Grundmann, W. Z. Physiol. Chem., 252, 151 (1936).

(16) Hamans, R. W., and Steenbock, H. Ind. Eng. Chem. Anal. Ed., 8, 291 (1936).

(17) Harris, L., Kaminsky, J., and Simard, R. G. J. Am. Chem. Soc., 57, 1151, 1154 (1935).

(18) Havinga, E., and Bots, J. P. L. Rec. trav. chim. Pays-Bas, 73, 393 (1954).

(19) Havinga, E., Koevoet, A. L., and Verloop, A. Ibid., 74, 1230 (1955).

(20) Havinga, E., Verloop, A., and Koevoet, A. L. Ibid., 75, 371 (1956).

(21) Huber, W., Ewing, G. W., and Kriger, J. J. Am. Chem. Soc., 67, 609 (1945).

(22) Inhoffen, H. H. Naturwiss. 43, 396 (1956).

(23) Inhoffen, H. H. Ber., 89, 2273 (1956).

(24) Inhoffen, H. H., Bruckner, K., Grundel, R., and Quinkert, G. Ber., 87, 1407, 1418 (1954).

(25) Inhoffen, H. H., Bruckner, K., and Irmscher, K. Ibid., 88, 1424 (1955).

(26) Inhoffen, H. H., and Bruckner, K. Fortschr. Chem. Org. Naturstoffe, 11, 83 (1954).

(27) Koevoet, A. L., Verloop, A., and Havinga, E. Rec. trav. chim. Pays-Bas, 74, 788 (1955).

(28) Lyness, W. I., and Quackenbush, F. W. Anal. Chem., 27, 1978 (1955).

(29) Mulder, F. J., Roborgh, J. R., DeMan, Th. J., Keuning, K. J., and Hanewald, K. Rec. trav. chim. Pays-Bas, 76, 733 (1957).

(30) Murdock, D. C., "Linear Algebra for Undergraduates," John Wiley & Sons, Inc., New York, 1957, pp. 60-61.

(31) Nield, C. H., Russel, W. C., and Zimmerli, A. J. Biol. Chem., 136, 73 (1940).

(32) Noyes, W. A. Jr., and Leighton, P. A. "The Photochemistry of Gases," Reinhold Publishing Corp., New York, 1941, p. 152.

(33) Rappoldt, M. P., Buisman, J. A. K., and Havinga, E. Rec. trav. chim. Pays-Bas, 77, 327 (1958).

(34) Rappoldt, M. P., Westerhof, P., Hanewald, K. H., and Buisman, J. A. K. Ibid., 77, 241 (1958).

(35) Scarborough, J. B. "Numerical Mathematical Analysis," The Johns Hopkins Press, Baltimore, 1950, pp. 469-472.

(36) Sebrell, W. H. Jr., and Harris, S. (editors), "The Vitamins," Vol. II, The Academic Press, Inc., New York, 1954.

(37) Sharpe, L. H. Ph. D. Thesis, Michigan State University, 1957.

(38) Sheely, M. L. Ind. Eng. Chem., 24, 1060 (1932).

(39) Shaw, W. H. C., Jefferies, J. P., and Holt, T. E. Analyst, 82, 2, 8 (1957).

(40) Shaw, W. H. C. Private Communication, 1958.

(41) Szwarc, M. J. Chem. Phys., 23, 204 (1955).

(42) Velluz, L., Amiard, G., and Petit, A. Bull. soc. chim. France, 1115 (1948); 16, 501 (1949).

(43) Velluz, L., and Amiard, G. Ibid., 205 (1955).

(44) Velluz, L., Amiard, G., and Goffinet, B. Ibid., 1341 (1955).

(45) Velluz, L., Amiard, G., and Goffinet, B. Compt. rend., 240, 2076, 2156, 2326 (1955).

(46) Verloop, A., Koevoet, A. L., and Havinga, E. Rec. trav. chim. Pays-Bas, 74, 1125 (1955).

(47) Verloop, A., Koevoet, A. L., and Havinga, E. Ibid., 76, 689 (1957).

(48) Westerhof, P., and Buisman, J. A. K. Ibid., 75, 1243 (1956).

(49) Westerhof, P., and Buisman, J. A. K. Ibid., 76, 679 (1957).

(50) Van de Vliervoet, J. L. J., Westerhof, P., Buisman, J. A. K., and Havinga, E. Ibid., 75, 1179 (1956).

(51) Yates, R. Ph. D. Thesis, Michigan State University, 1952.

(52) Zechmeister, L. "Progress in Chromatography 1938-1947," John Wiley & Sons, Inc., New York, 1951, p. 27.

(53) Handbook of Chemistry and Physics, Chemical Rubber Company, Cleveland, Ohio, 1947.

APPENDICES

APPENDIX I

CALIBRATION OF PHOTOMETER

Average Value of Scale Reading = $T_{\frac{1}{2}}$
Average Value of $T_{\frac{1}{2}}$ and Extrapolated Value of $\frac{q}{a}$ are in Parentheses.

Irrad. Time Min.	Scale Reading Solvent	Solution	Average	Percent Conversion	$q/a \times 10^{-15}$ quanta/in.^{2}
Run III-9 2537 A° Slit Width 1.50 mm. Conc. of Actinometer Compound 4.951×10^{-4} Molar					
0				0	(1.47)
5.5	6.05	0.17	3.11	0.54	1.47
11	5.96	0.14	3.05	1.08	1.48
16	5.97	0.15	3.06	1.57	1.47
Run III-4 2537 A° Slit Width 1.50 mm. Conc. of Actinometer Compound 3.961×10^{-5} Molar					
0				0	(1.42)
5	6.00	1.20	3.60	4.84	1.41
10	5.95	1.19	3.57	9.57	1.40
15	6.05	1.26	3.66	14.25	1.39
Run III-8 2537 A° Slit Width 1.50 mm. Conc. of Actinometer Compound 1.980×10^{-5} Molar					
0				0	1.47
5.5	6.60	2.98	4.79	8.26	1.45
11.5	6.55	3.08	4.82	16.62	1.43
17.5	6.50	3.16	4.83	24.50	1.41
Run III-2 2537 A° Slit Width 1.50 mm. Conc. of Actinometer Compound 1.980×10^{-5} Molar					
0			(4.62)	0	(1.52)
5	6.26	2.86	4.56	7.31	1.50
10.5	6.19	2.95	4.57	15.00	1.50
16	6.20	3.08	4.64	21.96	1.48
22.5	6.20	3.21	4.70	29.85	1.46
Run III-6 2537 A° Slit Width 1.50 mm. Conc. of Actinometer Compound 9.902×10^{-6} Molar					
0			(5.30)	0	(1.53)
5	6.36	4.13	5.24	9.55	1.50
10.5	6.33	4.20	5.32	18.90	1.45
16	6.26	4.26	5.26	27.50	1.42
21.5	6.34	4.41	5.38	35.52	1.40

Continued

APPENDIX I - Continued

Irrad. Time Min.	Scale Reading Solvent	Solution	Average	Percent Conversion	$q/a \times 10^{-15}$ quanta/in.^{2}
Run III-7 2537 A° Slit Width 1.50 mm.					
Conc. of Actinometer Compound 9.902×10^{-6} Molar					
0			(5.32)		(1.61)
5	6.41	4.26	5.34	9.64	1.57
10	6.31	4.26	5.28	18.05	1.50
15.5	6.27	4.33	5.30	26.41	1.47
21	6.27	4.45	5.36	34.38	1.44
Run II-36 2804 A° Slit Width 2.00 mm.					
Conc. of Actinometer Compound 4.951×10^{-4} Molar					
0			(3.02)	0	(2.82)
5.5	5.52	0.50	3.01	0.88	2.77
10.5	5.55	0.48	3.02	1.64	2.71
15.75	5.55	0.48	3.02	2.44	2.67
Run II-35 2804 A° Slit Width 2.00 mm.					
Conc. of Actinometer Compound 3.961×10^{-5} Molar					
0			(4.13)	0	(4.06)
5.5	5.40	2.91	4.16	7.81	3.92
10.0	5.40	2.86	4.13	13.27	3.68
15.5	5.37	2.84	4.10	19.50	3.49
23.5	5.37	2.87	4.12	28.53	3.38
Run II-42 2804 A° Slit Width 2.00 mm.					
Conc. of Actinometer Compound 9.902×10^{-6} Molar					
0			(4.92)	0	(5.81)
6.0	5.30	4.53	4.92	14.90	5.67
12.0	5.26	4.54	4.90	28.65	5.62
18.0	5.29	4.60	4.94	40.87	5.46
Run II-46 2967 A° Slit Width 1.50 mm.					
Conc. of Actinometer Compound 4.951×10^{-4} Molar					
0			(3.05)	0	(3.63)
6	6.81	0.16	3.16	1.60	3.48
12.5	6.89	0.18	3.18	3.38	3.51
19.5	6.80	0.20	3.10	4.88	3.26

Continued

APPENDIX I - Continued

Irrad. Time Min.	Scale Reading: Solvent	Solution	Average	Percent Conversion	$q/a \times 10^{-15}$ quanta/in.^{2}
Run II-49 2967 A° Slit Width 1.50 mm.					
Conc. of Actinometer Compound 3.961 x 10^{-5} Molar					
0			(5.73	0	(4.35)
8	7.03	4.72	5.875	10.19	3.83
16	7.01	4.44	5.725	18.07	3.24
24	6.95	4.25	5.600	25.78	2.96
Run II-74 2967 A° Slit Width 1.50 mm.					
Conc. of Actinometer Compound 3.961 x 10^{-5} Molar					
0			(6.17)	0	(4.27)
6	7.48	5.15	6.32	7.78	3.90
11	7.47	4.94	6.20	13.61	3.59
17	7.35	4.67	6.01	20.11	3.30
Run II-75 2967 A° Slit Width 1.50 mm.					
Conc. of Actinometer Compound 1.980 x 10^{-5} Molar					
0			(6.62)	0	(4.71)
5	7.54	6.27	6.90	7.78	4.35
10.5	7.24	5.89	6.56	14.52	3.70
16	7.23	5.81	6.52	20.87	3.40
21.5	7.26	5.77	6.52	27.03	3.18

APPENDIX II

ABSORBANCY OF IRRADIATED ERGOSTEROL SOLUTIONS AT ANALYTICAL WAVELENGTHS

Time, Min.	Wavelength, A° 252	256	260	264	268	272	276	280	284	288	292	296
2537 A° Isopropyl Alcohol Run III-10												
0	.259	.319	.437	.480	.580	.684	.580	.681	.651	.393	.391	.359
20	.266	.326	.439	.479	.575	.671	.572	.664	.635	.391	.383	.351
40	.275	.331	.441	.482	.575	.667	.570	.658	.630	.389	.382	.346
60	.281	.339	.443	.483	.571	.658	.567	.649	.622	.390	.378	.341
90	.290	.346	.449	.488	.574	.661	.570	.646	.617	.393	.379	.340
120	.302	.357	.461	.498	.583	.659	.574	.651	.615	.395	.383	.336
185	.317	.376	.477	.515	.598	.674	.596	.663	.629	.415	.401	.356
245	.335	.395	.492	.530	.616	.682	.615	.680	.637	.443	.420	.368
305	.350	.413	.509	.553	.636	.705	.642	.710	.660	.467	.447	.382
365	.365	.429	.524	.571	.661	.725	.670	.740	.680	.497	.476	.407
410	.374	.441	.533	.585	.677	.739	.689	.758	.694	.521	.496	.422
2537 A° Isopropyl Alcohol Run III-14												
0	.255	.311	.428	.477	.568	.681	.579	.668	.659	.401	.384	.363
20	.261	.316	.429	.473	.563	.664	.570	.644	.640	.394	.377	.352
40	.270	.326	.435	.480	.564	.669	.575	.654	.639	.398	.379	.352
60	.281	.335	.443	.486	.569	.666	.575	.646	.637	.400	.379	.356
90	.290	.347	.449	.492	.575	.669	.578	.650	.631	.402	.381	.352
120	.295	.352	.453	.495	.574	.663	.578	.645	.624	.403	.382	.350
180	.310	.369	.469	.508	.588	.671	.594	.653	.635	.419	.396	.358
240	.325	.386	.486	.531	.609	.640	.619	.679	.656	.448	.419	.378
330	.343	.406	.500	.550	.630	.705	.645	.706	.669	.485	.453	.400
420	.371	.436	.531	.583	.668	.739	.690	.755	.710	.526	.495	.431
2537 A° n-Hexane Run III-22												
0	.212	.263	.366	.393	.492	.564	.473	.578	.518	.311	.335	.280
20	.215	.267	.366	.390	.483	.554	.464	.563	.495	.304	.320	.269
40	.219	.267	.360	.386	.470	.546	.457	.543	.495	.298	.313	.262
60	.223	.272	.362	.389	.473	.538	.456	.544	.490	.299	.310	.264
90	.230	.278	.367	.393	.476	.535	.454	.538	.477	.298	.312	.262
120	.235	.284	.370	.396	.475	.532	.454	.534	.480	.300	.309	.262
185	.249	.297	.380	.403	.483	.531	.463	.534	.484	.310	.317	.265
240	.261	.310	.391	.416	.491	.541	.477	.544	.493	.331	.329	.279
330	.276	.326	.403	.431	.503	.550	.496	.558	.504	.351	.348	.289
420	.294	.346	.420	.455	.528	.570	.526	.589	.527	.388	.377	.315

Continued

APPENDIX II - Continued

Time, Min.	Wavelength, A° 252	256	260	264	268	272	276	280	284	288	292	296
2537 A°	20% Mineral Oil				Run III-18							
0	.212	.261	.362	.394	.479	.568	.474	.565	.539	.322	.324	.296
20	.212	.261	.357	.388	.467	.552	.463	.543	.520	.309	.314	.288
40	.220	.268	.362	.392	.469	.551	.462	.538	.521	.314	.312	.288
60	.224	.273	.361	.391	.469	.543	.459	.531	.508	.310	.308	.282
90	.236	.282	.370	.399	.473	.544	.463	.531	.511	.315	.309	.283
120	.242	.289	.372	.402	.476	.542	.464	.532	.505	.316	.310	.278
185	.264	.310	.389	.419	.487	.550	.479	.540	.510	.331	.326	.291
240	.273	.320	.398	.427	.498	.555	.489	.547	.506	.346	.338	.301
330	.284	.333	.407	.440	.507	.562	.508	.565	.535	.375	.362	.320
404	.296	.347	.419	.456	.528	.575	.533	.588	.542	.397	.385	.334
2804 A°	Isopropyl Alcohol				Run II-14							
0	.252	.313	.434	.477	.583	.681	.574	.680	.641	.393	.398	.352
14	.257	.316	.429	.473	.568	.662	.561	.654	.614	.385	.382	.345
29	.270	.330	.438	.476	.568	.655	.557	.636	.617	.381	.371	.338
49	.283	.342	.447	.480	.564	.643	.546	.622	.589	.369	.359	.320
58	.294	.352	.453	.488	.571	.640	.546	.618	.581	.376	.363	.322
88	.316	.371	.462	.499	.566	.633	.551	.607	.582	.383	.358	.324
118	.339	.394	.482	.518	.584	.651	.573	.618	.593	.402	.367	.339
213	.387	.444	.520	.558	.618	.661	.603	.638	.597	.431	.399	.347
273	.408	.470	.543	.587	.648	.684	.638	.666	.618	.471	.432	.371
2804 A°	20% Glycerol				Run II-9							
0	.247	.314	.429	.479	.576	.686	.579	.680	.657	.401	.396	.365
15	.254	.316	.430	.476	.560	.666	.567	.640	.639	.400	.379	.365
30	.272	.330	.441	.480	.571	.655	.555	.640	.601	.385	.376	.336
45	.284	.342	.444	.487	.565	.652	.557	.624	.606	.383	.369	.337
60	.294	.354	.450	.488	.562	.644	.554	.610	.599	.389	.365	.328
90	.315	.375	.467	.504	.573	.644	.560	.616	.594	.389	.364	.333
120	.334	.394	.483	.515	.587	.638	.558	.619	.572	.384	.371	.316
150	.355	.413	.497	.531	.598	.647	.575	.621	.576	.404	.381	.330
240	.392	.452	.529	.573	.634	.674	.620	.648	.613	.458	.421	.368
305	.420	.485	.561	.603	.671	.698	.655	.692	.627	.485	.456	.384
365	.436	.503	.578	.622	.688	.715	.682	.715	.658	.521	.484	.410

Continued

APPENDIX II - Continued

Time, Min.	Wavelength, A° 252	256	260	264	268	272	276	280	284	288	292	296
2804 A° n-Hexane Run II-18												
0	.202	.258	.366	.395	.491	.570	.471	.577	.531	.320	.343	.293
15	.212	.264	.369	.395	.486	.560	.465	.565	.502	.306	.331	.282
30	.259	.305	.405	.428	.523	.600	.500	.593	.523	.322	.332	.273
45	.259	.307	.401	.424	.512	.567	.475	.562	.498	.313	.321	.253
60	.263	.314	.404	.426	.510	.567	.481	.553	.491	.308	.312	.260
90	.296	.341	.421	.447	.509	.561	.481	.547	.492	.317	.309	.250
120	.313	.357	.433	.455	.523	.564	.490	.544	.488	.326	.314	.262
150	.323	.370	.443	.462	.526	.568	.491	.539	.488	.332	.321	.261
230	.368	.419	.489	.516	.570	.586	.539	.573	.509	.366	.352	.278
290	.383	.436	.497	.526	.588	.609	.567	.602	.527	.402	.377	.299
350	.396	.446	.506	.541	.602	.615	.586	.617	.538	.422	.397	.314
2804 A° 20% Mineral Oil Run II-24												
0	.208	.263	.368	.393	.489	.566	.471	.574	.517	.311	.330	.273
15	.219	.271	.370	.394	.488	.553	.464	.559	.496	.309	.322	.266
30	.232	.280	.374	.397	.483	.546	.460	.548	.490	.303	.314	.256
44	.239	.286	.376	.396	.472	.532	.452	.530	.479	.299	.306	.253
59	.257	.303	.386	.409	.483	.536	.457	.529	.474	.302	.307	.254
89	.271	.314	.393	.414	.483	.530	.451	.514	.460	.304	.300	.242
119	.285	.329	.401	.424	.483	.525	.453	.508	.456	.306	.300	.244
189	.318	.363	.431	.450	.509	.541	481	.526	.462	.331	.319	.256
249	.330	.379	.443	.468	.520	.549	.500	.536	.478	.357	.336	.282
324	.344	.394	.455	.484	.542	.562	.536	.560	.494	.385	.362	.291
2967 A° Isopropyl Alcohol Run II-61												
0	.257	.318	.436	.476	.585	.675	.578	.682	.628	.384	.393	.341
30	.267	.325	.434	.474	.570	.658	.564	.655	.602	.380	.375	.337
60	.283	.338	.438	.477	.567	.648	.555	.634	.605	.371	.366	.322
90	.297	.353	.450	.485	.572	.636	.549	.629	568	.358	.360	.299
120	.305	.358	.454	.484	.568	.625	.655	.609	.561	.361	.352	.302
195	.338	.391	.475	.504	.571	.622	.548	.604	.548	.367	.351	.293
285	.370	.421	.497	.525	.586	.625	.562	.600	.544	.381	.358	.301
375	.395	.446	.516	.544	.600	.630	.575	.605	.550	.400	.366	.301
2967 A° 20% Glycerol Run II-64												
0	.257	.319	.436	.482	.579	.682	.580	.682	.636	.388	.392	.342
30	.274	.332	.441	.478	.571	.661	.569	.657	.618	.386	.377	.331
60	.285	.342	.444	.485	.567	.655	.566	.640	.608	.385	.370	.334
90	.298	.353	.451	.487	.566	.645	.558	.622	.594	.379	.358	.326
120	.316	.370	.461	.499	.574	.642	.561	.621	.583	.380	.361	.313
200	.347	.400	.482	.516	.579	.639	.565	.611	.566	.382	.356	.310
290	.374	.425	.502	.535	.592	.640	.574	.610	.565	.399	.365	.313
380	.401	.451	.520	.555	.609	.646	.593	.617	.572	.418	.380	.322

Continued

APPENDIX II - Continued

Time, Min.	Wavelength A° 252	256	260	264	268	272	276	280	284	288	292	296
2967 A°	n-Hexane			Run II-53								
0	.230	.281	.381	.406	.504	.576	.486	.586	.531	.317	.338	.285
30	.231	.279	.372	.399	.482	.553	.465	.552	.509	.308	.317	.276
60	.243	.289	.378	.403	.480	.542	.460	.536	.490	.304	.309	.270
90	.255	.297	.380	.403	.475	.535	.453	.516	.487	.302	.300	.256
120	.263	.305	.384	.405	.471	.526	.448	.509	.478	.300	.291	.254
180	.284	.328	.401	.419	.482	.524	.453	.504	.460	.300	.291	.245
270	.311	.354	.417	.438	.492	.526	.464	.500	.455	.310	.294	.244
330	.323	.365	.426	.449	.495	.526	.471	.504	.453	.319	.300	.243
375	.335	.380	.437	.459	.507	.530	.479	.509	.452	.326	.305	.253
2967 A°	n-Hexane			Run II-67								
0	.217	.273	.372	.397	.492	.568	.477	.578	.530	.319	.335	.293
330	.323	.369	.432	.454	.507	.535	.476	.516	.459	.324	.305	.251
375	.337	.383	.440	.462	.513	.537	.482	.516	.461	.330	.310	.256
435	.349	.391	.452	.472	.522	.539	.491	.519	.456	.337	.314	.255
495	.360	.405	.459	.483	.529	.545	.504	.525	.462	.346	.324	.254
560	.371	.416	.466	.489	.535	.545	.506	.525	.461	.352	.325	.259
2967 A°	20% Mineral Oil			Run II-57								
0	.228	.276	.376	.406	.502	.578	.483	.578	.546	.325	.335	.286
30	.220	.269	.364	.392	.478	.549	.463	.549	.506	.305	.315	.272
60	.242	.288	.376	.403	.477	.543	.461	.533	.496	.301	.308	.267
90	.250	.296	.378	.402	.472	.536	.454	.518	.489	.304	.299	.260
120	.267	.308	.388	.411	.476	.532	.453	.515	.470	.299	.297	.251
180	.286	.327	.399	.420	.480	.523	.455	.504	.461	.303	.295	.247
285	.313	.357	.419	.439	.490	.520	.465	.502	.449	.315	.298	.252
360	.331	.373	.431	.453	.501	.528	.475	.506	.452	.327	.303	.251
2967 A°	40% Mineral Oil			Run II-70								
0	.212	.263	.359	.394	.477	.568	.473	.559	.544	.321	.326	.299
31	.224	.274	.364	.395	.466	.553	.466	.532	.529	.317	.313	.289
61	.237	.280	.365	.396	.460	.538	.456	.516	.509	.312	.303	.277
91	.249	.296	.374	.403	.464	.534	.456	.512	.498	.309	.297	.271
121	.262	.306	.381	.406	.466	.531	.454	.509	.485	.308	.296	.269
211	.290	.332	.398	.423	.472	.523	.457	.495	.472	.315	.294	.262
301	.314	.355	.415	.440	.487	.526	.469	.499	.463	.328	.304	.268
391	.332	.376	.431	.456	.500	.532	.483	.509	.469	.342	.317	.270

APPENDIX III

IRRADIATION RESULTS--ACTINOMETRIC DATA

(Note: Units of $\int_o^t I_a A_i dt$ = moles of quanta per liter of solution.)

Interval, Min.	$\bar{I}_a \times 10^{-14}$, Quanta Per Min.	$\int_t^{t'} A_E dt$	$\int_t^{t'} A_P dt$	Interval, Min.	$\int_o^t I_a A_E dt$ x 10^5	$\int_o^t I_a A_P dt$ x 10^5
2537 A°	Isopropyl Alcohol		Run III-10			
0-20	4.32	18.96	.80	0-20	.453	.019
20-40	4.26	17.29	2.28	0-40	.861	.073
40-60	4.22	16.06	3.44	0-60	1.236	.153
60-90	4.20	22.41	6.39	0-90	1.757	.302
90-120	4.41	20.83	7.35	0-120	2.234	.470
120-150	4.23	19.40	8.20			
150-185	4.33	21.00	10.48	0-185	3.192	.913
185-215	4.42	16.78	9.52			
215-245	4.46	15.76	9.86	0-245	3.991	1.390
245-275	4.54	14.83	10.19			
275-305	4.58	13.94	10.51	0-305	4.717	1.912
305-335	4.82	13.05	10.76			
335-365	4.89	12.19	10.88	0-365	5.395	2.493
365-395	5.05	11.35	10.99			
395-410	5.04	5.41	5.54	0-410	5.863	2.955
2537 A°	20% Glycerol		Run III-14			
0-20	3.87	18.77	0.77	0-20	.402	.016
20-40	3.78	17.29	1.97	0-40	.764	.058
40-60	3.78	16.35	3.12	0-60	1.106	.123
60-90	3.96	23.09	6.10	0-90	1.612	.257
90-120	3.73	21.52	7.30	0-120	2.056	.407
120-150	4.01	20.03	8.13			
150-180	4.00	18.55	8.81	0-180	2.911	.783
180-210	4.08	17.10	9.33			
210-240	4.11	15.68	10.04	0-240	3.654	1.222
240-270	4.30	14.56	10.54			
270-300	4.34	13.79	10.74			
300-330	4.42	13.16	10.80	0-330	4.654	1.995
330-360	4.54	12.68	10.80			
360-390	4.65	12.23	10.80			
390-420	4.78	11.74	10.80	0-420	5.598	2.830

Continued

APPENDIX III - Continued

Interval, Min.	$\bar{I}_a \times 10^{-14}$, Quanta Per Min.	$\int_t^{t'} A_E dt$	$\int_t^{t'} A_P dt$	Interval, Min.	$\int_o^t I_a A_E DT$ x 10^5	$\int_o^t I_a A_P dt$ x 10^5
2537 A°	n-Hexane	Run III-22				
0-20	3.58	19.40	.58	0-20	.384	.012
20-40	3.54	18.20	1.74	0-40	.741	.046
40-60	3.56	17.07	2.88	0-60	1.077	.102
60-90	3.60	23.74	6.10	0-90	1.550	.224
90-120	3.51	21.90	7.50	0-120	1.976	.370
120-150	3.33	20.32	8.48			
150-185	3.38	21.83	10.94	0-185	2.758	.730
185-215	3.46	17.18	10.26			
215-240	3.53	13.33	9.12	0-240	3.348	1.105
240-270	3.70	14.94	11.39			
270-300	3.75	13.89	11.89			
300-330	3.83	12.92	12.31	0-330	4.216	1.846
330-360	4.07	12.00	12.71			
360-390	4.17	11.08	13.06			
390-420	4.26	10.11	13.29	0.420	4.980	2.747
2537 A°	20% Mineral Oil		Run III-18			
0-20	3.55	19.08	1.01	0-20	.375	.020
20-40	3.56	17.54	2.42	0-40	.720	.068
40-60	3.60	16.37	3.35	0-60	1.046	.134
60-90	3.71	22.86	5.09	0-90	1.516	.239
90-120	3.69	21.19	6.11	0-120	1.949	.364
120-150	3.70	19.64	7.02			
150-185	3.77	21.00	11.29	0-185	2.789	.743
185-215	4.02	16.48	10.72			
215-240	3.98	12.80	9.55	0-240	3.438	1.192
240-270	4.10	14.33	11.93			
270-300	4.09	13.24	12.30			
300-330	4.21	12.18	12.67	0-330	4.346	2.036
330-360	4.36	11.13	12.97			
360-390	4.52	10.18	13.23			
390-404	4.51	4.40	6.23	0-404	4.979	2.835

Continued

APPENDIX III - Continued

Interval, Min.	$\bar{I}_a \times 10^{-14}$, Quanta Per Min.	$\int_t^{t'} A_E dt$	$\int_t^{t'} A_P dt$	Interval, Min.	$\int_o^t I_a A_E dt \times 10^5$	$\int_o^t I_a A_P dt \times 10^5$
2804 A°	Isopropyl Alcohol		Run II-14			
0-14	14.42	13.68	.22	0-14	1.092	.018
14-29	13.79	13.98	.74	0-29	2.159	.074
29-49	13.48	17.56	1.76	0-49	3.469	.205
49-58	13.52	7.51	1.08	0-58	4.031	.286
58-88	13.18	23.35	4.55	0-88	5.734	.618
88-118	13.33	21.04	5.49	0-118	7.286	1.023
118-148	13.46	19.09	6.12			
148-178	13.25	17.26	6.75			
178-213	13.09	17.94	8.59	0-213	11.273	2.596
213-243	13.37	13.59	7.84			
243-273	13.17	12.07	8.04	0-273	13.159	3.757
273-293	14.09	7.31	5.38			
293-318	13.99	8.47	6.72	0-318	14.384	4.702
2804 A°	20% Glycerol		Run II-9			
0-15	13.99	14.52	.38	0-15	1.124	.029
15-30	13.38	13.67	.98	0.30	2.136	.102
30-45	13.23	12.98	1.42	0-45	3.087	.206
45-60	12.89	12.37	1.80	0-60	3.969	.334
60-90	12.93	23.10	4.64	0-90	5.622	.666
90-120	12.58	21.16	5.87	0-120	7.096	1.075
120-150	12.77	19.33	6.80	0-150	8.462	1.556
150-180	12.86	17.41	7.31			
180-210	12.94	15.46	6.43			
210-240	12.98	13.55	7.69	0-240	11.781	3.089
240-270	13.09	11.96	8.16			
270-305	13.05	12.74	9.75	0-305	13.568	4.384
305-335	13.14	10.33	8.57			
335-365	13.27	10.09	8.71	0.365	15.060	5.647

Continued

APPENDIX III - Continued

Interval, Min.	$\bar{I}_a \times 10^{-14}$, Quanta Per Min.	$\int_t^{t'} A_E dt$	$\int_t^{t'} A_p dt$	Interval, Min.	$\int_o^t I_a A_E dt$ x 10^5	$\int_o^t I_a A_p dt$ x 10^5
2804 A°	n-Hexane	Run II-18				
0-15	10.61	14.69	.15	0-15	.862	.009
15-30	8.65	14.07	.48	0-30	1.536	.032
30-45	10.97	13.45	.86	0-45	2.353	.084
45-60	10.21	12.84	1.27	0-60	3.078	.156
60-90	10.21	23.90	3.79	0-90	4.429	.370
90-120	10.25	21.51	5.30	0-120	5.649	.670
120-150	10.66	19.22	6.50	0-150	6.783	1.054
150-180	10.55	17.01	7.14			
180-210	10.46	14.90	7.58			
210-230	10.82	8.76	5.28	0-230	9.163	2.226
230-260	10.96	11.39	8.23			
260-290	10.88	9.43	8.54	0-290	10.422	3.239
290-320	11.09	7.65	8.84			
320-350	10.82	6.22	9.06	0-350	11.264	4.324
2804 A°	20% Mineral Oil		Run II-24			
0-15	11.41	14.49	.33	0-15	.915	.021
15-30	11.31	13.55	.96	0-30	1.763	.081
30-44	10.92	11.91	1.42	0-44	2.483	.167
44-59	11.17	12.05	2.02	0-59	3.228	.292
59-89	11.07	22.13	5.23	0-89	4.584	.612
89-119	10.90	19.75	6.46	0-119	5.775	1.002
119-154	11.05	20.49	8.69			
154-189	10.84	18.13	9.38	0-189	8.116	2.096
189-219	11.34	13.74	8.37			
219-249	11.46	12.19	8.62	0-249	9.751	3.168
249-284	11.09	12.25	10.32			
284-324	11.03	11.34	12.14	0-324	11.195	4.542

Continued

APPENDIX III - Continued

Interval, Min.	$\bar{I}_a \times 10^{-14}$, Quanta Per Min.	$\int_t^{t'} A_E dt$	$\int_t^{t'} A_p dt$	Interval, Min.	$\int_o^t I_a A_E dt$ x 10^5	$\int_o^t I_a A_p dt$ x 10^5
2967 A°	Isopropyl Alcohol		Run II-61			
0-30	6.32	29.31	.74	0-30	1.025	.026
30-60	6.16	27.86	1.80	0-60	1.975	.087
60-90	6.17	26.40	2.56	0-90	2.876	.175
90-120	6.10	24.98	3.31	0-120	3.720	.286
120-150	6.43	23.47	3.98			
150-195	6.53	32.19	7.19	0-195	5.718	.688
195-225	6.73	19.56	5.53			
225-255	6.87	18.13	5.94			
255-285	7.17	16.76	6.26	0-285	7.801	1.368
285-315	7.44	15.45	6.53			
315-345	7.65	14.20	6.79			
345-375	7.72	13.02	7.02	0.375	9.595	2.224
2967 A°	20% Glycerol		Run II-64			
0-30	6.06	28.52	.80	0-30	.956	.027
30-60	6.12	26.23	1.97	0-60	1.845	.094
60-90	6.35	24.56	2.81	0-90	2.708	.192
90-120	6.37	23.16	3.51	0-120	3.524	.316
120-150	6.38	21.85	4.10			
150-180	6.51	20.60	4.60			
180-200	6.78	13.05	3.34	0-200	5.528	.752
200-230	6.87	18.52	5.32			
230-260	6.88	17.31	5.65			
260-290	7.16	16.13	6.00	0-390	7.530	1.407
290-320	7.49	14.91	6.34			
320-350	7.72	13.72	6.60			
350-380	7.85	12.58	6.77	0-380	9.281	2.246

Continued

APPENDIX III - Continued

Interval, Min.	$\bar{I}_a \times 10^{-14}$, Quanta Per Min.	$\int_t^{t'} A_E dt$	$\int_t^{t'} A_P dt$	Interval, Min.	$\int_o^t I_a A_E dt$ x 10^5	$\int_o^t I_a A_P dt$ x 10^5
2967 A°	n-Hexane	Runs II-53, II-67				
0-30	5.77	28.89	.71	0-30	.922	.023
30-60	5.67	26.96	1.80	0-60	1.768	.079
60-90	5.58	25.30	2.70	0-90	2.550	.162
90-120	5.62	23.77	3.45	0-120	3.289	.270
120-150	5.58	22.32	3.97			
150-180	5.57	20.91	4.41	0-180	4.623	.528
180-210	5.63	19.47	4.81			
210-240	5.64	17.96	5.19			
240-270	5.86	16.47	5.57	0-270	6.324	1.021
270-300	5.90	15.06	5.91			
300-330	6.13	13.86	6.19	0-330	7.286	1.424
330-350	6.37	8.67	4.24			
350-375	6.46	10.21	5.39	0-375	7.957	1.766
375-405	6.77	11.34	6.58			
405-435	6.93	10.28	6.71	0-435	8.776	2.270
435-465	7.20	9.25	6.82			
465-495	7.35	8.27	6.88	0-495	9.481	2.822
495-525	7.52	7.42	6.93			
525-560	7.64	7.88	8.14	0-560	10.123	3.454
2967 A°	20% Mineral Oil		Run II-57			
0-30	5.60	29.62	.55	0-30	.918	.017
30-60	5.70	28.28	1.57	0-60	1.810	.067
60-90	5.78	26.64	2.60	0-90	2.662	.150
90-120	5.68	24.99	3.56	0-120	3.448	.262
120-150	5.97	23.40	4.37			
150-180	6.06	21.81	5.04	0-180	4.952	.575
180-210	6.22	20.26	5.53			
210-240	6.12	18.86	5.94			
240-285	6.37	25.85	9.58	0-285	7.200	1.304
285-315	6.88	15.68	6.79			
315-360	6.85	21.18	10.64	0-360	8.600	1.966
360-390	7.22	12.57	7.34			
390-420	7.27	11.31	7.47	0-420	9.557	2.560

Continued

APPENDIX III - Continued

Interval, Min.	$\bar{I}_a \times 10^{-14}$, Quanta Per Min.	$\int_t^{t'} A_E dt$	$\int_t^{t'} A_P dt$	Interval, Min.	$\int_o^t I_a A_E dt$ x 10^5	$\int_o^t I_a A_P dt$ x 10^5
2967 A°	40% Mineral Oil		Run II-70			
0-31	5.73	29.78	.79	0-31	.944	.025
31-61	5.83	26.82	2.09	0-61	1.810	.092
61-91	5.52	25.08	2.90	0-91	2.576	.181
91-121	5.66	23.44	3.60	0-121	3.310	.294
121-151	5.89	21.85	4.25			
151-181	5.94	20.20	4.88			
181-211	6.06	18.59	5.50	0-211	5.310	.777
211-241	6.32	17.02	6.06			
241-271	6.47	15.58	6.46			
271-301	6.70	14.21	6.74	0-301	6.990	1.470
301-331	7.12	12.92	6.93			
331-361	7.25	11.75	7.06			
361-391	7.19	10.86	7.20	0-391	8.403	2.313